The Ret receptor mediates sensory neuron dendrite growth through TGFβ

Dissertation with the aim of achieving a doctoral degree
at the Faculty of Mathematics, Informatics and Natural Sciences
Department of Biology of the Universität of Hamburg

submitted by
Nina Hoyer

2016 in Hamburg

Day of oral defense: 21.10.2016

The following evaluators recommend the admission of the dissertation:

Prof. Dr. Arp Schnittger

PD Dr. Sabine Hoffmeister-Ullerich

Eidesstattliche Versicherung

Declaration on oath

Hiermit erkläre ich an Eides statt, dass ich die vorliegende Dissertationsschrift selbst verfasst und keine anderen als die angegebenen Quellen und Hilfsmittel benutzt habe.
I hereby declare, on oath, that I have written the present dissertation by my own and have not used other than the acknowledged resources and aids.

Hamburg, den: …… Unterschrift: ……

Universitätsklinikum Hamburg-Eppendorf

Center for Molecular Neurobiology Hamburg

Research Group: Neuronal Translational Control

Martinistraße 52
20246 Hamburg

Kent Duncan, PhD

Phone: +49(0)40 7410-56274
Fax: +49(0)40 7410-53436
Kent.Duncan@zmnh.uni-hamburg.de
www.zmnh.uni-hamburg.de

Delivery address:
Falkenried 94
20251 Hamburg

Universitätsklinikum Hamburg-Eppendorf Martinistraße 52 20246 Hamburg
Zentrum für Molekulare Neurobiologie - Forschergruppen

June 9, 2016

English language Thesis Certification: Nina Hoyer

To whom it may concern:

Nina Hoyer, who was born on 07. Oktober 1985 in Bremerhaven, is submitting her doctoral dissertation in English. The title of her thesis is: **'The Ret receptor mediates sensory neuron dendrite growth through TGFb'**.

I hereby certify as a native speaker and molecular biologist that the English language used in this thesis is sufficiently correct for submission.

Yours truly,

Universität Hamburg
Universitätsklinikum Hamburg-Eppendorf
Zentrum für Molekulare Neurobiologie
AG Duncan
Falkenried 94 · D-20251 Hamburg

Kent Duncan, Ph.D.

Hamburg, June 9, 2016

1 ZUSAMMENFASSUNG

Die Entwicklung eines funktionellen Nervensystems erfordert korrekte neuronale Spezifikation, um die sensorische Informationsverarbeitung und Kommunikation innerhalb des neuronalen Netzwerks zu gewährleisten. Hierbei ist insbesondere die Entwicklung neuronaler Dendriten von hoher Wichtigkeit und auf Grund dessen streng durch eine Vielzahl von Substrat- und Gewebe-Interaktionen reguliert. Neurone etablieren art-spezifische und hoch stereotype Strukturierungsmuster, wodurch die Abdeckung ihres rezeptiven Feldes erlangt wird. Demzufolge korreliert die funktionale Komplexität mit der der morphologischen Komplexität, die durch die Form des Dendritenbaums, die -verzweigung und seiner Größe gekennzeichnet ist (Ramon y Cajal S, 1911). Aufgrund der hohen Komplexität ist das Verständnis der mechanistischen und molekularen Grundlagen während der Entwicklung von Dendriten jedoch weiterhin begrenzt.

Das periphere Nervensystem (PNS) der Larven von *Drosophila melanogaster* hat sich als ein sehr gutes genetisches Modell für die Analyse von Dendritenentwicklung und deren Funktion etabliert. Innerhalb des PNS der *Drosophila* Larven bieten die gut charakterisierten “dendritic arborization“ (da) Neurone ein ausgezeichnetes System zur Untersuchung von Dendritenentwicklung *in vivo.* Die C4da Neurone verfügen über klassenspezifische hochkomplexe dendritische Felder, welche die gesamte Körperwand der Larve abdecken.

In der vorliegenden Arbeit wurde die konservierte Rezeptor-Tyrosinkinase (RTK) Ret als ein wichtiger Regulator des Dendriten-Wachstums und der Entwicklung des rezeptiven Feld von C4da Neuronen identifiziert.

Die Analyse eines generierten *Ret* „Knock-out“ Allels (Ret^{ko}) ergab, dass der Verlust von *Ret* zu starken Wachstums- und Adhäsionsdefekten der Dendriten von C4da Neuronen führt. Durch die spezifische Expression von *Ret* in C4da Neuronen konnte dieser Phänotyp in Ret^{ko} Tieren vollständig gerettet werden. Eine anschließende Struktur-Funktions-Analyse von Ret ergab, dass sowohl die extra- als auch die intrazelluläre Domäne für die Dendritenentwicklung von C4da Neuronen erforderlich ist, welches darauf hinweist, dass extrazelluläre Signale von Ret aufgenommen und innerhalb der Zelle weitergeleitet werden.

Hierbei zeigte sich, dass die Aktivität der Tyrosinkinase nicht an der Funktion von Ret in der Dendritenentwicklung beteiligt ist, da die Expression einer Kinase-inaktiven Form von Ret eine vollständige Rettung des Phänotyps von Ret^{ko} Tieren aufzeigte. Diese Ergebnisse belegen, dass Ret zell-autonom für die Strukturierung der Dendriten von C4da Neuronen erforderlich ist, und zwar unabhängig von der Kinaseaktivität. Darüber hinaus zeigten Ret^{ko} Tiere Verhaltensdefekte, welche mit der Funktion von C4da Neuronen verknüpft sind.

Des Weiteren wurde in dieser Studie der TGFβ Ligand maverick (mav) als potentieller Interaktionspartner von Ret identifiziert, welcher Ret-abhängige Dendriten-Entwicklung von C4da Neuronen vermittelt. Eine detaillierte Funktionsanalyse von mav konnte zeigen, dass mav wahrscheinlich von Epithelzellen exprimiert und sekretiert wird. Die Analyse eines neu

generierten *mav* „Knock-out“ Allels (*mav*^{ko}) konnte bestätigten, dass mav eine funktionelle Komponente des Ret Signalwegs in C4da Neuronen darstellt. Darüber hinaus zeigte sich, dass eine Überexpression von *mav* und *Ret* ausreichend ist, um Dendritenwachstum in heterologen Neuronen zu induzieren. Dieses Ergebnis deutet daraufhin, dass der zugrundeliegende Signalweg von mav und Ret grundlegende Wachstumssignale aktivieren kann. Insgesamt liefern die erhaltenen Daten in dieser Arbeit Hinweise darauf, dass Ret und mav bei der Entwicklung von C4da Neuronen im selben Signalweg agieren und es sich hierbei um einen potentiellen neuen Rezeptor-Ligand-Komplex handelt. Zudem dient mav vermutlich als permissives Signal, welches für die Verzweigung und Morphologie von Dendriten der C4da Neurone entscheidend ist.

Die Analyse des zugrundeliegenden Signalweges deutet jedoch darauf hin, dass die Aktivierung klassischer TGFβ Signalwege bei der Funktion von Ret und mav nicht beteiligt ist. Mit Hilfe einer genomweiten „Microarray“-Analyse von *Ret*^{ko} C4da Neuronen wurde RanBPM als potenzieller Vermittler von Ret induzierten intrazellulären Signalwegen identifiziert. Eine tiefergehende Analyse konnte die Expression von RanBPM in C4da Neuronen zeigen. Des Weiteren wies der Verlust von *RanBPM*-Funktion einen Ret-ähnlichen Phänotyp in C4da Neuronen auf. Zusätzlich konnte eine funktionelle genetische Interaktion zwischen RanBPM und Ret in der Entwicklung von C4da Neuronen festgestellt werden. Diese Ergebnisse deuten darauf hin, dass RanBPM eine neu identifizierte Komponente im Signalweg von Ret darstellt.

Diese Arbeit gibt neue Einblicke in den zugrundeliegenden Signalweg von Ret, welcher für die Dendritenentwicklung von C4da Neuronen erforderlich ist, einschließlich der Identifizierung von mav als potentieller Ligand. Basierend auf dem hohen Grad der Konservierung von Ret legen diese Ergebnisse potentielle konservierte Funktionen in der Dendritenentwicklung von Wirbeltieren nahe.

2 SUMMARY

The development of a functional nervous system requires correct neuronal specification to allow proper sensory information processing and communication within the neuronal network. In particular, neuronal dendrite development is highly complex and therefore strictly regulated by a variety of substrate and tissue interaction. Neurons establish subtype specific, often highly stereotyped branching patterns to cover their receptive field. Cell type specific functional complexity correlates with the morphological complexity characterized by the dendritic shape, arborization and size (Ramon y Cajal S, 1911). However, due to this complexity, mechanistic and molecular insight into dendrite development is still limited.

The *Drosophila melanogaster* larval peripheral nervous system (PNS) is a powerful genetic model for the analysis of dendrite development and function. Within the larval PNS, the well characterized dendritic arborization (da) neurons provide an excellent system to study dendrite development *in vivo*. C4da neurons feature class specific highly complex dendritic fields tiling the entire larval body wall. In this study, the conserved receptor tyrosine kinase (RTK) Ret (re-arranged during transfection) has been identified as an important regulator of C4da neuron dendrite development and patterning. A newly generated *Ret* knock-out (Ret^{ko}) allele revealed strong C4da neuron dendrite growth and adhesion defects. This phenotype could be fully rescued by C4da neuron specific expression of transgenic *Ret* in Ret^{ko} animals. Subsequent structure-function analysis of Ret revealed that the extra- and intracellular domain are both required for C4da dendrite development indicating that Ret transduces extracellular signals into the cell. Surprisingly, Ret tyrosine kinase activity is dispensable for Ret function in dendrite development, as expression of kinase-inactive Ret showed complete rescue activity. These results provide evidence that Ret is cell-autonomously required for C4da neuron dendrite patterning independently of its kinase activity. Furthermore, Ret^{ko} animals displayed behavioural defects linked to C4da neuron function.

A candidate screen for Ret ligands identified the TGFβ ligand maverick (mav) as a potential interactor mediating Ret function in C4da neuron development. Mav is likely expressed and secreted by epithelial cells and analysis of mav function by generation of a *mav* knock-out allele (mav^{ko}) confirmed a role for mav in Ret dependent C4da neuron development. Moreover, mav likely acts as a permissive guidance signal required for C4da neuron dendrite patterning. Additionally, overexpression of *mav* and *Ret* is sufficient to induce dendrite growth in heterologous neurons suggesting that mav/Ret signaling is able to transduce growth signals. Overall, the data provide evidence that Ret and mav are acting in same signaling pathway in C4da neuron development, potentially as a novel receptor-ligand protein complex.

Analysis of the underlying signaling pathway indicated that canonical TGFβ signaling is not involved in Ret and mav function. Instead, genome wide microarray profiling of Ret^{ko} C4da neurons identified RanBPM as a potential mediator of Ret intracellular signaling. Further

analysis showed that RanBPM is expressed in C4da neurons and its loss-of-function displays Ret-like phenotypes in C4da neurons. In addition, a functional genetic link between RanBPM and Ret in C4da neurons development could be identified suggesting that RanBPM is a novel component of the Ret signaling pathway.

This work provides novel insight into the Ret signaling pathway required for C4da neuron dendrite development, including the identification of mav as a potential ligand. Based on the high degree of conservation of Ret, these findings suggest potentially conserved functions in dendrite development of vertebrates.

3 ACKNOWLEDGEMENT

The writing of this dissertation has been one of the most significant academic challenges I have ever had to face. Without the support, patience and guidance of the following people, this study would not have been completed. It is to them that I owe my deepest gratitude.

First, I would like to express my sincere gratitude to my thesis advisor, Dr. Peter Šoba, for the continuous support of my PhD study and related research, for his patience, motivation, immense knowledge and the opportunity to participate in conferences. The door of his office was always open whenever I had a question about my research or writing, ran into a trouble spot or simply to sit down for a cup of coffee.

Besides my advisor, I would like to thank my thesis committee: Prof. Dr. Schnittger, PD Dr. Hoffmeister-Ullerich, Prof. Dr. Ganzhorn, Prof. Dr. Dobler and Prof. Dr. Oertner.

I thank all the members and former members of the research group 'Neuronal Patterning and Connectivity' in the Center for Molecular Neurobiology Hamburg (ZMNH): Meike Petersen, Chun Hu, Alisa Gruschka, Dr. Denan Wang, Federico Tenedini, Philip Zielke, Kathrin Sauter, Dörte Clausen, Hanna Schmidt, Dr. Assia Hijazi and Dr. Bettina Spitzweck. Thank you for the great atmorphere within the lab. Especially, I would like to thank Meike and Alisa for all the fun we had in the last years!

I would like to thank the members of the research groups of the ZMNH, in particular the research groups of Dr. Kent Duncan and Dr. Froylan Calderon de Anda, and the PhD students of the ASMB program, for their comments and passionate discussions.

My gratitude also goes to Prof. Dr. Jay Z. Parrish and Dr. Charles Kim, who gave access to their laboratory and research facilities; as well as to Dr. Irene Miguel-Aliaga who provided the Ret-antibody. Without their support it would not be possible to conduct this research.

To my friends in Bremerhaven and Bremen: Thank you all for your support, encouragement, profound understanding and the varied events during free time.

At the end, I would like to thank my partner, Peter Kampmann. He was always there cheering me up and supported me the whole time. I am really looking forward to our future. It will be fantastic!

Lastly, I must express my very profound gratitude to my mum, Monika Hoyer. She supported me in so many ways and my years of study and the whole process of doing research and writing this thesis would not have been possible…Thank you so much.

4 TABLE OF CONTENTS

5 ABBREVIATIONS

AEL after egg laying
Amp Ampicillin
babo baboon
BN Bolwig's nerve
BO(s) Bolwig's organ/s
BSA Bovine serum albumine
C4da neurons Class IV da neurons
Cas9 CRISPR associated protein 9
CD4 Cluster of differentiation 4
CD8 Cluster of differentiation 8
CLD Cadherin-like domain
CNS Central nervous system
CRD Cysteine-rich domain
CRISPR Clustered Regularly Interspaced Short Palindromic Repeats
CyO Curly of oster
da dendritic arborization
dAct dActivin (TGFβ ligand)
daw dawdle (TGFβ ligand)
DEG/ENaC Degenerin/Epithelial sodium channel
dH_2O deionized water
D-Ret Drosophila-Ret
Dvl Dishevelled
Drl Derailed
Gal4 yeast transcription factor Gal4
gbb glass-bottom boat (TGFβ ligand)
GDNF Glial-cell-line-derived neurotrophic factor
GFLs GDNF family ligands
GFP Green fluorescent protein
GFRα GDNF family receptor α
GMR Glass multimer reporter
h/hrs hour/s
hid head involution defective
HRP Horseradish peroxidase
Kan Kanamycin
L liter
LB Lysogeny Broth, liquid media for culturing bacteria
mav maverick (TGFβ ligand)
min minute/s
mL milliliter/s
mm millimeter/s
myo myoglianin (TGFβ ligand)
PBS Phosphate buffered saline
PBS-T PBS with 0.3 % Triton x-100
PDF pigment dispersing factor
pdf neurons PDF-expressing neurons
PG Prothoracic gland
PI Performance index

PN projecting neurons
PNS Peripheral nervous system
ppk pickpocket, Degenerin/Epithelial sodium channel (DEG/ENaC) subunit
ptth Prothoracicotropic hormone
ptth neurons PTTH-producing neurons
put punt
RanBPM Ran-binding protein M
Ret "rearranged during transfection"
RNA Ribonucleic acid
RNAi RNA interference
RT Room temperature
sax saxophone
s(ec) second/s
SEM Standard error mean
tdGFP tandem dimer GFP
tdTom tandem dimer Tomato
TGFβ Transforming Growth Factor beta
TK Tyrosine kinase
tkv thickveins
TMD Transmembrane domain
TrpA1 Transient receptor potential cation channel A1
UAS Upstream activating sequence
VNC Ventral nerve cord
wit wishful thinking

6 INTRODUCTION

6.1 General features of dendrite development

The development of a functional neuronal network is essential for every living organism. For this purpose, neurons have to develop different subcellular compartments (dendrites, soma, axon), each providing its specialized function by distinctive molecular and morphological features. Comparing the cellular compartments, dendritic arbors are more complex in contrast to axonal arbors. In general, neurons develop one axon but have several distinct dendrites to receive and to convey different incoming information. Neuronal differences and their specialization can be already seen on the morphological level since each neuron type displays its own characteristic dendritic arborization. For instance, Purkinje cells develop enormously complex dendritic trees to transmit incoming information from many different presynaptic connections, whereas other neurons as sensory neurons display more simple dendritic structures. Besides that, dendrites display mostly postsynaptic specialization compared to axons having mostly presynaptic specializations. Further, the cytoskeleton of dendritic and axonal compartments differs from each other: While axons usually display higher amounts of stable microtubules, dendrites display a higher ratio of actin filaments to microtubules.
The generation of this polarity and intracellular compartmentalization enables each neuron to grow properly and to be guided to the appropriate target to make synaptic connections between dendrites and incoming axons and thus forming a proper functional network.

To respond and react to environmental sensory cues, the peripheral nervous system is connected to the central nervous system to generate appropriate behavioral motor outputs. External stimuli activate sensory receptors, which are specifically located throughout the body surface. The sensory response to painful stimuli is termed as nociception. In nociception, harmful chemical, mechanical or thermal stimulation of sensory nerve cells (nociceptors) results in their activation and behavioral responses. In humans, special cutaneous receptors respond to certain external stimuli. The free nerve endings are the simplest receptors and respond to temperature, touch, pressure and pain of sensory neurons. These receptors transmit external information via neuronal pathways in the spinal cord to the brain. Here, the sensory information is processed and evaluated (Purves et al., 2011).
In terms of pain perception it has been shown that evolutionarily conserved proteins and the underlying signaling pathways are likely extensively conserved between vertebrates and invertebrates (Kang et al., 2010; Neely et al., 2011).

6.2 The peripheral nervous system of *Drosophila melanogaster* as a model system for dendrite development

6.2.1 Dendrite arborization neurons: development, molecules and their characteristic functions

Similar to humans, the existence and survival of *Drosophila* larvae and adult flies within their environment require a functional neuronal circuitry. The peripheral nervous system (PNS) of *Drosophila melanogaster* larvae consists of segmentally repeated sensory neurons lining the larval body wall. Based on the characteristic dendrite projection pattern, these neurons are categorized into type I or type II.

Type I sensory neurons display monopolar dendrites and are located in external sensory organs and chordotonal organs. In contrast, type II sensory neurons display a multidendritic (md) branching pattern. This group is further subdivided into tracheal dendrite (td) neurons, bipolar dendrite (bd) neurons, and dendritic arborization (da) neurons (Bodmer and Jan, 1987) (Figure 1).

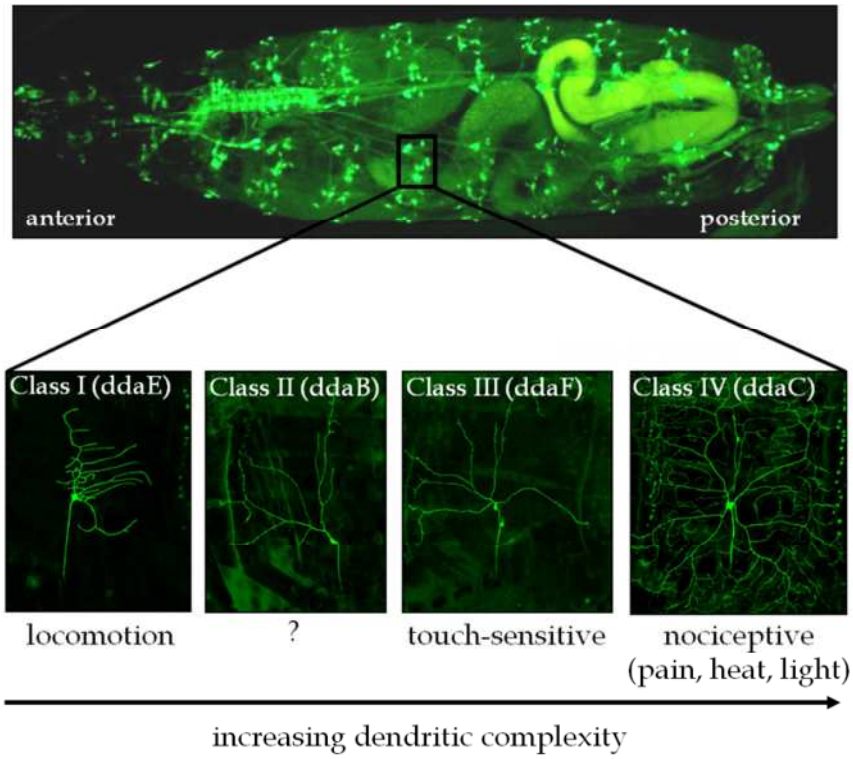

Figure 1. Morphology and function of class I-IV da sensory neurons in the larval peripheral nervous system. Sensory da neurons in *Drosophila* larvae are categorized into four distinct classes according to their increasing morphological complexity. All types of sensory neurons feature different specific functions (modified from Grueber et al. 2002).

The dendritic patterning of da neurons has been characterized extensively. Based on their dendritic branching morphology, each of the 15 da neurons found per abdominal

hemisegment can be classified into one of four distinct subtypes ranging from class I, II, III to IV (C1da, C2da, C3da and C4da) in order of increasing dendritic complexity (Grueber et al., 2002).

The dendritic morphology of C1da and C2da neurons is simple and each class only covers a portion of the abdominal segment. C1da neuron secondary dendrites mostly extend along the anterior-posterior axis and perpendicular to the primary dendrite, whereas C2da neurons display more symmetrically branching dendrites. Dendritic arbors of C3da neurons have larger dendritic fields and exhibit higher branching complexity. They also show an abundant number of short dendritic spikes, which are actin-rich and lack stable microtubules. C4da neurons are the most complex da neurons and achieve almost complete coverage of the larval body wall (Grueber et al., 2003, 2002).

Even though each C3da and C4da neuron shows almost complete dendritic field coverage, dendrites of neighboring neurons within each class do not cross one another. This phenomenon is known as 'tiling' and well documented in both vertebrates and invertebrates (Breuer et al., 2005; Grueber et al., 2002; Wassle et al., 1981). It allows dendrites of a distinct neuronal type to cover the receptive field and detect incoming signals without redundancy and to hold down the rate of energy consumption. Molecules involved in the control of this mechanism will be introduced in a following chapter (6.3.3).

Besides their morphological differences, the four classes can be distinguished by their functional properties as well. C1da neurons are involved in locomotion and likely function as proprioceptors (Cheng et al. 2010). C2da neuron function is not completely understood. So far, there is evidence that these sensory neurons are implicated in gentle touch response since silencing of driver lines targeting C2da neurons showed an impaired touch sensation. However, these driver lines are also expressing C1da or C3da neurons and likely contribute to this behavioral response (Tsubouchi et al., 2012). Indeed, C3da neurons are described to act as touch-sensitive (innocuous touch) neurons (Yan et al., 2013). The most complex C4da neurons have polymodal functions (Guo et al., 2014) and are essential for sensing nociceptive stimuli (e.g. temperature, painful touch, light) (Hwang et al., 2007; Robertson et al., 2013; Tsubouchi et al., 2012; Xiang et al., 2010).

6.2.2 Class IV da neuron function in the perception of noxious stimuli

In order to increase the chances of survival, larvae instinctively avoid exposure to light and remain in the food during larval stages. Thus they avoid predators, heat and dehydration (Gong & Gong 2012). This typical phototactic behavior has been described as light avoidance (Hassan et al. 2000; Keene et al. 2011, Yamanaka et al. 2013).

In *Drosophila* larvae, the stimulus "light" can be processed through two different light sensing pathways.

Drosophila larvae can perceive light stimuli through C4da sensory neurons along the entire larval body wall (Xiang et al., 2010, Yamanaka et al., 2013). Xiang et al. revealed that C4da neurons respond to ultraviolet, violet and blue light and are major mediators of light avoidance, particularly at high intensities. Calcium imaging analysis using the calcium indicator GCaMP3 showed that dendritic illumination with ultraviolet and blue light (340 - 470 nm) but not green or red light (525 - 620 nm) activates C4da neurons (Xiang et al., 2010).
Besides C4da neurons, phototaxis or light avoidance in *Drosophila* larvae is also mediated by photoreceptors clustered as the Bolwig organ (BO), which functions as the primary light sensing organ. Genetic ablation of BOs by using a GMR-hid transgene induces larval blindness, showing BOs are a major component in light detection and avoidance (Hassan et al. 2000, Xiang et al., 2010). These primary light sensing organs are located at the anterior end of the larval head inside the body and connect the brain with the larval head skeleton (Green et al., 1993). Each BO is comprised of 12 photoreceptors. Four photoreceptors expressing the blue light sensitive rhodopsin 5 and eight expressing the green light sensitive rhodopsin 6 (Sprecher et al., 2011). Downstream of BOs, the pigment-dispersing factor (PDF)-expressing lateral neurons (pdf neurons) in the larval central brain are innervated via the Bolwig's nerve (BN) (Yuan et al., 2011).

To detect noxious stimuli is therefore under strict evolutionary pressure. Parasitoid wasps (e.g. L. boulardi) prey on *Drosophila* larvae by using their ovipositor to inject eggs into their bodies. The *Drosophila* larva is then eaten from the inside and the adult wasp ecloses out of the *Drosophila* pupa. Robertson et al. described that larvae display the ability to respond very precisely to the location of the wasp attack and that C4da neurons are necessary and respond to this noxious stimulus (Robertson et al., 2013). This nocifensive escape response is performed by stereotypical corkscrew-like rolling around the anterior/posterior axis in response to noxious thermal or mechanical stimulation.
The highly branched C4da neurons function as polymodal nociceptors that are necessary for behavioral responses to noxious heat (>39°C) or noxious mechanical (>30 mN) stimuli (Zhong et al., 2010). Several observations indicate that specific expression of ion channels play a crucial role in neuronal mechanotransduction in invertebrates.
Zhong et al. reported that the *pickpocket* (*ppk*) gene is required for mechanical nociception but not thermal nociception in these sensory cells. *Ppk* encodes an ion channel subunit of the Degenerin/Epithelial sodium channel (DEG/ENaC) family and is specifically expressed in nociceptive C4da neurons (Adams et al., 1998). *Ppk* mutant larvae display strongly reduced nociceptive behavior in response to mechanical stimuli. However, they exhibit normal behavioral responses to gentle touch (Zhong et al., 2010). Analyzing DEG/ENaCs in vertebrate hair cells revealed that they are implicated in painful touch sensation as well, suggesting that neurons that detect these mechanical forces in *Drosophila* use similar mechanosensory molecules (Corey et al., 2004; Nagata et al., 2005).

In the studies from Guo et al. (2014), Gorczyca et al. (2014) and Maunther et al. (2014), the gene *ppk26* (also known as *CG8546* or *balboa*) was identified as being required for mechanical nociception as well. *Ppk26* also encodes a DEG/ENaC ion channel subunit with high similarity to the amino acid sequence of *ppk*. Detailed analysis revealed ppk26 as well as ppk being highly enriched in nociceptive C4da neurons. In their analysis a direct interaction between these DEG/ENaC subunits was detected and it was shown that ppk26 distribution in C4da neurons depends on ppk. These observations indicate a mechanical nociceptive function for the ppk/ppk26 heteromeric ion channel complex *in vivo* (Gorczyca et al., 2014; Guo et al., 2014; Mauthner et al., 2014).

High-throughput behavioral methods performed by Neely et al. (2011) determined further genes contributing to pain perception. Within their analysis, the conserved gene encoding the thermoreceptor TrpA1 was identified as an essential "pain-sensor" in both adult and larval *Drosophila*. The TrpA1 channel is required in the *Drosophila* nervous system to sense noxious stimuli and shows specific expression within multi-dendritic (md) sensory neurons (Neely et al., 2011). Furthermore, a genetic screen for mutants defective in noxious heat response identified the *painless* gene, which is required for both thermal and mechanical nociception, but not for sensing gentle touch. The painless mRNA encodes a protein of the transient receptor potential ion channel family. Expression analysis showed painless localization in peripheral neurons that extend multiple branched dendrites beneath the larval epidermis (Tracey et al., 2003).

Recently, mammalian *Piezo1* and *Piezo2* were identified as components of channels activated by mechanical stimulation (S. E. Kim et al., 2012). These genes are evolutionarily conserved and encode for proteins belonging to the Piezo transmembrane protein family. Within the *Drosophila* genome one single member of *Piezo* (*DmPiezo*) is known and it has been shown that the knock-down of *DmPiezo* in sensory C4da neurons reduced the nocifensive response of *Drosophila* larvae. However, other noxious stimuli or touch were not affected. Electrophysiological recordings confirmed the function of *DmPiezo* in C4da neurons. It was also shown that both *ppk* and *DmPiezo* function in two parallel pathways. In human cells, the expression of *DmPiezo* induces mechanically activated currents, similar to its mammalian homologs, confirming its evolutionarily conserved function (Coste et al., 2010; S. E. Kim et al., 2012).

6.2.3 The larval peripheral nervous system of *Drosophila melanogaster* as model system to study dendrite development

The model organism *Drosophila melanogaster* is a powerful system to study the mechanisms underlying dendrite development and function. Compared to the billions of cells within the human nervous system, the *Drosophila* nervous system is fairly simple with only about 100.000 in adults and about 10.000 in larvae.
Fundamental mechanisms of development which are conserved in the mammalian system have originally been identified using *Drosophila* as a model organism. The peripheral nervous system of *Drosophila* larvae offers a number of advantages to identify novel genes and signaling pathways involved in dendrite development. One major aspect is that there are many useful genetic tools available to easily manipulate spatial and temporal gene expression (Venken et al., 2011). Further, the neurons of the PNS are well characterized and accessible to *in vivo* confocal microscopy techniques, which allow high-resolution imaging of single neurons.
An additional feature is its short life cycle of two weeks (Figure 2).

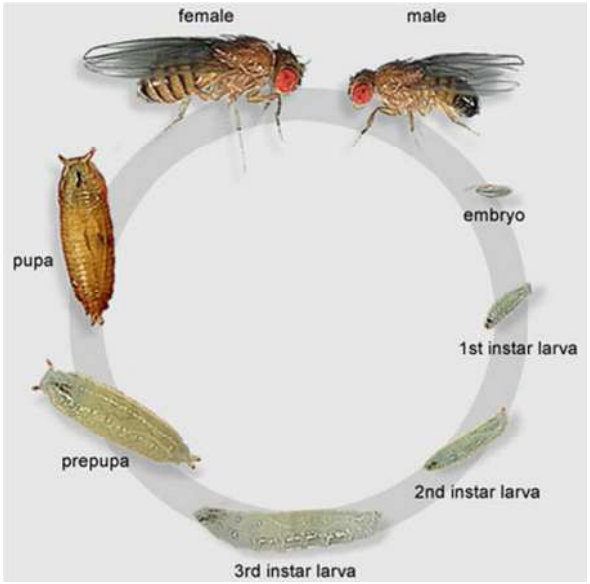

Figure 2. The life cycle of *Drosophila melanogaster*. At 25°C the development from egg via three larvae stages to an adult fly takes nine to ten days (modified from Weigmann et al., 2003).

After female and male adult flies have mated, the females lay fertilized eggs into the fly food. 20-22 h after egg laying (AEL) the 1st instar larvae hatch. During development, *Drosophila* larvae have to pass through three larval stages. Before reaching adulthood, late 3rd instar larvae crawl out of the fly food and form pupae to undergo metamorphosis until adult flies eclose from the puparium (Weigmann et al., 2003). This life cycle makes it possible to study and generate numerous generations within a short time frame.

6.3 Molecular mechanisms of dendrite development

During their developmental stages, neurons exhibit a variety of possible dendritic interactions, including self-avoidance (dendrites from the same neurons do not cross with the others), tiling (different neurons of the same class have their own specific dendritic field without invading to the adjacent area), and coexistence (different types of neurons share the same territory). Although some of the molecules controlling dendrite morphogenesis and regulating specific dendrite interactions have been identified, details of the underlying processes are still largely unknown.

Several studies have shown that molecular mechanisms regulating dendrite growth and development can be categorized into cell-extrinsic and cell-intrinsic mechanisms.

Cell-extrinsic regulators mainly refer to the chemoattractive/chemorepulsive cues, cell surface proteins and the interaction between the extracellular matrix and cellular dendrites (by receptors or membrane-bound proteins). Cell-intrinsic regulators refer to transcriptional regulators, cytoskeletal regulators, secretory and endocytic pathways. However, external cues may influence their activity (Puram & Bonni, 2013).

Some of those fundamental mechanisms for dendrite development will be introduced in the following chapter.

6.3.1 Exogenous factors: secreted proteins, cell surface proteins and receptor-ligand interaction

During development, dendrites grow to their correct locations in response to environmental cues allowing them to target their final positions. The orientation is controlled by a number of different factors, which can be categorized into different groups.

First, diffusible cues can act in a long-range manner by forming a gradient to help dendrites navigating their environment. Second, secreted or transmembrane proteins can act locally and control the branching pattern in a more precise manner (Figure 3). Based on that, fundamental mechanisms such as 'tiling', 'self-avoidance' and 'co-existence' are able to control proper dendrite interaction and formation, which will be introduced in a following chapter (6.3.3).

Neurotrophins

Many studies have shown that secreted factors play a crucial role in regulating growth and retraction of dendrites; for instance neurotrophins, which are secreted proteins, including nerve growth factor (NGF), brain-derived growth factor (BDNF), neurotrophin 3 (NT-3) and neurotrophin 4 (NT-4). They act on neurons expressing their receptor, which are members of the receptor tyrosine kinase (RTK) family. As an example, experiments in granule cell cultures showed that neurotrophin-4/5 (NT-4/5) and BDNF promoted neurite extension and

survival of differentiated cerebellar granule cells. These effects can be blocked pharmacologically by a specific inhibitor for Trk tyrosine kinases (Gao et al., 1995).

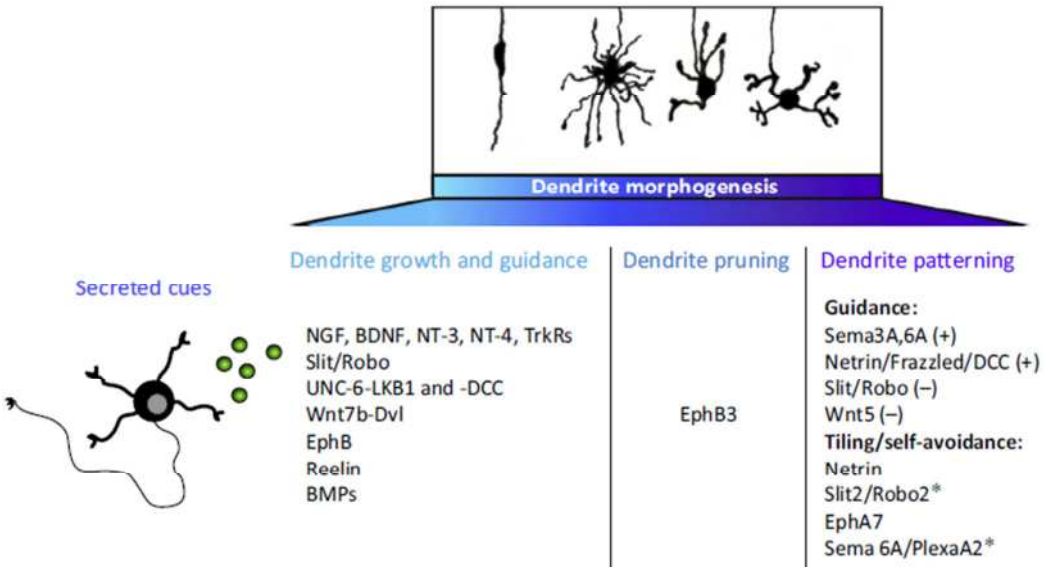

Figure 3. Cell-extrinsic regulators of dendrite morphogenesis. Several secreted molecules regulate different stages of dendrite development. *Molecules mediating isoneural repulsion of dendrites (modified from Valnegri et al., 2015).

Semaphorins

Neuronal dendrites are also responsive to extrinsic factors which can trigger or repress growth and semaphorins are a well-studied family of proteins mediating dendritogenesis. Semaphorins are a large family of both secreted and membrane-bound proteins. Semaphorin binding to its neuronal receptors, neuropilins and plexins, can act both as an attractive or repulsive cue in dendrite and axon formation.

For instance, Semaphorin 3A (Sema3A) is implicated in mediating axon guidance as well as affecting dendritic growth. More specifically, in the mammalian system this molecule acts both as a repulsive cue for cortical axons and as an attractive signal for apical dendrites of cortical neurons. It is thought to be secreted by cells within the cortical layer 1 and the interaction of Sema-3A and its receptor neuropilin-1 mediating the initial growth of cortical neuron axons towards the Sema3A source. This is regulated by diffusible repulsive signaling and plays an important role in the initial patterning of projections in the developing cortex (Polleux et al., 1998, Polleux et al., 2000).

In *Drosophila*, membrane bound Semaphorin-1a is an important factor within the olfactory system to control the dendritic targeting of projecting neurons (PNs) and also to regulate their axon targeting into higher olfactory centers.

Its paralogs, Sema-2a and -2b, function as spatial signals to regulate proper PN dendrite targeting. These molecules are secreted and form a gradient inverse to the Sema-1a protein

gradient. Dendrites with high levels of Sema-1a are targeted to regions with low levels of Sema-2a and -2b and vice versa. This sophisticated interaction leads to proper dendrite targeting and correct olfactory information processing in the brain (Komiyama et al., 2007; Sweeney et al., 2011; Zlatic et al., 2009).

Recent data from *Drosophila* concerning the function of Sema-2b showed that this secreted ligand is also implicated in dendrite patterning of C4da sensory neurons. Its loss-of-function results in increased dendrite crossing defects due to a loss of adhesion between sensory neuron dendrites and the extracellular matrix. C4da neurons express the Sema-2b receptor Plexin B, which can interact with integrins and is linked to the downstream TORC2 complex and Trc/Fry signaling pathway (Meltzer et al., 2016).

Wnts

Secreted Wnt proteins and their receptors regulate fundamental patterning processes in early development. Thus, Wnts are described as morphogens that can act over short- or long distances (Neumann and Cohen, 1997).

Their expression is tightly controlled and regulates broad functions from cell polarity, embryonic patterning, neuronal morphogenesis, axon guidance, dendrite development, synapse formation to neuronal plasticity (Ackley, 2014; Purro et al., 2014).

Wnt signaling can be subdivided into three different pathways (canonical or β-catenin pathway, planar cell polarity pathway and calcium pathway), all of which are intracellularly transduced by the scaffold protein Dishevelled (Dvl). Dysregulation of Wnt signaling is implicated in neurodegenerative diseases including Alzheimer's disease (De Ferrari and Inestrosa, 2000).

In *Drosophila*, Wnt5 and its receptor Derailed (Drl) are regulators of dendrite morphogenesis. Drl is a member of the RYK subfamily of atypical receptor tyrosine kinases (RTK) and is expressed in different levels along PN dendrites. The secreted Wnt5 molecule acts as an extrinsic repulsive cue for dendrites of PNs. The spatially limited expression pattern allows an appropriate extension of PN dendrites to their final positions (Lahaye et al., 2012).

In addition, Drl is involved in controlling axon routing across the midline by acting as a guidance receptor. In *Drosophila*, axons cross the midline in one of two distinct tracts, the anterior or posterior commissure (AC or PC). In *wild type*, Drl is expressed by neurons that project in the AC. Bonkowsky and Thomas showed that loss of *Drl* results in an abnormal projection pattern of those neurons into the PC (Bonkowsky and Thomas, 1999). Conversely, misexpression of Drl in PC neurons results in crossing into the AC. In this system, Yoshikawa et al. identified Wnt5 as the ligand of Drl. Loss-of-function mutations in *wnt5* exhibit Drl-like mutant phenotypes and they showed that Wnt5 is expressed by midline cells. Thus, Wnt5 together with Drl is required for proper projection of AC axons across the midline of the CNS (Yoshikawa et al., 2003).

In mice, secreted Wnt7b is implicated in dendrite growth in cultured hippocampal neurons. Rosso et al. identified that Wnt7b and Dvl regulate dendrite branching by activating the GTPase Rac (Rho family) and the downstream signaling partner protein kinase JNK (c-Jun N-terminal kinase) (Rosso et al., 2005).

TGFβ

Besides those previously mentioned factors, the development of a multicellular organism is also strongly regulated by ligands belonging to the family of transforming growth factors (TGFβ). Like Wnts, these polypeptides are classified as morphogens and are secreted by different cell types. TGFβ ligands form gradients and act in a dose-dependent manner to control many aspects of cellular functions, such as growth, migration, adhesion, differentiation, polarity and also apoptosis. Not surprisingly, due to their broad spectrum of cellular functions, deregulation of TGFβs results in severe diseases, including cancer or wound-healing disorders (Massagué, 2000).

In mammals, the TGFβ ligand family comprises ~ 30 genes, whereas in *Drosophila* seven members are known (Schmierer and Hill, 2007). Before secretion, the polypeptides are translated as preproproteins in a dimeric form. The prodomain is needed for dimerization. Afterwards, the prodomain is cleaved by proteases and the active ligand is directly secreted by the cell (Constam and Robertson, 1999).

In mammals, ligands of TGFβ superfamily include Bone Morphogenetic Proteins (BMP), Transforming Growth Factors beta (TGFβ), Growth and Differentiation Factors (GDF), Activin, Anti-Müllerian Hormone (AMH) and Nodal. Their signal transduction is highly conserved and occurs through the binding of the ligand to its cognate transmembrane receptor. These receptors are single transmembrane proteins, comprise a conserved intracellular serine-threonine kinase domain and can be subdivided into two classes, namely type I and type II. The activated ligand-receptor complex is formed by binding of the ligand to a type II receptor which recruits a type I receptor-ligand complex. The formation of a heterotetramer induces intracellular serine and threonine phosphorylation by the type II receptor kinase, which is thought to be constitutively active. Within the intracellular compartment, binding activates the recruitment and signaling of different SMAD proteins which transduce the outside signal into the nucleus to directly regulate gene expression (Shi and Massagué, 2003).

In *Drosophila*, the accurate gradient formation of the TGFβ ligand decapentaplegic (dpp) is very important to establish the dorso-ventral polarization in the developing embryo. Studies in *Drosophila* embryos showed that dpp is enriched throughout the dorsal side of the embryo and that dpp levels influence the ectoderm cell fate (Ferguson and Anderson, 1992). The ubiquitous expression of the related TGFβ morphogen Screw (Scw) and the subsequent

formation of a gradient sharpens the dorso-ventral axis and thus organizes defined embryonic patterning (Arora et al., 1994).

Besides its function in polarization, TGF signaling has been shown to function in regulating dendritic morphogenesis. Using the *Drosophila* medulla as a model system, which exhibits similarities to the mammalian visual cortex, Ting et al. demonstrated that afferent-derived TGFβ Activin regulates the dendritic field size of their postsynaptic partners to ensure proper synaptic connectivity. The medulla is organized in layers and columns and innervated by medulla neuron dendrites and photoreceptor axons. Thus, all visual input is received by the medulla layers either layer specific or broadly in different layers depending on the photoreceptor axonal projections. They investigated the direction of dendrites of medulla neurons (Tm) in 3D and identified that dActivin signaling derived from photoreceptors (R7 and R8) selectively restricts dendritic arborization and size on their respective postsynaptic targets (projection neuron Tm20 and the wide-field amacrine neuron Dm8). The loss-of-function of canonical Activin signaling in Tm20 neurons resulted in enlarged dendritic field size and unspecific synaptic connections with neighboring photoreceptors. Screening analysis focused on Tm20 dendritic morphological phenotypes identified the type I TGFβ receptor babo as being required for this canonical Activin signaling pathway in both cell culture and in photoreceptors (Ting et al., 2014).

TGFβ ligand maverick

In *Drosophila*, the TGFβ family members include three proteins with homology to vertebrate bone morphogenetic proteins (BMPs): decapentaplegic (dpp), screw (scw), and glass bottom boat-60A (gbb). All of these genes are highly important for body axes patterning, the regulation of cell proliferation and cell fate (Raftery and Sutherland, 1999). The TGFβ members myoglianin (myo), dActivin (dAct) and dActivin-like ligand dawdle (daw) exhibit protein similarity related to the TGFβ/dActivins.

The gene *Maverick* (*mav*) was identified by Nguyen et al. and encodes a new member of the TGFβ superfamily, a large group of soluble extracellular proteins that are potent regulators of development in both vertebrates and invertebrates. Mav is located on the fourth chromosome in *Drosophila*, which only comprises 2% of the whole *Drosophila* genome, more precisely within the cytogenetic region 102C. This gene was identified by a BLAST search of the Berkeley Drosophila Genome Project (BDGP) EST database by checking for sequences similarly to the carboxyl-terminal ligand domain of screw (scw), a member of TGFβ ligands. The identified gene encodes a 378 amino acid peptide and at least two alternatively spliced transcripts (Nguyen et al., 2000). The longest mav isoform (Mav1) encodes a putative protein of 701 amino acids in length. In this isoform the first Methionine for starting translation is followed by a stretch of hydrophobic amino acids indicating a signal sequence. The shorter isoform (Mav2) encodes a predicted protein of 433 amino acids. Since the protein lacks a signal sequence it indicates that this isoform might not be secreted. In Mav1 the consensus

sequence for proteolytic cleavage site (RKDK) is located at residues 586-89 and would generate a mature ligand of 112 amino acids (Massagué, 1998). Based on situ hybridization and RT-PCR analysis, mav is expressed throughout embryonic and larval stages and persists until adulthood. More detailed analysis of the spatial distribution of the transcript during development revealed that mav mRNA is ubiquitously distributed throughout the embryo at stage of early syncytial blastoderm and post-cellular blastoderm embryos (stages 1-5). During gastrulation and germ band elongation (stages 6±8 and stages 9±11, respectively), mav is located throughout the embryo at low levels and shows a dynamic expression pattern in germ layers forming the gut. Here, mav mRNA is observed in the endoderm (stage 9-10), in the hindgut and posterior midgut (stage 10). Besides gut expression, mav transcript is also present in distinct segmental patches of cells likely belonging to the dorso-lateral epidermal region.

In terms of mav function, so far studies showed that mav is implicated in fine modulation of synapse formation and growth. The development of pre- and postsynaptic synapse compartments at the neuromuscular junction (NMJ) is highly coordinated and studies have shown that a muscle-secreted retrograde signal, the TGFβ gbb is crucial for this function. However, the interaction of neurons and glia during synapse formation *in vivo* is largely unknown. Recently, Fuentes-Medel et al. (2012) uncovered that mav is secreted by NMJ glia and likely activates the muscle dActivin-type receptor punt. The loss of mav specifically in glia leads to a reduction of mad phosphorylation at the NMJs, a decrease of gbb mRNA in the muscle and a reduction in gbb-dependent retrograde signaling from muscle to motor neurons. With respect to their observation, they propose the model that the secretion of mav by glia controls gbb release by muscles and as a consequence fine tunes the formation of new synaptic boutons and general synapse growth *in vivo*. With this study a novel glial-derived factor has been identified as being important for neuron-glia interaction in synapse formation (Fuentes-Medel et al., 2012).

6.3.2 Adhesion: Cellular and extracellular matrix interaction mediated by integrins

A fundamental mechanism for the appropriate development of a multicellular organism is the interaction between cells, and cells and the extracellular matrix (ECM). The ECM mainly consists of a highly dynamic mass of insoluble proteins that has multiple roles during development (Rozario and DeSimone, 2010). Cell-ECM interaction includes cell fusion, migration and epidermal attachment. As a consequence, adhesion mechanisms of different tissues are highly important and involved at various developmental stages (Figure 4).

Tissue formation is mainly mediated by the expression of cell-surface transmembrane proteins. Primarily it is mediated by the integrin family of cell surface receptors (Murooka and Mempel, 2012). Cells expressing integrin receptors are able to anchor the basal ECM which

consequently provides a common adhesive substrate with cellular ensembles being connected via the ECM.

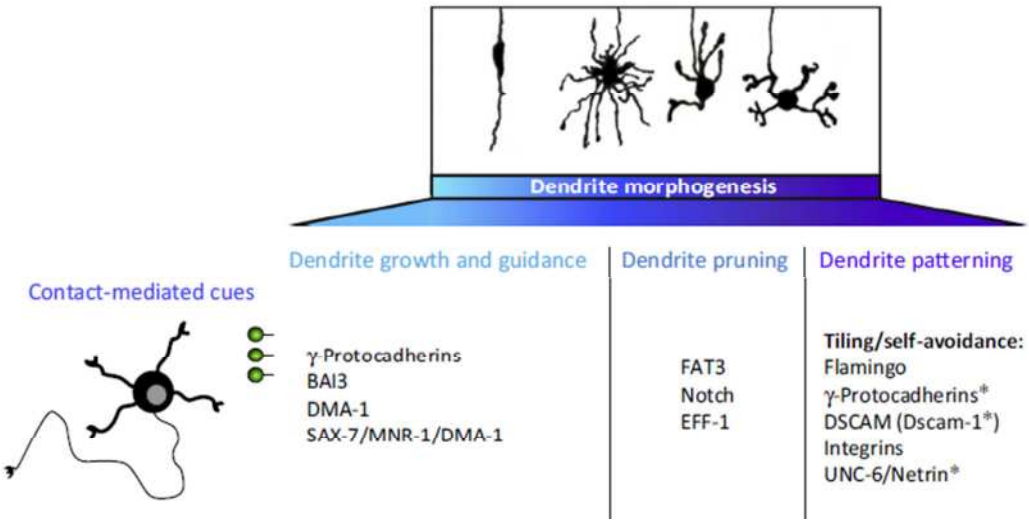

Figure 4. Cell-extrinsic regulators of dendrite morphogenesis. Several molecules mediate dendrite development by direct contact. *Molecules regulating isoneural repulsion of dendrites (modified from Valnegri et al., 2015).

Integrins are glycoproteins and function as heterodimeric transmembrane receptors. They consist of an α and β subunit and bind ECM components with their extracellular domains. The ectodomain of these transmembrane proteins exhibits a RGD-recognition and -binding domain for fibronectin in fibroblasts. Besides that, intercellular adhesion molecules (ICAMs) displaying no RGD-domain, like collagens and laminin, are able to bind to integrins as well. Furthermore, the short C-terminal domain of integrins can act as an adaptor for intracellular proteins, the integrin-associated proteins (IAPs). This provides a connection between the ECM and the actin cytoskeleton and consequently a link to different intracellular downstream signal cascades (Campbell and Humphries, 2011; Zaidel-Bar et al., 2007).

In *Drosophila*, five α subunits (αPS1 to 5) and two β subunits (βPS and βv) are tissue-dependently expressed. The integrin βPS is broadly expressed, whereas βv shows a more tissue-specific expression pattern (Yee and Hynes, 1993; Hynes and Zhao, 2000). Further, different heteromeric pairing provides functional diversity as integrins PS1 and PS2 bind ligands with high specificity. It has been shown that heterodimers of αPS1 and βPS bind Laminin (a collagen-like glycoprotein and major component of the basal lamina), while αPS2 and βPS bind to extracellular matrix molecules containing RGD sites, such as the ECM protein tiggrin (Brown, 2000).

Furthermore, heterodimers of integrins are expressed in an opposite manner displaying an additional strategy of development control. In *Drosophila*, a well characterized example for integrin function being required for interactions between epithelial cells is the wing blister phenotype. The wing blade of the adult fly is made up of two layers of epidermal cells, and

integrins mediate the adhesion between the basal surfaces of these two cell layers, in which the two integrins PS1 and PS2 have complementary expression patterns. PS1 is expressed on the dorsal side and PS2 on the ventral side and each integrin is required primarily on the side where it is highly expressed. One explanation might be that it helps the two surfaces to attach only to the opposing surface, thus avoiding wrinkles caused by adhesion within the same surface (Brabant and Brower, 1993).

Besides that, loss of integrin function in *Drosophila* has been observed to disrupt axon outgrowth and neuromuscular junction growth and function (Hoang and Chiba, 1998; Beumer et al., 1999). Moreover, integrin heterodimers have an essential function in midgut cell migration and differentiation in *Drosophila* embryos (Brower et al., 1995; Devenport and Brown, 2004).

In *Drosophila,* integrin-ECM adhesion is further essential for body wall muscles to translate the force of muscle contraction into movement of the exoskeleton. The proper interaction is required for both to organize the actin-myosin contractile structure into sarcomeres and to keep the muscles in the right place (Bloor and Brown, 1998).

In addition to integrins, other receptors such as cadherins or the immunoglobulin superfamily cell adhesion molecules (CAMs) work alongside to mediate cell–cell and cell–matrix communication (Halbleib and Nelson, 2006; Matsubara et al., 2011). Even further, tension and viscosity of the cytoplasm and membrane of the cell can have an influence on adhesion as well (Lecuit and Sonnenberg, 2011). Taken together, all of these factors play a critical role in the construction and maintenance of tissues during dendrite development. This is mainly achieved by repulsive interactions of spatial expression of these cell surface proteins between isoneuronal and heteroneuronal dendritic branches and plays an essential role in self-avoidance and tiling mechanism (Emoto et al., 2004; Grueber et al., 2002). These mechanisms and the involved known factors will be introduced in the following chapter.

6.3.3 Self-avoidance and tilling as mechanisms for proper dendrite development

Specification of dendritic patterning is entailed by secreted proteins, gradients of guidance cues, cell surface receptors or transcription factors. Dendrite morphogenesis is governed by both, autonomous and non-autonomous mechanisms, which rely on different molecular mechanisms conserved in vertebrates and invertebrates.

First, self-avoidance is a mechanism ensuring non-redundant coverage of dendrites by recognition and repulsion of isoneuronal dendrites. During development, this process is essential to prevent extensive overlap in the arborization pattern and to facilitate the coverage of the neuronal processes across different regions (Hattori et al., 2008). Cell adhesion molecules have been found to be involved in this process in both vertebrates and invertebrates. In *Drosophila*, Dscam (Down syndrome cell adhesion molecule) is essential for

self-avoidance of dendrites in da sensory neurons. Dscam belongs to the immunoglobulin (Ig) superfamily of cell adhesion molecules and through alternative splicing gives rise to up to 19,008 different extracellular domain isoforms. *In vitro* studies demonstrated that Dscam isoforms show homophilic interaction in an isoform-specific manner (Schmucker et al., 2000; Wojtowicz et al., 2007, 2004).
The expression of unique isoforms on the neuronal cell surface of the same neuron leads to specific homophilic recognition and repulsion, resulting in self-avoidance of isoneuronal processes. Several studies reported that Dscam controls cell-autonomous dendrite self-avoidance in all da sensory neuron classes and its loss-of-function in single neurons causes a strong increase in self-crossing (Hughes et al., 2007; Matthews et al., 2007; Soba et al., 2007). Studies of DSCAM and DSCAML1 in mice could demonstrate its role in promoting neurite self-avoidance as well as tiling of retinal cells, which is similar to the function of *Drosophila* Dscam in sensory neurons (Fuerst et al., 2009, 2008). In cultured dissociated cortical neurons, Zhang et al. could show that downregulating DSCAM or DSCAML1 increases the complexity of proximal dendritic branching and delays axon growth. Thus, both genes play an important role in the development of cortical neural network during the postnatal development (Zhang et al., 2015).

The second mechanism is tiling, in which dendrites of functionally uniform neurons avoid dendrites of neighboring neurons of the same type to maximize their surface coverage. In vertebrates, tiling has been analyzed in alpha ganglion cells of the mammalian retina (Wassle et al., 1981). Two functionally distinct subpopulations of ganglion cells, ON- and OFF-center, have been identified. Their cell bodies are organized in an independent mosaic and the dendrites completely cover the surface of the retina with minimal dendrite overlap in order to achieve high effectiveness and economic savings (Breuer et al., 2005).
In *Drosophila*, C3da and C4da neurons are examples for this mechanism. Both exhibit high but non-overlapping receptive field coverage of the larval body wall. In terms of the underlying signaling pathway, Tricornered (trc, NDR family kinase) and Furry (fry) have been identified to mediate tiling of C4da sensory neurons. The loss-of-function of these conserved genes resulted in overbranching of da neuron dendrites and in strong overlap of C4da neuron dendritic fields demonstrating its regulation of homotypic repulsion (Emoto et al., 2004).
Koike-Kumagai et al. reported that Sin1, Rictor, and target of rapamycin (TOR) are required for dendritic tiling of C4da neurons and mutants of *sin1* and *rictor* show abnormal dendritic overlap of the receptive fields. Both proteins are reported to physically and genetically interact with trc indicating a shared role in regulating dendritic tiling (Koike-Kumagai et al., 2009). Additionally, the GTPase Rac has been identified to regulate controlling dendritic branching via trc. There is further evidence for a role of the Hippo (hpo) kinase, an upstream regulator of Trc, in dendrite maintenance and tiling as well. In summary, the trc/fry signaling

pathway is essential for the patterning of da neuron dendritic fields (Emoto et al., 2006, 2004).

Consequently, self-avoidance and tiling together ensure even spreading of dendrites to acquire appropriate receptive fields. Concerning *Drosophila* C4da neurons, these neurons tile the larval body wall and their dendrites grow in a 2D space between the ECM and the epidermis. Tiling and self-avoidance defects result in dendrite crossing due to a lack of branch recognition or repulsion. However, studies by Kim et al. (2012) and Han et al. (2012) could show that the relationship between dendrites and substrates in da sensory neurons has an impact on dendritic morphogenesis. They could show that integrins mediated adhesion is cell-autonomously required for dendritic self-avoidance by acting as a physical linker between the ECM and the cytoskeleton and thus promoting positioning of dendrites on the basal epidermal surface. The elimination of integrins resulted in dendritic overlap by non-contacting crossing and dendritic growth into the epidermis. The same phenotype of dendritic crossing is observed by blocking the production of laminin. Besides integrins, tiling mutants (*trc*, *fry*) fail to keep dendrites in a 2D plane and show impaired dendrite attachment to the ECM as well. Interestingly, integrin overexpression in these mutants rescued dendritic crossing defects and restored tiling demonstrating that the observed tiling defects in these mutants are not mediated by lack of repulsive signals (Han et al., 2012).

These studies uncovered that the interaction of integrins and laminin is crucial for dendrite-ECM attachment. Further, it shows the importance of integrins restricting dendrite self-crossing by regulating dendrite-ECM attachment and thus the capability of isoneuronal and heteroneuronal dendritic repulsion. Therefore, integrin-mediated mechanisms allow the appropriate positioning and spacing of sensory dendrites covering their sensory fields (Han et al., 2012; M. E. Kim et al., 2012).

6.3.4 Intrinsic factors

Besides extrinsic cues, cell type specific dendrite development and morphology is also controlled by intrinsic factors. Several studies have identified different transcription factors that are involved in cell identity mechanisms. Distinct dendrite morphology can be achieved by specific transcription factor expression in a single type of neuron, by varying the levels of single transcription factors and by combining mechanisms involving many transcription factors.

In terms of the dendritic arborization neurons in *Drosophila* PNS, the different classes exhibit differential expression or combinations of specific transcription factors to determine the neuronal type-specific dendritic pattern.

For instance, the transcription factor and BTB-zinc finger protein Abrupt is expressed in only C1da neurons and loss-of-function results in increased arbor complexity, whereas ectopic overexpression of *abrupt* in other da neurons leads to simplified dendritic trees (Li et al.,

2004). The transcription factor Collier/Olfactory-1/early B cell factor Knot is specifically expressed in C4da neurons and is required for their complex branching pattern. The misexpression of this transcription factor in other da neurons results in the transformation of simpler into more complex dendritic arbors, indicating that Collier/Knot is sufficient to initiate dendrite complexity. Collier is also required for the C4da-specific expression of Degenerin/Epithelial sodium channel subunit pickpocket (ppk), which is required for larval locomotion (Crozatier and Vincent, 2008) and mechano-nociception. A third example is the homeodomain-containing transcription factor Cut. This transcription factor is expressed in a complementary pattern in C2da-C4da neurons and shows intermediate expression levels in C2da and C4da and high levels in C3da. Thus, the expression levels do not correlate with dendrite complexity, but loss-of-function leads to lower dendrite complexity, while misexpression promotes dendrite complexity in lower branched da neurons (Blochlinger et al., 1990; Grueber et al., 2003). Co-expression of Collier and Cut ensures correct dendritic pattering of C4da neurons without spike formation. In contrast, C3da neurons express high levels of Cut but not Collier (Jinushi-Nakao et al., 2007). This combination favors dendritic spike formation in C3da neurons and is an example of combinatorial transcription factor expression to achieve neuronal type-specific dendritic morphology. Altogether, transcription factors are required for distinct programs to control morphological and sensory specificity of *Drosophila* da neurons.

6.4 The Receptor tyrosine kinase Ret and its developmental functions

6.4.1 Discovery, protein structure and biogenesis from the nucleus to the cell surface

The receptor tyrosine kinase (RTK) Ret is required for normal development, maturation and maintenance of different types of tissues and cell types. Takahashi et al. identified *Ret* as a novel oncogene, which was reported as a gene re-arrangement with transforming activity in human lymphoma transfected NIH3T3 cells (Takahashi et al., 1985). The novel gene resulted from a recombination of two unrelated DNA sequences and encodes a chimeric fusion protein with a dimerizing motif at the N-terminus and a tyrosine kinase domain. Consequently, the gene *Ret* ("rearranged during transfection") was classified as a receptor tyrosine kinase.

Ret encodes a transmembrane protein and is composed of four conserved domains: an extracellular domain with cadherin-like repeats and a cysteine-rich region, a hydrophobic transmembrane domain and an intracellular tyrosine kinase domain (Figure 5).

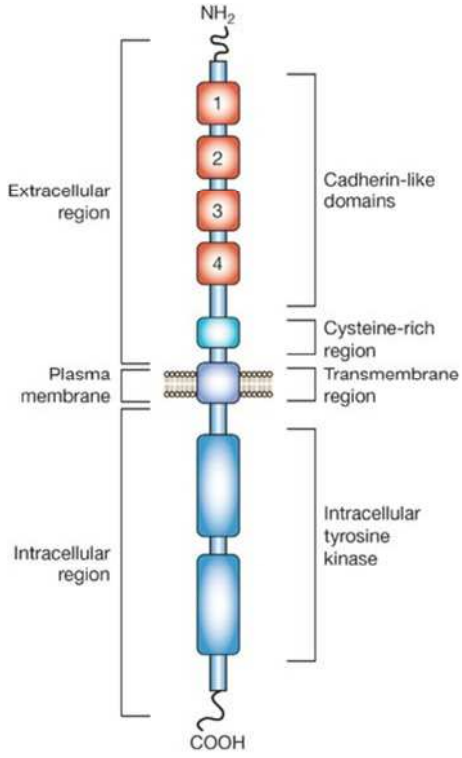

Figure 5. Structure of the receptor tyrosine kinase RET in vertebrates (Drosten and Pützer, 2006). The RET receptor is a transmembrane protein and contains four cadherin-like domains and a cysteine-rich region extracellularly as well as a tyrosine kinase domain in the intracellular region in vertebrates.

In mammals, the extracellular domain includes four cadherin-like repeats, which are crucial for stabilizing Ret dimers. The membrane-proximal cysteine-rich domain is important for

ligand binding and conformation of the protein (Amoresano et al., 2005; Anders et al., 2001; Wang, 2013). Ret is glycosylated in the endoplasmic reticulum (ER) and further processed in the Golgi network. The immature nascent protein displays a mass of 155 kDa, and after posttranslational modification it is described to have an approximate mass of 175 kDa when it is finally localized at the plasma membrane (Richardson et al., 2012). Three different isoforms of mammalian Ret are generated by alternative splicing of 3' exons. Those isoforms differ in their C-Terminus and are named RET9, RET43 and Ret51 (Myers et al., 1995).

6.4.2 Ret signaling

In the mammalian system, the signaling receptor Ret is part of a complex that binds extracellular proteins belonging to the glial cell line-derived neurotrophic factor (GDNF) family ligands (GFLs). Ret-GFL interaction requires a ligand-binding subunit acting as a co-receptor known as the GDNF family receptor α (GFRα) (Durbec et al., 1996, Trupp et al., 1996). Biochemical analysis of GDNF and RET indicates direct contact between both molecules although the binding affinity is too low to stabilize this complex showing that RET is unable to bind GDNF on its own. Instead, GDNF displays high affinity for GFRα1 independently of RET. The GFRα1 co-receptor is tethered to the cell surface by a GPI–(glycosylphosphatidylinositol) anchor (Vieira et al., 2003). Based on these results, a model was proposed that GDNF first forms a high-affinity complex with GFRα1. This complex, containing GDNF and GFRα1 homodimers, recruits two RET molecules resulting in dimerization and intracellular signal transduction (Airaksinen et al., 1999). However, GDNF mutants deficient in GFRα1 binding still exhibit the ability to activate RET, indicating an alternative model where RET is to some extend weakly associated with GFRα1 before GDNF binding (Eketjäll et al., 1999).

After ligand binding to the extracellular portion of the receptor and complex formation, signal transduction by the GDNF/GFRα1/RET tripartite complex activates several second messenger pathways by inducing RET autophosphorylation of intracellular tyrosine residues. Once stimulated, distinct protein complexes carrying specific binding domains assemble on phosphorylated tyrosine residues, which consequently activate different downstream signaling pathways (Figure 6).

The intracellular domain of Ret displays multiple docking sites for effector proteins, including Shc (Src homology 2 domain containing protein), Grb2 (Growth factor receptor-bound protein 2), Src kinase or PLCγ (phospholipase C-γ) (Jain et al., 2006; Manié et al., 2001). These signaling pathways activate the Ras/RAF pathway, which leads to activation of the mitogen-activated protein kinases ERK1 and ERK2 (Worby et al., 1996), phosphatidylinositol 3-kinase (PI3K) resulting in activation of the serine/threonine kinase Akt and cell survival (Segouffin-Cariou and Billaud, 2000), Jun NH2-terminal protein kinase (JNK) (Chiariello et al., 1998), p38MAPK (Gire, 2004), and PLCγ (Jain et al., 2006). So far, extensive studies have

identified some of the tyrosine residues present in the intracellular region of RET that can be phosphorylated. The tyrosine residues Tyr900 and Tyr905 within the kinase domain were shown to be essential for full kinase activation. Further, the phosphorylation of the Tyr1062 and Tyr1096 residues is required for activation of Ras/MAP kinase and PI3 kinase/AKT (Besset et al., 2000; Jain et al., 2006).

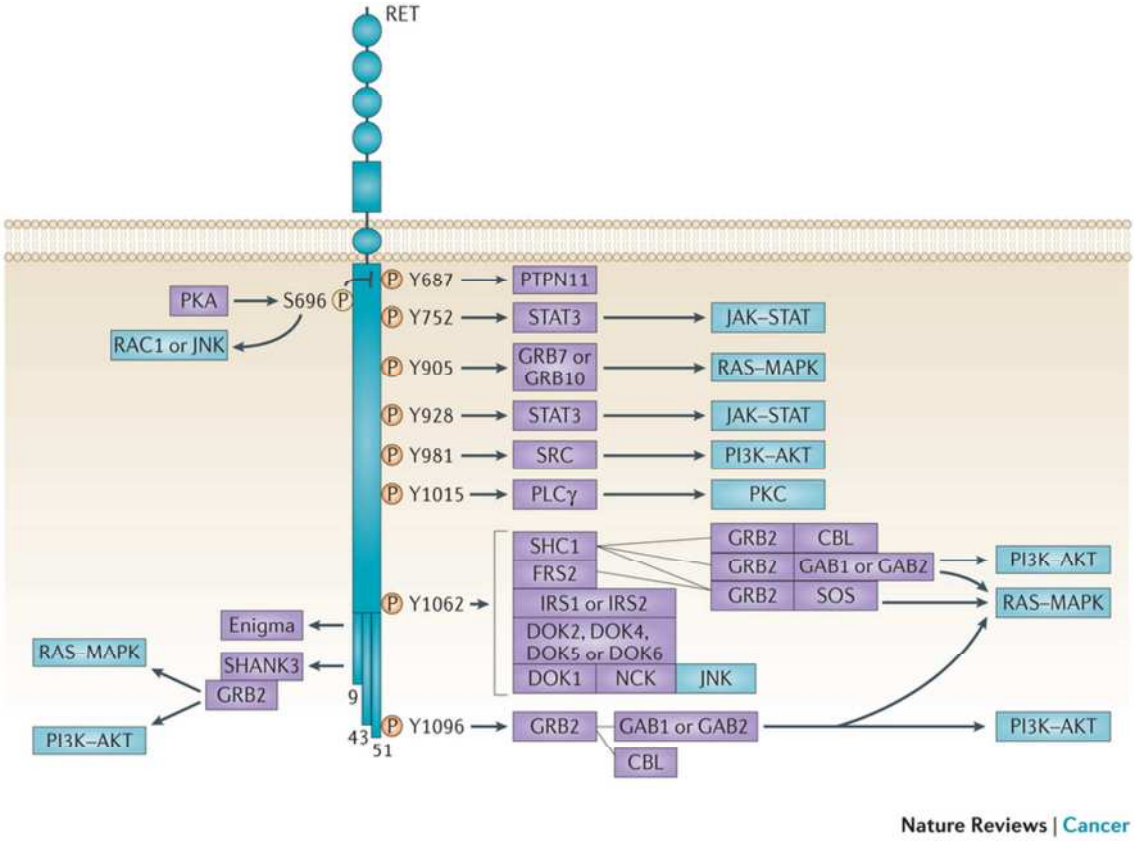

Figure 6. Signaling pathway of RET receptor tyrosine kinase in vertebrates (Mulligan, 2014). In vertebrates, RET has three protein isoforms, which differ in their carboxy-terminal amino acids. Upon activation, RET becomes phosphorylated (P) on multiple intracellular tyrosine residues. These facilitate direct interactions with signaling molecules, which lead to the activation of multiple downstream signaling pathways to promote cell growth, proliferation, survival or differentiation.

Besides GDNF, three highly related proteins belonging to the GDNF family of ligands (GFLs) have been identified as ligands of RET. The GDNF paralogues are known as Neurturin, Artemin and Persephin and each of these GFLs displays high-affinity to additional co-receptors belonging to the GFRα family (GFRα2-4, respectively) (Zihlmann et al., 2005).

It should be noted that Ret receptor is described to function together with additional cell surface proteins, receptor tyrosine kinases and cell adhesion molecules, namely Met, integrins, Ephrin and protocadherins (Ruco et al., 2001, Soba et al., 2015, Bonanomi et al., 2012, Schalm et al., 2010).

6.4.3 Functions of Ret in nervous system and organ development

During development the expression of Ret is described to have its highest level at early embryonic stages.
In vertebrates, Ret plays an essential role in the development of the ureter and kidneys. In these organs, Ret is implicated in the onset of growth and morphological formation of the ureteric bud during development and the lack of Ret results in cells being excluded from the tips of the branching ureteric bud (Chi et al., 2009). Furthermore, Ret is essential for proper regulation of motor neuron axon guidance. Kramer et al. described that Ret and GDNF function together as guidance cues to instruct lateral motor neuron axon growth to into the dorsal limb (Kramer et al., 2006). In addition, Ret function is implicated in the maintenance of dopaminergic neurons (Kowsky et al., 2007; Kramer et al., 2007). Ret also has a developmental role in intrinsic ganglia innervation of the smooth muscle layers of the gastro-intestinal tract (Romeo et al., 1994; Schuchardt et al., 1994). Ret expression is further detected in neuroendocrine-derived cells of different organs (e.g. thyroid C cells). During early development Ret is expressed in neural crest cells as well. These cells are responsible for the migration of neuroblasts to their targets within the enteric nervous system (Durbec et al., 1996). Interestingly, there is evidence that Ret contributes to the development and maintenance of the immune system modulating the response of immune cells during inflammation (Rusmini et al., 2014).

Due to Ret's high impact during early development, mutations in the *Ret* locus have been found in a number of human diseases and many different substitutions and rearrangements in the *Ret* gene underlie these syndromes. These mutations are subdivided into two groups, affecting either the extracellular domain or the intracellular tyrosine kinase domain of Ret.
The malfunction of Ret includes several different cancer types of neuroendocrine origin and an intestinal gut syndrome known as Hirschsprung´s disease. In humans, four different cancer types carry mutations in the *Ret* gene, including papillary thyroid carcinoma (PTC), medullary thyroid carcinoma (MTC) and the multiple endocrine neoplasias type 2 (MEN 2) (Donis-Keller et al., 1993; Grieco et al., 1990; Hofstra et al., 1994).
In human cancer, somatic chromosomal rearrangements involving the *Ret* gene represent the most frequent genetic alteration in PTC, which is the most common thyroid malignancy. Those follicular-cell-derived tumors are the most prevalent malignancies of the endocrine system. The rearrangements lead to the fusion of the tyrosine kinase domain with the 5'-terminal regions of the heterologous gene. These fusions of Ret and different activation genes result in ligand-independent dimerization and constitutive activation of the chimeric oncogenes.
MTC is a malignant tumor arising from calcitonin-secreting parafollicular C cells. This tumor form occurs sporadically in 75% or as a component of the MEN 2 syndrome in 25% of patients. MEN 2 is an inherited cancer syndrome resulting in carcinomas of thyroid C cells,

as well as occasional pheochromocytomas of adrenal glands and neuromas of the enteric neurons. MEN 2 is divided into three different variants: MEN 2A, 2B and familial medullary thyroid carcinoma (FMTC). The phenotypes of MEN 2 variants are depending on the strength of the MTC phenotype. Within these different forms MEN 2B is the most aggressive and distinctive subtype. It is characterized by an early onset of MTC and associated with developmental defects including intestinal ganglioneuromatosis, ocular and skeletal abnormalities. FMTC is described as the least aggressive form of MEN 2 variants. Mutations of this variant are similar to those causing MEN 2A, but the frequency of affected cysteine residues are more homogeneously distributed.

The mechanism of *Ret* in MEN 2 as a dominant activation gene has been studied in different model systems. In MEN 2 tumors and Hirschsprung´s disease, affected cells are derived from the neural crest and diffusely migrate during embryogenesis (Hahn and Bishop, 2001). Studies in fibroblasts and transgenic animals could show that germline point mutations of Ret are the major component for all types of MEN 2 carcinomas. Gain-of-function mutations of *Ret* are associated with MEN 2, arising as a result of kinase activating mutations in the *Ret* gene. In MEN 2A patients, the phenotypes are caused by substitution of cysteine residues in the extracellular domain (affecting Codon 609, 611, 618, 620 in exon 10, and codon 630 or 634 in exon 11). Studies showed that most MEN 2A patients carry a mutation of Cys634. MEN 2B is caused by the highly specific substitution of codon 883 (<5%) or 918 (95%). All these point mutations show “gain-of-function” effects of *Ret*.

Conversely, loss-of-function mutations of human *Ret* have been implicated in Hirschsprung´s disease. This developmental disorder is characterized by the partial absence of enteric neurons in the gut (Romeo et al., 1994). The different mutations invariably result in targeting its kinase activity, docking sites of signaling partners, or affect residues in the extracellular domain of Ret which disturb the processing within the endoplasmatic reticulum (ER) and prevent the recruitment of Ret to the cell surface (Pelet et al., 1998; Kjær and Ibáñez, 2003).

In mice, targeted *Ret* disruption results in perinatal lethality. In human patients, the null mutation of *Ret* is homozygous lethal. The number of allelic Ret mutations implies that Ret is a fundamental component required for normal morphogenesis. This is suggested by the observation that accidental dysfunction of Ret signaling can subsequently convert it to tumor outgrowth (Romeo et al., 1994).

In addition, Ret function is potentially associated with Parkinson´s disease (PD). In mice, loss-of-Ret leads to a reduced number of midbrain neurons and degeneration of nerve terminals within parts of the dopaminergic system. These defects were identified in 2 year old animals suggesting Ret as a mediator of long-term maintenance of neurons within the dopaminergic system (Kramer et al., 2007).

Comparison of *Drosophila* Ret and mammalian RET revealed high sequence identity (Hahn and Bishop, 2001). Ret comprises homologous elements within its protein structure and

displays a similar expression pattern suggesting similar functions in vertebrates and invertebrates (Hahn and Bishop, 2001). Consistently, Gal4 lines driven by fragments of the Ret promoter indicated Ret expression in a subset of migrating neural stomatogastric nervous system (SNS) precursors and also in a distinct set of midgut associated cells (Hernández et al., 2015). In vertebrates, the RET receptor tyrosine kinase is implicated in the migration of enteric neuron precursors and mutations are a key cause of Hirschsprung's disease, in which the colon and rectum have severely decreased innervation suggesting a shared evolutionary origin of Ret.

Little is known about Ret function in *Drosophila* so far. Recently, it has been shown that Ret is implicated in the regulation of dendrite patterning, adhesion and stability of C4da neurons in the PNS (Soba et al., 2015). Here, loss of Ret resulted in severe dendritic patterning defects. Soba et al. showed that Ret is physically interacting with integrins to mediate C4da dendrite-ECM adhesion, which is required for dendrite adhesion and 2D growth of C4da neuron dendrites during dendrite development.

In mammals, Ret signaling is mediated by binding of its cognate ligand GDNF and the co-receptor GFRα. However, a homologous GDNF ligand has not been found in the *Drosophila* genome (Anders et al., 2001). Moreover, Kallijärvi et al. provided evidence that in *Drosophila*, Ret and the GFRα homolog GFR-like do not function together, since expression patterns in the central and peripheral nervous systems were largely non-overlapping throughout development (Kallijärvi et al., 2012). Therefore, the required extracellular and intracellular mediators of Ret signaling in dendrite development are so far largely unknown.

7 OBJECTIVES OF THE DISSERTATION

The receptor tyrosine kinase (RTK) Ret is required for normal development, maturation and maintenance of different types of tissues and cell types and is conserved in the nervous system of mammals and *Drosophila* (Hahn and Bishop, 2001; Schuchardt et al., 1994). In vertebrates, Ret functions in maintenance of dopaminergic neurons, guidance of motor neuron axons and differentiation of subsets of mechanosensory neurons. Here, Ret receptor activation is mediated by a complex of glial cell line-derived neurotrophic factor (GDNF) and GDNF family receptor α-1 (GFR α-1).
In *Drosophila*, the Ret receptor was recently identified in an *in vivo* RNAi screen as a novel regulator of dendrite development in *Drosophila* C4da neurons. Soba et al. (2015) showed that Ret is expressed in C4da neurons and its loss-of-function resulted in severe dendrite defects caused by the loss of extracellular matrix adhesion and impaired dendritic patterning.
However, the underlying mechanism of Ret signaling in dendrite development and the potential ligand and downstream signaling in this system are so far unknown.

In this thesis, the precise role of Ret in controlling dendrite development and Ret dependent signaling was addressed using newly generated knock-out alleles and morphological, functional and genome wide analyses:

1. **Ret structure-function analysis *in vivo***
   To gain information about the functional requirement and importance of different Ret extra- and intracellular domains in dendrite development, a structure-function analysis was performed. For this purpose, novel generated Ret domain deletion transgenes were used to analyze their capacity to rescue C4da neuron dendrite defects in *Ret* mutant animals.

2. **Screening of a potential ligand of Ret and its functional characterization in C4da neuron development and behavior**
   To identify potential ligand/s required for Ret signaling in C4da neurons, a candidate screen of members of the TGFβ family was performed to investigate their impact on C4da neuron morphology.
   The TGFβ ligand maverick could be identified as a potential interaction partner in Ret-mediated signalling in C4da development and a newly generated CRISPR/Cas9 mutant allele was further characterized.

3. **Insight into Ret downstream signaling in C4da dendrite development**

   Genome wide microarray analysis allowed the identification of genes implicated in Ret signaling in C4da neuron dendrite development. This analysis uncovered several genes with up- or downregulated transcript levels in Ret^{ko} C4da neurons compared to *controls*.

   One gene, RanBPM, exhibited a strong decrease of expression in Ret^{ko} C4da sensory neurons. RanBPM expression and function in C4da neuron development and the potential link to Ret signaling *in vivo* were analyzed.

4. **Impact of Ret function in C4da neuron dependent behavior**

   C4da neurons have polymodal functions (Guo *et al.*, 2014) and are essential for sensing nociceptive stimuli (e.g. temperature, painful touch, light) (Hwang et al., 2007; Robertson et al., 2013; Tsubouchi et al., 2012; Xiang et al., 2010).

   To test the functional impact of Ret loss-of-function, Ret^{ko} animals were assayed for functional defects in C4da neuron dependent locomotion, light avoidance and mechano-nociception.

8 MATERIALS

8.1 Chemicals and reagents

All chemicals and reagents used in this work are commercially available.

Table 1: Chemicals, reagents and kits

	Company
Agar-Agar, Kobe I (powdered)	Roth, Karlsruhe, Germany
Baysilone® silicon grease (medium viscous)	Bayer AG, Leverkusen, Germany
Deoxynucleotide (dNTP) Mix	Invitrogen, Darmstadt, Germany
Donkey serum	Dianova, Hamburg, Germany
Ethanol 99.9 % (technical grade)	Th. Geyer GmbH & Co. KG, Renningen, Germany
Formaldehyde solution 30 % (methanol-free)	Roth, Karlsruhe, Germany
Gene Ruler 1 kb Plus DNA	Fermentas, Thermo Fisher Scientific, Darmstadt, Germany
DreamTaq Green PCR 2x Master Mix	Thermo Fisher Scientific, Darmstadt, Germany
Orange DNA Loading Dye (6x)	Thermo Fisher Scientific, Darmstadt, Germany
PCR clean-up Gel extraction Kit, NucleoSpin® Extract II	Macherey-Nagel GmbH & Co. KG, Düren, Germany
Platinum® Pfx DNA Polymerase	Invitrogen, Darmstadt, Germany
Propionic acid	Roth, Karlsruhe, Germany
Proteinase K	Roche, Basel, Switzerland
Q5® High-Fidelity DNA Polymerase	New England BioLabs, Ipswich, USA
Q5® High-Fidelity 2x Master Mix	New England BioLabs, Ipswich, USA
QIAGEN Plasmid Mini Kit	QIAGEN, Hilden, Germany
Roti®-Safe GelStain	Roth, Karlsruhe, Germany
SlowFade® Antifade Kit (mounting medium)	life Technologies, Darmstadt, Germany
T4 DNA Ligase	Roche, Basel, Switzerland
T4 DNA Ligase 10x buffer	Roche, Basel, Switzerland
Triton x-100	Roth, Karlsruhe, Germany
Zero Blunt-II® TOPO® PCR Cloning Kit	life technologies, Darmstadt, Germany

For 1 L of 10 x PBS solution the following ingredients were dissolved in dH_2O:

Table 2: Ingredients for 1 L of 10 X PBS solution

Quantity	Ingredient	Company
14.4 g	di-Sodium hydrogen phosphate dihydrate (141.96 g/mol)	Roth, Karlsruhe, Germany
80 g	Sodium chloride (58.44 g/mol)	Roth, Karlsruhe, Germany
2.4 g	Potassium dihydrogen phosphate (136.09 g/mol)	Merck, Darmstadt, Germany
2 g	Potassium chloride (74.55 g/mol)	Roth, Karlsruhe, Germany

dissolved in 1 L dH_2O

For 1 L of 10 x TBS solution the following ingredients were dissolved in dH_2O:

Table 3: Ingredients for 1 L of 10 X TBS solution

Quantity	Ingredient	Company
60.6 g	Tris (121.14 g/mol)	Roth, Karlsruhe, Germany
87.6 g	Sodium chloride (58.44 g/mol)	Roth, Karlsruhe, Germany
1 M	Hydrochloric acid (HCl)	Roth, Karlsruhe, Germany

dissolved Tris and NaCl in 800 mL of deionized water, adjusted pH to 7.6 with 1 M HCl, added deionized water to 1 L

For 50 mL of Ringer Buffer the following ingredients were dissolved in dH_2O:

Table 4: Ingredients for 50 mL Ringer Buffer

Quantity	Ingredient	stock solution	Company
2 mL	Sodium chloride (58.44 g/mol)	3.25 M	Roth, Karlsruhe, Germany
2 mL	Potassium chloride (74.55 g/mol)	125 mM	Roth, Karlsruhe, Germany
500 µL	Magnesium chloride hexahydrate (203.3 g/mol)	200 mM	Roth, Karlsruhe, Germany
5 mL	Sucrose (342.3 g/mol)	360 mM	Roth, Karlsruhe, Germany
500 µL	HEPES (238.31 g/mol)	500 mM	Roth, Karlsruhe, Germany

add to 50 mL dH_2O

For 1 L of 10 x TAE solution the following ingredients were dissolved in dH_2O:

Table 5: Ingredients for 1 L of 10 X TAE solution

Quantity	Ingredient	Company
48.4 g	Tris (121.14 g/mol)	Roth, Karlsruhe, Germany
20 mL	EDTA (0.5 M)	Roth, Karlsruhe, Germany
11.44 mL	glacial acetic acid	Roth, Karlsruhe, Germany

dissolved Tris, EDTA and glacial acetic acid in 800 mL of deionized water, diluted the buffer to 1 L

8.2 Agar plates

For light avoidance trials and mechano-nociception assays 2 % agar plates were used. Kobe agar I was dissolved in dH_2O and petri dishes (Ø 10 cm) were filled with a defined volume of 12 mL.

8.3 Consumable supplies

Table 6: Consumable supplies

	Company
Cover slips (22 x 22 mm, 60 x 24 mm)	Roth, Karlsruhe, Germany
Drosophila vials (wide, K-Resin)	Genesee Scientific, San Diego, USA
Flugs® fly plugs, stock bottles	Genesee Scientific, San Diego, USA
Flugs® fly plugs, plastic vials (wide)	Genesee Scientific, San Diego, USA
Micro Slides (76 x 26 mm)	Glaswarenfabrik K. Hecht GmbH & Co KG, 'Assistent'
Omniflex monofilament fishing line Shakespeare (6 lb test, diameter 0.23 mm)	Zebco, Tulsa, USA
Petri dishes (Ø 10 cm; Ø 6 cm)	Sarstedt, Nümbrecht, Germany
Stock bottles 80z round bottom (polypropylene)	Genesee Scientific, San Diego, USA

8.4 Antibodies

Table 7: Primary and secondary antibodies

Primary antibody	**Host**	**Dilution**	**Company / Source**
Anti-Ret 70	guinea pig	1:1000	Dr. Miguel-Aliaga, MRC Clinical Sciences Centre, London, UK
Secondary antibody	**Host**	**Dilution**	**Company / Source**
Cy3 anti-guinea pig	Donkey	1:250	Jackson ImmunoResearch, Westgrove, PA
DyLight649 anti-HRP	Donkey	1:500	Jackson ImmunoResearch, Westgrove, PA

8.5 Primers

For sequencing of DNA, 10 pmol of a suited primer was used and pure water to a final volume of 8 µL was added. For PCR, 10 pmol of each primer was used and dH_2O to a final volume of 50 µL was added.

Table 8: Primer

Primer name	**Recognition sequence (5'-3')**	**Annealing (°C)**	**usage / vector**
as-3' (*mav*^{ko})$^{\#}$	GAACCAAATGAGAAACAAAAC		validation/sequencing
as-5' (*mav*^{ko})$^{\#}$	TTGACGTTTGGCGGAATATGC		validation/sequencing

Primer name	Recognition sequence (5'-3')	Annealing (°C)	usage / vector
M13 forward[+]	GTAAAACGACGGCCAG		sequencing
M13 reverse[+]	CAGGAAACAGCTATGAC		sequencing
mav 3' targeting (CRISPR/Cas9)	5'-NGG-3'-CCGTCCATGCTGTACTCCTTC		*mav*^{ko} generation
mav 5' targeting (CRISPR/Cas9)	5'-NGG-3'-GTTTTCTCCGCATGGCCATT		*mav*^{ko} generation
Ret-5´-2seq (as)	GAGAACTTCATGCCCCAAATTTTATGCCACAATA		validation/sequencing
Ret-5´-2seq (s)	GGCAAATGGGAATCTCGCAAAAGGC		validation/sequencing
Ret-del5´ (as)	TGGGAAAGTAAACATCGACGGCTGAAAA		*Ret*^{ko} generation
Ret-del5´ (s)	CTTTTTATTCATTTATTCCAGCTGTTTACATTTACCTTCA		*Ret*^{ko} generation
Ret-del5´-2 (as)	ACGAGGCAAAGTCCAATACAAGCGATAAATAAA		*Ret*^{ko} generation
Ret-del5´-2 (s)	TGAGCGAAAATTGCCGACTGATAACTGAC		*Ret*^{ko} generation
s-3' (*mav*^{ko})[#]	TTCACCAAATCATGCTGACCA		validation/sequencing
s-5' (*mav*^{ko})[#]	ATTTAACCTAATAAGTAATGG		validation/sequencing
s-Ret-1[#]	GTAGTTCCCATTTTGTTTTG		sequencing
s-Ret-2[#]	TACCGCAAGCTCTTCCCCTAC		sequencing
s-Ret-3[#]	ATCCTATGGCCTGTCCGCAG		sequencing
s-Ret-4[#]	GCTTGCCGGGAATAACCACG		sequencing
s-Ret-5[#]	GAATTTGTGGTCCTTGCTGA		sequencing
as-Ret-6[#]	CGTGGTTATTAAGGCGGAATC		sequencing
s-pUAST[#]	CAACTGCAACTACTGAAATC	59 55 55	*for sequencing,* *UAS-Ret-CLDΔ* *UAS-Ret-CRDΔ* *UAS-Ret-CTΔ*
asCLD-longseq (EcoRI)[#]	CTTAGAGCTACTCTCCTGGGATACATGAGGACACAG	59	*UAS-Ret-CLDΔ*
asCRD[#]	CAGATCTATGTACTTGGC	57	*UAS-Ret-NTΔ*
asCRD_del[#]	TGATCGAGACTTGACCTT	55	*UAS-Ret-CRDΔ*
sTMD/sTyrKD[#]	CGATCTCTAAGTCCTCCG	55	*UAS-Ret-TKΔ*
asTyrKD(BglII)[#]	CAGATCTATGTACTTGGCTTCCCTGGGAAACTCCCA	55	*UAS-Ret-TKΔ*
asCTdel(XbaI)[#]	TTTTTTTCTAGAAGTGCTATCCAGTCCAAGGAGTGGGTTAGGTATAGGTTTGCCTTGCGACGTTGGAGCATCTT	55	*UAS-Ret-CTΔ*
sNTdel[#]	TTTTTTCGGCCGACCACGTCGGTGAAATTCAATATGGCCTCGGGTACCTGCATTTGC	57	*UAS-Ret-NTΔ*

source/order from: [+]life technologies, [#]invitrogen

8.6 Restriction enzymes

Table 9: Restriction enzymes

Enzyme	Recognition site	Buffer (Company)	vector
BglII	A|GATCT	Roche, Basel, Switzerland	*UAS-Ret-TKΔ*
EagI-HF	C|GGCCG	NEBuffer4 (New England BioLabs, Ipswich, USA)	*UAS-Ret-CRDΔ* *UAS-Ret-NTΔ* *UAS-Ret-CTΔ*
EcoRI-HF	G|AATTC	NEBuffer4 (New England BioLabs, Ipswich, USA)	*UAS-Ret-CLDΔ*
KpnI	GGTAC|C	Roche, Basel, Switzerland	*UAS-Ret-TKΔ*
XbaI	T|CTAGA	NEBuffer4 (New England BioLabs, Ipswich, USA)	*UAS-Ret-CTΔ*
XhoI	C|TCGAG	NEBuffer4 (New England BioLabs, Ipswich, USA)	*UAS-Ret-CRDΔ* *UAS-Ret-NTΔ*

8.7 Fly strains

Table 10: Fly stocks

strain	Chromosome	Reference
21-7-Gal4	2nd	Song et al., 2007
A58-Gal4	3rd	Han et al., 2011
Df(2L)Bsc^{312}	3rd	Bloomington Drosophila Stock Center, Indiana, USA
engrailed-Gal4	2nd	Bloomington Drosophila Stock Center, Indiana, USA
mav^{ko}	4th	RG Šoba, ZMNH, Hamburg (unpublished)
nompC-Gal4	3rd	Bloomington Drosophila Stock Center, Indiana, USA
ppk-Gal4	3rd	Han et al., 2012
ppk-CD4-tdGFP	3rd	Han et al., 2012
ppk-CD4-tdTomato	3rd	Han et al., 2012
RanBPM^{k0521}	2nd	Bloomington Drosophila Stock Center, Indiana, USA
RanBPM^{ts7}	2nd	Bloomington Drosophila Stock Center, Indiana, USA
Ret^{C168}	2nd	Bloomington Drosophila Stock Center, Indiana, USA
Ret^{ko}	2nd	RG Šoba, ZMNH, Hamburg (unpublished)
trol-GFP	x	Bloomington Drosophila Stock Center, Indiana, USA
TrpA1^{1}	3rd	Bloomington Drosophila Stock Center, Indiana, USA
UAS-CD4-tdGFP	3rd	Han et al., 2012
UAS-CD4-tdTomato	3rd	Han et al., 2012
UAS-CD8-tdTomato	3rd	Yuan et al., 2011
UAS-dAct	3rd	Gift from M. O'Connor, Minneapolis, USA
UAS-daw	3rd	Gift from M. O'Connor, Minneapolis, USA
UAS-gbb	3rd	Bloomington Drosophila Stock Center, Indiana, USA
UAS-mav	2nd	Gift from M. O'Connor, Minneapolis, USA
UAS-mav	3rd	Gift from M. O'Connor, Minneapolis, USA
UAS-mav	3rd	Gift from V. Budnik, University of Massachusetts

		Medical School, USA
mav-GFP (reporter) ***mav^{MI05038}***	3rd	Bloomington Drosophila Stock Center, Indiana, USA
UAS-mav-RNAi	2nd	Bloomington Drosophila Stock Center, Indiana, USA
UAS-mav-RNAi	3rd	Bloomington Drosophila Stock Center, Indiana, USA
UAS-myo	3rd	Gift from M. O'Connor, Minneapolis, USA
UAS-Ret-CLDΔ	3rd	This study RG Šoba, ZMNH, Hamburg (unpublished)
UAS-Ret-CRDΔ	3rd	RG Šoba, ZMNH, Hamburg (unpublished)
UAS-Ret-CTΔ	3rd	RG Šoba, ZMNH, Hamburg (unpublished)
UAS-Ret-K805M	3rd	Soba et al. 2015
UAS-Ret	3rd	Soba et al. 2015
UAS-Ret-mCherry	3rd	Soba et al. 2015
UAS-Ret-NTΔ	3rd	RG Šoba, ZMNH, Hamburg (unpublished)
UAS-Ret-RNAi	3rd	Bloomington Drosophila Stock Center, Indiana, USA
UAS-Ret-TKΔ	3rd	RG Šoba, ZMNH, Hamburg (unpublished)
w^{1118}	x	Bloomington Drosophila Stock Center, Indiana, USA

w^{1118} strain was used as '*wild type*' control.

8.8 Fly food

The following ingredients were used for 1 L of standard fly food:

Table 11: Ingredients for 1 L of standard fly food

Quantity	Ingredient	Company
8.75 g	Agar (strings)	Probio GmbH, Eggenstein, Germany
0.08 g	Corn flour	Spielberger-GmbH Brackenheim, Germany
10 g	Soy flour	Spielberger-GmbH Brackenheim, Germany
25 g	Brewer's yeast (ground)	Gewürzmühle Brecht, Eggenstein, Germany
0.08 g	Malt syrup	MeisterMarken – Ulmer Spatz, Bingen am Rhein, Germany
21.88 g	Treacle (molasses)	Grafschafter Krautfabrik, Meckenheim, Germany
1.88 g	Nipagin (Methyl 4-hydroxybenzoate)	Merck, Darmstadt, Germany
9.38 mL	Propionic acid	Roth, Karlsruhe, Germany

dissolved in 1 L dH_2O

8.9 Software

Table 12: Software

	Company
DNASTAR Lasergene 12	DNASTAR, Inc., Madison, Wisconsin, USA
Ethovision XT-X2	Noldus Information Technology, Wageningen, Netherlands
Fiji	Free software, http://fiji.sc/Downloads
Imaris 8.0.1	Bitplane's core scientific software, Bitplane AG
Origin Pro 9.0	OriginLab, Northampton, USA
Zeiss Zen imaging software	Carl Zeiss AG, Oberkochen, Germany

8.10 Technical equipment

Table 13: Technical equipment

	Company
Basler ace GigE camera	Basler AG, Ahrensburg, Hamburg, Germany
Centrifuge 5417C	Eppendorf AG, Hamburg, Germany
Forceps (Dumont, #3, 4, 5)	Fine Science Tools Inc., Heidelberg, Germany
Gel electrophoresis	Manufactured in-house, ZMNH, Hamburg, Germany
Infrared light frame (850 nm)	Manufactured in-house, ZMNH, Hamburg, Germany
Light source (white light)	ZMNH, Hamburg, Germany (equipment)
PCR thermocycler Biometra® T-Gradient	Biometra GmbH, Göttingen, Germany
Power Supply, Standard Power Pack P25	Biometra GmbH, Göttingen, Germany
SZX7 stereo microscope	Olympus, Hamburg, Germany
SZX12 stereo microscope	Olympus, Hamburg, Germany
Zeiss LSM700 confocal microscope	Carl Zeiss AG, Oberkochen, Germany

9 METHODS

9.1 Fly handling and genetics

All experiments were performed using 3rd instar larvae at 96 hours (hrs) after egg laying (AEL). In order to ensure that all larvae were about the same age, the egg laying was restricted to four to six hrs. Fly stocks were raised on standard fly food at 25°C with 70 % humidity and a 12 hrs light/12 hrs dark cycle. Flies were anaesthetized via a CO_2-dispensing fly pad. Females and males of the desired genotypes could be selected according to their phenotypic markers for experimental crosses or to establish new stocks. New fly stocks were established following standard *Drosophila* genetics (Greenspan, 2004). The following balancer chromosomes were used for maintaining lethal fly strains and to prevent homologous recombination:

Table 14: Balancer chromosomes and phenotypic markers

Chromosome	Balancer/Marker	Phenotypic marker
2	CyO GB	curly wings, kr-Gal4, UAS-GFP insertion
	CyO wee-P	curly wings, ubiquitously expressed green fluorescent marker
	sp	sternopleural, marker
3	TM2, ubx	ultrabithorax, larger halteres with bristles
	TM3, sb, ser	serrate, notched wings, short bristles
	TM3, sb	stubble, short bristles
	TM6B, hu, tb	humeral, extra humeral bristles, tubby, shorter larvae
4	unc^{13}, actin-GFP	actin green fluorescent marker
	pan^{ciD}	Inversion in which the promotor regions and first exons of transcription factors pan (pangolin) and Ci (Cubitus interruptus) have been swapped

9.2 The Gal4-UAS system for directed gene expression

The binary Gal4-UAS system was used for transient gene expression approaches. This system requires a driver line with a genomic enhancer and the yeast transcriptional activator Gal4 as well as an effector line carrying an upstream activating sequence (UAS). The yeast transcriptional activator Gal4 can be used to regulate gene expression in *Drosophila* by putting a gene/protein of interest (gene X) under UAS control. 'Enhancer-trap' lines that express Gal4 under the control of nearby genomic enhancers in a cell-type and tissue-specific patterns are available (Figure 7). Therefore, the expression of gene X can be driven in any of these patterns by crossing the appropriate Gal4 enhancer-trap line to flies that carry the UAS–gene X transgene (Brand and Perrimon, 1993; reviewed in Duffy, 2002; St Johnston, 2002).

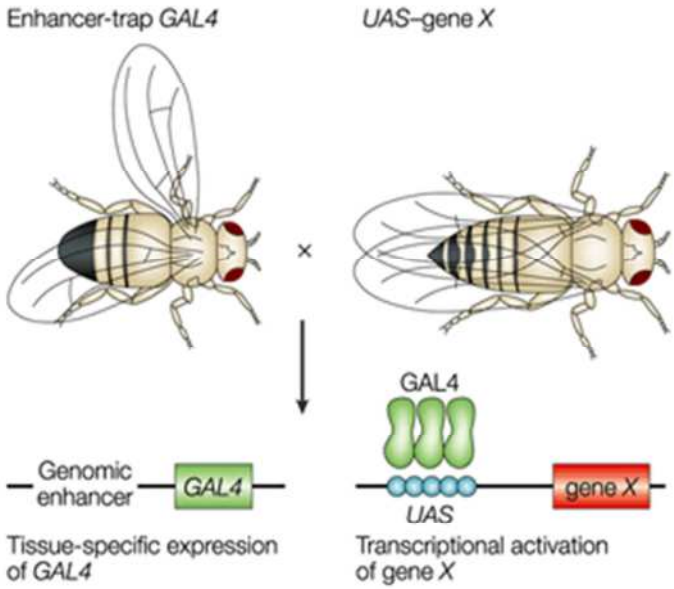

Figure 7. Schematic overview of the Gal4-UAS system in *Drosophila* (St Johnston, 2002). The system can be used to enable tissue or cell type specific expression of a transgene of interest. Expression can be visualized by using a fluorescent marker (e.g. tdGFP or tdTomato) fused to 'gene X'.

9.3 Fillet preparation and immunochemistry

3rd instar larvae fillets were prepared to investigate the distribution of specific proteins by using antibody immunostainings and the neuronal morphology of sensory neurons. The preparation and staining was essentially performed as described (Han et al., 2012). The larvae were prepared in Ringer solution. The animals were cut open ventrally after pinning the anterior and the posterior ends using insect pins (FST). The interior organs and fat bodies were removed and the body wall was then flattened with additional pins. Fillets were washed with Ringer solution and fixed with 4 % Formaldehyde/PBS for 15 min. After fixation the larval fillets were washed with 0.3 % Triton x-100 in PBS (PBS-T) and blocked for 1 h at room temperature (RT) in 5 % donkey serum. The samples were incubated with the primary antibody over night at 4°C in 5 % donkey serum/PBS, while the secondary antibody was applied at RT for 1 h. As a marker for all sensory neurons, anti-Horseradish peroxidase (anti-HRP) antibody was used as a reference. Between primary and secondary antibody incubation the fillets were washed with PBS-T to remove the antibody solution. After the immunostaining procedure, the samples were transferred to an equilibration buffer and mounted on a glass slide with the muscle side facing down. Silicon was applied on the slide to serve as a spacer and fillets were covered with a cover slip by carefully pressing it down. The mounting medium (Slowfade reagent with 50 % glycerol in PBS) was applied to the sample between the slide and the coverslip. A lead weight was used to flatten the samples and cover slips were then sealed with nail polish. Images were taken on a Zeiss LSM700 confocal microscope with a 20x/0.8NA air lens or with a 40x/1.3NA oil lens.

9.4 Live imaging

For live imaging 3rd instar larvae (96hrs AEL) C4da neurons (ddaC) were imaged by confocal stack microscopy (Zeiss LSM700). C4da neurons were visualized by using *ppk-CD4-tdTomato, ppk-CD4-tdGFP* or *ppk-Gal4>UAS-CD4-tdGFP* (Han et al., 2011). For comparison, abdominal segments A3 and A4 were chosen. Confocal stacks were taken with a 20x objective (air lens, 0.8NA) to image the whole dendritic field of ddaC neurons. For higher resolution and magnification a 40x objective was used (oil lens, 1.3NA). The chosen step size of a stack varied from 0.3 - 0.7 µm depending on the experiment.
For time lapse imaging, one C4da neuron (96 hrs AEL) was imaged over a time period of 25 - 30 min in 5 min time steps. The analyzed larva was kept in a special customized larval chamber to facilitate survival of the animal during the imaging procedure (Mishra et al., 2014).

9.5 Genomic DNA preparation – Single fly preparation

For the isolation of genomic DNA or cDNA one male fly was placed in a 0.5 mL tube and mashed for 5-10 seconds with a pipette tip containing 50 µL of squishing buffer (SB), without expelling any liquid. After squishing the remaining SB was expelled. The single fly preparation was performed on ice. Incubation at 37°C for 30 min, followed by inactivation of the Proteinase K at 95°C for 10 min. For PCR reactions typically 1 µL of the DNA preparation was used.

Table 15: Ingredients for squishing buffer

Concentration	Ingredient
10 mM	Tris-Cl pH, 8.2
1 mM	EDTA
25 mM	NaCl
200 µg/mL	Proteinase K (diluted fresh from a frozen stock)

9.6 Molecular biology

Standard molecular biology methods were used according to Sambrook and colleagues (1989) and Ausubel and colleagues (1992) and are not described here in detail (Ausubel et al., 1992; Sambrook et al., 1989).

9.6.1 Plasmid DNA amplification

The PCR reaction was performed in a 50 µL volume and the reagents are listed in Table 16. Sense and antisense oligonucleotide primers were designed based on DNA sequences using DNASTAR Lasergene 12 Core Suite. All constructs generated in this study contain fragments that were PCR-amplified from clone pUAttB-Ret-V5 (generated by Dr. Peter Šoba). A different strategy was based on blunt-end PCR cloning into pCR™-BluntII-TOPO® vector (life technologies), in which the amplified PCR product was first cloned into TOPO® vector. All constructs were confirmed by sequencing using M13 forward/reverse vector primers. The correct fragment was cloned into the final vector (pUAttB-Ret-V5) using restriction enzymes.

Table 16: Ingredients for PCR approach

Quantity	Ingredient
x µL	Template DNA (50 ng)
5 / 12.5 µL	10x / 2x buffer (Pfx/Q5)
1 µL	dNTPs (10 mM)
2 µL	Forward Primer (10 pmol)
2 µL	Reverse Primer (10 pmol)
0.5 µL	Pfx / Q5 Polymerase (2.5U/µL / 2 U/µL)

add dH_2O to 50 / 25 µL (Pfx/Q5 Polymerase)

The following PCR profile was used:

1. Initial denaturation 95°C 5 min
2. Denaturation 95°C 30 s
3. Annealing (primer specific °C) 30 s
4. Extension 68 / 72°C (1 min/1000 bp) (Pfx/Q5 Polymerase)
5. Cycle from step 2 to step 4 (25x)
6. Final extension 68 / 72°C 10 min (Pfx/Q5 Polymerase)

(7. Storage at 4°C)

The details about the used primers and their annealing temperatures are provided in Table 8. For DNA amplification, Pfx or Q5 polymerase was selected. Both high fidelity polymerase enzymes have 3'-5' exonuclease proof reading activity that reduces the errors in nucleotide incorporation during PCR amplification and hence was used in generating all fragments for DNA cloning.

9.6.2 Agarose Gel electrophoresis

Conventional agarose gel electrophoresis was used to analyze DNA fragments. The electrophoretic mobility of linear DNA fragments mainly depends on the fragment size and to a lesser extent on the conformation of the DNA, type end concentration of agarose used as well as applied voltage and electrophoresis buffer used. For separating PCR fragments or restricted plasmid DNA, 1 % agarose gels were prepared (in TAE). DNA bands were visualized by non-carcinogenic Roti®-GelStain (5 µL/100 mL agarose gel solution) and fragment size was identified by using DNA fragments ladder GeneRuler 1 kb Plus.

9.6.3 Gel extraction and PCR purification

The gel extraction kit (Macherey-Nagel) was used according to the manufacturer's instructions to extract DNA fragments from agarose gels and for PCR product purification. The gel fragment was excised with a clean scalpel. For each 100 mg of agarose gel 200 µL buffer NT was added into the 1.5 mL tube. For PCR clean-up 1 volume of sample was mixed with 2 volumes of Buffer NT. The samples were incubated for 5-10 min at 50°C and vortexed briefly every 2-3 min until the gel slice was completely dissolved. For binding the DNA the solution was loaded into an Extract Column and centrifuged for 1 min at 11.000 x g. The flow-through was discarded and the column was placed back into the collection tube. The DNA was washed with 700 µL Buffer NT3 and centrifuged twice for 1 min at 11.000 x g to dry the silica membrane. The elution of the DNA was done by adding 30 µL Buffer NE, was incubated for 1 min at RT and centrifuged for 1 min at 11.000 x g.

9.6.4 Restriction digest of PCR products or plasmid DNA

Analytical or preparative restriction digests were done using 1 µg of DNA. The commercially available reagents are shown in Table 17. All single or double digests were made up to a final volume of 20 µl according to the company´s protocols. The digests were mixed and incubated at 37°C for 1-1.5 h. The digested DNA was viewed on a 1 % agarose gel.

Table 17: Ingredients for analytical and preparative restriction approach

Quantity	Ingredient
x µL	Plasmid DNA (1 µg)
2 µL	10x NEB restriction buffer (#4) / Roche restriction buffer
2 µL	10x BSA
0.5-1 µL	Restriction enzyme (Table 9) (10,000-20,000 U/mL)

add dH_2O to 20 µl

9.6.5 Ligation of plasmid DNA

100 ng of vector was used with the molar ratio of vector to insert being set at 1:3. The final reaction volume for ligation was 10 µl. The reaction mixture including T4-DNA-Ligase and T4-Buffer was incubated at RT for 1 h or overnight at 4°C. 5µl of ligated mixture was used for transformation into competent DH5α bacteria.

Table 18: Ingredients for ligation approach

Quantity	Ingredient
x µL	Vector (50 ng)
x µL	3x insert
1 µL	10x T4 buffer
1 µL	T4-DNA-ligase

add dH_2O to 10 µL

9.6.6 Zero Blunt-II® TOPO® Cloning reaction

Zero Blunt-II® TOPO® Cloning reaction provides a highly efficient cloning strategy to insert blunt-end PCR products into a plasmid vector. This vector is supplied linearized with *Vaccinia* virus DNA topoisomerase I covalently bound to the 3‘ end of each DNA strand. The procedure to perform TOPO® Cloning reaction was used according to the manufacturer’s instructions (Life technologies). To perform this reaction 0.5-1 µL fresh blunt-end PCR product, 0.5 µL salt solution and 1 µL pCR™II-Blunt-TOPO® were mixed and water was added to a total volume of 5 µL. The reaction was mixed gently and incubated for 5-20 min at RT and transformed into competent cells after incubation on ice.

9.6.7 Chemotransformation

Chemically competent DH5α bacteria were thawed on ice for 5-10 min. For a single transformation 1 aliquot (50 µL) of bacterial suspension was mixed with 5 µl of ligation product plasmid DNA in a reaction tube. Immediately after heat-shock (42°C for 45 sec) the tube was placed on ice and 400 µL of LB-medium was added. This suspension was incubated with shaking at 37°C for 30 min (Ampicillin resistance) or 45 min (Kanamycin resistance). After incubation, 50-450 µL were plated on an LB agar plate containing the appropriate selection antibiotic for the plasmid and incubated at 37°C over night.

9.6.8 Colony PCR

Colony PCR is a commonly used method to quickly screen for plasmids containing a desired insert directly from bacterial colonies. After transforming a ligation reaction and incubation on LB agar plates overnight, individual colonies can be picked by a sterile yellow pipette tip and dipped into the reaction tube for PCR analysis.

Table 19: Ingredients for colony PCR approach

Quantity	Ingredient
6.25 µL	DreamTaq Green PCR 2x Master Mix
5.25 µL	Nuclease-free water
0.5 µL	forward primer (10 pmol)
0.5 µL	reverse primer (10 pmol)
	bacterial colony

9.6.9 Isolation of plasmid DNA

3 mL LB media supplemented with appropriate selection antibiotics were inoculated with a single colony and grown overnight at 37°C on a shaker. Cells were centrifuged at 3.000 rpm for 10 min. Plasmid DNA was isolated using the QIAGEN Plasmid Mini Kit, which is based on a modified alkaline lysis procedure, followed by binding of plasmid DNA to an anion exchange resin under appropriate low salt and pH conditions, according to the protocol. The DNA pellet was washed with 70 % ethanol and dissolved in 30-50 µL 1x TE buffer.

9.6.10 DNA sequencing

For sequencing 500 ng of purified plasmid DNA and 0.5 µL of sequencing primer (10 pmol) was added and dissolved in sterile water to a total reaction volume of 8 µL. The samples were analyzed on an ABI 3130 Genetic Analyzer by the sequencing facility service in-house.

9.7 CRISPR/Cas9-system

Correct targeted gene disruption in *Drosophila* has been achieved by deletion of flanking sequences by imprecise excision of transposons or by gene replacement using homologous recombination (Rong, 2002; Ryder and Russell, 2003). However, each of these systems has its own limitations: Using imprecise excision of transposons existing transposon near the target locus are required and for quite a few genes not available (Ryder and Russell, 2003). For homologous recombination, a screening of more than 1000 flies is sometimes needed because of its low efficiency (Huang et al., 2009).

To generate a mav^{ko} allele, the simple and efficient CRISPR/Cas9 system for systematic gene targeting in *Drosophila* was used. This system was originally identified as a component of the CRISPR (***C****lustered* ***R****egularly* ***I****nterspaced* ***S****hort* ***P****alindromic* ***R****epeats)* bacterial innate immunity system. Cas9 was found to encode a novel class of sequence-specific endonuclease whose target specificity is determined by its guide-RNA (gRNA) component (Cong et al., 2013; Jinek et al., 2012; Mali et al., 2013). This method is described as a robust system in which any gene can be mutated with high efficiency and consistency (Kondo and Ueda, 2013).

9.7.1 Targeting of mav by CRISPR/Cas

In *Drosophila*, several strategies and reagents have been developed that allow efficient targeting of any gene by CRISPR/Cas9 (Cong et al., 2013; Jinek et al., 2012; Kondo and Ueda, 2013; Mali et al., 2013).
For generation of a *mav* knock-out (mav^{ko}), two specific guide RNA sequences were cloned into pCFD4 and expressed both guide RNA under control of U6-1 and U6-3 promoter to target the 5' and 3' regions of the mav CDS on the 4th chromosome, respectively (see primer sequence in chapter 8.5). pRK2 (Huang et al., 2009) was used to generate an HDR template with 1kb genomic regions 5' and 3' of the mav coding exons, respectively, which flanked a GMR white cassette as a selection marker. Both plasmids were co-injected (pCFD4-mav: 0.2 µg/µL, pRK2-mav: 0.5 µg/µL) into *yw,vasa-Cas9* syncytial embryos to target mav in the germ-line. F^0 animals were backcrossed to double balancer virgins (sp/CyO ; TM2/TM6b) and positive transgenic animals (F^1) were identified by red eye color. Candidate flies were backcrossed to a fourth chromosome balancer and lines were established from individual F^1 transformants. PCR analysis was performed to verify correct targeting of the mav locus. In total, screening of less than 20 animals was sufficient to get 3 independent mav^{ko} lines.

9.8 *Drosophila* larval behavior assays

For all behavioral assays 3rd instar larvae (96 hrs AEL) were tested and raised in an incubator at 25°C.

9.8.1 Locomotion behavior assay

To analyze locomotion behavior, foraging 3rd instar larvae (96 hrs AEL) were placed on a 2% agar plate. Before imaging, the animals were equilibrated for 2–3 min. The plate was illuminated by a light source from below. The larvae were tracked for 10 min using automatic video tracking system EthoVision XT software.

9.8.2 Mechano-nociception assay

The mechanical nociception assay was performed as described in Zhong et al., 2010, with slight modifications. 3rd instar larvae (96 hrs AEL) were washed and placed on a 2 % agar plate (Ø 10 cm) with 2 mL dH_2O. Each larva was stimulated with a 50 mN calibrated tool, equivalent to *Von Frey* filament (Figure 8). Omniflex monofilament fishing line Shakespeare (6 lb test, diameter 0.009 inch [0.23 mm]) was cut to a length of 18 mm. 10 mm were attached to a toothpick such that 8 mm of the fiber protruded from the end of the toothpick. The force of the fiber was calibrated by using it to depress a balance until the fishing line was seen to bend.

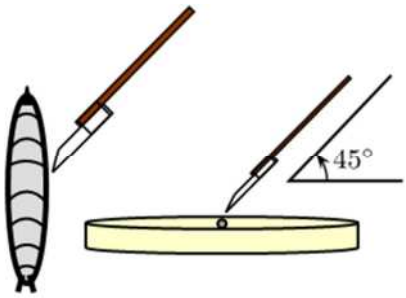

Figure 8. Experimental setup of the mechanonociception assay. The assay was performed by placing 3rd instar larvae on a 2% agar plate. The behavioral response of each larvae after nociceptive stimulation with a 50 mN calibrated tool was analyzed and afterwards scored (response classification: 1=no response, 2=stop, 3=stop and turn, 4=bending, 5=rolling). Each larva was tested twice with a pause of 2-3 sec.

The force (in grams) was recorded and converted to milli-Newtons by multiplying the measured grams by a factor of 9.8. Noxious mechanical stimuli were delivered by rapidly depressing the larva with the fiber on the dorsal side (abdominal segments four, five, or six). The stimulus was delivered and released as quickly as possible. The quick release allows the larvae to perform escape locomotion behavior. A positive nociceptive response was scored if at least one rotation around the A/P axis occurred in response to the mechanical stimulus (response classification: 1=no response, 2=stop, 3=stop and turn, 4=bending, 5=rolling). Each larva was tested twice with a pause of 2-3 sec, and only the 2nd response was plotted.

9.8.3 Light avoidance assay

Light avoidance is a particular behavior *Drosophila* larvae exhibit prior to pupation (Sawin-McCormack et al., 1995). In order to gain insights into the neuronal network responsible for the photophobic behavior, neurons can be genetically modified and the behavioral readout can be analyzed in light avoidance assays. The light avoidance assays were performed as described (Gong et al., 2010; Yamanaka et al., 2013), with slight modifications using 2 % agar plates and illumination from below. The light avoidance assay was carried out in a black box designed to exclude daylight (Figure 9). For this assay standardized petri dishes (Ø 10 cm) with 2 % agar were placed on a Plexiglas plate positioned above a white light source (450 lux). The Plexiglas plate served as an insulation shield against the radiated warmth of the light source to be able to maintain a constant temperature of 24°C ± 2 of the agar surface. By positioning a template below the agar plate, one half of the petri dish was illuminated whereas the other half was kept darkened. For each trial 20 staged 3rd instar larvae were collected, washed in dH_2O and then aligned along the border between the light and the dark side. Employing an infrared light frame, the larvae became detectable in the dark for the recording with a camera at 60 Hz and 7.5 frames per second. The larval light

avoidance behavior was assessed for a total duration of 15 min. During the trial, larvae on the light side of the agar plate were counted after 5, 10 and 15 min.

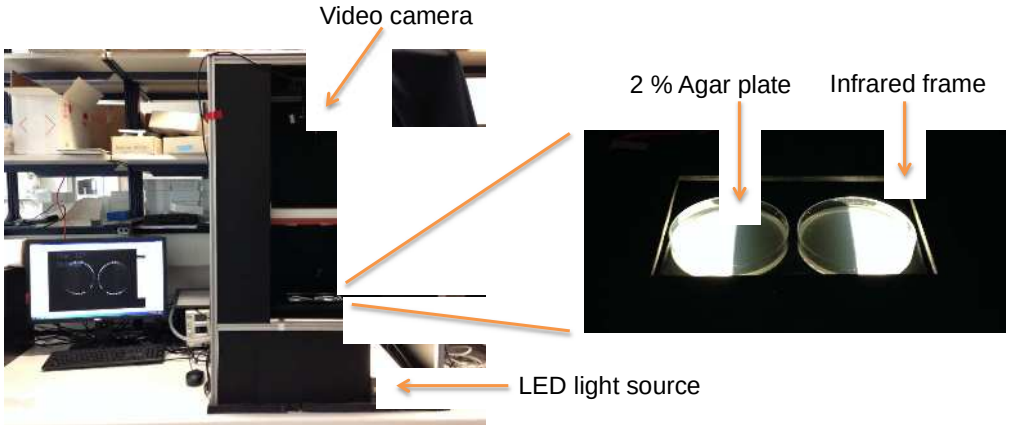

Figure 9. Experimental setup of the light avoidance assay. The assay was performed in a black box to exclude daylight. A white light source and a template were used to illuminate one half of the agar plate, keeping the other half darkened. For each trial and genotype, 20 3rd instar larvae were placed on the midline of the agar plate and recorded with a camera. The total duration was 15 min/trial and the dark preference index (PI) was calculated (see chapter 9.8.4).

9.8.4 Dendrite analysis and statistics

Dendrites of C4da neurons were traced semi-automatically using the Imaris Filament Tracer module (BitPlane AG, Zürich, Switzerland) to describe dendrite morphology and their phenotype. Used parameters are: dendritic field coverage, total dendrite length, normalized dendrite crossing points, number of terminal dendrite ends, Sholl analysis, Strahler analysis and dendrite-ECM interaction.

Dendritic field coverage was calculated by measuring the area covered by dendrites divided by the total area of the segment (Fiji). Statistical significance was calculated using a two-tailed t-test. The following parameters were calculated by filament tracing of confocal z-stacks (Imaris).

The analysis of dendrite and extracellular matrix (ECM) interaction was performed as described in Han et al., 2012. After deconvolution (AutoQuant, Bitplane), a colocalization analysis of C4da neuron dendrites and the ECM was performed. Non-contacting and contacting domains were semi-automatically traced and verified manually. Percentages of detached dendrites were calculated by the ratios of detached and total dendrite length.

To quantify dendrite dynamics, confocal stacks of the same neuron at different time points were analyzed (5 min time lapse intervals). In detail, the length of each dendrite terminal was measured and compared to its length after 5 min (Fiji). Growth was defined as a terminal branch which was shorter at timepoint 0. Retraction was defined as a terminal branch which was longer at timepoint 0. Afterwards, growth and retraction speed of terminal dendrites (µm/min] and the frequency of growing, retracting and stable dendritic terminals were plotted.

The light avoidance data were obtained by determining the performance index (PI). The PI was calculated using the following formula:

$$\mathrm{PI} = \frac{(\text{number of larvae in dark}) - (\text{number of larvae in light})}{(\text{total number of larvae})}$$

The statistical significance was analyzed via the software Origin Pro using the nonparametric Mann-Whitney U-Test. The data is presented as mean ± SD. In all figures the level of significance was indicated by $p<0.05$ (*), $p<0.01$ (**) and $p<0.001$ (***).

10 RESULTS

10.1 Generation of a targeted *Ret* knock-out allele

An *in vivo* RNAi screen in *Drosophila* C4da neurons identified the conserved Ret receptor as an important regulator of dendrite development. Soba et al. (2015) demonstrated that Ret is expressed in C4da neurons and its loss resulted in severe dendrite defects caused by the loss of extracellular matrix adhesion, which impaired proper growth of those sensory neuron dendrites within their 2D plane. The study showed that Ret interacts with integrins to regulate dendrite adhesion to the extracellular matrix. In that study, a hypomorphic mutant allele of Ret (Ret^{C168}) was used containing a *P-element* insertion within the 3′UTR region of the *Ret* genetic locus. To further validate and analyze Ret function in C4da neurons in more detail, a targeted *Ret* knock-out allele (Ret^{ko}) was generated by an improved ends-out genomic targeting strategy (Huang et al., 2009) (Figure 10A).

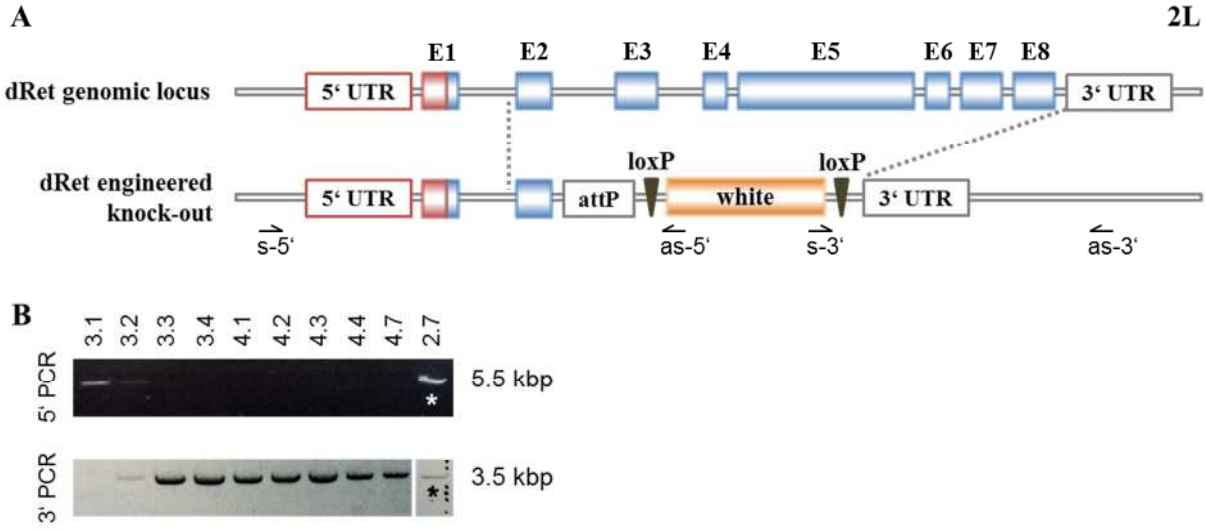

Figure 10. Targeting strategy of the *Drosophila melanogaster* Ret genomic locus (dRet) and Ret knock-out validation. A) Exons 3-8 (E3-8) were replaced by a cassette containing attP- and loxP-sites allowing further site-specific recombination, and a *GMR-white* cassette as a positive selection eye marker. The Ret targeted knock-out was generated using ends-out targeting. E1-8: Exon 1-8; signal peptide indicated in red (5'UTR and coding sequence of E1). Red eyed *Ret* mutant candidates were screened by PCR using primer pairs flanking the 5' and 3' targeting site in the *Ret* genomic locus to verify its correct gene replacement **(B)**. Ret mutant lines 2.7 and 3.2 showed correct PCR products with predicted size of 5.5 kbp (5' PCR, primer pair: s-5' and as-5') and 3.5 kbp (3' PCR, primer pair: s-3' and as-3') and thus correct targeting. Mutant 2.7 (indicated by asterisks) was chosen for further experiments.

Candidates with insertion of the targeting cassette on the correct chromosome were verified by PCR screening amplifying 5' and 3' flanking sequences of the targeting construct (Figure 10B). The verification revealed predicted PCR products of 5.5 kbp (5' PCR) and 3.5 kbp (3' PCR) for two *Ret* mutant lines (2.7 and 3.2) showing correct targeting. The Ret mutant allele

2.7 was chosen for further investigation and will be referred to as "*Ret*^{ko}". The *Ret*^{ko} allele was combined with the C4da neuron specific marker *ppk-CD4-tdTomato* and characterized.

10.2 Verification and characterization of the *Ret*^{ko} allele

In order to test *Ret*^{ko} larvae with respect to their Ret expression, *w*^{1118} and *Ret*^{ko} 3rd instar larval fillets were immunohistochemically stained with an anti-Ret antibody (Figure 11A). In *wild type* larvae (*w*^{1118}), C4da neurons showed specific expression of Ret in the soma and along all dendrites. In *Ret*^{ko} larvae, anti-Ret immunostaining was completely absent in C4da neurons and only non-specific background signal was detectable.

For quantitative analysis, the signal intensity of the antibody was measured. The comparison of *control* and *Ret*^{ko} larvae revealed significantly higher normalized signal intensity of the Ret-antibody in C4da *wild type* neurons (*wild type*: 7.39 ± 1.57, *Ret*^{ko}: 0.05 ± 0.03, p-value<0.05) (Figure 11B). These results confirmed the absence of Ret protein expression in *Ret*^{ko} animals.

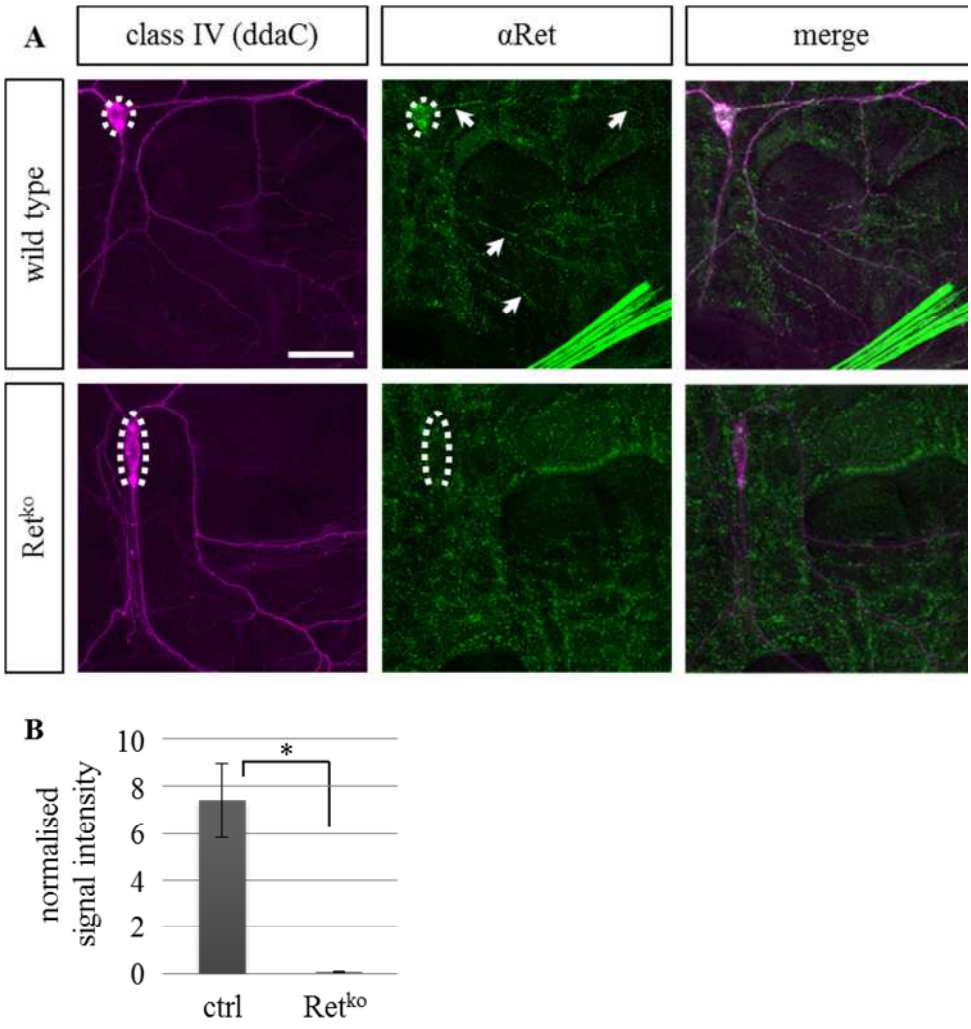

Figure 11. Ret expression in C4da neurons of *wild type* and *Ret*^{ko} 3rd instar larvae. A) Confocal images of a dorsal C4da neuron in 3rd instar larvae. Larval fillets were stained with an anti-Ret antibody (guinea pig) and *ppk-CD4-tdTomato* to visualize C4da neurons. In *wild type* (*w*^{1118}), soma

(dashed line) and dendrites of C4da neurons (arrows) show specific expression of Ret. Along the dendrites, anti-Ret immunostaining showed a punctuate localization (indicated by arrows). In Ret^{ko} larvae, anti-Ret immunostaining is completely absent in C4da neurons. Scale bar: 100 µm. **B)** Quantification of the Ret antibody signal intensity. The relative intensity was quantified by background subtraction of the signal intensity of the region of interest (cell soma) divided by the signal intensity of the background. The quantitative analysis confirmed the absence of Ret immunoreactivity in Ret^{ko} C4da neurons. All data are mean ± SD, Mann-Whitney-Test, $p<0.05$ (*), n=5.

10.3 *Ret* is required for C4da neuron dendrite development

To analyze morphological defects of C4da sensory neurons in Ret^{ko} animals, 3rd instar larvae were imaged by confocal microscopy *in vivo*. Accordingly, the dendritic morphology of C4da neurons in *control,* Ret^{ko} and C4da neuron specific overexpression in Ret^{ko} animals (*UAS-Ret*) were visualized by the expression of the C4da neuron specific marker *ppk-Gal4>CD4-tdGFP*.

The qualitatively observation revealed that Ret loss-of-function resulted in dramatically reduced dendritic field size and an increase of isoneuronal crossing defects compared to *control* larvae (Figure 12). These morphological defects were absent in Ret^{ko} animals specifically expressing transgenic full-length Ret in C4da neurons demonstrating that Ret is cell-autonomously required for C4da neuron dendrite patterning.

For detailed analysis, the total dendrite length, dendritic coverage index (ratio of dendrite field area and segment area), number of crossing points and neuron complexity of C4da neurons were quantitatively investigated (Figure 12B-D, Figure 13).

In Ret^{ko} animals (over the deficiency $Df(Bsc^{312})$), C4da sensory neurons revealed dramatic defects at the morphological level. Both, the total dendrite length and their dendritic field size were strongly reduced. Quantitative measurement of total dendrite length (18311 µm ± 2016) and dendritic field coverage (87% ± 0.03) of *control* and Ret^{ko} C4da neurons revealed a strong reduction in dendrite length (14237 µm ± 1634, $p<0.001$) and coverage (62% ± 0.02, $p<0.001$) due to *Ret* loss-of-function (Figure 12B and C). In terms of their dendritic self-avoidance properties, Ret^{ko} C4da neurons showed a significant increase of crossing of dendrites compared to *control* (12.34 ± 3.19, 4.69 ± 1.79 number of crossing points / 10 µm, accordingly, p-value<0.001) (Figure 12D). These observed morphological defects were fully rescued by C4da neuron specific *Ret* overexpression using *ppk-Gal4* (total dendritic length: 19542 µm ± 1783, dendritic field coverage: 88% ± 0.01, number of crossing dendrites / 10 µm: 5.29 ± 1.59).

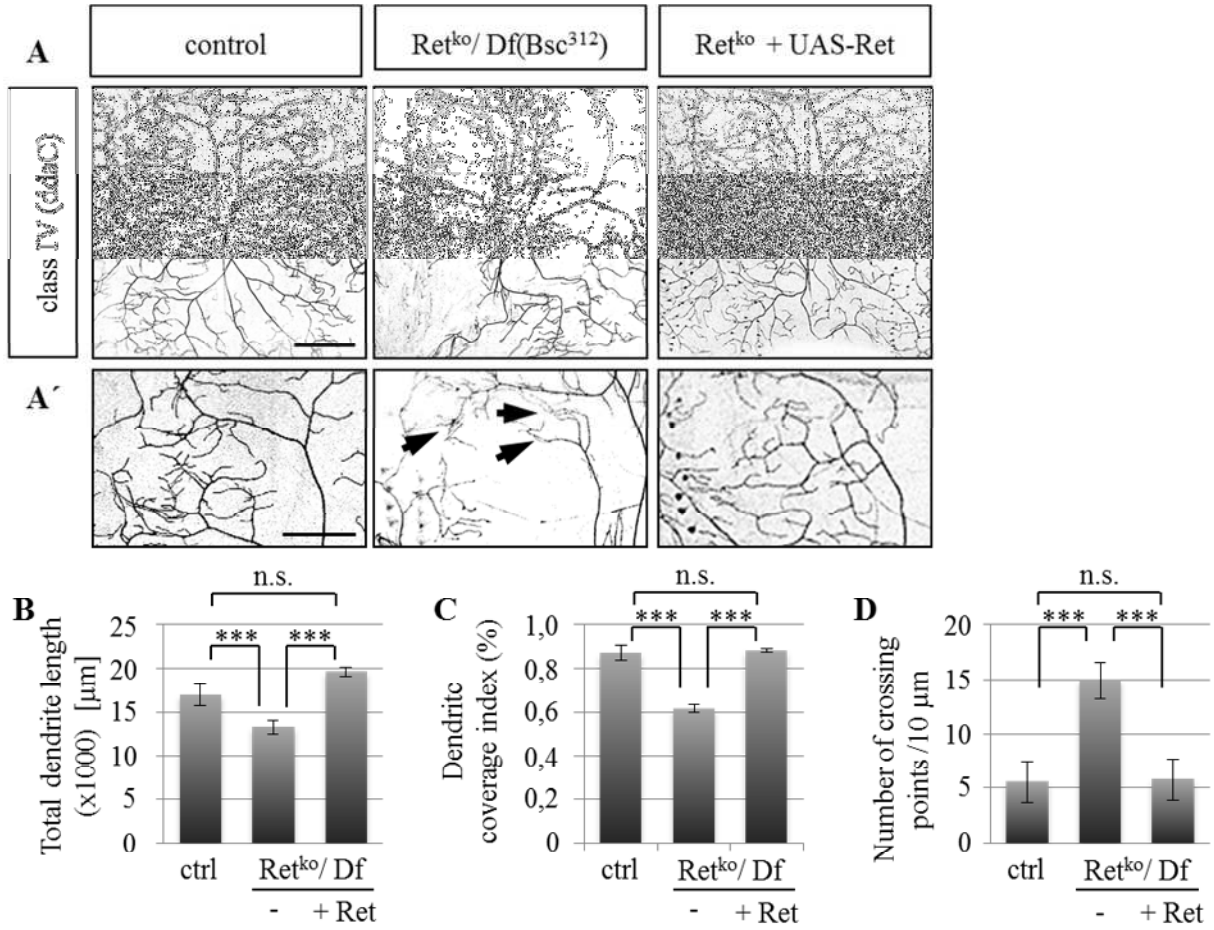

Figure 12. *Ret* loss-of-function causes cell-autonomous dendrite growth and coverage defects in C4da neurons. A) Dendritic morphology of C4da neurons in *control* and *Ret^{ko}/ Df(2L)Bsc^{312}* 3rd instar larvae visualized by the expression of the C4da specific marker *ppk-CD4-tdGFP.* Scale bar: 100 µm. An enlarged section is shown below indicated by a rectangle **(A´)**. Scale bar: 50 µm. **B-D)** Quantitative analysis of total dendrite length, dendritic coverage index (ratio of dendrite field area and segment area) and number of crossing points of C4da neuron dendrites. Note the dramatically reduced dendritic field size and crossing defects in *Ret^{ko}* C4da neurons (arrows). Ret overexpression (*UAS-Ret-mCherry*) specifically in C4da neurons rescues this phenotype. All data are mean ± SD, Mann-Whitney-Test p<0.05 (*), p<0.001 (***), n=5.

To analyze the dendrite complexity in more detail, Sholl analysis was performed to visualize the number of dendrite intersections in relation to the increasing distance from the soma (Figure 13A-D). In comparison to *control*, *Ret^{ko}* C4da neurons displayed significantly reduced dendrite complexity in medial and distal parts. In particular, at a distance of 200-300 µm from soma the number of dendritic intersections was highly reduced indicating a loss of distal branching. In addition, reverse Strahler analysis was performed to examine potential changes of branch orders in relation to the branch number (Figure 13E-F). In *Ret^{ko}* C4da neurons, the number of branches within each branch order was highly reduced compared to *control* neurons. However, a shift towards higher ordered branches was observed, which indicated increased dendritic branching of the remaining dendritic arbor in *Ret^{ko}* neurons. These defects were completely rescued by C4da neuron specific overexpression of a Ret

transgene, which validated the cell-autonomous requirement of *Ret* for C4da neuron dendrite development.

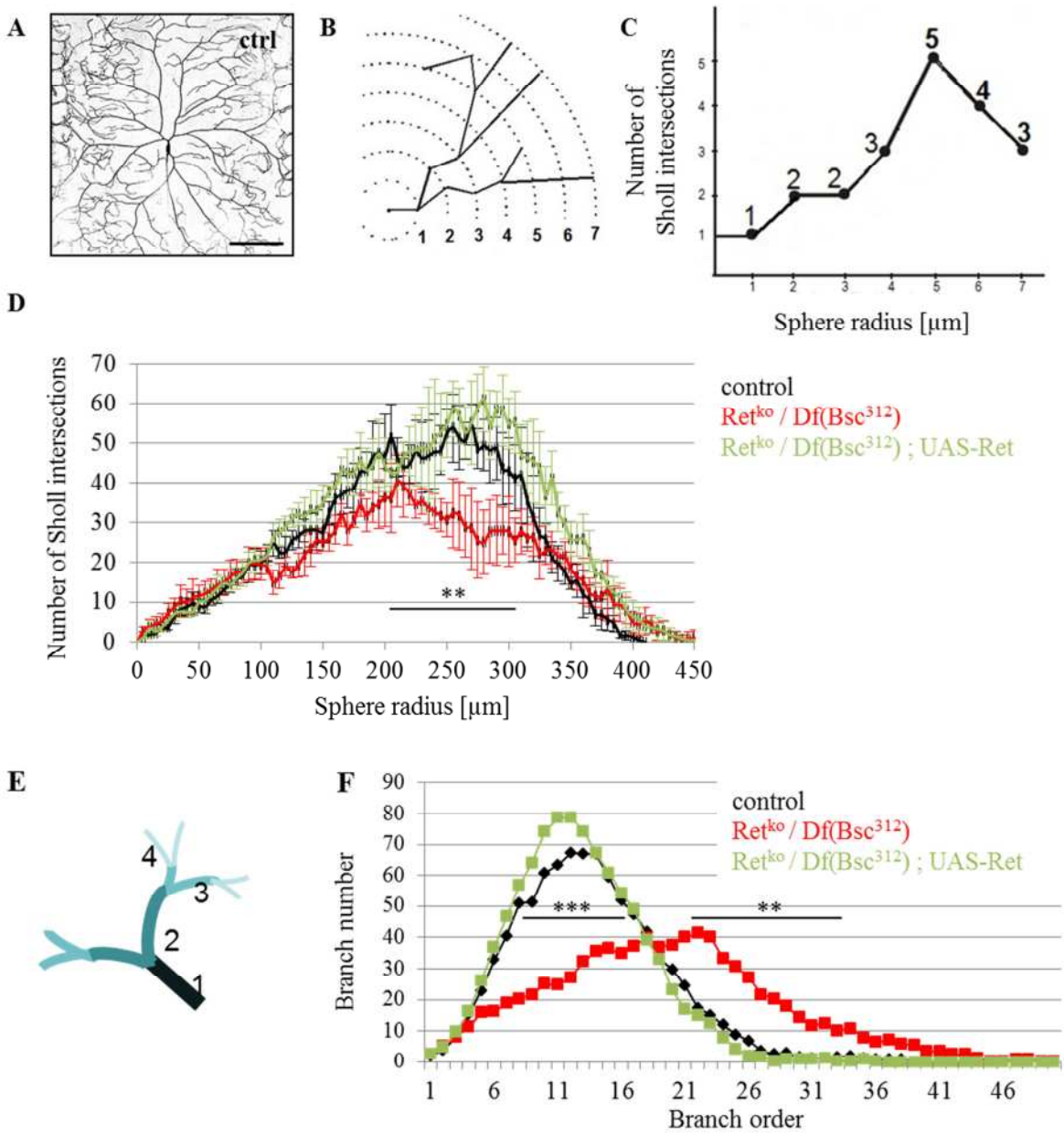

Figure 13. *Ret^{ko}* larvae display reduced C4da neuron dendrite complexity. A) Dendritic field of C4da *control* neuron of 3rd instar larvae visualized by the expression of *ppk-Gal4>CD4-tdGFP.* Scale bar: 100 µm. **B-C)** Sholl analysis to quantitatively visualize dendrite complexity. A series of equidistant, concentric spheres (every 5 µm) is placed around the center of a neuron and the numbers of dendrite intersections are plotted against the increasing radius. **D)** *Ret^{ko}* C4da neurons display reduced dendrite complexity in medial and distal parts compared to *control*. This defect could be rescued by C4da specific overexpression of a Ret transgene. **E)** Strahler analysis to quantitatively visualize dendrite complexity. The numbers of dendrites are plotted against the increasing branch order. **F)** *Ret^{ko}* C4da neurons display reduced numbers of dendrites of lower branch orders. In return, *Ret^{ko}* C4da neurons display an increased number of higher order dendrites. This defect can be rescued by C4da specific overexpression of a Ret transgene. All data are mean ± SD, Mann-Whitney-Test $p<0.01$ (**), $p<0.001$ (***), n=5.

10.4 Domain-function analysis of Ret in C4da neurons

As shown above, C4da neuron specific expression of transgenic Ret in *Ret*^{ko} animals completely rescued dendrite defects. To gain information about the functional requirement of different Ret extra- and intracellular domains in dendrite development, a structure-function analysis was performed using Ret domain deletion transgenes to analyze their capacity to rescue C4da neuron dendrite defects in *Ret* mutant animals (Figure 14).

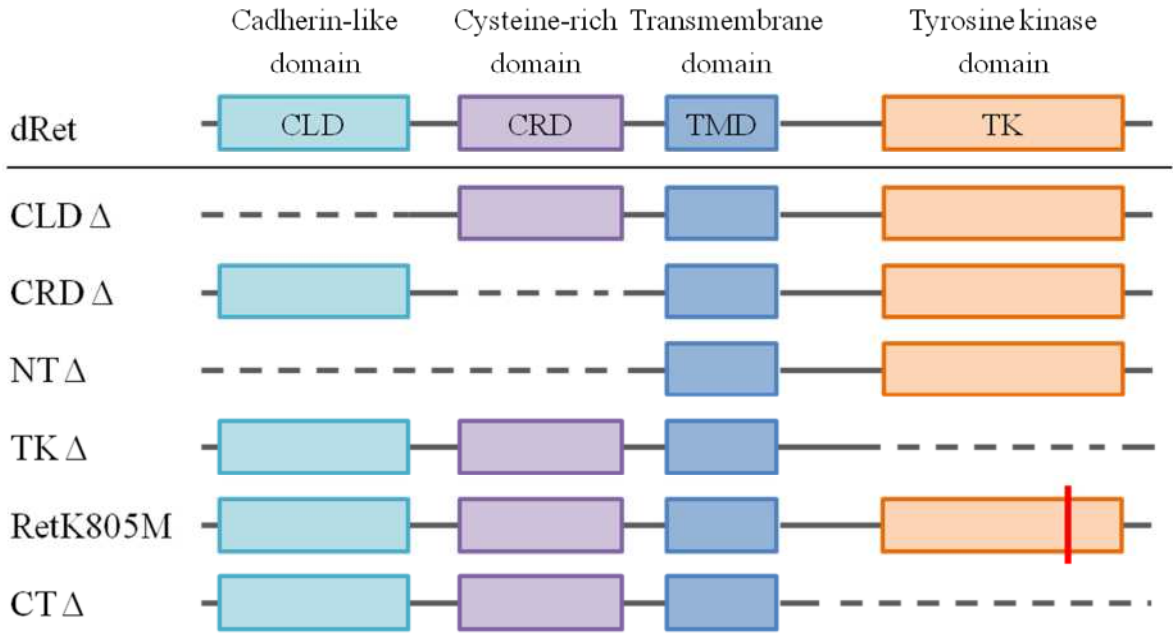

Figure 14. Scheme of Ret protein domain deletion constructs. Generated UAS-transgenes of Ret cDNA with different domain deletions for tissue specific rescue experiments. dRet: full-length Ret protein, CLDΔ: Cadherin-like domain deletion, CRDΔ: Cysteine-rich domain deletion, NTΔ: extracellular domain deletion, TKΔ: tyrosine kinase domain deletion, RetK805M: inactive Ret kinase mutant, CTΔ: intracellular domain deletion.

Qualitatively, this analysis showed that both extracellular domains of Ret (CLD and CRD) are essential for Ret function since C4da neuron patterning of larvae lacking these domains exhibit similar defects as in *Ret*^{ko} larvae. However, lacking of either the complete intracellular kinase domain or the mutation of the kinase activity was able to partially or complete rescue C4da neuron dendrite morphogenesis in *Ret*^{ko} larvae. However, transgenes lacking either the entire extracellular or intracellular domain of Ret were both unable to restore C4da neuron dendrite morphology (Figure 15).

For the quantitative analysis dendritic field coverage, total dendrite length, numbers of crossing dendrites and neuron complexity were analyzed and compared as before.

Quantitative analysis of the dendritic coverage index revealed that *Ret*^{ko} C4da neurons expressing extracellular domain deletion transgenes of Ret (partially or completely) still displayed significantly decreased dendritic field coverage compared to *control* (CLDΔ: 61% ±

0.05, CRDΔ: 58% ± 0.04, NTΔ: 43% ± 0.02) (Figure 15, Figure 16A). Interestingly, expression Ret transgenes with a deleted (TKΔ) or inactive kinase domain (RetK805M) showed a partial or complete rescue of the *Ret*^{ko} phenotype, respectively (TKΔ: 82% ± 0.02, RetK805M: 87% ± 0.03). However, neurons expressing Ret lacking the entire intracellular domain still exhibited reduced dendritic field coverage (CTΔ: 62% ± 0.02) (Figure 15, Figure 16A).

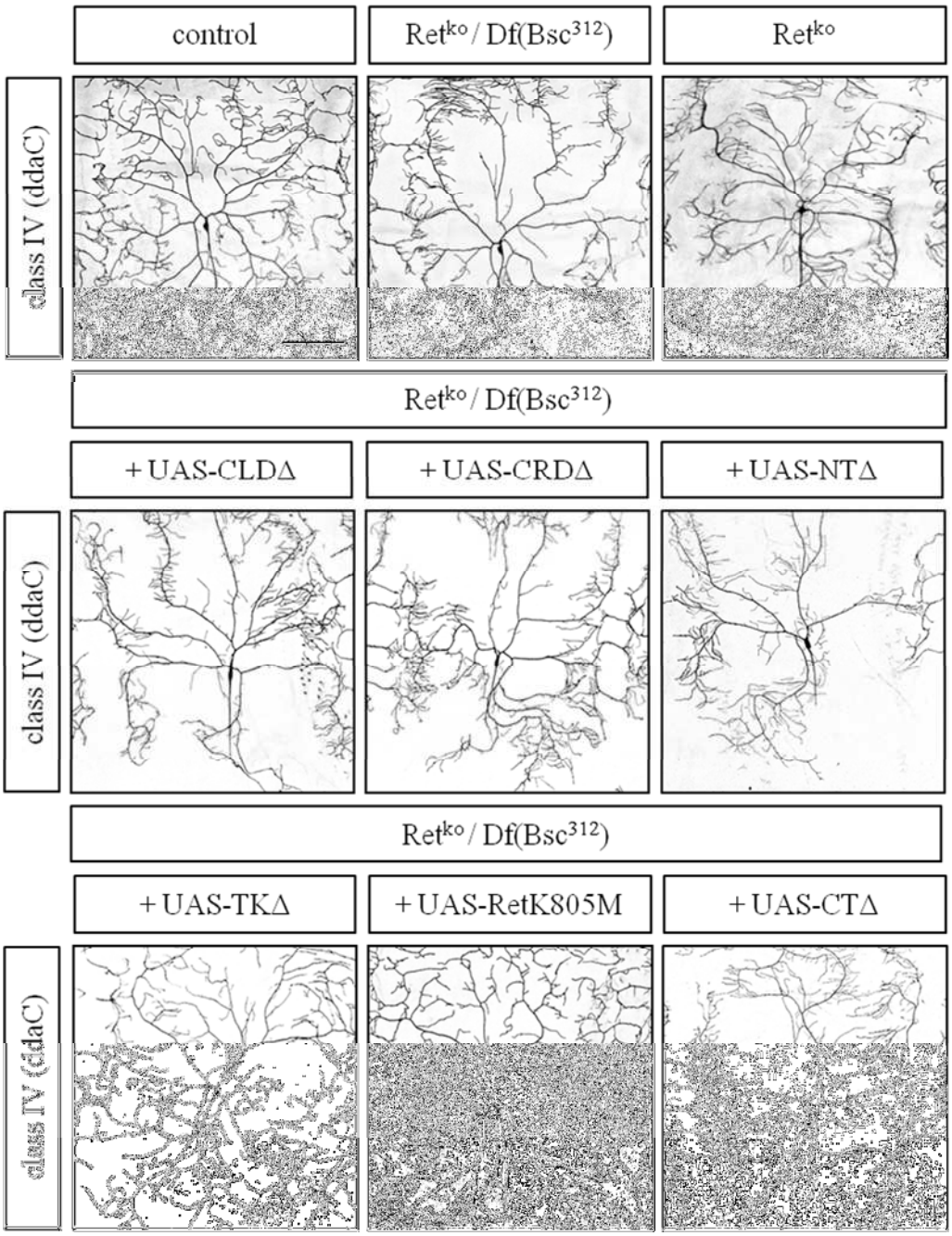

Figure 15. Ret function requires its extra- and intracellular domains but not its kinase activity for dendrite development. C4da neuron morphology in *Ret*^{ko} 3rd instar larvae expressing different Ret domain deletion transgenes (CLDΔ: Cadherin-like domain, CRDΔ: Cysteine-rich domain, NTΔ: extracellular domain deletion, TKΔ: Tyrosine kinase domain, RetK805M: Ret tyrosine kinase dead mutant CTΔ: intracellular domain deletion). Neurons were visualized by the expression of the C4da specific marker *ppk-Gal4>CD4-tdGFP*. Transgenes lacking extracellular domains of Ret (CLD and CRD) were not able to rescue C4da neuron morphology in *Ret*^{ko} background animals. In contrast, the

intracellular kinase domain (TK) and its activity were partially dispensable for C4da neuron dendrite morphogenesis. Transgenic rescue with transgenes lacking either the complete extracellular or intracellular domain of Ret were both unable to restore C4da neuron dendrite morphology. Scale bar: 100 µm.

In terms of total length of C4da neuron dendrites, Ret^{ko} animals expressing extracellular domain deletion transgenes of Ret still displayed significantly reduced dendritic length compared to *control* (CLDΔ: 13928 µm ± 1763, CRDΔ: 15941 µm ± 1098, NTΔ: 12617 µm ± 946) (Figure 15, Figure 16B). Expression of Ret transgenes with a deleted or inactive kinase domain showed a partial or complete rescue of the Ret^{ko} phenotype, respectively (TKΔ: 15928 µm ± 441, RetK805M: 15821 µm ± 1614), whereas Ret transgenes with a completely deleted C-terminus did not rescue the phenotype (CTΔ: 15053 µm ± 1450).

Examining isoneuronal dendritic crossing showed that Ret transgenes carrying extracellular domain deletions were not able to rescue crossing defects of Ret^{ko} C4da neurons (CLDΔ: 16.55 ± 1.95, CRDΔ: 17.7 ± 3.67, NTΔ: 10.11 ± 2.15). Ret transgenes with intracellular domain deletions however could completely rescue this phenotype (TKΔ: 6.24 ± 1.7, RetK805M: 7.28 ± 1.27, CTΔ: 4.27 ± 1.28) (Figure 15, Figure 16C).

For quantitative visualization of dendrite complexity, Sholl and Strahler analysis were performed. As described before, Ret^{ko} C4da neuron displayed reduced dendrite complexity in medial and distal parts compared to *control*. Further, Ret^{ko} C4da neurons displayed reduced number of dendrites of lower branch orders, but an increased number of higher ordered dendrites. These defects were rescued by C4da neuron specific overexpression of full-length Ret (Figure 17).

However, expression of Ret transgenes carrying extracellular domain deletions of Ret (CLDΔ, CRDΔ, NTΔ) were not able to rescue Ret^{ko} C4da neuron branching characteristics assayed by Sholl or Strahler analysis. They still exhibited a reduction of dendrite complexity and an increase in higher ordered branches (Figure 17A+C). With respect to intracellular domain deletion Ret transgenes, the kinase domain deletion or inactive Ret transgene could restore dendrite complexity. In contrast, the complete intracellular domain deletion of Ret was not able to rescue C4da neuron complexity defects (Figure 17B+D).

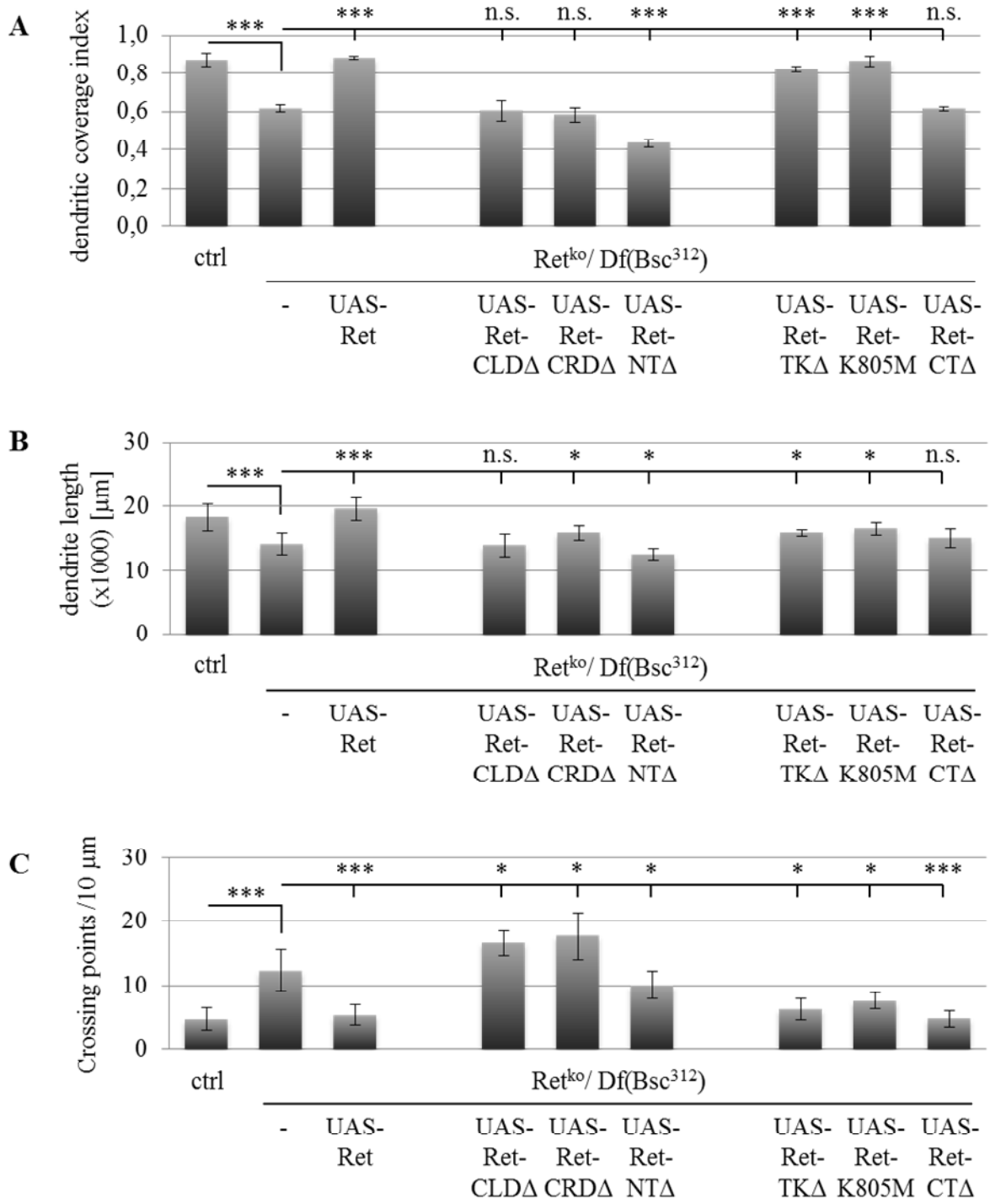

Figure 16. Ret function requires its extra- and intracellular domains but not its kinase activity are required for dendrite development. A) Quantitative analysis of the dendritic coverage index (ratio of dendrite field area and segment area) of C4da neurons of 3rd instar larvae. **B)** Quantitative analysis of the total length of C4da neuron dendrites. **C)** Quantitative analysis of isoneuronal dendritic crossing is shown for the indicated genotypes. C4da neurons expressing extracellular deletion transgenes of Ret (CLDΔ, CRDΔ, NTΔ) in *Ret^{ko}* larvae still displayed significantly severe C4da dendrite defects compared to *control*. Ret transgenes with a deleted (TKΔ) or inactive kinase domain (RetK805M) showed a partial or complete rescue of the *Ret^{ko}* phenotype, respectively. In contrast, neurons expressing Ret lacking the entire intracellular domain (CTΔ) did not show rescue capacity, except for the number of crossing points. All data are mean ± SD, Mann-Whitney-Test $p<0.05$ (*), $p<0.001$ (***), n=5.

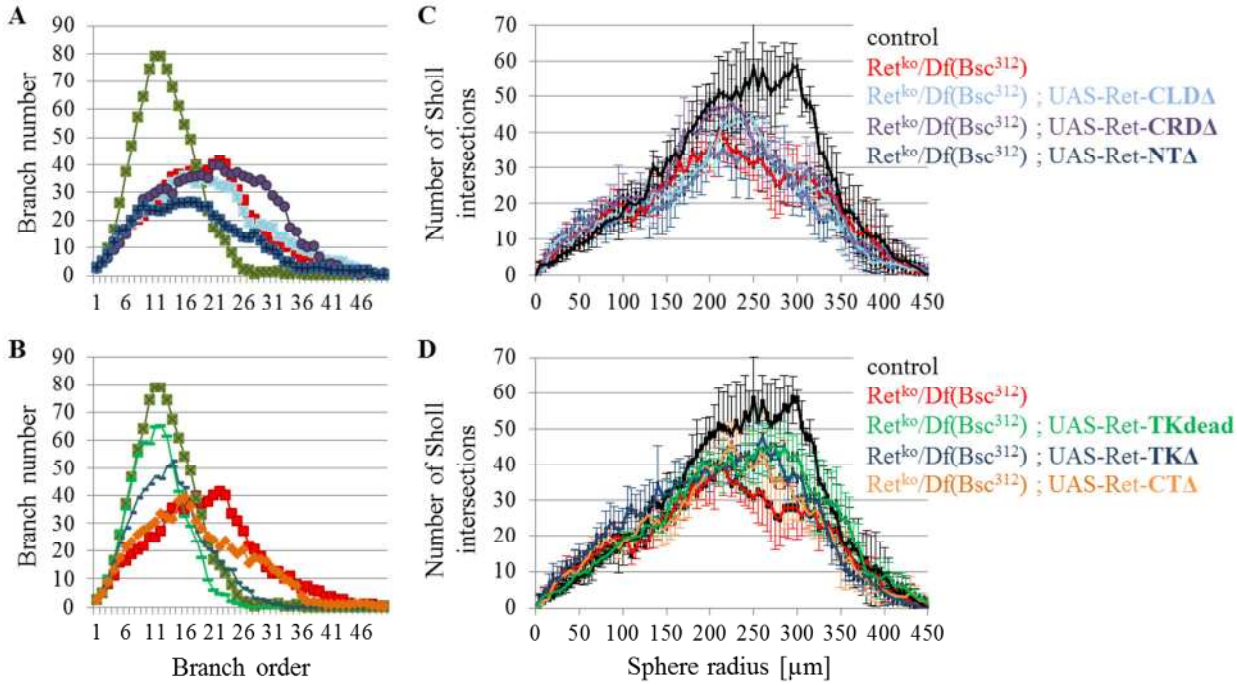

Figure 17. Characterization of *Ret* protein domain function in C4da neuron dendrite complexity. Strahler **(A-B)** and Sholl **(C-D)** analysis to quantitatively visualize dendrite complexity. *Ret*^{ko} C4da neurons display reduced number of dendrites of lower branch orders and an increased number of higher ordered dendrites. Specific C4da neuron expression of Ret transgenes lacking extracellular domains (CLDΔ: Cadherin-like domain, CRDΔ: Cysteine-rich domain, NTΔ: extracellular domain deletion) **(A+C)** or intracellular domains of Ret (TKΔ: Tyrosine kinase domain, RetK805M: Ret tyrosine kinase dead mutant CTΔ: intracellular domain deletion) in *Ret*^{ko} larvae **(B+D)**. Transgenes carrying extracellular domain deletions of Ret (CLDΔ, CRDΔ, NTΔ) were not able to rescue C4da neuron branching characteristics in *Ret*^{ko} larvae. In contrast, expression of a Ret kinase domain deletion or kinase-dead transgene could restore dendrite complexity. However, Ret lacking the entire intracellular domain was not able to rescue C4da neuron complexity defects. N=5.

To further analyze whether the overexpression of intra- or extracellularly truncated Ret already caused defects in dendrite morphology, *UAS-Ret-CTΔ* or *UAS-Ret-NTΔ* were expressed in C4da neurons using *ppk-Gal4>CD4-tdGFP* (Figure 18). The total length of C4da neuron dendrites in 3rd instar larvae was then quantitatively analyzed. The data showed that larvae overexpressing a Ret-transgene lacking the intracellular domain (*UAS-Ret-CTΔ*) displayed a mild but significantly increase in dendritic length of C4da neurons compared to *control* (*control*: 19782 µm ± 1106, CTΔ: 22797 µm ± 1429). In contrast, the dendritic length of neurons overexpressing Ret lacking the extracellular domain (*UAS-Ret-NTΔ*) was not significantly different from *control* (NTΔ: 20297 µm ± 1279).

This analysis showed that Ret is cell-autonomously required for C4da neuron dendrite patterning. Moreover, transgenic full-length Ret was able to completely rescue dendrite defects of C4da neurons in *Ret*^{ko} larvae.

The dataset further demonstrated that both extracellular domains of *Ret* are essential for C4da dendrite morphogenesis, whereas intracellular kinase domain and its activity are at

least partially dispensable for C4da neuron dendrite development. However, transgene lacking the entire intracellular domain did not show complete rescue activity indicating that other motifs within the C-Terminus of Ret protein are necessary for Ret function in C4da morphogenesis.

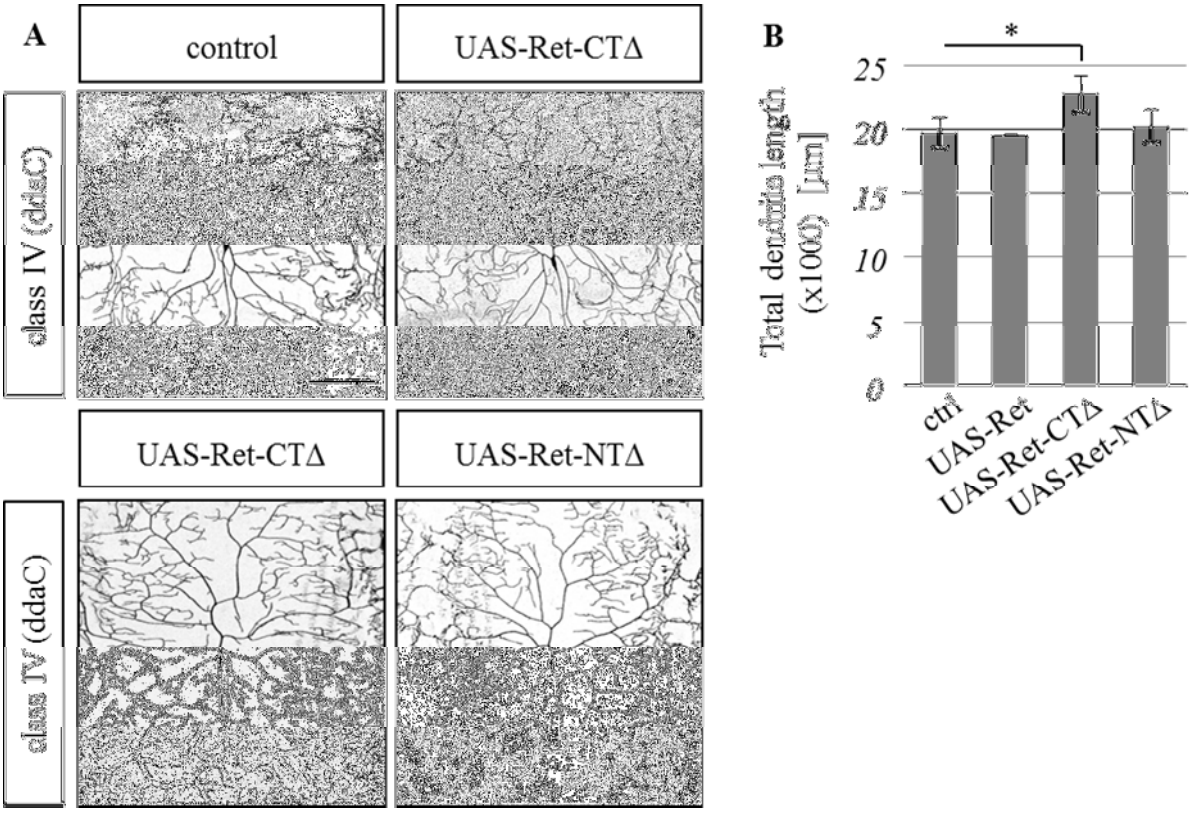

Figure 18. Overexpression of truncated Ret lacking its intracellular domain causes mild C4da dendrite overgrowth. A) Dendritic morphology of C4da neurons in 3rd instar larvae overexpressing full-length *Ret or* Ret lacking its intra- or extracellular domain (*UAS-Ret, UAS-Ret-CTΔ*, *UAS-Ret-NTΔ*) using *ppk-Gal4.* Neurons were visualized by the expression of the C4da specific marker *ppk-Gal4>CD4-tdGFP.* Scale bar: 100 µm. **B)** Quantitative analysis of the total length of C4da neuron dendrites. C4da neurons overexpressing a Ret transgene lacking the intracellular domain (*UAS-Ret-CTΔ*) displayed significantly increased dendritic length compared to *control*. All data are mean ± SD, Mann-Whitney-Test $p<0.05$ (*), n=5.

10.5 *Ret* is required for C4da neuron dendrite-ECM interaction

Ret^{ko} C4da neurons displayed dendritic crossing defects, which might be a consequence of loss of self-avoidance. C4da neuron dendrites are normally in close contact with the extracellular matrix (ECM), but can also detach and be embedded in the epithelium due to loss of adhesion to the ECM. To explore this in detail, C4da neuron dendrites were visualized by confocal microscopy using *ppk-CD4-tdTomato* together with a GFP protein trap labeling the ECM specific protein *trol* (*trol-GFP*) (Han et al., 2012) (Figure 19A'-A''').

The analysis revealed that under control conditions, most of the dendrites were in contact with the ECM and only a low number of dendrites showed no dendrite-ECM-interaction (1.85% ± 1.65). In contrast, *Ret*^{ko} C4da neurons displayed a significant increase of dendrites detached from the ECM (9.47% ± 1.1) (Figure 19B). Especially dendritic terminals of C4da neurons exhibited this defect, but detachment could also be observed along major branches.

To investigate whether these defects were Ret dependent and which domains of Ret are necessary for this function, cell-type specific C4da rescue experiments using full-length and truncated Ret transgenes (*UAS-Ret-NTΔ, UAS-Ret-CTΔ*) were performed.

Specific C4da neuron expression of full-length Ret in *Ret*^{ko} animals was able to rescue the ECM detachment phenotype (3.64% ± 0.91). However, both truncated Ret transgenes could not rescue these defects indicating that both, the intra- and extracellular domain are necessary for proper dendrite-ECM adhesion (*UAS-Ret-NTΔ*: 9.95% ± 1.41, *UAS-Ret-CTΔ*: 11.54% ± 2.12).

In summary, this dataset demonstrated that *Ret* is required for dendrite-ECM adhesion and 2D growth of C4da neurons. Further, it showed that Ret ectodomain interaction and appropriate intracellular downstream signaling in C4da neurons is likely required for its function.

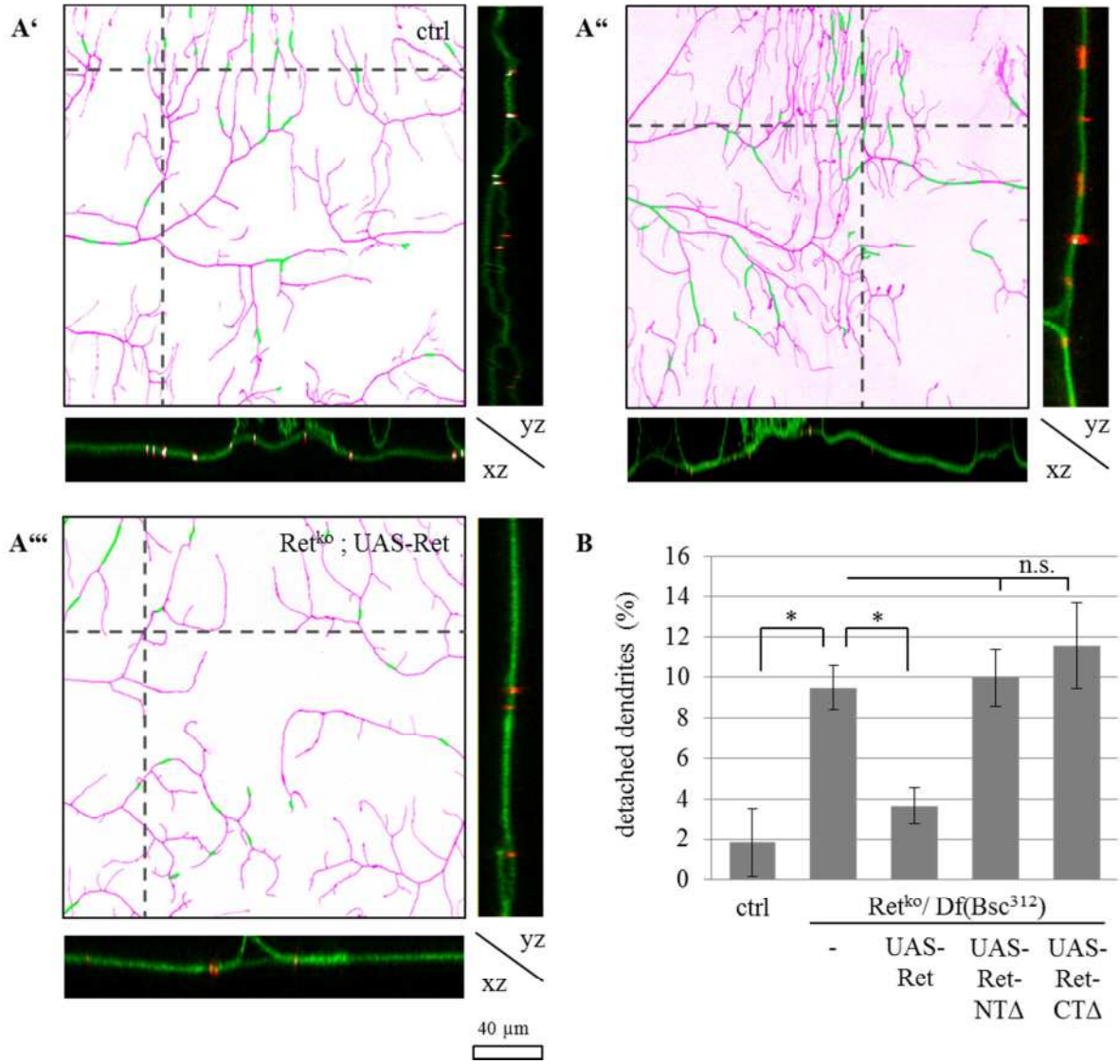

Figure 19. Loss of Ret impairs C4da neuron dendrite-ECM interaction. Analysis of dendrite-ECM interaction by high resolution two-color confocal imaging. 3rd instar larval C4da neuron dendrites along the dorsal midline were visualized together with the extracellular matrix by *ppk-CD4-Tom* and *trol-GFP*, respectively. Segments of ECM-detached C4da neuron dendrites along are indicated in green. **A')** As shown in cross sections (xz, yz; plane of cross section indicated by dashed line), *control* larvae exhibited a very small number of dendrites not being in contact with the ECM (dendrites: magenta, ECM: green, interaction: white). **A'')** In *Ret^{ko}* C4da neurons, a significant increase of detached dendrites could be observed, which could be rescued by C4da specific Ret transgene expression **(A''')**. Scale bar: 40 µm. **B)** Quantitative analysis of dendrite-ECM interaction in *control*, *Ret^{ko}* mutant larvae and after rescue by certain Ret transgenes (*UAS-Ret, UAS-Ret-NTΔ, UAS-Ret-CTΔ*) in C4da neurons (*ppk-Gal4*). Expression of full-length Ret in a *Ret^{ko}* background displayed a significant reduction of detached dendrites. Both truncated Ret transgenes lacking either the extra- or intracellular domain were not able to rescue detachment defects. All data are mean ± SD, Mann-Whitney-Test $p<0.05$ (*), n=4.

10.6 Ectopic but not cell-autonomous overexpression of Ret induces C4da neuron dendrite defects

The exclusive overexpression of Ret transgenes in C4da neurons showed that the increase in Ret protein had no morphologically negative effect on these neurons (Figure 20A).

To test whether ectopic overexpression of Ret in non-Ret expressing sensory neurons causes morphological changes, Ret was overexpressed in all sensory da neurons using *21-7-Gal4* to test if ectopic Ret overexpression might affect C4da neuron morphogenesis.

Surprisingly, pan-sensory neuron overexpression of full-length Ret using the *21-7-Gal4* driver resulted in a severe C4da neuron specific phenotype (Figure 20B) characterized by reduced dendritic field coverage similarly to a *Ret* loss-of-function phenotype. C4da neuron specific defects were still present when overexpressing a Ret transgene lacking the intracellular domain, but not when lacking the extracellular domain (*UAS-Ret-NTΔ*) (Figure 20B).

This result indicated that the ectodomain of Ret is required for ectopic influence on C4da neuron dendrite growth. The most severe defects were typically observed within the anterior part of the C4da neuron dendritic field correlating with the domain of class I or class II neurons.

These results raised the question whether ectopic Ret overexpression in surrounding tissues affected C4da neuron dendrite morphology similarly to pan-sensory neuron overexpression.

For this purpose, full-length and truncated Ret transgenes (*UAS-Ret, UAS-Ret-CTΔ, UAS-Ret-NTΔ*) were overexpressed in the epidermis using an epithelial cell-specific *Gal4* line (*A58-Gal4*). The morphology of C4da neurons of 3rd instar larvae was visualized by *ppk-CD4-tdTomato* using confocal microscopy (Figure 21). In *control* larvae, epithelial overexpression of Ret showed a dramatic C4da neuron dendrite phenotype which depended on the extracellular, but not the intracellular domain of Ret. Epithelial expression of full-length Ret resulted in a very strong reduction of the of C4da neuron dendritic tree with only a part of the major branches being developed. Furthermore, the C4da neuron axon diameter was enlarged compared to *control* axons. This phenotype was less dramatic but still severe upon overexpression of the Ret transgene lacking the intracellular domain (*UAS-Ret-CTΔ*). The coverage of C4da neuron dendrites was highly reduced, but axon morphology seemed not to be affected. Epithelial overexpression of the Ret transgene lacking the extracellular domain (*UAS-Ret-NTΔ*) did not affect C4da neuron dendrite morphology and was comparable to *control*.

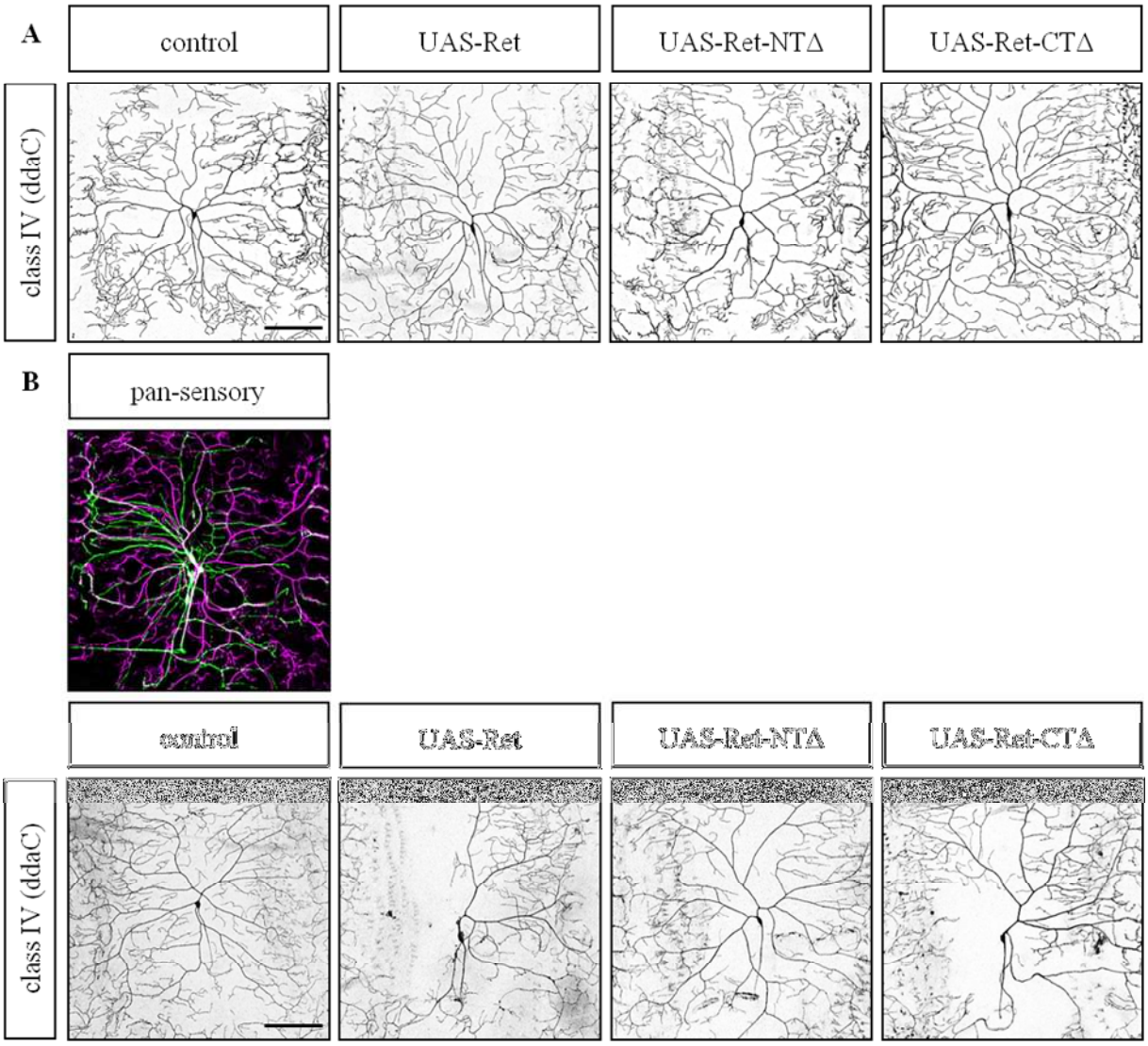

Figure 20. Ectopic but not cell-autonomous overexpression of Ret induces C4da neuron dendrite defects. A) Dendritic morphology of C4da neurons in *control* larvae compared to overexpression of different Ret transgenes (*UAS-Ret, UAS-Ret-CTΔ, UAS-Ret-NTΔ*) using C4da specific driver (*ppk-Gal4*). Neurons of 3rd instar larvae were visualized by the expression of the specific marker *ppk-Gal4>CD4-tdGFP*. **B)** Dendritic morphology of C4da neurons in *control* animals compared to overexpression of different Ret transgenes (*UAS-Ret, UAS-Ret-CTΔ, UAS-Ret-NTΔ*) using a pan-sensory *Gal4*-driver (*21-7-Gal4*). 3rd instar C4da neurons were visualized by the expression of the specific marker *ppk-CD4-tdTomato* (shown in magenta). Sensory da neurons were visualized by *UAS-CD8-GFP* transgene (green). Overexpression of Ret transgenes in C4da neurons showed no morphologically negative effect. Pan-sensory da neuron overexpression of full-length Ret using the *21-7-Gal4* driver resulted in a severe C4da neuron specific phenotype. This effect depended on the ectodomain of Ret since C4da neuron defects were still present when overexpressing a Ret transgene lacking the intracellular domain, but not when lacking the extracellular domain. Scale bar: 100 µm.

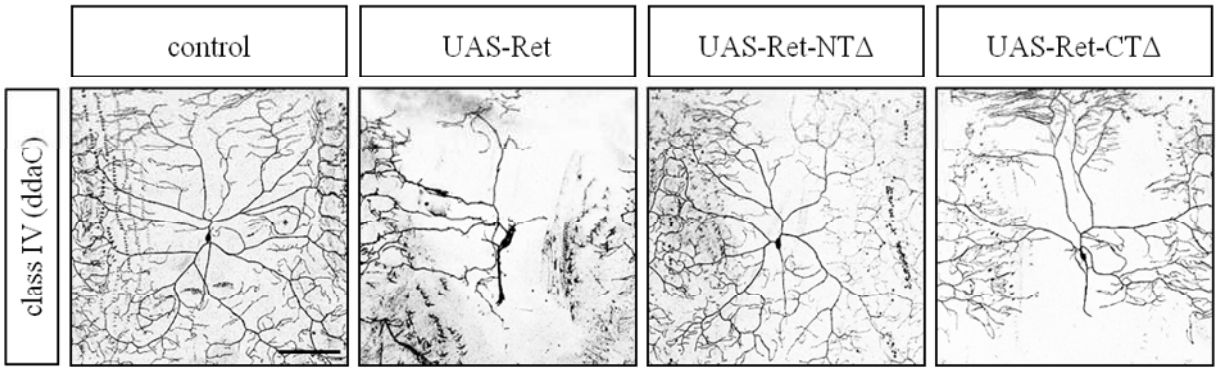

Figure 21. Epithelial overexpression of Ret impairs C4da neuron dendritic field development. Morphology of C4da neurons in *control* animals compared to overexpression of different Ret transgenes (*UAS-Ret, UAS-Ret-CTΔ, UAS-Ret-NTΔ*) using the epithelial *Gal4*-driver *A58-Gal4*. C4da neurons of 3rd instar larvae were visualized by the expression of the specific marker *ppk-CD4-tdTomato*. Epithelial overexpression of Ret resulted in a dramatic C4da neuron dendrite phenotype which depended on the extracellular, but not the intracellular domain of Ret indicated by a very strong reduction of the of C4da neuron dendritic tree with only a part of the major branches being developed. Scale bar: 100 µm.

It has previously been shown that a hypomorphic mutant of Ret (*Ret^{C168}*) showed a C4da neuron dendritic phenotype already at early larval stages (Soba et al., 2015). The epithelial *Gal4*-driver (*A58-Gal4*) used here starts expression at larval stage (L1), however its broad expression pattern within the epithelium impeded a more restricted analysis.
To examine the effect of Ret overexpression within a restricted epithelial domain the early epithelial driver *engrailed (en)-Gal4* was used. *En-Gal4* expression is restricted to the posterior compartment within each body wall segment. The anterior part of each C4da neuron dendrite field could thus be used as an internal control. The following overexpression analysis was performed as described above. The morphology of C4da neurons of 3rd instar larvae was visualized by the expression of the specific marker *ppk-CD4-tdGFP*. The posterior expression domain of the *engrailed-Gal4* driver was visualized by nuclear mCherry.

Strikingly, ectopic overexpression of *Ret* (*UAS-Ret-mCherry*) in the epithelium using *en-Gal4* prevented ingrowth of C4da neuron dendrites into the *engrailed* expression domain (Figure 22A). This severe effect on C4da neuron development depended on the Ret extracellular but not intracellular domain, as overexpression of the corresponding truncated transgenes showed an equally strong (*UAS-Ret-CTΔ*) or no (*UAS-Ret-NTΔ*) phenotype, respectively. The quantification of dendritic coverage revealed that ectopic expression of the full-length Ret or *Ret-CTΔ* led to a reduced coverage of 15-20% within the posterior compartment compared to ~ 90% within the anterior compartment. This result was significantly different from *control* conditions (p-value<0.01). By contrast, expression of truncated Ret lacking its ectodomain had no significant effect on dendritic coverage showing that the ectodomain of Ret is required for ectopic influence on C4da neuron dendrite growth (Figure 22B).

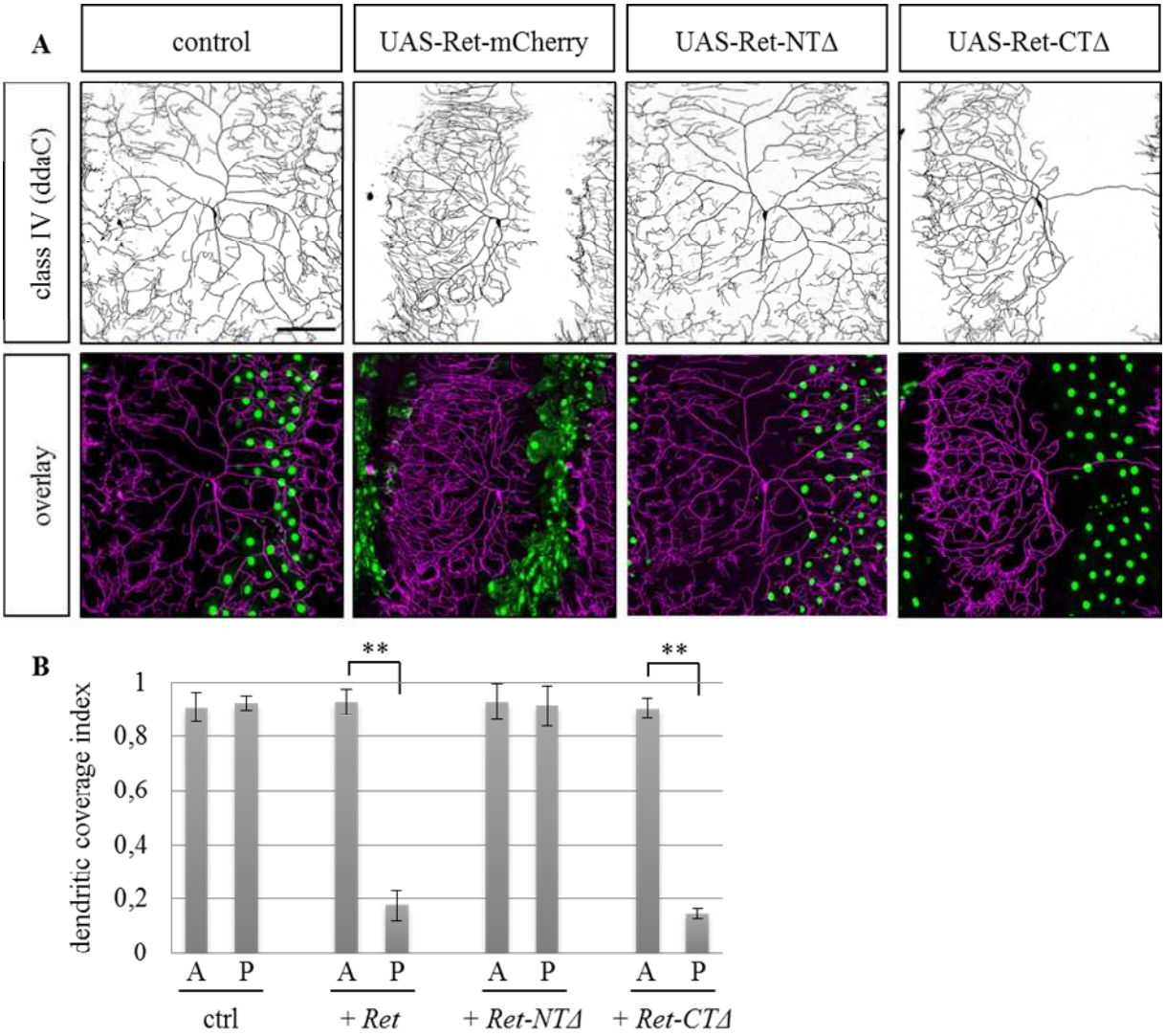

Figure 22. Ret overexpression in the posterior epithelium causes C4da neuron specific dendrite defects and depended on the Ret N-Terminus. A) Dendritic morphology of C4da neurons in *control* animals compared to overexpression of different Ret transgenes (*UAS-Ret, UAS-Ret-CTΔ, UAS-Ret-NTΔ*) using the early epithelium *Gal4*-driver (*engrailed-Gal4*), with its posterior expression domain visualized by nuclear mCherry (green). C4da neurons of 3rd instar larvae were visualized by the expression of the specific marker *ppk-CD4-tdGFP* (magenta). Scale bar: 100 µm. **C)** Quantitative analysis of the dendritic coverage in the anterior (A) or posterior (P) field of C4da neuron. Ectopic overexpression of *Ret* prevented ingrowth of C4da neuron dendrites into the restricted expression domain and depended on the Ret extracellular but not intracellular domain. Quantification of the dendritic coverage revealed that ectopic expression of the full-length Ret or *Ret-CTΔ* significantly reduced dendritic coverage within the posterior compartment compared to the anterior compartment. Overexpression of Ret lacking the ectodomain had no significant effect on dendritic coverage. All data are mean ± SD, Mann-Whitney-Test $p<0.01$ (**), n=6.

To investigate whether other da sensory neurons are affected by Ret transgene overexpression, sensory neurons were visualized immunohistochemically in larval fillet preparations using an anti-HRP antibody. Ectopic overexpression of Ret exclusively affected dendrite development of C4da neurons, as other sensory neurons did show normal growth into the *en* expression domain (Figure 23). At the morphological level other da neurons were

not affected by epidermal Ret overexpression showing its specific effect on C4da neuron morphology.

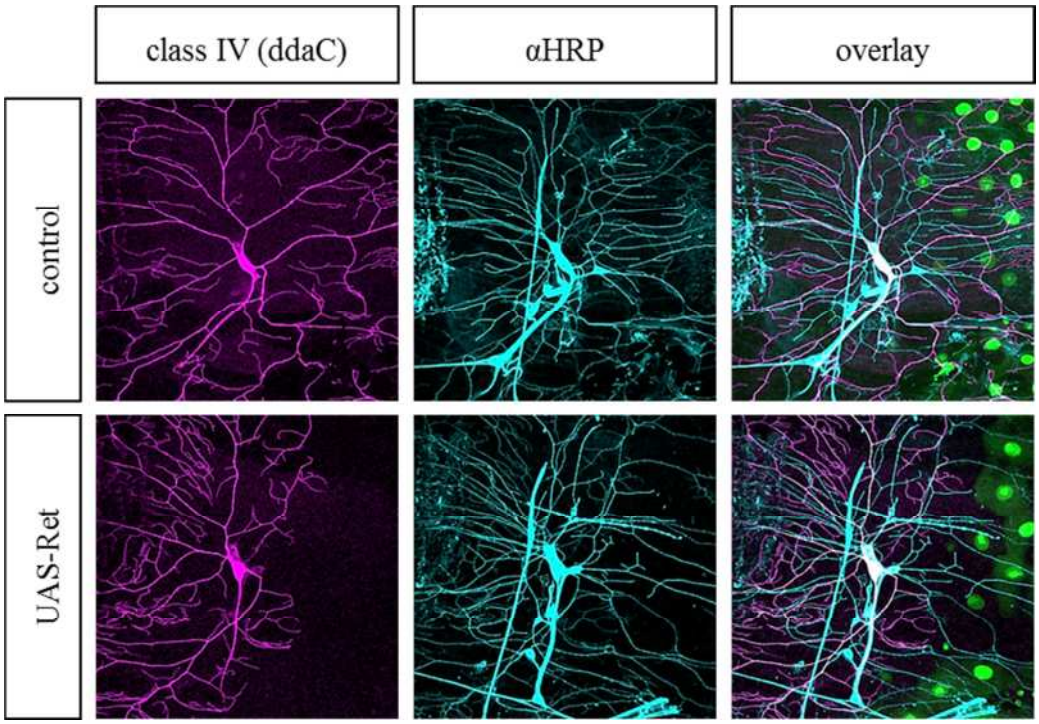

Figure 23. Epidermal overexpression of Ret specifically affects C4da neuron dendrite growth. To investigate whether da sensory neurons are generally affected by Ret transgene overexpression, fillet preparations of 3rd instar larvae were immune-stained with anti-HRP antibody (cyan). Dendritic morphologies were compared under control conditions or with epithelial overexpression of Ret *engrailed-Gal4*). The *engrailed*-driver domain was visualized by nuclear mCherry (green). C4da neurons were visualized by the expression of the specific marker *ppk-CD4-tdGFP* (magenta). The result showed that ectopic overexpression of Ret exclusively affected dendrite development of C4da neurons. Scale bar: 100 µm.

10.7 Ectopic overexpression of Ret alters C4da neuron dendrite dynamics

As described in chapter 10.6, the ectopic expression of Ret in the epithelium resulted in a severe C4da neuron dendrite phenotype. Especially Ret overexpression under the control of *en-Gal4* resulted in a virtually complete absence of C4da neuron dendrites within the expression domain.

C4da neuron dendrites are highly dynamic and terminal dendrites display significant turnover by growth and retraction (Stewart et al., 2012; Zheng et al., 2008), which might be altered due to ectopic Ret expression. To analyze possible alterations in dendrite dynamics of C4da neurons Ret was overexpressed with *en-Gal4*, which allowed for internal comparison of dendrite dynamics within the posterior Ret overexpression domain and the anterior control field within the same neuron.

The morphology of C4da neurons of 3rd instar larvae were visualized by the expression of the specific marker *ppk-CD4-tdGFP*. The C4da neuron dendrite field was imaged at 96 hrs AEL and dendrite growth and the dynamics within a 5 min time period were compared between anterior and posterior compartments (retraction: red, stability: grey, growth: green) (Figure 33A). It is worth noting that overexpression of full-length Ret induced a phenotype in epithelial cells resulting in abnormal cell shape compared to *control* cells (data not shown). As this effect was likely due to its tyrosine kinase activity, a Ret transgene lacking the intracellular domain was chosen instead.

As shown in the previous experiment (Figure 22), no ingrowth of C4da neuron dendrites was observed within the *engrailed* domain expressing the Ret-CTΔ. For a more detailed analysis, the relative speed of terminal dendrites [µm/min] of *control* C4da neurons was compared to larvae overexpressing Ret-CTΔ in the *engrailed* domain.

The quantitative analysis revealed no significant difference of growing (green) and retracting (red) terminal ends of *control* neurons within the anterior (A) and posterior (P) dendritic field (Figure 24B). For growing terminal dendrites a speed of 0.23 µm/min ± 0.04 (A) and 0.27 µm/min ± 0.11 (P) was measured, and for retracting terminal dendrites a speed of -0.21 µm/min ± 0.03 (A) and -0.26 µm/min ± 0.07 (P) was calculated. Ectopic overexpression of Ret-CTΔ showed no significant difference in the speed of retracting C4da neuron terminal endings (-0.27 µm/min ± 0.06 (A) and -0.30 µm/min ± 0.08 (P)). However, the speed of growing terminal endings was significantly slower in the posterior compared to the anterior compartment (0.30 µm/min ± 0.08 (A) and 0.16 µm/min ± 0.07 (P), p-value<0.05).

This result showed that ectopic Ret expression negatively influences dendrite growth dynamics of C4da neurons and this effect depends on the ectodomain of Ret.

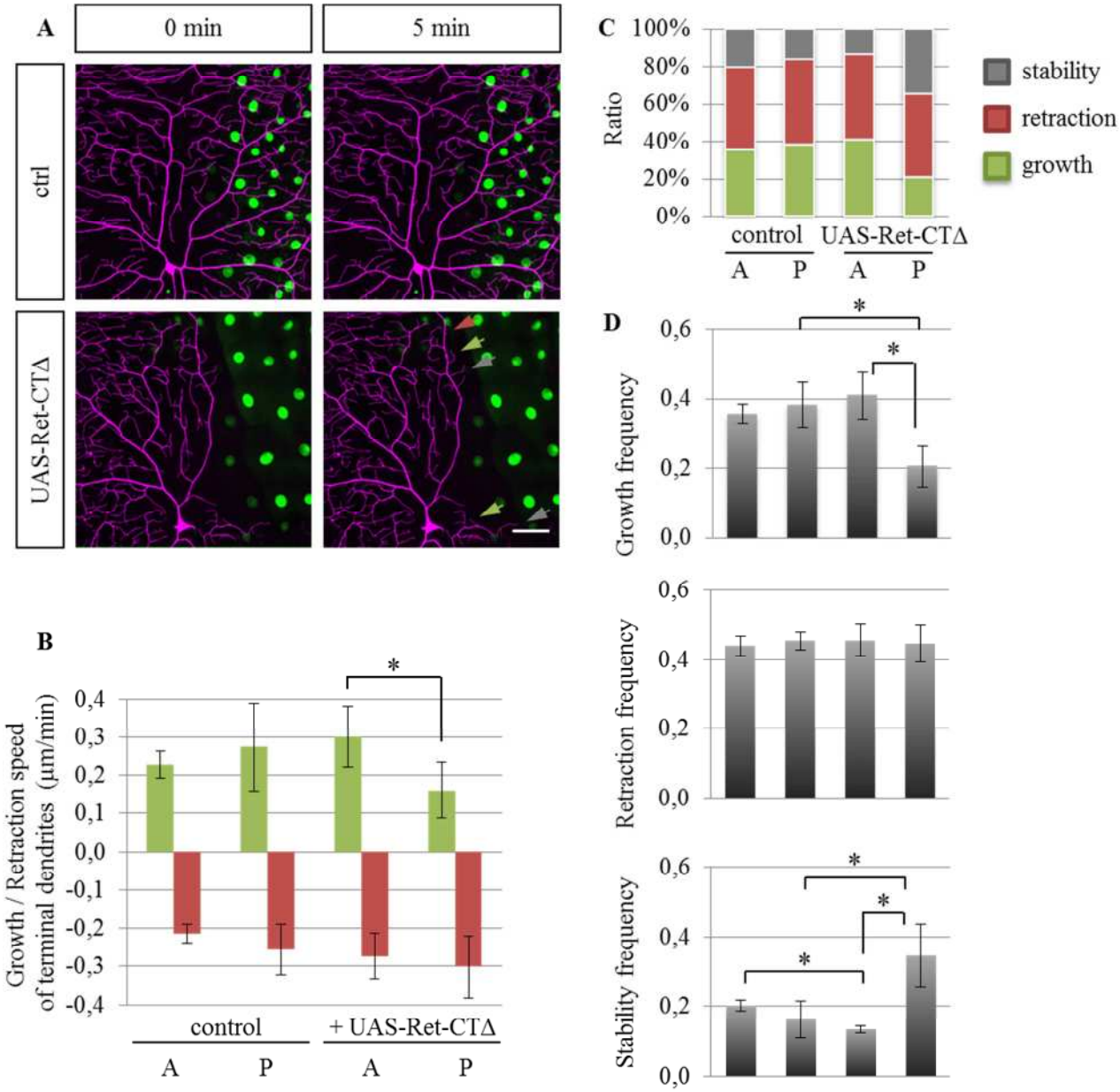

Figure 24. Ectopic Ret expression affects C4da neuron dendrite dynamics. A) Dorsal dendritic field of ddaC in *control* 3rd instar larvae compared to larvae overexpressing Ret lacking the intracellular domain (*UAS-Ret-CTΔ*) using *engrailed-Gal4* (green). C4da neurons were visualized by the expression of the specific marker *ppk-CD4-tdGFP* (magenta). Representative images show the dynamic changes of terminal dendrites after 5 min (arrows; green: growing, grey: stable, red: retracting) in the anterior (A) and posterior (P) domain of the dendritic field. N=347,149 (number of all terminals of 3 and 5 neurons in *control* and *UAS-Ret-CTΔ* larvae, respectively). Scale bar: 50 µm. **B)** Quantification of growth (green) and retraction (red) speed of terminal branches (µm/min). Ectopic Ret expression resulted in decreased growth speed within the posterior domain of C4da neurons. **C)** Quantification of relative amount of growth (green), stability (grey) and retraction (red) after 5 min of time-lapse imaging. Ectopic Ret overexpression resulted in a reduction of growing dendrites within the posterior compartment of C4da neurons. In contrast, the number of stable dendrites was increased. **D)** Quantification of growth, stability and retraction frequency after 5 min of time-lapse imaging. Ectopic Ret overexpression resulted in a reduction of growing dendrites within the posterior compartment of C4da neurons. The frequency of retracting terminal endings was not affected. The frequency of stable dendrites was increased in the posterior domain after ectopic Ret overexpression. Compared to *control* neurons, the stability frequency was also decreased in the anterior domain.

To analyze relative dendrite dynamics, the number of growing, stable and retracting terminal endings within a 5 min timeframe was calculated. For *control* neurons, similar percentages of each category were found for the anterior (A) and posterior (P) domain: 44% (A) and 46% (P) of retracting dendrites, 36% (A) and 38% (P) of growing dendrites and 20% (A) and 16% (P) of stable dendrites (Figure 24C).
In larvae expressing Ret-CTΔ in the *engrailed* domain, the analysis of C4da neuron terminal endings within the anterior (A) domain revealed a quite similar distribution as *control* larvae: 46% retracting, 41% growing and 14% of stable terminal endings. Unlike the anterior domain, the percentile distribution within the posterior domain was changed. Here, the relative value of growing terminal endings was decreased by half (21%) compared to growing terminal endings within the anterior domain, whereas the percentage of stable terminal endings was increased 2-fold (35%). Only the relative value of retracting terminal endings was comparable to all other previous results (45%).
Furthermore, the relative change of dendritic growth/stability/retraction was normalized by the total changes to calculate the frequency of each event (Figure 24D). As already indicated before, the frequency of retracting terminal endings (retracting events/total number) was not affected. For all states a frequency of ~ 0.45 was calculated (*control*: 0.44 ± 0.03 (A), 0.46 ± 0.03 (P), *UAS-Ret-CTΔ*: 0.46 ± 0.05 (A), 0.45 ± 0.05 (P)).
For *control* neurons, no difference in growth frequency between the two compartments was measured (*control*: 0.36 ± 0.03 (A), 0.38 ± 0.06 (P)). In contrast, ectopic overexpression of Ret-CTΔ using *engrailed-Gal4* showed a significantly decreased growth frequency reducing growing terminals by 50% within the posterior domain. Interestingly, the frequency within the anterior domain was similar to *control* (*UAS-Ret-CTΔ*: 0.41 ± 0.07 (A), 0.21 ± 0.06 (P), p-value<0.05).
The frequency of stable terminals of *control* neurons was rather similar in both, the anterior and posterior compartment (0.20 ± 0.02 (A), 0.16 ± 0.05 (P)). However, ectopic Ret overexpression led to a significant increase of stable dendrite terminals within the *engrailed* expression domain compared to anterior (0.13 ± 0.01 (A), 0.35 ± 0.09 (P), p-value<0.05).

In summary, epithelial overexpression of Ret induced a C4da neuron dendrite phenotype resulting in strongly reduced coverage of their receptive field. Besides that, the amount of stable dendrites exhibiting less dendritic growth was increased within the *engrailed* domain correlating with the non-coverage of C4da neuron dendrites. Combining these two results might be an explanation that the presence of ectopic Ret prevented C4da dendrite ingrowth into the *engrailed* expression domain by changing the dendrite stability and dynamics of C4da neurons.

10.8 Candidate screening of TGFβ family members as potential interaction partners in Ret signaling

To identify potential ligand/s required for Ret signaling in C4da neurons, a candidate screen was performed using transgenic UAS lines. In the mammalian system, Ret receptor activation is mediated by a complex of glial cell line-derived neurotrophic factor (GDNF) and GDNF family receptor α-1 (GFR α-1). However, GDNF is not conserved in *Drosophila melanogaster*. The co-receptor GFR-like is not expressed in C4da neurons and its loss-of-function did not reveal a phenotype in C4da neurons. Therefore, the closest homologs of GDNF in *Drosophila*, the transforming growth factor-beta (TGFβ) family ligands *melanogaster*, were investigated as potential candidate ligands for Ret.

10.8.1 The TGFβ *maverick* is implicated in C4da neuron dendrite development

To identify a potential role of TGFβ members in C4da neuron dendrite morphogenesis, an *in vivo* overexpression screen was performed. Five transgenic UAS lines of TGFβs (dActivin [dAct], dawdle [daw], glass-bottom boat [gbb], maverick [mav] and myoglianin [myo]) were expressed in either C4da neurons (*ppk-Gal4>CD4-tdGFP)* or in the epidermis *(A58-Gal4; ppk-CD4-tdTomato)*.

Overexpression of each TGFβ member in C4da neurons did not affect their dendrite morphology (Figure 25A). Interestingly however, the epithelial overexpression of maverick (mav), but none of the other TGFβ members induced a strong C4da neuron dendrite phenotype (Figure 25B). Mav overexpression led to reduced C4da neuron dendritic field coverage, but proximal branching and growth was highly increased with higher ordered branches showing an increase in isoneuronal dendritic crossing events. Moreover, the higher order branches and terminals appeared thinner than *control* dendrites. These results provided the first evidence that the TGFβ ligand mav is implicated in C4da neuron dendrite development.

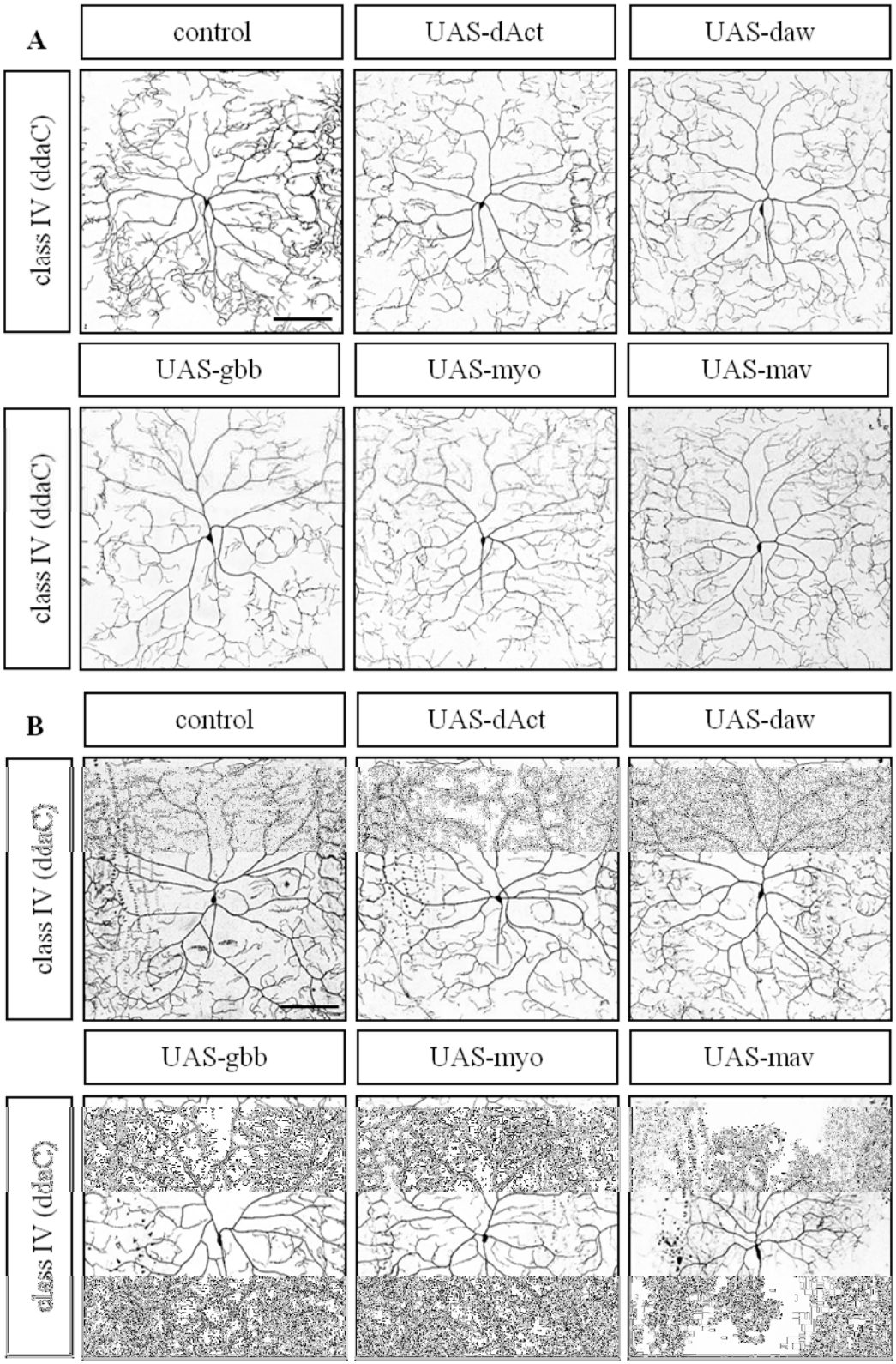

Figure 25. Epithelial overexpression of the TGFβ ligand *maverick* impairs C4da neuron dendrite growth. Dendritic morphology of C4da neurons under control conditions compared to overexpression of *UAS-TGFβ* transgenes (dAct, daw, gbb, myo and mav) using the C4da neuron *Gal4*-driver (*ppk-Gal4* (A)) and an epithelial driver (*A58-Gal4* (B)). C4da neurons of 3rd instar larvae were visualized by the expression of the specific marker *ppk-Gal4>CD4-tdGFP* (A) or *ppk-CD4-tdTomato* (B). Epithelial overexpression of maverick but none of the other TGFβ members induced a strong C4da neuron dendrite phenotype indicated by reduced dendritic field coverage. Scale bar: 100 µm.

10.8.2 *Mav* is endogenously expressed in epithelial cells but not in sensory neurons

In order to investigate the source of mav expression, a GFP enhancer trap line containing a Minos-mediated integration cassette (MiMIC) transposon inserted within the 5'UTR in front of the coding sequence of *mav* gene was used (Mi{MIC}mav^{MI05038}), which allowed the analysis of the *mav* expression domain *in vivo*. For this purpose, the *mav* GFP enhancer trap line was crossed to the C4da neuron specific marker *ppk-CD4-tdTomato* to detect mav enhancer activity and its distribution or occurrence along C4da neuron dendrites. No GFP-signal was detected within sensory neurons including C4da neurons. Instead, GFP expression was limited to epithelial cells and not detected in muscle attachment cells or muscles (Figure 26C). It remains to be determined if *mav* forms an expression gradient or if it is expressed in certain hot spots during development.

Since epithelial cells showed mav protein expression and also act as a substrate promoting sensory neuron dendrite growth, this finding supports the hypothesis that mav protein expressed in the epidermis is secreted and regulates C4da neuron dendrite growth.

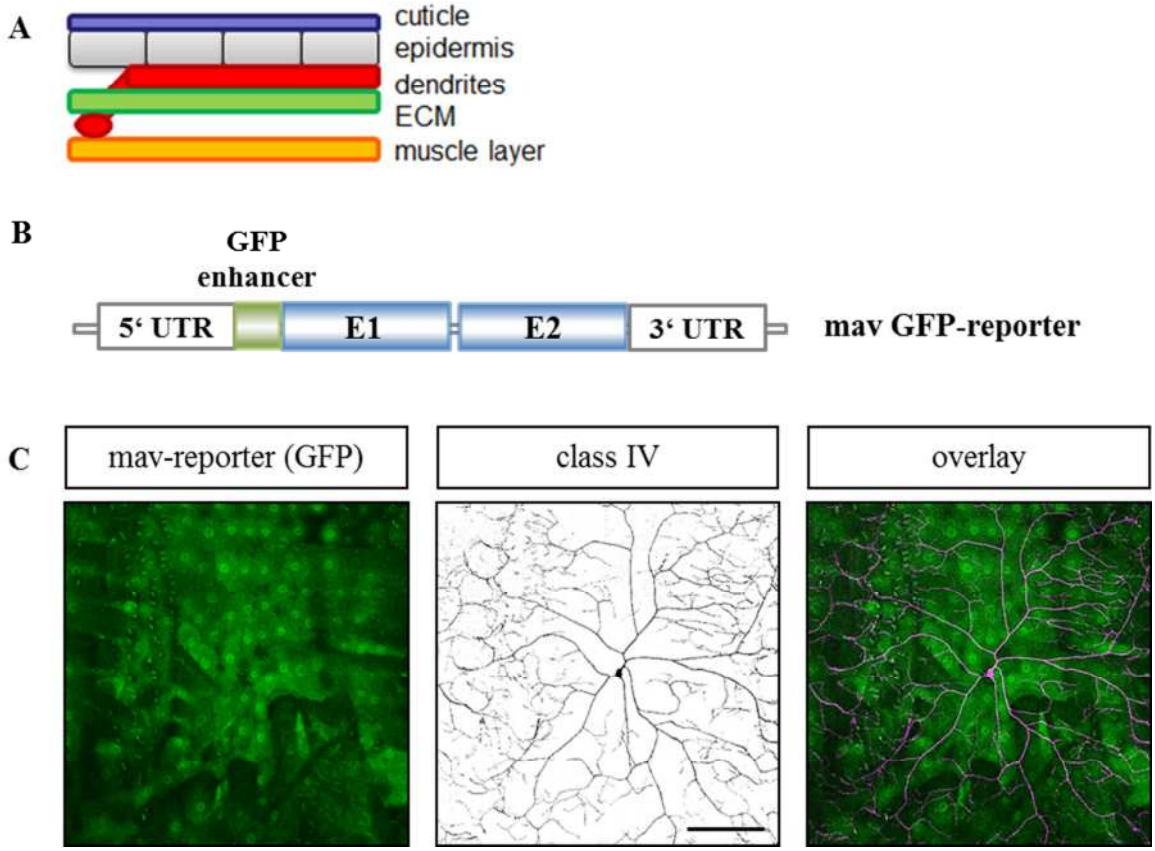

Figure 26. *Mav* is expressed in epithelial cells but not in sensory neurons. A) Schematic illustration of C4da neuron dendrites, extracellular matrix (ECM) and epithelial interaction. Dendrites of C4da neurons grow in a 2D plane and are attached to the ECM. The soma is located between the ECM and the muscle layer. **B)** Scheme of mav enhancer reporter carrying a GFP fluorescent marker inserted in the 5' region of the *mav* genomic locus. **C)** Analysis of mav expression using the mav enhancer reporter. The reporter line was crossed to a C4da neuron marker (*ppk-CD4-tdTomato*). GFP-signal was detected in epithelial cells but not in sensory neurons. Scale bar: 100 µm.

10.8.3 Epithelial downregulation of *mav* affects C4da neuron dendrite development

To verify that the observed morphological defects induced by mav overexpression were specific and to test whether endogenous mav plays a role in C4da neuron development, mav expression was targeted by RNAi. Two independent RNAi-transgenes of mav (either on 2nd or 3rd chromosome) were expressed in the epithelium by using the epithelial driver *A58-Gal4* together with the C4da neuron specific marker *ppk-CD4-tdTomato* (Figure 27A). Quantitative analysis showed that the RNAi mediated knock-down of mav significantly decreased dendritic length of C4da neurons using either RNAi-transgene (2nd or 3rd chromosome) when compared to *control*. (18088 µm ± 845, 15882 µm ± 1385, 15381 µm ± 454, p-value<0.05) (Figure 27B). Further, Strahler analysis revealed reduced dendrite complexity of C4da neuron dendrites after *mav* knock-down compared to *control* (Figure 27C). The reduced field coverage and dendrite complexity were similarly impaired with both independent mav RNAi-transgenes indicating a specific role of mav in C4da neuron dendrite growth.

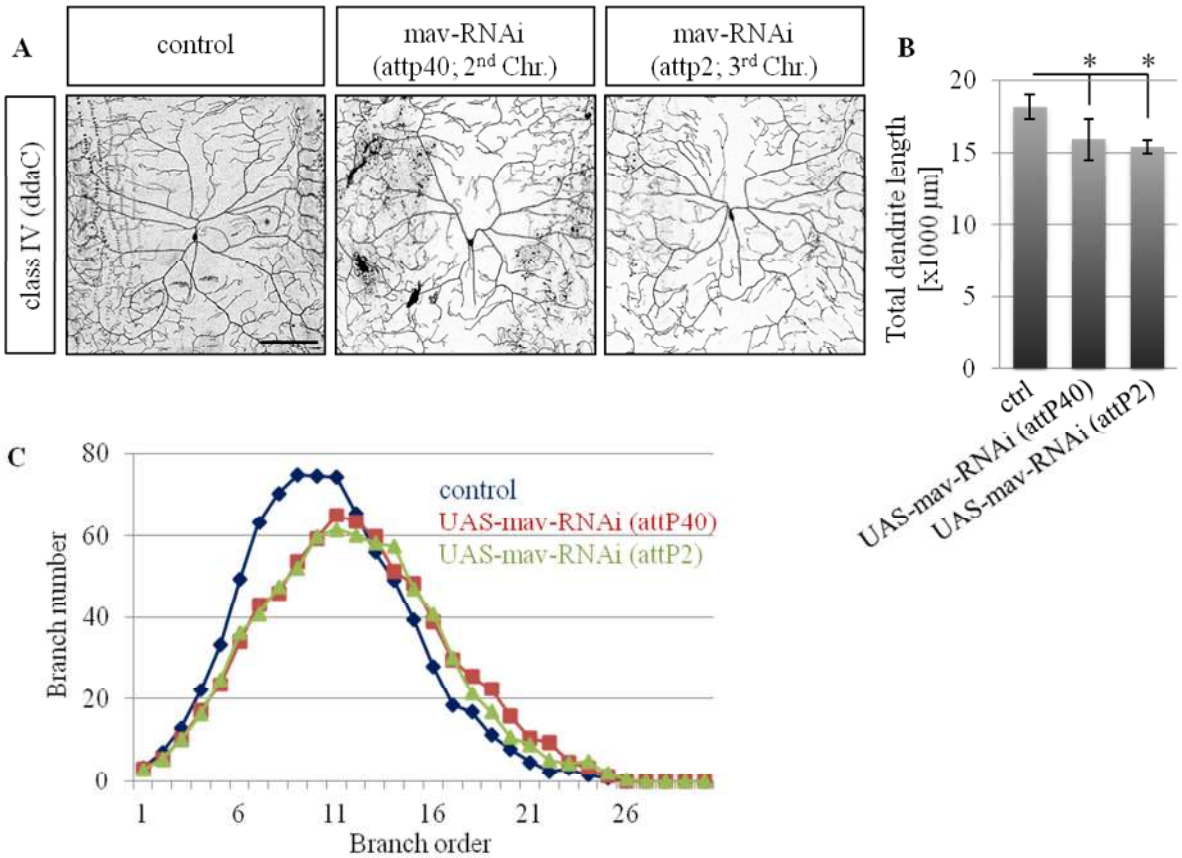

Figure 27. *Mav* knock-down in the epithelium causes mild C4da neuron dendrite phenotypes. A) Dendritic pattern of 3rd instar larvae C4da neurons in *control* compared to neurons expressing RNAi-transgenes of mav (2nd or 3rd chromosome) in the epithelium using *A58-Gal4*. Neurons were visualized by the expression of the C4da specific marker *ppk-CD4-tdTomato.* Scale bar: 100 µm. **B)** Quantitative analysis of the total length of C4da neuron dendrites of the indicated genotype. **C)** Strahler analysis to quantitatively visualize dendrite complexity. The numbers of dendrites are plotted against the increasing branch order. RNAi mediated knock-down of mav significantly decreased dendritic length and reduced dendrite complexity of C4da neuron dendrites compared to *control*. All data are mean ± SD, Mann-Whitney-Test p<0.05 (*), n=5.

10.8.4 Epithelial *mav* expression promotes and directs C4da neuron dendrite growth

The up- and downregulation of mav within the epithelium seemed to have opposite effects on C4da neuron dendrite growth. To analyze this in more detail, *engrailed-Gal4* was used to verify whether *mav* deregulation affects dendrite growth directionality during development.
Control larvae were compared to animals overexpressing mav (*UAS-mav*) or RNAi mediated knock-down of mav (*mav-RNAi*) in the posterior epithelium using *en-Gal4* (Figure 28A). The driver expression domain in the posterior compartment was visualized by nuclear mCherry together with the C4da neuron marker *ppk-CD4-tdGFP*.
The overexpression of mav enhanced dendrite growth of C4da neurons into the *en-Gal4* expression domain. In contrast, the knock-down of mav within the posterior field resulted in a reduction of C4da neuron dendrites. The quantitative analysis of the dendritic coverage index and filament dendrite length in the anterior (A) or posterior (P) field of C4da neurons of 3rd instar larvae confirmed this observation (Figure 28B). In the anterior compartment of the C4da neuron dendritic field, mav-overexpression (*UAS-mav*) resulted in significantly reduced dendritic coverage compared to *control* (*control*: 0.88 ± 0.05, *UAS-mav*: 0.38 ± 0.07, p-value<0.05), but the dendritic length was not affected (*control*: 2031 µm ± 193, *UAS-mav*: 2176 µm ± 513). In comparison, mav-overexpression exhibited significantly reduced dendritic field coverage in the posterior compartment compared to *control* (*control*: 0.87 ± 0.06, *UAS-mav*: 0.58 ± 0.08, p-value<0.05), but showed 2-fold enhanced dendritic growth compared to the anterior compartment (*control*: 1966 µm ± 189, *UAS-mav*: 4724 µm ± 837). The opposite effect occurred when mav was downregulated in the *engrailed*-domain by RNAi. Here, mav downregulation resulted in a significant decrease of the dendritic length (*mav-RNAi*: 1535 µm ± 233, p-value<0.05), but the dendritic coverage was not affected (*mav-RNAi*: 0.93 ± 0.02).
Anteriorly, C4da neuron dendritic field coverage was identical to *control*, but the total dendrite length was 2-fold higher than within its posterior compartment of the same dendritic field (*mav-RNAi*: 0.89 ± 0.02, 4249 µm ± 586). Analysis of the ratio of total dendrite length between anterior and posterior compartments showed that the overexpression of mav significantly shifted the dendritic length ratio posteriorly (*control*: 0.98 ± 0.16, *UAS-mav*: 2.23 ± 0.28, p-value<0.05), while the knock-down of mav led to a significant anterior shift (*mav-RNAi*: 0.37 ± 0.06, p-value<0.05) (Figure 28C).
Comparison of the field coverage ratio between anterior and posterior compartments showed that the overexpression of mav resulted in significantly increased dendritic coverage, while the knock-down of mav did not exhibit changes in dendritic field coverage compared to *control (*Figure 28F). Interestingly, total dendrite length was not affected in any of the genotypes (*ctrl*: 20867 µm ± 799, *UAS-mav*: 22069 µm ± 727, *mav-RNAi*: 20209 µm ± 1862) (Figure 28D).
This data suggests that up- or downregulation of mav protein levels regulates dendrite growth preference of C4da neurons.

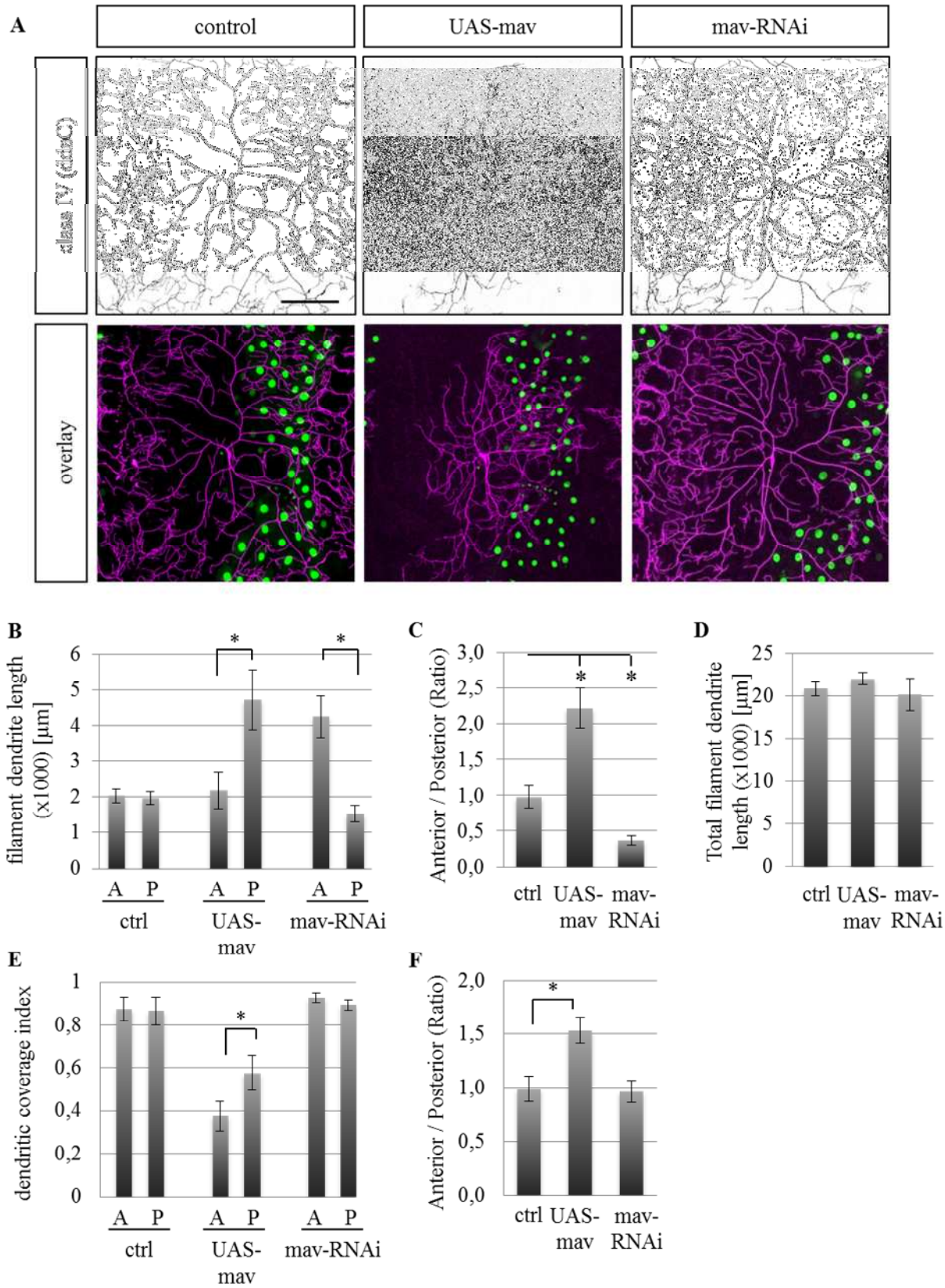

Figure 28. *Mav* directs growth and growth preference of C4da neuron dendrites A) Dendritic morphology of C4da neurons in *control* animals compared to overexpression of mav (*UAS-mav*) or mav knock-down (*mav-RNAi*) in the posterior epithelium using *en-Gal4*. The *en-Gal4* expression domain in the posterior compartment was visualized by nuclear mCherry (green). C4da neurons of 3rd instar larvae were visualized with the specific marker *ppk-CD4-tdGFP* (magenta). Scale bar: 100 µm. **B)** Quantitative analysis of the dendritic filament length in the anterior (A) or posterior (P) field of C4da neurons. **C)** Ratio of dendritic filament length in the anterior (A) to posterior (P) field of C4da neurons.

For filament length analysis: 100 µm from anterior or posterior end. **D)** Quantitative analysis of the total dendritic filament length of C4da neurons**. E)** Quantitative analysis of the dendritic field coverage in the anterior (A) or posterior (P) field of C4da neurons. **(F)** Ratio of the dendritic field coverage in the anterior (A) to posterior (P) field of C4da neurons. The overexpression of mav enhances dendrite growth of C4da neurons into the posterior domain. In contrast, the knock-down of mav within the posterior part resulted in a reduction of C4da neuron dendrites. However, total dendrite length was not affected in any of the genotypes. All data are mean ± SD, Mann-Whitney-Test $p<0.05$ (*), n=5.

10.8.5 Ectopic mav overexpression does not affect short-term dynamics of C4da neuron dendrites

The epithelial expression of mav resulted in drastic C4da neuron dendrite overbranching and preferred growth within the domain with higher mav levels when using *engrailed-Gal4* (10.8.4). This result was opposite to ectopic Ret overexpression, which raised the question how growth dynamics of C4da neurons were affected by mav.

The experiment was performed and analyzed as described above using *engrailed-Gal4* for mav overexpression in the posterior segment (10.7). The previous results of increased dendritic ingrowth of C4da neuron dendrites into the *engrailed* domain overexpressing mav was confirmed (Figure 29A).

The relative numbers of growing, stable and retracting terminal dendrites within a 5 min timeframe were examined. The quantification of *control* neurons displayed no significant difference between the anterior (A) and posterior (P) field in relative numbers of growing, stable or retracting terminals: 36% (A) and 36% (P) of growing dendrites, 44% (A) and 45% (P) of retracting dendrites and 20% (A) and 19% (P) of stable dendrites (Figure 29B).

Similarly, larvae overexpressing ectopic mav in the *engrailed* domain also displaying a comparable distribution of C4da neuron dynamics: 34% (A) and 38% (P) of growing dendrites, 50% (A) and 41% (P) of retracting dendrites and 17% (A) and 21% (P) of stable dendrites. No significant differences between *control* and mav overexpression were detected, including the frequency of growth and retraction events (growth: *control* 0.36 ± 0.03 (A), 0.36 ± 0.05 (P), *UAS-mav* 0.34 ± 0.04 (A), 0.38 ± 0.11 (P); retraction: *control* 0.44 ± 0.03 (A), 0.45 ± 0.03 (P), *UAS-mav* 0.50 ± 0.08 (A), 0.41 ± 0.02 (P)).

Since the overexpression of mav resulted in a severe branching phenotype but no significant differences in dendrite growth this result indicated that mav overexpression had at least no short-term effect on C4da dendrite dynamics.

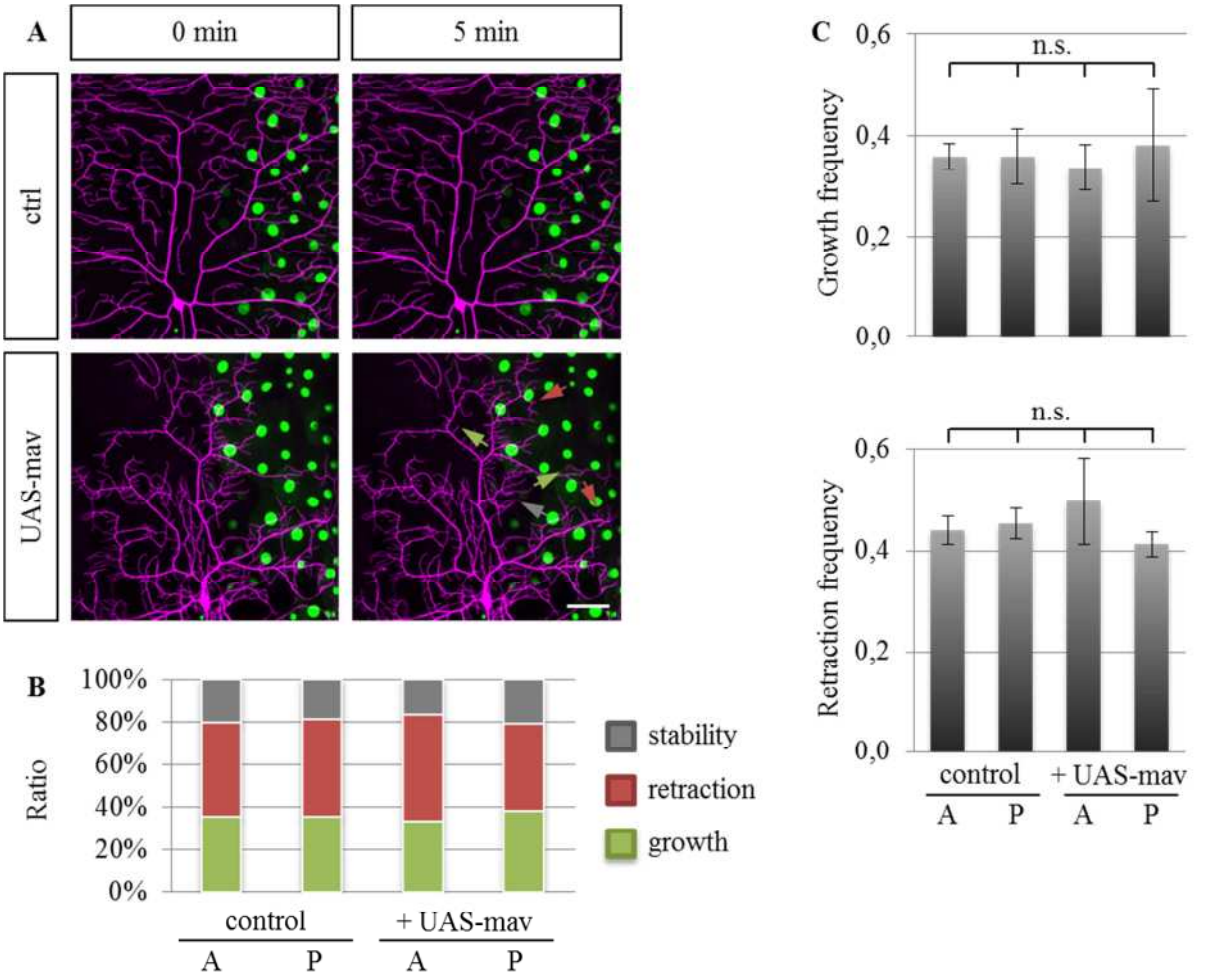

Figure 29. Ectopic overexpression of mav does not alter short-term dynamics of C4da neuron dendrites. A) Dorsal field of C4da neuron dendrites in *control* 3rd instar larvae compared to larvae overexpressing mav in the posterior segment using *engrailed-Gal4* (green).Neurons were visualized with the specific marker *ppk-CD4-tdGFP* (magenta). Representative images illustrate the dynamic changes of terminals after 5 min (arrows; green: growing, grey: stable, red: retracting) in the anterior (A) and posterior (P) domain of C4da neuron dendrite fields. Scale bar: 50 µm. **B)** Quantification of the relative amount of dendrite growth (green), stability (grey) and retraction (red) after 5 min of time-lapse imaging. Ectopic mav overexpression did not change the ratio of growing, retracting or stable terminals of C4da neurons. **C)** Quantification of growth, stability and retraction frequency after 5 min of time-lapse imaging. Ectopic mav overexpression did not change the frequency of dendrite retraction. N=397,156 (number of all terminals of 3 neurons per genotype).

10.8.6 Mav promotes C4da neuron dendrite growth and branching in a Ret dependent manner

To explore a possible functional genetic and molecular receptor-ligand link between Ret and mav, genetic interaction analysis was performed *in vivo*. Heterozygous *Ret* knock-out larvae (*Ret^{ko}*/+) already exhibited C4da neuron dendrite defects which might be rescued by providing more ligand, while the complete lack of the receptor should not be rescuable anymore. Therefore, the hypothesis was tested if neuronal mav overexpression could rescue dendrite defects in Ret heterozygous but not homozygous *Ret^{ko}* animals.

To this end, the dendrite morphologies of C4da neurons in *control*, heterozygous *Ret* knock-out (*Ret^{ko}*/+) and *Ret* knock-out (*Ret^{ko}*) 3rd instar larvae were compared with or without overexpression of transgenic mav in C4da neurons using *ppk-Gal4*. The neurons were visualized by the expression of *UAS-CD4-tdGFP* and dendrite morphology was subsequently quantified (Figure 30A).

The analysis of C4da neuron morphology revealed that specific C4da neuron overexpression of transgenic *mav* in heterozygous *Ret^{ko}* (*Ret^{ko}*/+) larvae resulted in an increase of C4da neuron dendrite branches compared to *control* animals (*control, Ret^{ko}*/+*, +UAS-mav/*+). The overexpression of mav in homozygous *Ret^{ko}* larvae did not show a difference in neuron morphology compared to homozygous *Ret^{ko}* larvae alone.

Quantitative analysis showed that overexpression of mav in a *wild type* background had no growth effect on C4da neuron dendrites and exhibited similar dendrite length as *control* neurons (*control*: 19851 µm ± 1680, *UAS-mav*: 19871 µm ± 1768). Heterozygous *Ret^{ko}* (*Ret^{ko}*/+) C4da neuron dendrites displayed a non-significant reduction of dendritic length compared to *control* larvae (*Ret^{ko}*/+: 18319 µm ± 1382). Interestingly, C4da neurons overexpressing *mav* in heterozygous *Ret^{ko}* (*Ret^{ko}*/+) larvae exhibited a significant increase of C4da neuron dendrite length (*Ret^{ko}*/+*;+mav*: 21285 µm ± 957, p-value<0.05), whereas the overexpression of mav in homozygous *Ret^{ko}* larvae did not affect C4da neuron dendrite length (*Ret^{ko}*: 17478 µm ± 789, *Ret^{ko};+mav*: 15929 µm ± 1937) (Figure 30B).

Quantitative analysis of the number of terminal ends of C4da neuron dendrites in 3rd instar larvae showed a similar result as for the dendritic length analysis. Mav overexpression in C4da neurons did not affect the number of terminals compared to *control* or heterozygous *Ret^{ko}* (*Ret^{ko}*/+) larvae (*control*: 611 ± 67, *UAS-mav*: 592 ± 58, *Ret^{ko}*/+: 571 ± 79).

However, the overexpression of mav in heterozygous *Ret^{ko}* (*Ret^{ko}*/+) larvae resulted in a significant increase of C4da neuron terminal dendrites (*Ret^{ko}*/+*;+mav*: 800 ± 59, p-value<0.05). Interestingly, the opposite effect occurred in complete *Ret^{ko}* larvae. Here, the number of C4da neuron terminals was significantly decreased when mav was overexpressed in comparison to *Ret^{ko}* larvae (*Ret^{ko}*: 580 ± 12, *Ret^{ko};+mav:* 467 ± 72, p-value<0.05) (Figure 30C). Potential changes of dendrite complexity were visualized by Strahler analysis. The C4da neuron specific overexpression of mav in *Ret^{ko}*/+ larvae showed a mild shift towards an

increase of higher order branches. Conversely, overexpression of mav in *Ret*^{ko} larvae resulted in even more reduced distal branch numbers (Figure 30D).

Taken together, these data showed that mav overexpression in C4da neurons was able to promote dendritic length, number of terminals, complexity in Ret heterozygous animals but not in the complete absence of Ret demonstrating that *mav* and *Ret* are functionally linked in the same genetic pathway with mav acting upstream of Ret.

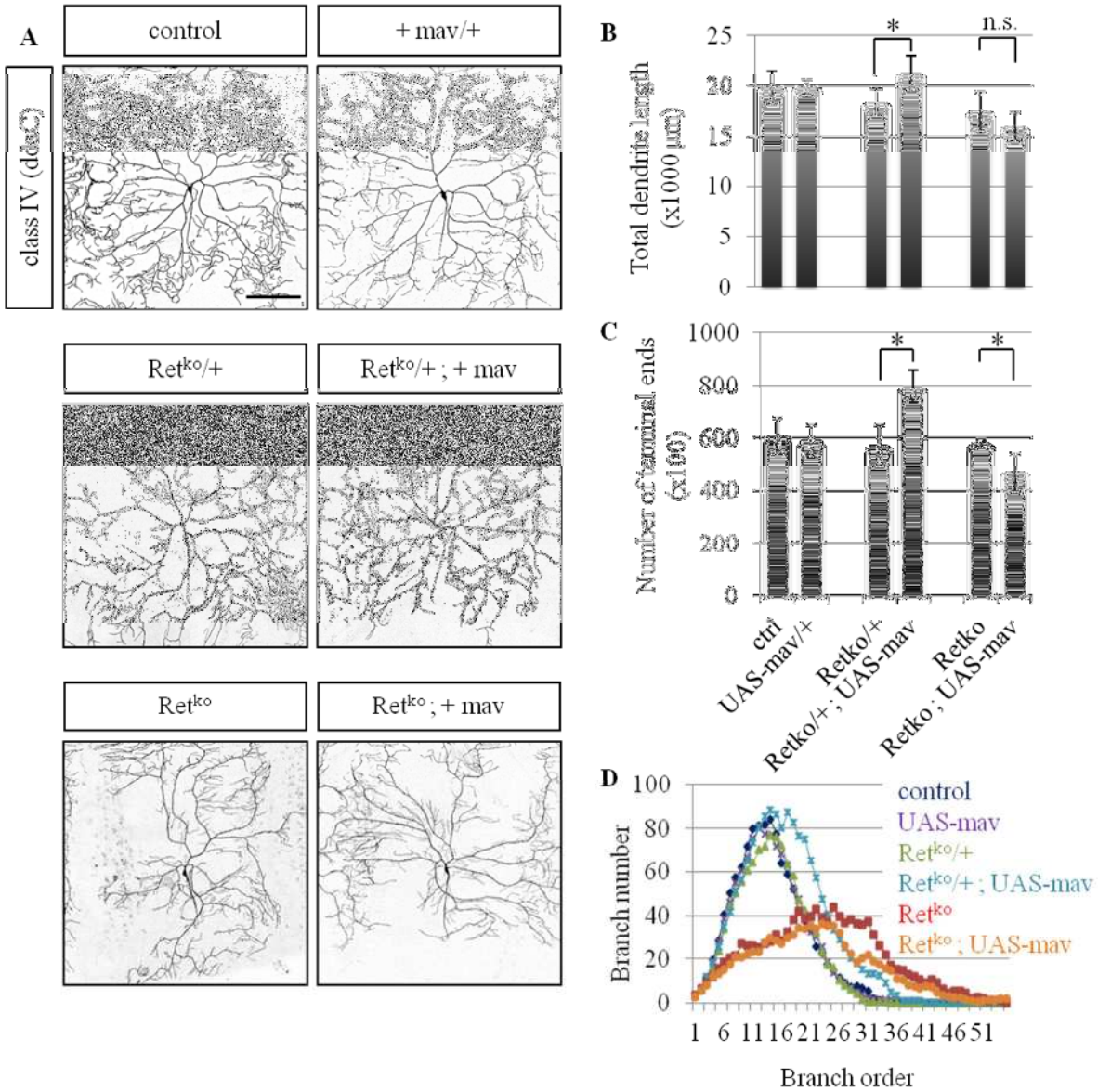

Figure 30. *Mav* promotes C4da neuron dendrite growth and branching in a Ret dependent manner. A) Dendrite morphology of C4da neurons in *control*, heterozygous *Ret*^{ko}/+ and *Ret*^{ko} 3rd instar larvae compared to mav overexpression using *ppk-Gal4*. Neurons were visualized using the specific marker *ppk-Gal4>CD4-tdGFP.* Scale bar: 100 µm. **B)** Quantitative analysis of total length of C4da neuron dendrites of the indicated genotypes. **C)** Quantitative analysis of the number of terminals of C4da neuron dendrites. **D)** Strahler analysis to quantitatively visualize dendrite complexity. The number of dendrites is plotted against the increasing branch order. Specific C4da neuron overexpression of *mav* in heterozygous *Ret*^{ko} (*Ret*^{ko}/+) larvae resulted in a significant increase of C4da neuron dendritic length, number of terminals and branching complexity compared to controls. The overexpression of mav in homozygous *Ret*^{ko} larvae did not affect C4da neuron dendrite length or complexity, but reduced the number of terminal branches. All data are mean ± SD, Mann-Whitney-Test $p<0.05$ (*), n=5.

10.8.7 Perturbation of C4da neuron dendrite morphology by epithelial mav overexpression is Ret-dependent

Mav overexpression in a subset of epithelial cells resulted in enhanced dendrite growth of C4da neurons into the expression domain (10.8.4). Based on the previous findings that Ret and *mav* are genetically linked, the mav overexpression phenotype was explored in *wild type* and Ret^{ko} larvae to examine its dependence on *Ret* expression. Mav was overexpressed in the epithelium using *A58-Gal4* and C4da neurons were visualized by *ppk-CD4-tdTomato* (Figure 31).

The quantitative analysis showed that epithelial overexpression of mav resulted in a significant increase of C4da neuron dendrite length and a striking increase of crossing dendrites and number of terminals compared to *controls* (Figure 31B - *control*: 16536 µm ± 1360, *UAS-mav*: 22179 µm ± 2047; Figure 31C - *control*: 5 ± 1, *UAS-mav*: 58 ± 10; Figure 31D - *control*: 386 ± 33, *UAS-mav*: 879 ± 109, p-value<0.05).

This effect was completely Ret-dependent since mav overexpression in Ret^{ko} mutant animals resulted in a *Ret* loss-of-function phenotype. Interestingly, comparing the total dendrite length and number of isoneuronal crossing events of Ret^{ko} animals with or without epithelial mav overexpression showed a mild but significant reduction (Figure 31B - Ret^{ko}: 13407 µm ± 1213, Ret^{ko} + *UAS-mav*: 10550 µm ± 467; Figure 31C - Ret^{ko}: 9 ± 1, Ret^{ko} + *UAS-mav*: 3 ± 1, p-value<0.05). The number of terminals was not affected comparing both genotypes, even though a tendency towards a reduction could be observed (Figure 31D - Ret^{ko}: 289 ± 42, Ret^{ko} + *UAS-mav*: 235 ± 17). These results revealed that epithelial mav overexpression affects C4da neuron morphology in a Ret-dependent manner. In addition, mav overexpression seems to have a negative effect on C4da neuron dendrite growth in Ret mutant animals, a phenomenon which remains to be investigated in more detail.

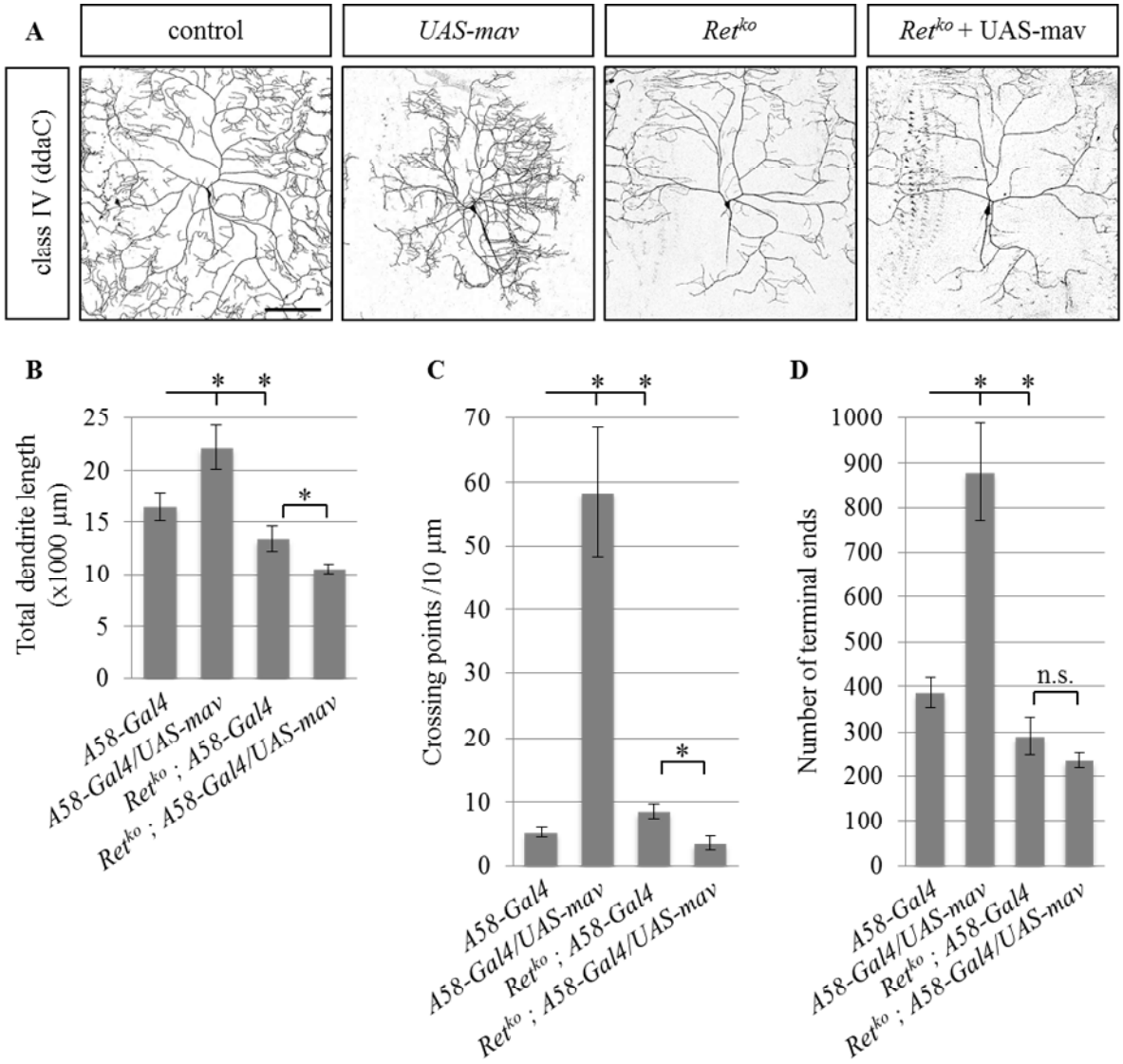

Figure 31. C4da neuron phenotypes due to epithelial overexpression of mav are Ret-dependent. A) Dendrite morphology of C4da neurons in *control* and *Ret*^{ko} 3rd instar larvae with or without epithelial overexpression of *mav* using *A58-Gal4*. Neurons were visualized using *ppk-CD4-tdTomato.* **B)** Quantitative analysis of total length of C4da neuron dendrites of the indicated genotypes. **C)** Quantitative analysis of isoneuronal dendritic crossing of the indicated genotypes. **D)** Quantitative analysis of the number of terminals of C4da neuron dendrites of the indicated genotypes. Epithelial overexpression of mav strongly effected C4da neuron dendrites. This effect was Ret-dependent and did not occur in complete *Ret*^{ko} background. Scale bar: 100 µm. All data are mean ± SD, Mann-Whitney-Test $p<0.05$ (*), n=5.

10.8.8 *Ret* and *mav* expression in C1da neurons is sufficient to promote dendrite growth

The previous data showed that mav can affect C4da neuron dendrite growth in a Ret-dependent manner. To test if Ret and mav are sufficient to promote dendrite growth, both were ectopically expressed in class I da (C1da, *nompC-Gal4*) neurons, which normally neither express Ret nor mav.

Class I ddaD neurons were used to quantitatively assess dendrite growth effects by overexpression of *UAS-Ret*, *UAS-mav*, *UAS-Ret-CTΔ* and *UAS-Ret-NTΔ* transgenes (+mav, +Ret, +Ret-CTΔ, +Ret-NTΔ) in 3rd instar larvae. C1da neurons were visualized with *nompC-Gal4* driven *UAS-CD4-tdTomato* (Figure 32A).

Analysis of the total length of C1da neuron dendrites revealed that overexpression of *Ret* resulted in a significant increase of total dendrite length compared to *control* neurons (*control*: 1854 µm ± 100, *UAS-Ret*: 2017 µm ± 61, p-value<0.05). This effect could be strongly enhanced by co-overexpression of *Ret* and *mav* (*UAS-mav/UAS-Ret*: 2507 µm ± 138), whereas overexpression of *mav* alone was not significantly different from *control* (1838 µm ± 96, p-value<0.05) (Figure 32B).

To investigate whether the growth promoting effect depended on the presence of the extra- or intracellular Ret domains, N-or C-terminally truncated Ret transgenes were overexpressed with or without mav. The co-overexpression of truncated Ret and mav did not significantly promote dendrite growth, indicating that both extra- and intracellular domains of Ret are necessary for mav induced dendrite growth (*UAS-mav/UAS-Ret-CTΔ*: 2184 µm ± 166, *UAS-mav/UAS-Ret-NTΔ*: 2035 µm ± 121, p-value<0.05).

The quantification of the number of terminals of class I neuron dendrites showed that only co-overexpression of *UAS-Ret* and *UAS-mav* transgenes resulted in a significant increase of C1da neuron terminals (*control*: 28 ± 3, *UAS-Ret*: 28 ± 3, *UAS-mav*: 30 ± 3, *UAS-Ret;UAS-mav*: 37 ± 6, p-value<0.05). None of the truncated Ret transgenes when expressed together with mav were able to increase C1da neuron terminal numbers. (*UAS-Ret-CTΔ*: 32 ± 6, *UAS-mav/UAS-Ret-CTΔ*: 30 ± 5, *UAS-Ret-NTΔ:* 30 ± 6, *UAS-mav/UAS-Ret-NTΔ:* 33 ± 4) (Figure 32C). Using Strahler analysis to visualize dendrite complexity confirmed these findings. Only co-overexpression of Ret and mav resulted in an increased C1da neuron branch numbers distally demonstrating that these neurons increased their dendritic complexity (Figure 32D).

This experiment strengthened the hypothesis Ret and mav function together. The data demonstrate that Ret and mav are sufficient to promote dendrite growth in heterologous neurons which do not express these proteins endogenously. These data show that Ret and mav have a general growth promoting function which depends on both the extra-and intracellular domain of Ret.

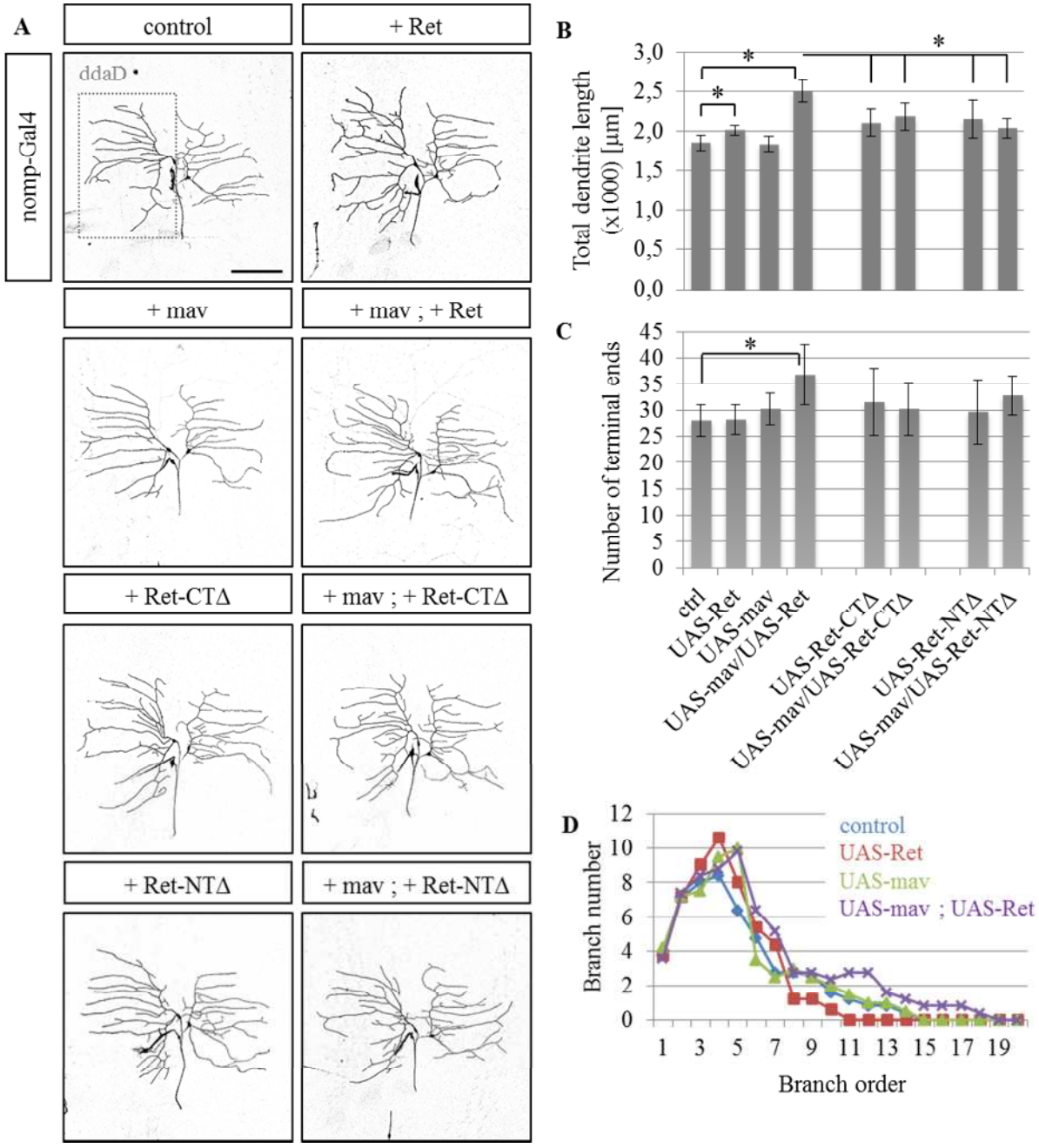

Figure 32. *Ret* and *mav* enhance dendrite growth of C1da neurons. A) Dendritic morphology of class I da neurons (C1da): ddaD and ddaE neurons. Using a C1da specific driver *(nompC-Gal4*) the effects of *UAS-Ret*, *UAS-mav*, *UAS-Ret-CTΔ* and *UAS-Ret-NTΔ* transgene overexpression (+mav, +Ret, +Ret-CTΔ, +Ret-NTΔ) on C1da neuron dendrites in 3rd instar larvae were analyzed and compared to *control*. Neurons were visualized by the co-expression of *UAS-CD4-tdTomato.* For quantification ddaD was selected (dashed line). Scale bar: 100 µm. **B)** Quantitative analysis of the total length of ddaD neuron dendrites. **C)** Quantitative analysis of the number of terminals of ddaD neuron dendrites. **D)** Strahler analysis to quantitatively visualize dendrite complexity. The numbers of dendrites are plotted against the increasing branch order. Co-overexpression of *Ret* and *mav* transgenes enhanced dendrite growth, the number of terminal ends and the complexity of ddaD neurons and both extra- and intracellular domains of Ret were required for mav dependent growth signaling. All data are mean ± SD, Mann-Whitney-Test $p<0.05$ (*), n=5.

10.8.9 Mav overexpression cannot rescue ectopic Ret overexpression induced C4da neuron dendrite defects

The ectopic overexpression of Ret and mav resulted in virtually opposite phenotypes in C4da neurons when using the *engrailed-Gal4* driver (10.6, 10.8.4). Therefore the idea was tested that co-overexpression of Ret and mav might mitigate on the effects on C4da neuron dendrite morphology.

For this experiment *engrailed-Gal4* was used to overexpress Ret and mav separately or together. As before, the overexpression of mav enhanced dendrite growth of C4da neurons into the *engrailed* expression domain (Figure 33). In contrast, the overexpression of Ret resulted in a complete non-coverage of C4da neuron dendrites within the posterior domain. The parallel co-overexpression of both transgenes however exhibited only the ectopic Ret overexpression phenotype demonstrating that the parallel overexpression of mav was not able to rescue the dominant Ret phenotype.

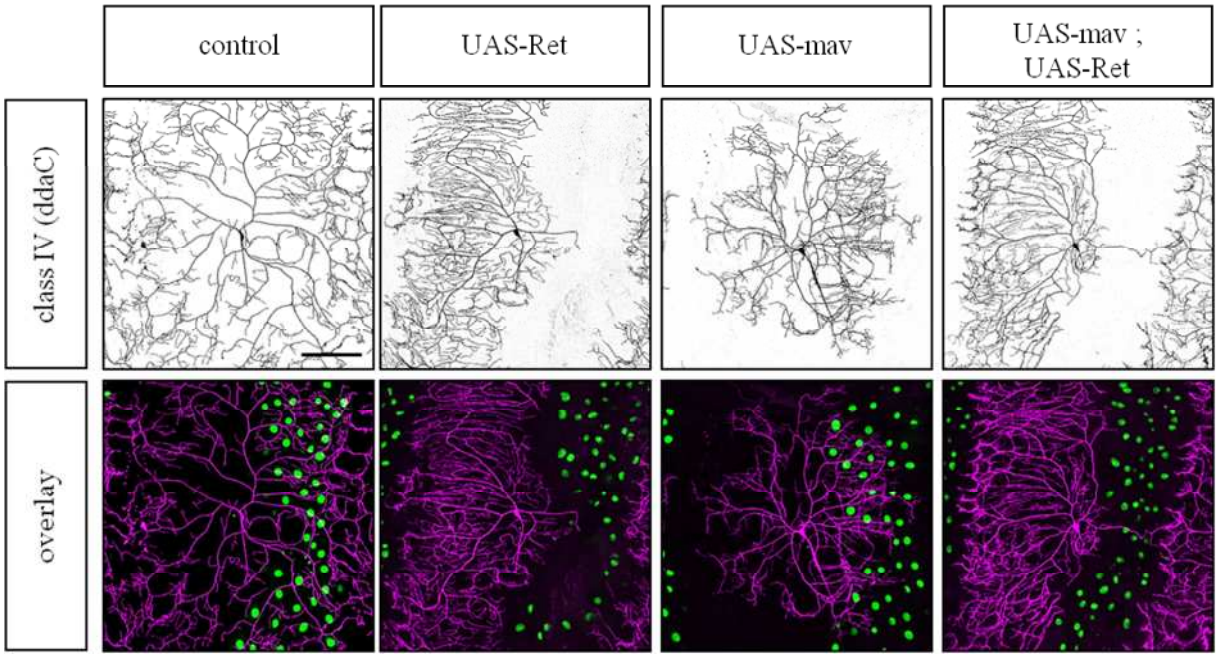

Figure 33. Epidermal co-overexpression of mav does not rescue Ret-overexpression induced C4da neuron dendrite defects. Dendritic morphology of C4da neurons in *control* animals compared to single or co-overexpression of Ret and mav (*UAS-Ret, UAS-mav, UAS-mav;UAS-Ret*) using *en-Gal4*. The *Gal4*-driver expression domain in the posterior compartment was visualized using a nuclear mCherry marker (green). C4da neurons of 3rd instar larvae were visualized by the expression of the specific marker *ppk-CD4-tdGFP* (magenta). Mav overexpression enhanced dendrite growth into the *engrailed* expression domain, whereas Ret overexpression resulted in a complete non-coverage of C4da neuron dendrites within the posterior domain. However, co-overexpression of both transgenes showed only the ectopic Ret overexpression phenotype. Scale bar: 100 µm.

10.9 Generation and validation of a *mav* loss-of-function allele using CRISPR/Cas9

The described functional connection of *mav* with the Ret receptor and its strong influence on C4da neuron dendrite development prompted the generation of a *mav* knock-out allele, since no alleles of *mav* were available at that time.

Therefore, CRISPR/Cas9 was used to engineer *mav* mutant lines (Port et al., 2014). The endogenous *mav* locus on the 4th chromosome was targeted by co-injecting an appropriate guide RNA (pCFD4-mav) and donor template serving as a template for homology directed repair (pRK2 vector including a white marker cassette and 5' and 3' flanking sites of genomic mav) (~ 1 kb each) into *Drosophila* embryos with germline specific Cas9 expression (Figure 34A). 510 embryos were injected and the progeny was screened for expression of the white marker. Positive candidates were verified by PCR screening using primer combinations flanking the *mav* genomic locus (Figure 34B). 10 out of 10 tested candidates revealed a predicted PCR product of 1.8 kbp (5' PCR) and 1.5 kbp (3' PCR) confirming correct targeting. For further investigation, the *mav* mutant line 7.1 was chosen and will be referred to as "*mav^{ko}*". The generated allele was combined with the C4da neuron specific marker *ppk-CD4-tdTomato* and characterized.

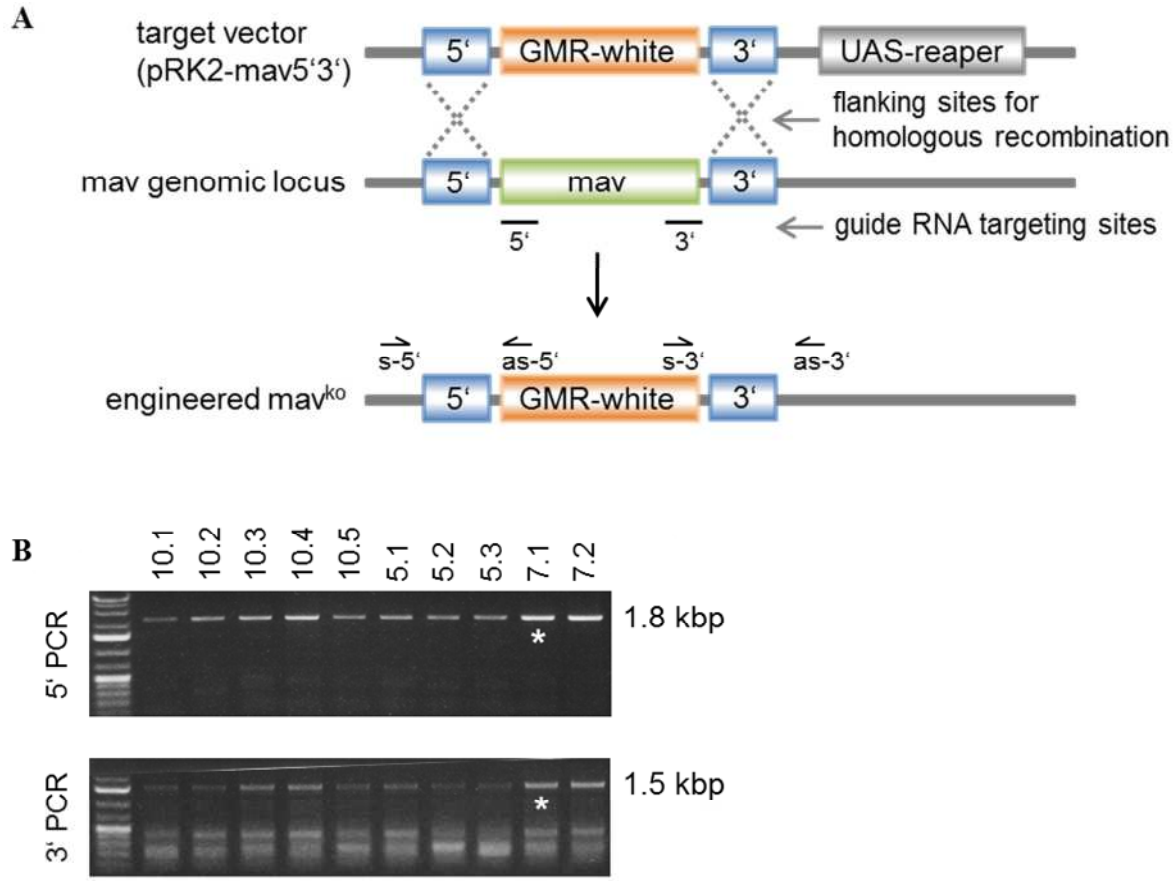

Figure 34. Generation of a *mav^{ko}* mutant allele by CRISPR/Cas9. A) Schematic illustration of the employed strategy to generate a *mav^{ko}* allele using CRISPR/Cas9. A donor vector (pRK2-mav5'3') was designed to provide a template with 5' and 3' genomic sequences flanking the two mav coding exons and including a GMR-white cassette as a marker for positive mutant candidates. A UAS-reaper

cassette was flanking the 3’ region and served as an additional selection marker (induces apoptosis under *Gal4* expression). Cas9 nuclease is guided to its target cut site by guide RNAs (pCFD4-mav, not shown), which feature 18 nucleotide homology to the target DNA (mav genomic locus). The targeted genomic DNA is cleaved and then repaired by HDR (homology directed repair) using the donor vector as the template, which resulted in a cassette exchange. Red eyed mutant candidates (fly strains 5, 7, 10) were screened by PCR using primer pairs flanking the 5’ or 3’ targeting sites in the *mav* genomic locus to verify correct targeting **(B)**. All candidates showed positive PCR products of the predicted size. The *mav* mutant allele 7.1 (indicated by asterisks) was chosen for further experiments.

10.9.1 Characterization of mav loss-of-function and C4da neuron morphogenesis

The visualization of C4da neurons in *mav*^{ko} 3rd instar larvae clearly confirmed the previous results of mav being implicated in C4da neuron dendrite development. Similarly to *Ret*^{ko} C4da neurons, complete loss of *mav* function led to morphological defects, characterized by reduced and uneven coverage of the dendritic field (Figure 35A). To verify the observed morphological defects, dendritic length, the number of terminals and Strahler analysis were quantified.

C4da neurons in *mav*^{ko} larvae exhibited significantly reduced total dendrite length compared to *control* neurons (*control*: 19663 µm ± 1720, *mav*^{ko}: 15998 µm ± 1115, p-value<0.05), but not when compared to *Ret*^{ko} larvae (*Ret*^{ko}: 13936 µm ± 1627) (Figure 35B). Compared to *control* neurons, *Ret*^{ko} larvae displayed a difference in the significance level (p-value<0.01). Similarly, the number of C4da neuron terminal dendrites in *mav*^{ko} 3rd instar larvae was decreased compared to *control* to a comparable extent as in *Ret*^{ko} larvae (*control*: 501 ± 44, *mav*^{ko}: 345 ± 27, p-value<0.05). Analysis of dendrite terminal numbers of *mav*^{ko} and *Ret*^{ko} C4da neurons exhibited no significant difference (*Ret*^{ko}: 360 ± 51) (Figure 35C).

Examination of C4da neuron dendrite complexity by Strahler analysis revealed that *mav*^{ko} larvae displayed a reduced complexity of C4da neurons compared to *control* indicated by a decreased branch number along the entire curve. This effect was identical to *Ret*^{ko} C4da neurons (Figure 35D).

For a more detailed analysis of the C4da neuron dendrite distribution within the receptive field, the field was subdivided into eight even parts and the relative amount of dendrites was depicted in a rose plot (Figure 35E). This analysis revealed the already qualitatively observed shift in dendrite distribution. In controls, C4da neurons dendrites were evenly distributed within their receptive field. The loss of *mav* resulted in a significant increase of dendrites within their dorsal-posterior field (*control*: 10.9% ± 2.1 (d-p), *mav*^{ko}: 20.2% ± 4.1 (d-p), p-value<0.05), whereas their anterior-ventral compartment was less covered, but not significant different to *control* C4da neurons. Similarly, *Ret* loss-of-function resulted in a significant shift in dendrite distribution. *Ret*^{ko} C4da neurons exhibited less coverage within their anterior-ventral field, whereas the anterior-dorsal field showed an increased coverage (*control*: 15.3% ± 1.9 (a-v), 9.4% ± 2.2 (a-d), *Ret*^{ko}: 6.8% ± 1.2 (a-v), 14.2% ± 1.6 (a-d), p-value<0.05).

In comparison, *mav*^{ko} C4da neurons exhibited a shift towards dorsal-posterior, whereas *Ret*^{ko} C4da neurons dendrites displayed a pronounced distribution along the anterior-posterior axis.

In summary, analyzing the branching pattern *mav* loss-of-function exhibited severe dendrite defects in C4da neurons resulting in reduced dendrite length, less terminals and decreased dendrite complexity compared to *control* C4da neurons. These defects were largely similar to *Ret*^{ko} C4da neurons showing that *mav* and *Ret* have a similar function in C4da neuron dendrite development.

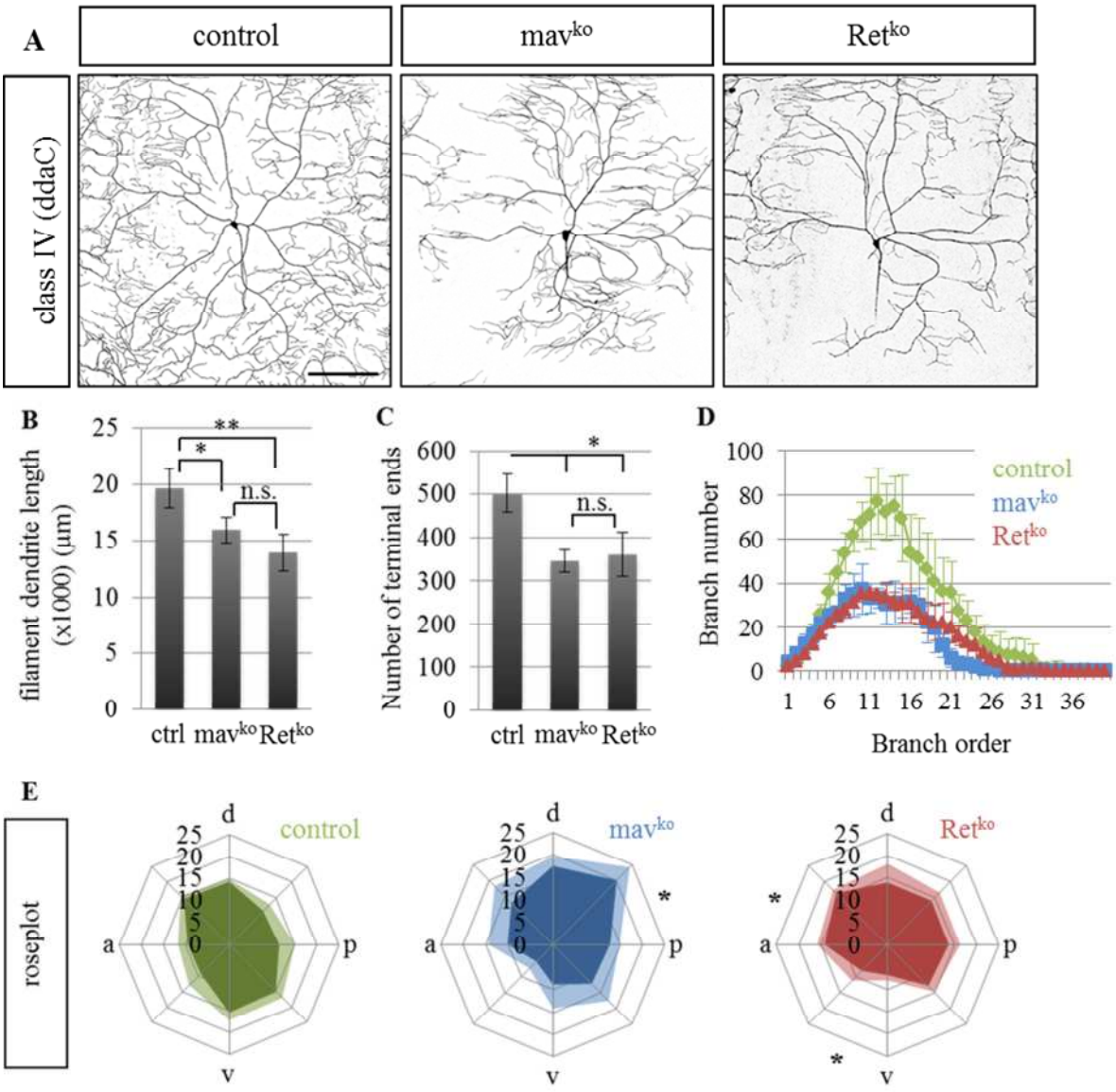

Figure 35. *Mav*^{ko} C4da neurons exhibit similar defects as the *Ret* loss-of-function. A) Dendritic morphology of C4da neurons in *control*, *mav*^{ko} and *Ret*^{ko} 3rd instar larvae. Neurons were visualized by the expression of the specific marker *ppk-CD4-tdTomato.* Scale bar: 100 µm. **B)** Quantitative analysis of the total length of C4da neuron dendrites of indicated genotypes. **C)** Quantitative analysis of the number of terminals of C4da neuron dendrites. **D)** Strahler analysis to quantitatively visualize dendrite complexity. The numbers of dendrites are plotted against the increasing branch order. **E)** Rose plot, representing the relative amount of C4da neuron dendrites within its dendritic field (a=anterior, d=dorsal, p=posterior, v=ventral). P-values (indicated by asterisks) are in comparison to *control*. *Mav* loss-of-function resulted in a severe C4da neuron phenotype which was largely similar to *Ret* loss-of-function. Both exhibited reduced dendrite length, less terminals and a decreased dendrite complexity. All data are mean ± SD, Mann-Whitney-Test p<0.05 (*), p<0.01 (**) n=5.

10.9.2 *Ret* and *mav* are genetically linked

To analyze the possibility of Ret and mav being genetically linked, an *in vivo* genetic interaction test was performed. This assay is based on the assumption that removing one copy of two functionally linked genes results in a synthetic phenotype. For this purpose, the morphology of C4da neuron dendrites of heterozygous *Ret* hypomorphic (Ret^{C168}/+) and mav^{ko} (mav^{ko}/+) animals was compared to the transheterozygous combination (Ret^{C168}/+ ;; mav^{ko}/+) (Figure 36A). C4da neurons were visualized using the specific marker *ppk-CD4-tdTomato*.

The morphological examination indicated that trans-heterozygous mutant larvae indicated a tendency towards decreased dendrite length and branching complexity of C4da neurons in comparison to *control* and heterozygous larvae.

The quantitative analysis of the total dendritic length of C4da neurons revealed no significant difference between *control*, Ret^{C168} and mav^{ko} heterozygous larvae (*control*: 19663 µm ± 1720, Ret^{C168}/+: 20960 µm ± 1545, mav^{ko}/+: 18734 µm ± 1009). However, trans-heterozygous C4da neurons displayed a significant reduction of dendritic length compared to *control* and heterozygous larvae (Ret^{C168}/+, mav^{ko}/+: 15552 µm ± 1422, p-value<0.05) (Figure 36B).

Heterozygous Ret^{C168} mutant but not mav^{ko} C4da neurons displayed a significant increase of crossing points compared to *control* (*control*: 3.85 ± 1.19, Ret^{C168}/+: 10.68 ± 1.65, p-value<0.05) (mav^{ko}/+: 4.5 ± 1.22). In the transheterozygous animals isoneuronal crossing was increased as well but not significantly different form heterozygous Ret knock-out larvae (Ret^{C168}/+, mav^{ko}/+: 8.97 ± 1.56, p-value<0.05) (Figure 36C).

Quantitative analysis of the number of C4da neuron terminals in 3rd instar larvae showed a significant reduction in heterozygous mav^{ko} but not Ret mutant larvae when compared to *control* (*control*: 501 ± 44, Ret^{C168}/+: 488 ± 45, mav^{ko}/+: 345 ± 57, p-value<0.05). The transheterozygous combination of both genotypes was not significantly different from mav^{ko} heterozygous larvae (Ret^{C168}/+, mav^{ko}/+: 295 ± 39, p-value<0.05) (Figure 36D).

Strahler analysis was then used to assess dendrite complexity for each genotype. Compared to *control* larvae, heterozygous *Ret* mutants exhibited a mild shift towards lower branch orders. In heterozygous mav^{ko} larvae this effect was much stronger and the number of branches was decreased as well, which was already indicated by the decreased dendritic length and the number of terminals. This phenotypic effect was mildly enhanced towards a decreased branching order in the transheterozygous larvae (Figure 36E).

Taken together, these data provide evidence for *Ret* and *mav* being genetically linked. It showed that the genetic link between both genes is only present for the phenotype in dendritic growth. The other observed phenotypes were already dominant in either heterozygous Ret mutant or mav^{ko} animals and were not enhanced in transheterozygous genotypes. It further suggests that *Ret* is mainly involved in crossing defects, whereas *mav* predominantly controls dendritic growth and the number of terminals.

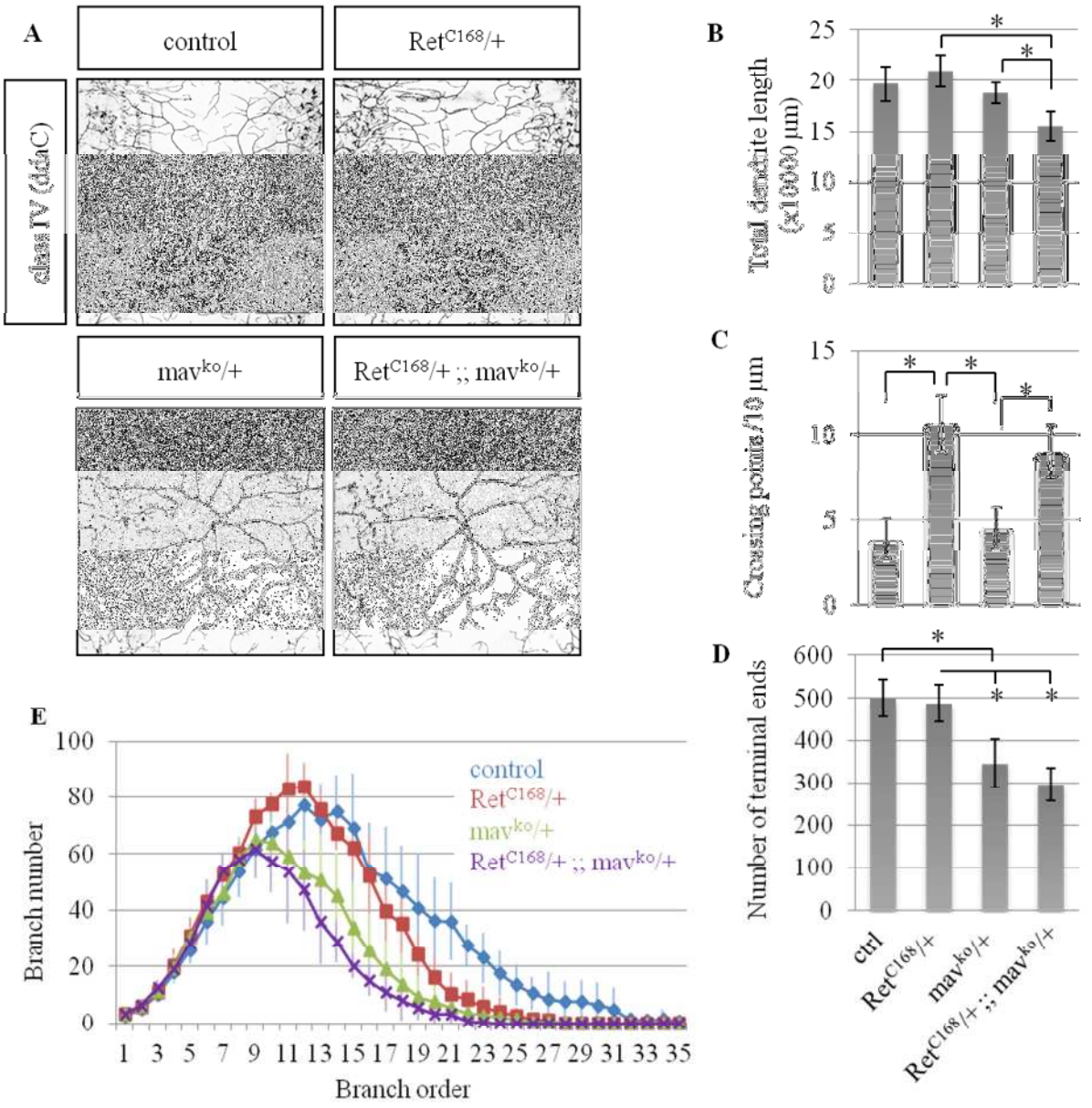

Figure 36. *Ret* and *mav* are genetically linked. A) C4da neuron dendrite morphology of *control*, *Ret* hypomorphic (*Ret*^{C168}) and *mav* knock-out (*mav*^{ko}) in heterozygous and transheterozygous 3rd instar larvae. C4da neurons were visualized by the expression of the specific marker *ppk-CD4-tdTomato*. Scale bar: 100 µm. **B)** Quantitative analysis of the total length of C4da neuron dendrites of the indicated genotypes. **C)** Quantitative analysis of crossing points/10 µm. **D)** Quantitative analysis of the number of terminals of C4da neuron dendrites for each indicated genotype. **E)** Strahler analysis to quantitatively visualize dendrite complexity. The numbers of dendrites are plotted against the increasing branch order. Trans-heterozygous mutants displayed a significant reduction of dendritic length of C4da neurons and a tendency towards less complexity compared to *control* and heterozygous larvae. Defects in crossing events and the number of terminal ending were not enhanced in transheterozygous animals. All data are mean ± SD, Mann-Whitney-Test $p<0.05$ (*), n=5.

10.9.3 *Mav* functions upstream of Ret in C4da neuron development

The previous experiments concerning *mav* and *Ret* clearly showed their genetic link and function in C4da neuron dendrite development.
Subsequently, *mav* and *Ret* double knock-out larvae were analyzed to test the hypothesis of both genes being part of the same signaling pathway. If so, complete loss-of-function of both should not differ from the individual mutant phenotypes. C4da neuron morphology of the different genotypes (*control*, mav^{ko}, Ret^{ko}, Ret^{ko} mav^{ko}) was visualized using *ppk-CD4-tdTomato* and subsequently quantified (Figure 37A).
The qualitative analysis revealed that C4da neuron dendrite defects in Ret^{ko} and mav^{ko} were not enhanced in double knock-out larvae. Indeed, quantitative analysis showed that total length of C4da neuron dendrites was similarly reduced in Ret/mav single and double knock-out animals (*control*: 18291 µm ± 784, Ret^{ko}: 13407 µm ± 1213, mav^{ko}: 13314 µm ± 1400, Ret^{ko};;mav^{ko}: 13049 µm ± 552, p-value<0.05) (Figure 37B).
Dendritic crossing was increased to a similar extent in all knock-out genotypes compared to *control* neurons (*control*: 3.01 ± 0.23, Ret^{ko}: 7.66 ± 1.76, mav^{ko}: 8.61 ± 2.34, Ret^{ko};;mav^{ko}: 9.56 ± 1.71) (Figure 37C).
Moreover, the number of C4da neuron terminals was reduced in both single and double knock-out animals without any phenotypic enhancement (*control*: 420.25 ± 35.93, Ret^{ko}: 289.2 ± 41.73, mav^{ko}: 261.0 ± 45.28, Ret^{ko};;mav^{ko}: 296.6 ± 50.13, p-value<0.05) (Figure 37D).
This result indicated that Ret and mav are functioning in the same pathway concerning the regulation of C4da dendrite length and their dendritic branching behavior.

If mav might function as a ligand it should act upstream of Ret. In this case expression of mav should rescue the mav^{ko}: phenotype, but not the Ret^{ko} and double knock-out phenotype. To test if expression of mav is able to rescue, a bacterial artificial chromosome (BAC) transgene containing a duplication of the mav genomic region was used.
The mav duplication (mav dupl.) was indeed able to rescue C4da neuron dendritic defect in *mav* single knock-out animals but not in Ret^{ko} larvae (Ret^{ko} +mav dupl.: 12111 µm ± 759, mav^{ko} +mav dupl.: 16304 µm ± 882, p-value<0.05). Interestingly, combining the mav duplication with the mav/Ret double knock-out resulted in an even stronger reduction of C4da neuron dendritic length (Ret^{ko};;mav^{ko} +mav dupl.: 11149 µm ± 619), similarly to epithelial mav overexpression (see Figure 28). The mav duplication itself did not affect C4da neuron dendrite length (mav dupl.: 17868 µm ± 1212) (Figure 37B).
The number of dendritic crossing points, was significantly increased in the mav duplication compared to *control* larvae (*control*: 3.01 ± 0.23, mav dupl.: 6.34 ± 2.07, p-value<0.5) (Figure 37C). Accordingly, the ability of the mav duplication to rescue crossing defects could not be assessed.

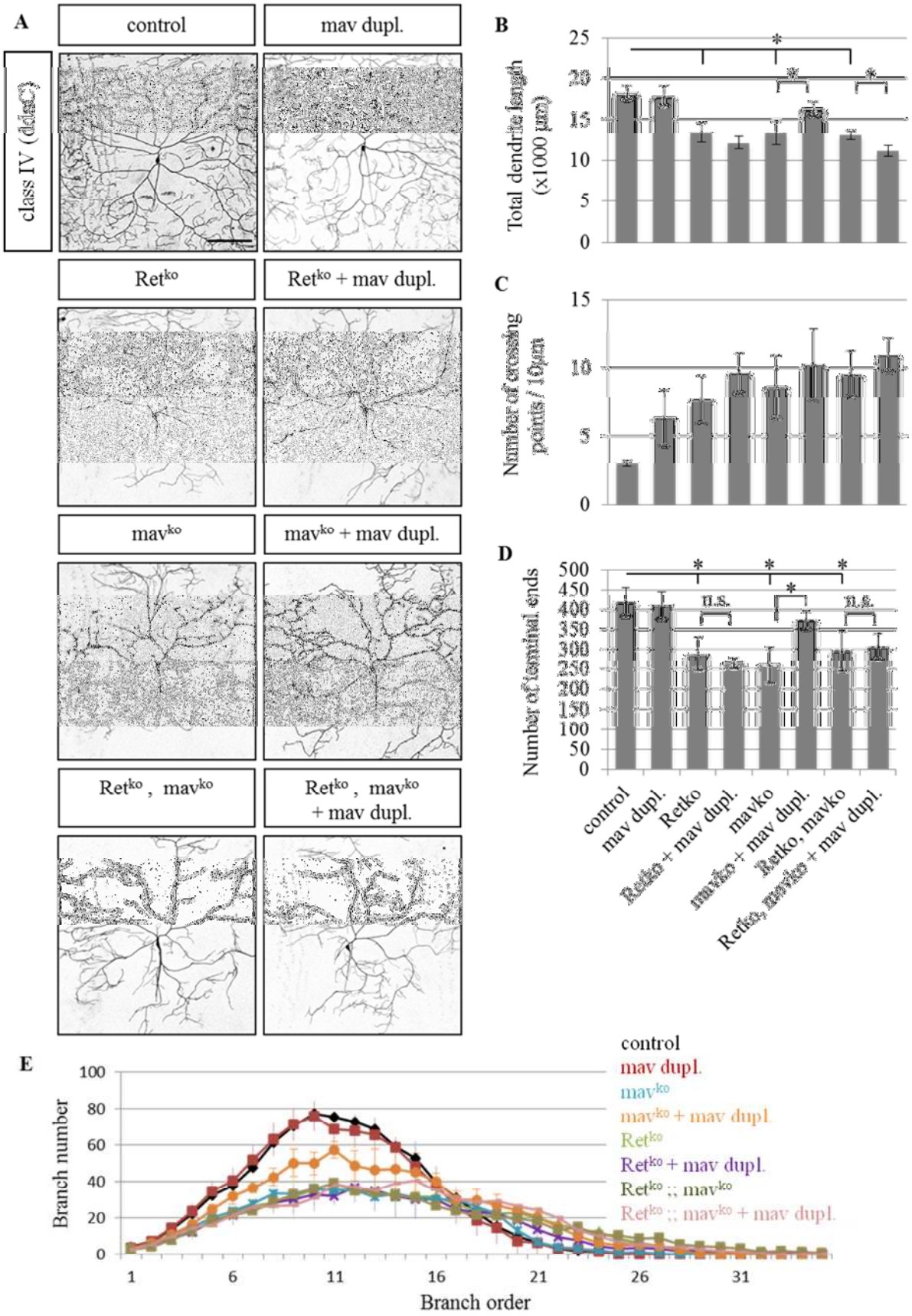

Figure 37. *Ret* and *mav* double knock-out larvae do not display increased C4da neuron defects and genomic mav expression rescues *mav* but not Ret phenotypes. A) Dendritic pattern of C4da neurons of *control*, *Ret*^{ko}, *mav*^{ko} and double knock-out (*Ret*^{ko};;mav^{ko}) with/without a mav duplication (mav dupl.) in 3rd instar larvae. Neurons were visualized by the expression of the C4da neuron-specific marker *ppk-CD4-tdTomato*. Scale bar: 100 µm. **B)** Quantitative analysis of the total length of C4da

neuron dendrites of indicated genotypes. **C)** Quantitative analysis of the crossing points/10 µm. **D)** Quantitative analysis of the number of terminals of C4da neuron dendrites. **E)** Strahler analysis to quantitatively visualize dendrite complexity. The numbers of dendrites are plotted against the increasing branch order. C4da neuron dendrite defects in Ret^{ko} and mav^{ko} were not enhanced in double knock-out larvae. The genomic mav duplication was able to rescue mav^{ko} but not Ret^{ko} or double knock-out defects in C4da neurons demonstrating that both genes act in the same genetic pathway with Ret acting downstream of mav. All data are mean ± SD, Mann-Whitney-Test $p<0.05$ (*), n=5.

The reduced number of C4da neuron terminal could only be rescued in mav^{ko} larvae using the mav duplication, but not in Ret^{ko} or double knock-out larvae (mav^{ko} +mav dupl.: 373.6 ± 23.22, Ret^{ko} +mav dupl.: 265.8 ± 14.09, Ret^{ko};;mav^{ko} + mav dupl.: 308.4 ± 32.1, p-value<0.05).

Accordingly, analysis of dendrite complexity by Strahler analysis confirmed these findings. Compared to *control* (*control*, mav dupl.), single *Ret* and *mav* knock-out C4da neurons exhibited a similar decrease in dendrite complexity as Ret^{ko}/mav^{ko} double knock-outs (Figure 37E). Only larvae expressing the endogenous mav duplication in the mav^{ko} background displayed a shift towards normal dendrite complexity observed in *controls*. Neither Ret^{ko} larvae nor the double knock-out mutant animals displayed a change in their dendritic complexity in combination with the mav duplication.

This data clearly shows that mav^{ko} and Ret^{ko} larvae exhibited similar C4da neuron dendrite defects which were not enhanced in double knock-out larvae. Moreover, a genomic mav duplication was able to rescue mav^{ko} but not *Ret* or double knock-out defects. Taken together, this dataset clearly shows that *mav* and *Ret* are in the same genetic pathway with Ret acting downstream of mav.

10.9.4 Classical TGFβ-receptors are not involved in C4da neuron dendrite development

The *mav* gene encodes a ligand belonging to the transforming growth factor β (TGFβ). In *Drosophila*, the of TGFβ signaling is subdivided into the BMP and Activin pathway, which both employ type I and type II TGFβ receptors.

To explore the importance of TGFβ signaling in C4da neuron dendrite development and the possible interaction with Ret, all type I (Thickveins [*tkv*], Saxophone [*sax*], Baboon [*babo*]) and type II (Punt [*put*], Wishful Thinking [*wit*]) receptors were investigated. The morphology of C4da sensory neurons of TGFβ receptor mutants was visualized using *ppk-CD4-tdTomato*.

Except for *tkv* and *sax*, mutations of TGFβ receptors were homozygously viable until the 3rd instar larval stage. For *tkv*, a dominant negative transgene (*UAS-tkvQ253D*, Riesgo-Escovar and Hafen, 1997) was expressed in all sensory neurons under UAS control (*21-7-Gal4*

driver). For *sax*, transheterozygous larvae of available EMS (Ethylmethylsulfonate) alleles were analyzed (*sax*^{4}/*sax*^{5}, Twombly et al., 1996). For baboon, the *babo*^{32} allele was selected which contains a deletion that removes the translation start site and the first 53 amino acids (part of the extracellular domain) (Brummel et al., 1999). For type II receptors, the alleles *wit*^{A12} and *put*^{10460} were tested (Marqués et al., 2002, Letsou et al., 1995;). *Wit*^{A12} contains a nucleotide substitution (C684T) introducing a stop codon prior to the transmembrane segment. For *put*, a mutant derived by insertional mutagenesis using the *P-element* construct was selected.

Analysis of all genotypes revealed that none of the known TGFβ receptors in *Drosophila* showed defects in C4da neuron morphology, indicating that classical TGFβ signaling is not involved in C4da neuron dendrite development (Figure 38). Furthermore, TGFβ receptors and Ret showed no genetic interaction (data not shown). These data show that Ret signaling via the TGFβ ligand mav is TGFβ receptor-independent.

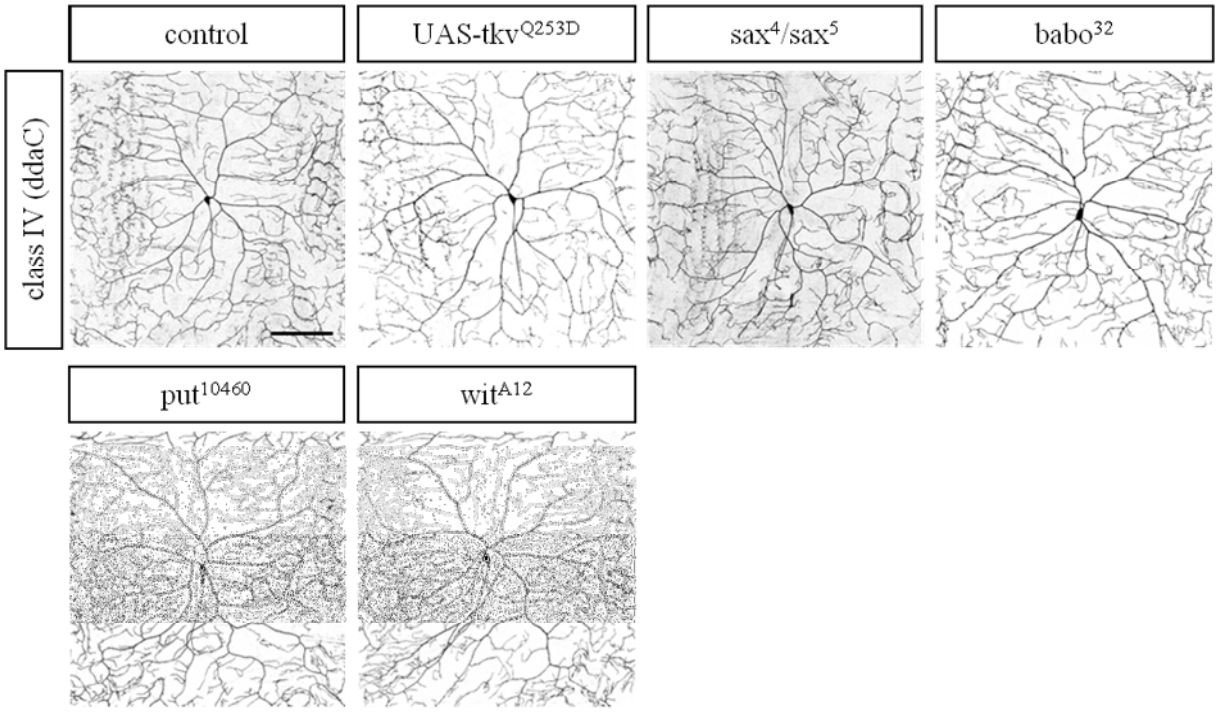

Figure 38. Classical TGFβ-receptor loss-of-function does not affect C4da neuron dendrite morphology. Dendrite morphology of C4da neurons of *control* 3rd instar larvae compared to transgenes and alleles of TGFβ receptors type I (upper row) and type II (bottom row) visualized by the expression of *ppk-CD4-tdTomato*. Transgenes: *UAS-tkv*^{Q253D} (dominant negative transgene under UAS control, expressed pan-neuronal using *21-7-Gal4* driver). Alleles: *sax4*, *sax5* (EMS induced point mutation), *babo*^{32} (deletion of start codon and part of the extracellular domain), *wit*^{A12} (C684T nucleotide substitution, stop codon in transmembrane segment), *put*^{10460}: (*P-element* P{PZ} insertion in genomic locus of *put*). None of the TGFβ receptor alleles induced C4da neuron morphological phenotypes. Scale bar: 100 µm.

10.10 Discovery of downstream partners in Ret signaling pathway

To find genes implicated in Ret signaling in C4da neurons FACS assisted sorting of C4da neurons and subsequent genome wide microarray analysis was employed. To this end, the transcriptome of *control* and *Ret*^{ko} C4da neurons was compared to uncover genes implicated in Ret signaling in dendrite development. The experiments and analysis was performed in collaboration with Jay Parrish (University of Washington, Seattle) and Charles Kim (University of California, San Francisco).

10.10.1 RanBPM: regulator of Ret downstream signaling in C4da neurons?

The genome wide microarray analysis uncovered several genes with up- or downregulated transcription levels showing a 2-fold or higher level differences in *Ret*^{ko} C4da neurons compared to *controls* (Figure 39). Particularly one gene, *RanBPM*, exhibited a strong decrease of expression in *Ret*^{ko} C4da sensory neurons (Figure 39C, red circle). In the following chapters, this candidate will be validated by analysing mutant alleles and its function in C4da dendrite development. One further focus will be its potential link to Ret signaling *in vivo*.

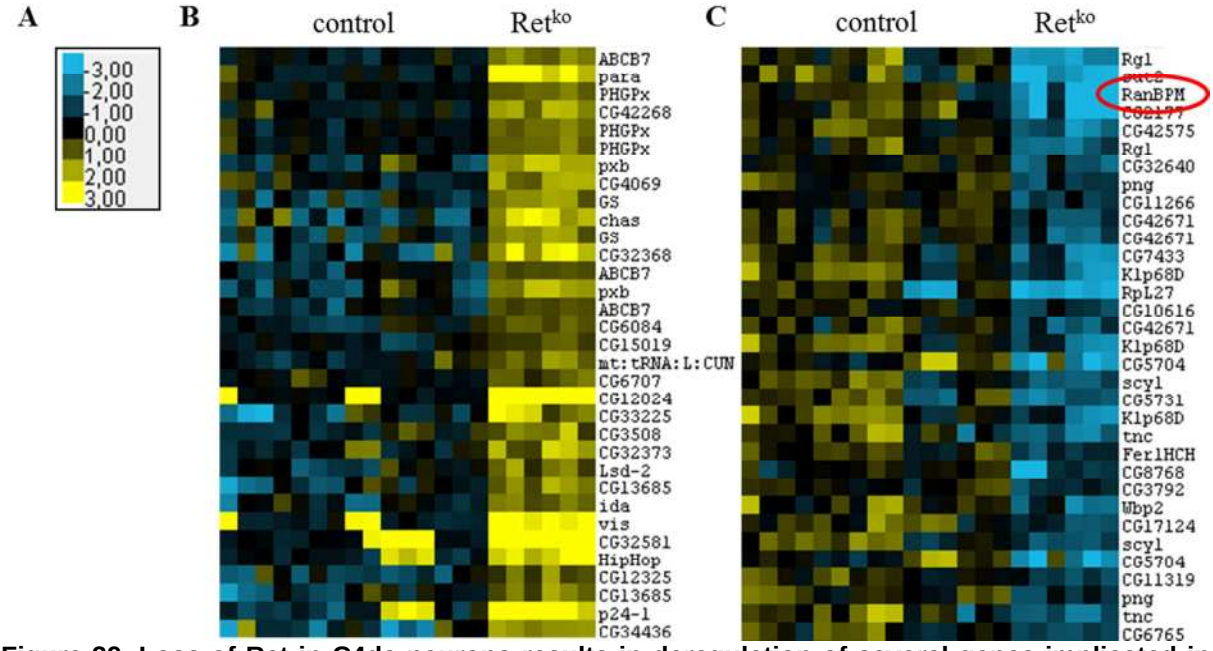

Figure 39. Loss of Ret in C4da neurons results in deregulation of several genes implicated in many aspects of cell signaling. Representative data set of genome wide microarray analysis of up- **(B)** and down-regulated **(C)** genes in *Ret*^{ko} larvae compared to *control*. The change of transcription level is shown color-coded (from blue to yellow) **(A)**. One biological repeat is shown in each column consisting of cells from 50-100 animals. The candidate gene *RanBPM* is indicated by a red circle.

10.10.1.1 *RanBPM* is expressed in C4da sensory neurons and its loss-of-function leads to Ret-like dendrite development defects

To investigate if RanBPM is expressed in C4da neurons a *Gal4 P-element* insertion within the *RanBPM* 5'-UTR was used (*RanBPM*^{NP6392}). Crossing this line to a *UAS-CD4-tdTomato* marker revealed that expression was restricted to C4da neurons and a subset of epithelial cell in close proximity to C4da neurons (Figure 40A).

Phenotypic analysis of this allele showed a phenotype in C4da neurons with coverage defects of the dendritic field and atypical isoneuronal dendrite crossing. This finding was confirmed using a second allele (*RanBPM*^{k05201}), which carried a P{lacW} insertion in the second exon of the *RanBPM* genetic locus. Similarly, transheterozygous larvae (*RanBPM*^{k05201}/ *RanBPM*^{NP6392}) exhibited similar dendritic defects (Figure 40B, arrows).

These results suggest that *RanBPM* is expressed in C4da neurons and *RanBPM* mutations exhibited similar dendrite development defects as *Ret* loss-of-function.

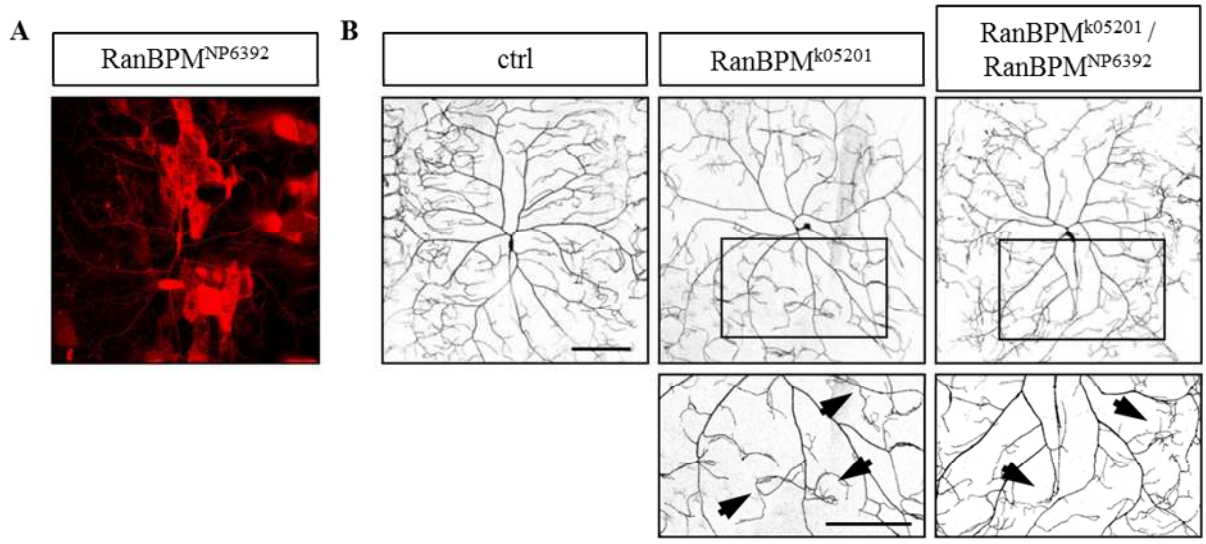

Figure 40. *RanBPM* is expressed in C4da sensory neurons and mutation leads to *Ret*-like defects in C4da neuron dendrite development. A) Expression pattern of RanBPM using a *Gal4 P-element* insertion within the 5'-UTR of *RanBPM* (*RanBPM*^{NP6392}). Crossing this line to a *UAS-CD4-tdTomato* marker revealed *RanBPM* expression in C4da sensory neurons and a subset of epithelial cell. **B)** Dendritic morphologies of C4da neurons of *control* and *RanBPM* alleles (*RanBPM*^{k0521}, *RanBPM*^{NP6392}) in 3rd instar larvae. Neurons were visualized by the expression of the C4da neuron specific marker *ppk-CD4-tdTom*. Scale bar: 100 µm. An enlarged section is shown below indicated by a rectangle. Scale bar: 50 µm. Note the growth and crossing defects in *RanBPM* alleles (indicated by arrows).

10.10.1.2 *Ret* and *RanBPM* are genetically linked

The previous investigations showed that *RanBPM* is expressed in C4da sensory neurons and implicated in dendrite development showing a mild but Ret-like phenotype (10.3).
Thus, the question was addressed whether *Ret* and *RanBPM* are genetically linked. To test genetic interaction between *Ret* and *RanBPM* two different RanBPM alleles were selected (*RanBPM*^{k0521}, *RanBPM*^{ts7}).
The morphology of C4da neuron dendrites of heterozygous *Ret* hypomorphic allele (*Ret*^{C168}/+) and *RanBPM* alleles (*RanBPM*^{k0521}/+, *RanBPM*^{ts7}/+) were compared to the corresponding transheterozygous combinations (Figure 41A). The neurons were visualized by the C4da neuron specific marker *ppk-CD4-tdTom*.
The quantitatively analysis of the total dendritic length of C4da neuron dendrites revealed no significant difference between *control*, *Ret*^{C168} and *RanBPM* heterozygous mutant larvae (*control*: 18291 µm ± 784, *Ret*^{C168}/+: 18723 µm ± 1293, *RanBPM*^{k0521}/+: 20622 µm ± 1059, *RanBPM*^{ts7}/+: 20367 µm ± 985). However, transheterozygous allelic combinations of *Ret* and *RanBPM*^{ts7} displayed a significant reduction in C4da neuron dendritic length compared to *control* and heterozygous animals (*Ret*^{C168}/*RanBPM*^{ts7}: 15781 µm ± 1851, p-value<0.05) (Figure 41B).
Isoneuronal crossing of C4da neuron dendrites was already significantly increased in heterozygous *Ret* mutated larvae da compared to *control* (*control*: 3.01 ± 0.23, *Ret*^{C168}/+: 9.75 ± 2.97, p-value<0.05) (Figure 41C). *RanBPM* heterozygous mutants displayed increased crossing of C4da neuron dendrites as well (*RanBPM*^{k0521}/+: 12.95 ± 1.39, *RanBPM*^{ts7}/+: 13.45 ± 1.52, p-value<0.05). However, the comparison of transheterozygous allelic combinations and heterozygous larvae revealed no enhancement of isoneuronal crossing.

Finally, the number of C4da neuron terminals was quantified. *Control* and heterozygous mutant animals exhibited no significant differences in their number of C4da neuron terminals (*control*: 420 ± 36, *Ret*^{C168}/+: 439 ± 38, *RanBPM*^{k0521}/+: 497 ± 44, *RanBPM*^{ts7}/+: 446 ± 33) (Figure 41D). The transheterozygous allelic combinations of *Ret* and *RanBPM*^{ts7} resulted in a significant reduction of terminals compared to *control* and heterozygous animals (*Ret*^{C168}/*RanBPM*^{ts7}: 361 ± 46, p-value<0.05). For *RanBPM*^{k0521}, this effect could not be observed. These different results might be explained by the differences of their strength of the *RanBPM* alleles, since the *RanBPM*^{k0521} allele carries a transposable element insertion P{lacW} in the second exon of *RanBPM* coding sequence suggesting it is a hypomorphic allele. In contrast, *RanBPM*^{ts7} contains a deletion from within 10 bp of the predicted start site extending upstream suggesting it is a null mutation.
In summary, these data show that *RanBPM* is also required for proper C4da neuron dendrite development and field coverage and exhibits Ret-like dendrite defects. Second, a functional genetic link between *Ret* and *RanBPM* was identified showing that they are acting in a

common pathway affecting total dendritic length and terminal numbers of C4da neurons. However, how precisely Ret and RanBPM are connected has to be investigated in more detail.

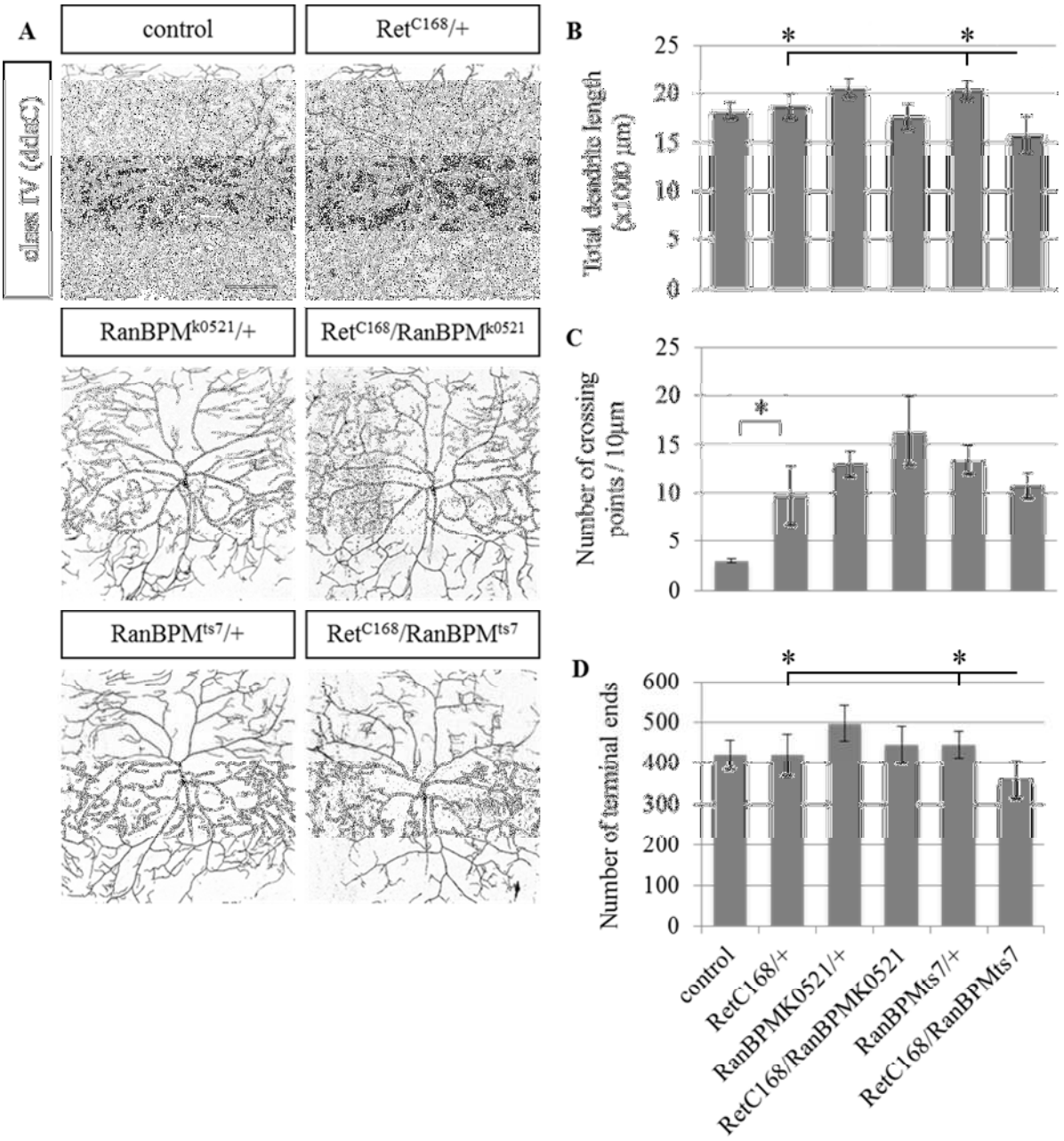

Figure 41. RanBPM is genetically linked to Ret. A) Dendrite morphology of *control*, *Ret* hypomorphic (*Ret*^{C168}) and *RanBPM* alleles (*RanBPM*^{k0521}, *RanBPM*^{ts7}) in heterozygous and transheterozygous C4da neurons in 3rd instar larvae. Neurons were visualized by the expression of the C4da neuron specific marker *ppk-CD4-tdTom*. Scale bar: 100 µm. **B)** Quantitative analysis of the total length of C4da neuron dendrites of indicated genotypes. **C)** Quantitative analysis of the crossing points/10 µm. **D)** Quantitative analysis of the number of terminals of C4da neuron dendrites. *RanBPM* is implicated in dendrite development of C4da neurons and genetically linked with *Ret* affecting total dendritic length and terminal numbers of C4da neurons. All data are mean ± SD, Mann-Whitney-Test $p<0.05$ (*), n=5.

10.10.1.3 Overexpression of *RanBPM* failed to rescue the *Ret*^{ko} phenotype

Based on the phenotypic similarities and positive genetic interaction between *Ret* and *RanBPM*, the hypothesis was tested if RanBPM is a downstream signaling partner of Ret. For this purpose, two RanBPM isoforms (short and long isoform) were overexpressed in C4da neurons using a specific C4da neuron driver (*ppk-Gal4*), and its ability to rescue *Ret*^{ko} deficits was tested. The long isoform contains a unique non-conserved glutamine rich region at the N terminus not present in the short isoform (Dansereau and Lasko, 2008). However, neither of the two RanBPM isoforms had the capacity to rescue C4da neuron defects upon overexpression in *Ret*^{ko} larvae (Figure 42).

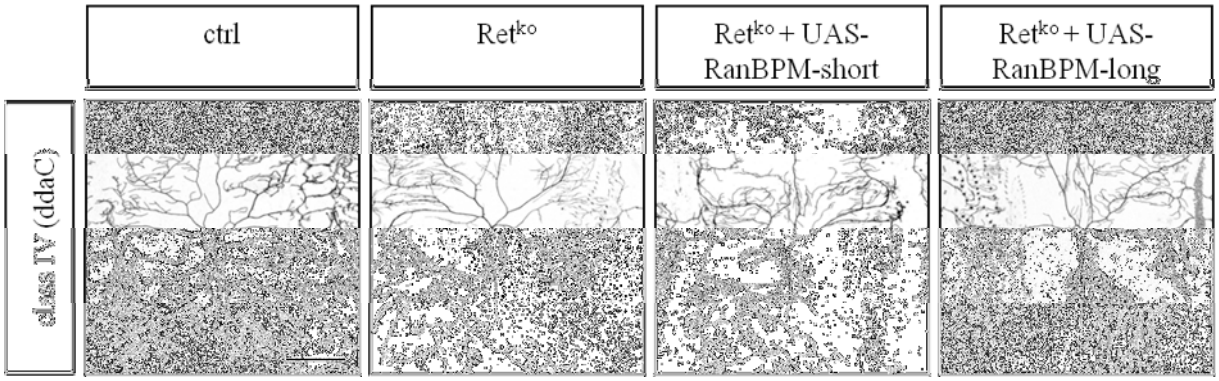

Figure 42. Expression of *RanBPM* in C4da neurons cannot rescue the *Ret* loss-of-function phenotype. Dendrite morphology of C4da neurons in *control*, *Ret*^{ko} and *RanBPM* overexpressing (*UAS-RanBPM-short* and *-long*) 3rd instar larvae using *ppk-Gal4*. Neurons were visualized by the expression of *UAS-CD4-tdGFP*. Scale bar: 100 µm.

10.11 Behavioral analysis of *Ret* in C4da neuron sensory function

The morphological analysis of C4da neurons in Ret^{ko} larvae revealed severe morphological defects including reduced dendritic field coverage and defects in dendritic self-avoidance. The dendrite defects could be completely rescued by cell-autonomous overexpression of Ret in C4da neurons.

C4da sensory neurons of *Drosophila* larvae have been identified as polymodal nociceptors and are necessary for sensing thermal and mechanical noxious stimuli, such as high temperatures, mechanical forces and strong light intensities. Based on the morphological defects in C4da neurons of Ret^{ko} animals, several behavioral paradigms were analyzed. For this purpose, larval light avoidance behavior, the response to mechanical forces and larval locomotion of Ret^{ko} mutants were tested (Xiang et al., 2010; Zhong et al., 2010).

10.11.1 Ret^{ko} larvae display locomotion defects

First, locomotion behavior of Ret^{ko} larvae was tested by placing individual wandering 3rd instar larvae on a 6 cm dish containing 2% agar. Before tracking, the animals were allowed to adjust for 2–3 min. The plate was illuminated by a light source from below and each larva was tracked using EthoVision XT software.

The quantification revealed that c*ontrol* larvae showed an average velocity of 0.84 mm/s (± 0.17) in accordance with published data (0.8 mm/s, Cheng et al., 2010) (Figure 43A). Ret^{ko} larvae displayed significantly decreased crawling speed compared to *control* larvae (0.42 mm/s ± 0.16, $p<0.001$). In addition, Ret^{ko} larvae exhibited an increase in turning behavior during locomotion. The turning angle normalized to the traveled distance was significant increased compared to *control* animals (*control*: 195.5°/mm ± 132.7, Ret^{ko}: 837.6°/mm ± 457.3, $p<0.001$) (Figure 43B).

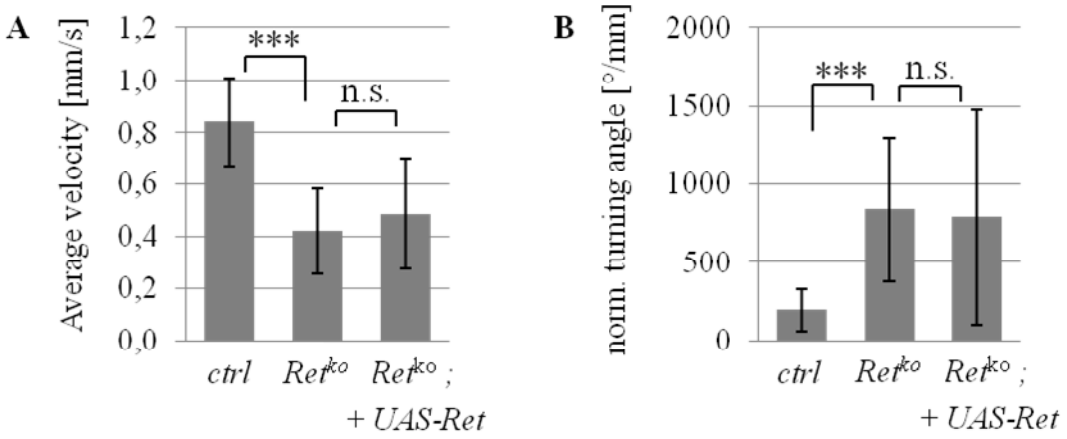

Figure 43. Ret^{ko} larvae exhibit defects in locomotion behavior. For locomotion behavior analysis, 3rd instar larvae were placed on a 2% agar plate and automatically tracked for 10 min using EthoVision XT. The average velocity **(A)** and normalized turning angle **(B)** was quantified. Ret^{ko} larvae displayed a significant locomotion defect combined with an increase in turning behavior. These defects were not rescued by Ret transgene expression in C4da neurons using *ppk-Gal4*. All data are mean ± SD, Mann-Whitney-Test, $p<0.001$ (***), n=25, 19, 26.

To test if these defects could be rescued, a Ret transgene (+*UAS-Ret*) was specifically overexpressed in C4da neurons using *ppk-Gal4*. Analysis of these animals showed that both locomotion defects could not be rescued. Ret mutant larvae overexpressing Ret in C4da neurons exhibited an average crawling speed of 0.42 mm/s (± 0.16) and their normalized turning angle was 789.7°/mm (± 685.8). This result was different from the morphological observation, where the phenotype was completely rescued by cell-autonomous overexpression of *Ret* in C4da neurons (Figure 12A). These results thus indicate that *Ret* function might be necessary but not sufficient in C4da neurons for normal larval locomotion.

10.11.2 *Ret* loss-of-function impairs innate light avoidance behavior

To further assess *Ret* function in C4da neuron dependent behavior, its requirement for innate larval light avoidance was investigated. Light avoidance of 3rd instar larvae was measured at three different time points (5, 10 and 15 min) as described in chapter 9.8.3. The calculated preference index (PI) was plotted for each time point. For this assay, larvae carrying a *ppk-Gal4* transgene served as a *control* (Figure 44A).

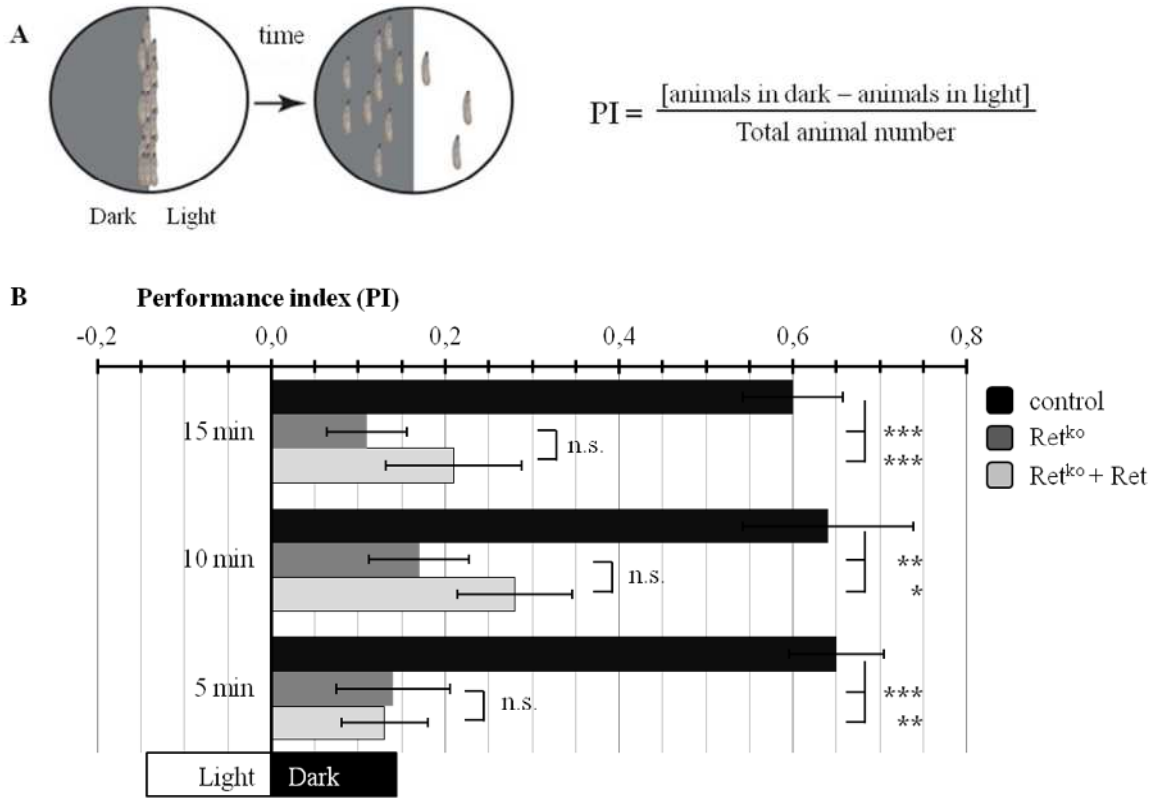

Figure 44. *Ret^{ko}* mutant larvae exhibit defects in light avoidance behavior. The performance index (P) for light avoidance was obtained after 5, 10 and 15 min. *Ret^{ko}* larvae displayed a significant light avoidance defect, which was not rescued by Ret transgene expression in C4da neurons using *ppk-Gal4*. All data are mean ± SD, Mann-Whitney-Test p<0.05 (*), p<0.01 (**), p<0.001 (***), n=10. In this and in subsequent figures the 'n-number' refers to the number of trials per genotype with 20 animals/trial.

Control larvae showed normal innate light avoidance behavior across the three time points (PI after 5 min: 0.65 ± 0.05, 10 min: 0.64 ± 0.10 and 15 min: 0.60 ±, 0.06, n=10) (Figure 44B). In contrast, Ret^{ko} larvae displayed a significant reduction in dark preference (PI after 5 min: 0.14 ± 0.07, 10 min: 0.17 ± 0.06 and 15 min: 0.11 ± 0.05, n=10).

To test if the light avoidance defect could be rescued, Ret (+Ret) was specifically overexpressed in C4da neurons using *ppk-Gal4*. Interestingly, this light avoidance defect could not be rescued by C4da neuron sspecific Ret overexpression (PI values after 5 min: 0.13 ± 0.05, 10 min: 0.28 ± 0.07 and 15 min: 0.21 ± 0.08, n=10). Similarly to the defects in locomotion, this result suggests that *Ret* is necessary for accurate larval light avoidance, but not sufficient when only expressed in C4da neurons.

10.11.3 *Ret* loss-of-function impairs mechano-nociceptive behavior

Lastly, the impact of Ret on C4da neuron function in mechano-nociceptive behavior was investigated. For this assay, a mechanical force (40-50 mN) was applied to the mid-abdominal segments of the larval body wall during their peristaltic movement (Figure 45A). The detectable behavioral reaction to this force was classified into five groups: no response, stop, stop + turn (non-nociceptive responses), bending and rolling (nociceptive responses).

Performing this assay revealed that Ret^{ko} larvae showed a decrease in nociceptive responses compared to *control* w^{1118} larvae (Figure 45B). 86% *of control* larvae displayed nociceptive responses (bending + rolling behavior). In contrast, only 32% of Ret^{ko} larvae showed this nocifensive response to the mechanical force.

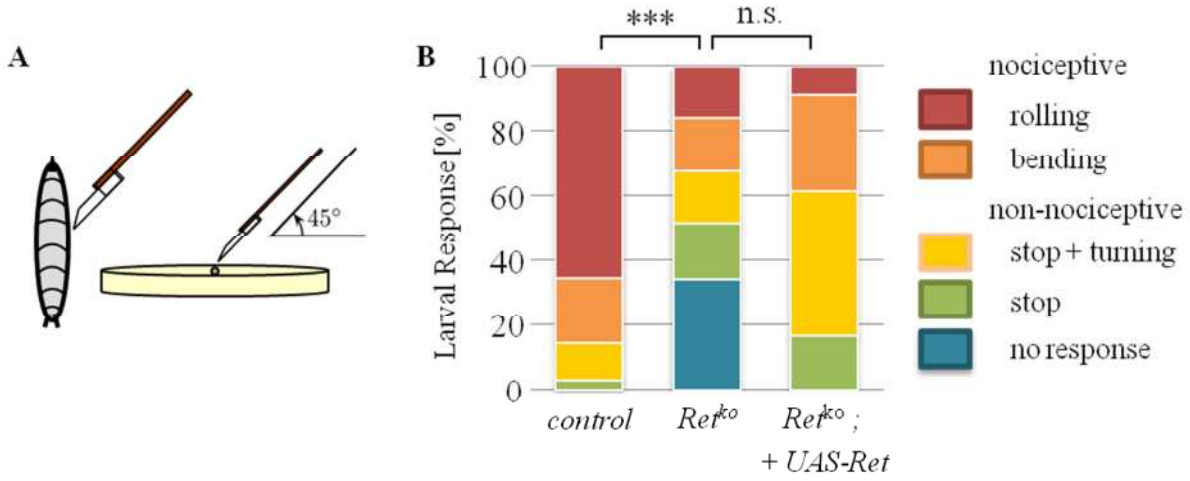

Figure 45. *Ret* is required for C4da neuron nociceptive circuitry function. A) Harsh mechanical touch results in nocifensive rolling behavior of *Drosophila* larvae. Larvae were analyzed on wetted 2% agar plates. The nociceptive stimulus was applied to mid-abdominal segments (force of 40-50 mN). The behavioral response was classified into nociceptive (rolling, bending) and non-nociceptive responses (stop and turn, stop no response). **B)** Relative values of classified responses of 3rd instar larvae. Behavior of *control*, Ret^{ko} and specific C4da neurons Ret rescue in Ret^{ko} mutants by using *ppk-Gal4* was compared. Chi-square test: χ^2 (1 degree of freedom, n=70,68,67), p-value<0.001 (***).

Additionally, 34% of *Ret^{ko}* larvae did not react at all (no response), which never occurred in *control* animals. To test whether these defects could be rescued, Ret (+Ret) was again specifically overexpressed in C4da neurons using *ppk-Gal4*. Unlike in the other assays, defects in mechano-nociception could be partially rescued by C4da neuron specific Ret overexpression (nociceptive response: 39%) (Figure 45B).
These animals displayed an increase in nociceptive bending behavior and the non-nociceptive responses were improved compared to *Ret^{ko}* animals as shown by an absence of "no response".
The statistical comparison of the different genotypes revealed a significant difference between *control* and *Ret^{ko}* larvae concerning their nocifensive or non-nocifensive behavior response. There was no significant difference in nociceptive responses between *Ret^{ko}* and C4da neuron specific Ret overexpression in *Ret^{ko}* larvae (*Ret^{ko} +Ret) animals.* However, their general behavioral response was significantly different compared to *Ret^{ko}* larvae (Kruskal-Wallis One-way ANOVA, all pair wise multiple comparison procedure, Dunn´s *post-hoc* analysis).
These data indicate that *Ret* is required in C4da sensory neurons for larval mechano-nociceptive behavior and overexpression can mitigate mechanosensory response defects but not nociceptive behavior.

10.11.4 *Mav^{ko}* and *Ret^{ko}* larvae display similar defects in C4da neuron dependent nociceptive behavior

Similarly to *Ret*, the loss of *mav* resulted in a severe C4da neuron dendrite phenotype. Based on the genetic link between *mav* and *Ret, mav^{ko}* animals were tested in nociceptive behavior as well. For this purpose, larval light avoidance behavior and mechano-nociception assays were tested as above.
Mav^{ko} larvae showed no significant difference in light avoidance behavior after 5 and 10 min (PI after 5 min: 0.27 ± 0.11. 10 min: 0.32 ± 0.06, n=10) compared to *control* larvae (*w^{1118}*, PI after 5 min: 0.41 ± 0.06, 10 min: 0.45 ± 0.05, n=10) (Figure 46).
However, after 15 min *mav^{ko}* larvae exhibited a significant light avoidance defect (*mav^{ko}* PI after 15 min: 0.26 ± 0.05, *w^{1118}* PI after 15 min: 0.51 ± 0.06, n=10, p-value<0.001). This light avoidance defect was weaker compared to *Ret^{ko}* larvae, as loss of Ret resulted in a stronger reduction in dark preference (PI after 5 min: 0.14 ± 0.07, 10 min: 0.17 ± 0.06 and 15 min: 0.11 ± 0.05) (Figure 44B).

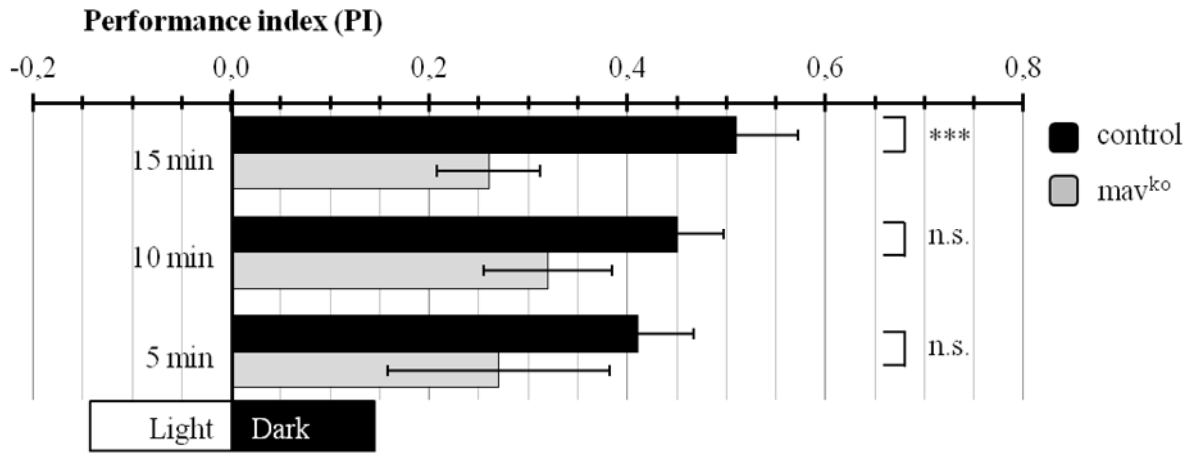

Figure 46. *Mav*^{ko} mutant larvae exhibited defects in light avoidance. The performance index (P) for light avoidance was obtained after 5, 10 and 15 min. *Mav*^{ko} larvae displayed a significant light avoidance defect after 15 min of testing. All data are mean ± SD, Mann-Whitney-Test p-value<0.001 (***), n=10. In this and in subsequent figures the 'n-number' refers to the number of trials per genotype with 20 animals/trial.

Next, the larval response to a painful mechanical stimulation (40-50 mN) was investigated and the detected behavioral reaction was classified as previously described.

The quantification showed that overall nocifensive behavior of *mav*^{ko} animals was not different compared to *control* animals (*control*: 84%, *mav*^{ko}: 76%) (Figure 47). However, regarding to the two types of nociceptive responses, *mav*^{ko} mutant animals displayed a decrease in rolling behavior (*control*: 62%, *mav*^{ko}: 27%) and concomitant increase of bending (*control*: 22%, *mav*^{ko}: 49%). This phenotype was weaker than in *Ret*^{ko} larvae.

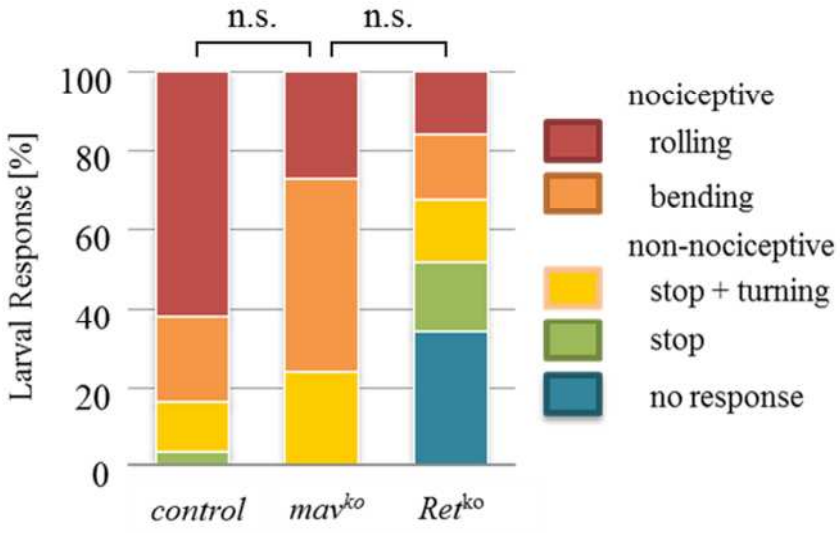

Figure 47. *Mav*^{ko} larvae exhibited defects in mechano-nociceptive behavior. Response of 3rd instar larvae to a mechanical nociceptive stimulus (force of 40-50mN). The behavioral response was categorized into nociceptive (rolling, bending) and non-nociceptive responses (stop and turn, stop, no response). Behavior of 3rd instar *control*, *mav*^{ko} and *Ret*^{ko} larvae was compared. Chi-square test: χ^2 (1 degree of freedom, n=70,64,68), p-value 0.001 (***).

Statistical comparison between *control* and *mav*^{ko} larvae revealed no significant difference regarding their nocifensive or non-nocifensive behavioral response. However, both genotypes displayed a significant difference in terms of the general behavior response (Kruskal-Wallis One-way ANOVA, all pairwise multiple comparison procedure, Dunn´s Method). The comparison of *Ret* and *mav* loss-of-function animals displayed a significant difference in both, their nocifensive and general behavioral responses.

In summary, *mav*^{ko} larvae showed defects in light avoidance and mechano-nociception similarly to *Ret*^{ko} animals, suggesting *mav* is required for C4da neuron sensory function as well. However, the observed behavioral alterations in *mav*^{ko} mutants were less severe than in *Ret*^{ko} animals (Figure 44B, Figure 45B).

11 DISCUSSION

11.1 Ret is required for C4da neurons dendrite morphogenesis

The development of the nervous system requires correct neuronal specification to allow proper sensory information processing and communication within the neuronal network.
This study demonstrates that the receptor tyrosine kinase Ret is a novel key regulator in dendrite growth and spreading of sensory C4da neurons, which has not yet been reported.
The loss of *Ret* results in a strong phenotype in C4da neurons *in vivo* exhibiting severe dendrite patterning defects on the morphological level indicated by reduced dendritic field coverage, dendrite length and an increase in crossing events. In general, the complexity of those sensory neuron dendrites was dramatically decreased. Moreover, C4da neuron dendrites display defects in extracellular matrix adhesion, which impaired proper growth of C4da sensory neuron dendrites within their 2D plane.
Astonishingly, all characteristics of this severe phenotype could be rescued by cell type specific C4da neuron expression of transgenic *Ret* in Ret^{ko} animals. These results provided evidence that Ret acts cell-autonomously in C4da neurons and Ret expression is both necessary and sufficient for normal development of C4da dendrites.

11.1.1 Ret function in C4da neurons does not require its kinase activity

In this study, the dissection of conserved *Ret* domain function by studying their phenotypic rescue capacity uncovered that both extra- and intracellular domains are required for C4da dendrite development. This already suggests that extracellular interaction with other proteins and intracellular signaling via Ret are essential for the control of C4da morphogenesis.
Surprisingly, the analysis revealed that the tyrosine kinase domain plays only a minor role in C4da sensory dendrite development. Even more surprisingly, activity of the Ret tyrosine kinase is completely dispensable for Ret function, since the expression of a kinase-dead Ret transgene (*UAS-Ret-K805M*) showed complete rescue capacity.
Besides the high degree of sequence conservation of the intracellular domain based on *in silico* analysis among different species, the kinase activity has been shown in both *in vitro* and *in vivo*. The functional conservation was shown by a chimeric molecule consisting of the human Ret ectodomain ($hRET^{ECD}$) and the *Drosophila* Ret kinase domain ($dRET^{KIN}$). The stimulation of transfected $hRET^{ECD}/dRET^{KIN}$ chimera PC12 cells with its cognate ligand GDNF resulted in neurite outgrowth as transfection with wild type hRET. This result confirmed the conserved functionality of the Ret tyrosine kinase activity and downstream signaling between human and *Drosophila* and its function in neuronal differentiation (Abrescia et al., 2005). *In vivo* studies could show that *Ret* transgene expression in the *Drosophila* eye caused phenotypes resulting in excessive proliferation and aberrant neuronal specification. Similar

phenotypes were observed using multiple endocrine neoplasia 2B (MEN 2B) mutations which are modulated by the Ras/ERK signaling pathway (Read et al., 2005; Runeberg-Roos et al., 2007). These studies demonstrate that the intracellular tyrosine kinase is active and functionally conserved in invertebrates and vertebrates. However, its function in C4da neuron development *in vivo* in *Drosophila* is dispensable, at least at the morphological level.

Similarly, *Drosophila* Derailed (Drl) is also a receptor tyrosine kinase which does not require kinase activity for its function. *Drl* is implicated in controlling axon guidance in the developing nervous system of *Drosophila*. During early development, *Drl* is expressed on the growth cones and axons of all neurons. Its function is to navigate the tracts of commissures in each segment to connect the opposite sides of the bilaterally symmetric *Drosophila* nervous system. Loss-of-function analysis of *Drl* showed abnormal midline crossing events form the anterior commissure (AC) neurons into the posterior commissure (PC). In *Drl* mutant animals, axons from the PC are switched to the AC. However, a kinase-deficient *Drl* mutant was able to rescue these observed axon guidance defects indicating that *Drl* does not require its kinase activity in this system (Yoshikawa et al., 2001). However, *Drl* contains several unusual amino acid substitutions in its catalytic domain, which are usually highly conserved in RTKs. Therefore, Drl is classified as member of the “related to tyrosine kinases” (RYK) subfamily of RTKs, of which several members display catalytically inactive forms of the tyrosine kinase domain (Hanks et al., 1988).

In mammals, stimulation of the Ret receptor activates several second messenger pathways by inducing Ret autophosphorylation of intracellular tyrosine residues. It is thought that after activation, distinct protein complexes carrying specific binding domains assemble on phosphorylated tyrosine residues, which consequently stimulate different downstream signaling pathways.

Ret signaling pathway has been studied in many different cell and mouse models. In the mammalian system, 16 tyrosines are present in the intracellular domain of RET9 and RET43 isoforms, and 18 tyrosines in RET51 isoform that can be phosphorylated. Once phosphorylated, the intracellular domain of RET displays multiple docking sites for certain effector proteins, including Shc (Src homology 2 domain containing), Grb2 (Growth factor receptor-bound protein 2), Src kinase or PLCγ (phospholipase Cγ) (Jain et al., 2006; Manié et al., 2001). These signaling adaptors activate the Ras/RAF pathway, which leads to activation of the mitogen-activated protein kinases ERK1 and ERK2 (Worby et al., 1996), phosphatidylinositol 3-kinase (PI3K), resulting in activation of the serine/threonine kinase Akt and cell survival (Segouffin-Cariou and Billaud, 2000), Jun NH2-terminal protein kinase (JNK) (Chiariello et al., 1998), p38MAPK (Kurokawa et al., 2003), and PLCγ (Knauf et al., 2003).

The alignment of human and *Drosophila* Ret indicates that several of these tyrosine residues are conserved. Y900 and Y905 are positioned within the predicted tyrosine kinase domain

and are essential for full kinase activation (Knowles et al., 2006). The finding that the transgenic rescue using a tyrosine kinase deletion transgene can partially rescue the *Ret*^{ko} C4da neuron defects indicates that phosphorylation of these tyrosine residues and the activation of the published Grb7/10 signaling pathway plays only a minor role in C4da dendrite development.

The analysis further revealed that full-length *Ret* can completely rescue *Ret* loss-of-function defects, whereas the deletion of the complete intracellular domain did not. This finding suggests that other motifs within the C-terminal domain are necessary for Ret function in C4da neuron morphogenesis. However, the complete absence of the intracellular domain might also influence Ret sorting and localization, which may affect its capacity of the transgenic rescue. Nonetheless, epidermal or pan-sensory overexpression of the C-terminally truncated Ret transgene was fully capable of inducing a C4da neuron phenotypes suggesting it is delivered to the cell surface and able to interfere with C4da neuron specific signals.

Regarding potential phosphorylation sites, conserved tyrosines Y1015 and Y1096 are located close to the C-terminal end of Ret. It has been shown that Y1015 (representing a binding site for PLCγ) is required for cell signaling mediated by both ligand-dependent and -independent activation of RET, which might be a potential site required for Ret signaling in C4da neuron development.

Further, the phosphorylation of the conserved Tyr1096 residue is required for activation of Ras/MAP/ERK and PI3K/Akt pathway (Besset et al., 2000; Jain et al., 2006). This phospho-site might be also an important residue for Ret function in C4da neuron dendrite development.

In the mammalian system, phosphorylation of Y1062 is described to activate signaling pathways including the Ras/MAPK/ERK, PI3K/AKT, p38MAPK, JNK and ERK5 by acting as a binding site for SHC, DOK1, DOK4 and 5, and Enigma (Durick et al., 1998; Grimm et al., 2001; Murakami et al., 2002; Ohiwa et al., 1997). This tyrosine residue is located in the catalytic core of the RET tyrosine kinase domain. The replacement of the tyrosine with phenylalanine (Y1062F) induces a conformational change and markedly alters Ret catalytic activity. This structural change results in activation without dimerization and is present in all types of MEN 2B patients (Jijiwa et al., 2004; Ohiwa et al., 1997). Based on sequence analysis, the localization of Y1062 is not conserved in *Drosophila* indicating that these pathways are not activated (see appendix, sequence alignment of dRet and RET). However, the sequence analysis showed that alternative tyrosines are located within the C-Terminus, which could be required to induce Ras/ERK and MAPK activation to contribute to cellular differentiation and proliferation.

In mammals, ligand binding to the extracellular portion of the receptor activates several second messenger pathways by inducing Ret autophosphorylation of intracellular tyrosine residues as described before.

Comparing the vertebrate and invertebrate extracellular sequence of Ret indicated a lower sequence identity (~ 40%) compared to the intracellular sequence homology (Hahn and Bishop, 2001). However, it comprises homologous elements among different species including the Cadherin-like domain (CLD) and the Cysteine-rich domain (CRD). Based on the degree of homology, it can be speculated that the known domain functions in the mammalian system are also crucial and thus transferable to invertebrates such as *Drosophila*. Vice versa, the high conservation and similar expression pattern (Hahn and Bishop, 2001) suggest similar functions in dendrite development in vertebrates.

The structure-function analysis of the extracellular compartments of Ret in C4da dendrite morphogenesis demonstrated that both domains, CLD and CRD, are essential for proper development. These truncated deletion transgenes do not have the capacity to rescue C4da neuron dendrite defects in *Ret* mutant animals. This result shows that extracellular interaction of Ret is essential for proper dendrite development and patterning of C4da sensory neurons.

The inability to rescue can be explained by different reasons due to their specific described functions. In mammalian Ret, four CLDs are present whereas *Drosophila* comprises one CLD domain. CLDs mediate Ca^{2+}-dependent cell–cell adhesion based on their amino acids repeats within the extracellular domain. However so far, Ret has not been shown to be involved in cell adhesion by homophilic interactions (Abrescia et al., 2005). Additionally, there are several publications focusing on the question which domains are implicated in GDNF binding. Baloh et al. provided insights into the GFRα1 and RET interaction and GDNF receptor binding sites and reported that sites along the domain 2 of GDNF as being critical for interacting with GFRα1 and activating RET (Baloh et al., 2000). Initially, it was proposed that GDNF–GFRα1 complex interacts with the CLD1– CLD3 domains of RET and it is suggested that the first CLD of RET contains the largest GFRα1 interface (Kjær and Ibáñez, 2003). Based on biochemical and mutagenesis analysis Leppänen et al. postulated the model that GFRα1 acts as scaffold to hold GDNF in place in a pocket-like structure acting with CLD1 and CLD4 of RET (Leppänen et al., 2004). However, this direct interaction involving CLD1–CLD3 domains of RET has not been confirmed in an independent analysis (Amoresano et al., 2005). Instead, it was reported that the CLD4 and CRD domains of RET are required for binding of RET to the GDNF– GFRα1 complex (Wang, 2013). These results indicate that the GDNF- GFRα1 complex is responsible for RET association; however, the structural details of the interaction are still controversial and an open question. With respect to Ret and its function in C4da neurons it can be postulated that lack of the CLD might either lead to prevent binding of the potential ligand or co-receptor directly to Ret, or the disability of receptor recruitment.

Concerning the functionality of the CRD it is described that the cysteine residues in the CRD are required for intramolecular di-sulphide bridges. These interactions are important for the tertiary structure and thus the stability of Ret protein (Anders et al., 2001). In humans, Multiple Endocrine Neoplasia 2A (MEN 2A) is associated with mutations of cysteine residues in the CRD (conserved residues 609, 611, 618, 620, 630 and 634). These mutations lead to abnormal di-sulphide bridges between RET molecules inducing dimerization and constitutive receptor activity (Donis-Keller et al., 1993; Takahashi, 2001). Within the CRD region, 14 of 28 cysteine residues are conserved between human, zebrafish and *Drosophila* Ret (Hahn and Bishop, 2001). In regard to this, it might be possible that lack of this domain disrupts dimerization of Ret molecules, or structural instability of the protein, both of which could interrupt intracellular signaling. Besides that, the general structure of Ret lacking the CRD transgene might impair its function, since the remaining CLD has a shorter membrane distance. This may affect the primary protein structure and CLD interactions which could have influence on the rescue capacity. The generation of a linker insertion instead of a complete domain deletion might be worthwhile to exclude this potential caveat.
Based on the structure-function analysis it can be speculated that unidentified proteins interact directly or indirectly with the Ret receptor to mediate C4da patterning and growth by downstream signaling pathways. This question will be pursued in the following sections in more detail.

11.1.2 C4da dendrite and extracellular matrix (ECM) interaction depend on Ret

The analysis of Ret function in C4da neuron dendrite development uncovered its function in dendrite crossing indicative of self-avoidance defects. However, detailed examination of C4da dendrites revealed Ret being necessary for dendrite-ECM interaction since its loss-of-function significantly increased the percentage of C4da neuron dendrites detached from the ECM. During development, C4da neuron dendrites grow in a 2D plane to establish their extensive receptive field, which supports their capacity to tile the whole larval body wall to sense and to react to noxious stimuli essential for survival (Grueber et al., 2007; Xiang et al., 2010). C4da neuron dendrites grow between the epidermis and the extracellular matrix (ECM) secreted by the epidermis with both serving as substrates permitting neurite outgrowth. In Ret^{ko} animals, C4da neuron dendrites lose their ability to grow in a defined 2D space. As a consequence, recognition programs for proper dendrite patterning cannot execute correctly since isoneuronal dendrites grow within an atypical 3D space.
Interestingly, Ret is cell-autonomously required for dendrite and ECM interaction, since C4da neuron specific overexpression of full-length *Ret* was able to rescue the detachment phenotype. Further, both intra- and extracellular domains are essential for proper dendrite-ECM adhesion.

On the one hand, this result can be explained by the interaction of Ret with a different cell surface protein - either expressed in C4da neurons or the ECM (*cis*- or *trans*-interaction, respectively) - acting as a functional complex involved in dendrite-ECM adhesion and 2D growth of C4da neurons.
It has been shown that a major group of cell surface proteins, integrins, act as receptors for ECM-interaction. Integrins mediate adhesion by linking the ECM and intracellular signaling to cytoskeletal anchoring (Cabodi et al., 2010). Han et al. demonstrated that C4da neurons lacking the integrins *mys* or *mew* exhibit an increase of dendrites growing into the epidermis. This embedding defect was further shown by downregulating epidermal derived laminin, which is an integrin ligand. They postulate that both integrin and laminin function as a complex to attach C4da neuron dendrites to the ECM (Han et al., 2012; M. E. Kim et al., 2012). Recently, the investigation of a *Ret* hypomorphic allele has shown that Ret and integrins are forming a physically interacting complex controlling C4da neuron development and regulating dendrite-ECM adhesion. The high amount of dendrite crossing events in *Ret* mutant animals could be rescued by overexpression of integrins. However, their defects in C4da neuron dendrite growth were still not rescued arguing for other molecules mediating aspects of Ret signaling (Soba et al., 2015). Based on these findings, it can be postulated that loss of *Ret* in C4da neurons leads to the disability to interact with other proteins located at the cell surface to induce proper dendrite growth. It is also possible that complex formation of Ret and integrins is essential for the proper location and recruitment of Ret along dendrites to influence dendritic growth and their field organization.
On the other hand, the interactions of intracellular proteins with motifs located within the C-terminus of Ret are likely also involved in dendrite-ECM adhesion, since a *Ret* transgene lacking the intracellular domain cannot rescue the Ret^{ko} phenotype. Besides the interaction between Ret and integrins, Soba et al. could reveal that Ret and integrin function in dendrite-ECM adhesion is linked to rac1 activity (Soba et al., 2015). But, it is not clear if this interaction is direct or indirect. However, it clearly demonstrates that Ret downstream signaling is necessary for proper dendrite-ECM adhesion and 2D growth of C4da neurons.
Since integrins are intracellularly connected to the cytoskeleton and display biochemical interaction with Ret, loss of *Ret* might also influence the cytoskeletal organization.

Besides the interaction with substrates embedded in the surrounding environment, additional basic mechanisms like self-avoidance are required to establish a receptive field. This whole machinery is highly controlled by protein-protein and protein-substrate interaction and recognition and allows the dendrites of a distinct neuronal type to cover its receptive field without overlap (Grueber et al., 2002; M. E. Kim et al., 2012; Soba et al., 2007). In particular, the cell adhesion molecule Dscam (Down syndrome cell adhesion molecule) has been shown to control self-avoidance in both vertebrates and invertebrates. In *Drosophila*, *Dscam* mutant animals display an increase of crossing defects in da sensory neurons (Hughes et al.,

2007; Soba et al., 2007). However, dendrite crossing in *Dscam* mutants is caused by defects in repulsion of isoneuronal dendrites, which is not observed in *Ret* mutant animals and thus have to be considered separately.

11.1.3 Ret functions in C4da neuron dendrite growth

Besides dendrite crossing due to ECM adhesion defects, C4da neurons lacking *Ret* displayed strongly decreased total dendrite length and reduced dendritic field coverage. The examination of the field distribution of Ret^{ko} C4da neuron dendrites further revealed a growth preference towards the dorso-posterior compartment.

During development, C4da neurons have to innervate an enormous receptive field. How this field organization is controlled and supported is still largely unknown.

Major branches of C4da neurons in Ret^{ko} animals are almost correctly developed by growing along the anterior-posterior and dorsal-ventral axis, which indicates that they exhibit an intrinsic program for axial growth. Besides cell-intrinsic factors, graded expression of cell surface receptors and secretion of molecules provide spatiotemporal cues for cells to discriminate between boundaries and allow fine-tuning of growth and position. Over the last years, specific expression and localization of cell surface proteins acting as guidance cues and being responsible for morphological cell polarity along the body axis have been identified.

The transmembrane protein Flamingo (Fmi) has been identified as an important player in planar cell polarity and dendrite development. Fmi belongs to the Cadherin superfamily and during prehair outgrowth Fmi is predominantly localized to proximal and distal cell-cell boundaries in the wing. *Fmi* loss-of-function resulted in a polarization defect of wing cells along the P-D axis (Usui et al., 1999). Besides its function in planar polarity, Fmi is required for the proper regulation of dendritic field formation in C4da neurons. During development, Fmi is implicated in the extension of sensory dendrites and the regulation of self-avoidance of homologous neurons. Gao et al. could demonstrate that both *Fmi* loss-of-function and gain of function mutations are defective in self-avoidance of dendritic branches and result in an overextension phenotype in dorsal dendrites (Gao et al., 2000).

In a follow-up study, Matsubara et al. could identify an intracellular interaction partner of Fmi-mediated dendritic self-avoidance. They showed that Espinas (Esn), which encodes a LIM domain protein, is able to bind to a juxtamembrane domain of the C-tail of Fmi. This intracellular interaction of Fmi and Esn is important for the regulation of dendritic repulsion of C4da sensory neurons in *Drosophila* (Matsubara et al., 2011):

In addition, mutation of the transmembrane protein Golden Goal (Gogo) exhibits similar defects in the dendritic field formation of C4da neurons as shown in *Fmi* loss-of-function. *Gogo* mutant neurons display dendrite overextension and growth beyond their normal receptive field (Hakeda and Suzuki, 2013). Satoko et al. showed that Gogo is required to

restrain C4da neuron dendrite growth and found that gogo and fmi are genetically linked by showing a synergistic enhancement of dendrite crossing (Hakeda and Suzuki, 2013).
Besides Fmi and Gogo, conserved factors such as Frizzled (Fz) or Van Gogh (Vang) have been studied extensively due to their role in cell polarity establishment. There is evidence that the localization of Fmi is controlled by the non-uniform distribution of Fz across the proximal/distal cell boundary. However, while Fmi functions downstream of Fz in regulating planar polarity, its role in dendritic outgrowth is Fz-independent (Gao et al., 2000).
These studies demonstrate the importance of expression and localization of cell surface proteins to establish complex and stereotypic dendritic fields. Since Ret is specifically expressed in C4da sensory neurons it can be postulated that the expression of this receptor contributes to the highly coordinated C4da neuron growth in concert with other cell-surface proteins expressed in this neuronal subtype.

One further aspect during receptive field innervation is the achievement of a dynamic balance to ensure both the stability of a dendritic field and the potential to react to environmental changes during development. The expression of *Ret* in C4da neurons is also implicated in this function. In the study of Soba et al., it has been shown that *Ret* mutant animals displayed an increase in growing and retracting dendrite terminal and a change in dendritic f-actin distribution. This might explain the observed defects in dendrite stabilization (Soba et al., 2015). For the future, this has to be investigated in more detail for *Ret* null-mutants (Ret^{ko}), since the studied Ret^{C168} mutant is described as a hypomorphic allele and might still exhibit extra- and intracellular interaction capabilities. Further evidence for this function was shown in this thesis, since ectopic *Ret* expression in the epithelium also influenced C4da neuron dendrites by inhibiting dendrite growth into the ectopic *Ret* expression domain by decreasing dendrite dynamics.

Taken together, this thesis provides evidence that Ret dependent signaling pathway/s mediate C4da neuron patterning. The next steps will be the investigation of further C-terminal deletion transgenes to dissect intracellular domain function in more detail. Further, single or combined tyrosine mutations might uncover residues important for Ret function in dendrite patterning and growth.
Besides Ret´s function in C4da dendrite development, this thesis demonstrated its impact on C4da neuron sensory function. The highly branched C4da neurons function as polymodal nociceptors necessary for behavioral responses to noxious stimuli (Hwang et al., 2007; Zhong et al., 2010) and as shown here, Ret loss-of-function resulted in a decreased nociceptive response. Interestingly, the differentiation of low threshold mechanoreceptors has been shown to be Ret-dependent in mouse (Bourane et al., 2009; Liu et al., 2009) (see chapter 11.6). Since Ret is highly conserved it is thus possible that its novel function in dendrite development might be conserved in vertebrates as well.

11.2 Mav is implicated in C4da neuron dendrite development

To identify a potential ligand required for Ret signaling in C4da sensory neuron development, a candidate screen of Transforming Growth Factor β (TGFβ) ligands was performed. These molecules have been selected because TGFβ are described as the closest related homologs to the GDNF family (Saarma, 2000).

In this analysis, only ectopic overexpression of the TGFβ *maverick* (*mav*) in the epithelium induced a strong dendrite phenotype specifically in C4da neurons. The overexpression resulted in reduced C4da neuron dendritic field coverage and shifted the complex dendrite network more proximally. Further, C4da neurons exhibited increased isoneuronal dendritic crossing events. Besides that, the *mav* overexpression effect was C4da neuron specific since other da neurons did not exhibit dendrite defects on the morphological level. However, no morphological phenotype was detected by *mav* overexpression in C4da neuron.

The generated *mav* knock-out (mav^{ko}) confirmed that *mav* is required for of C4da neuron dendrite development. *Mav* loss-of-function leads to reduced dendritic field coverage, decreased dendrite length and increased isoneuronal crossing of C4da neuron dendrites. Analysis of the dendritic field distribution of mav^{ko} C4da neuron dendrites revealed a growth preference into the dorso-posterior compartment. *Mav* was identified by Nguyen et al. as a new member of the TGFβ superfamily, a large group of soluble extracellular proteins that are potent regulators of development in both vertebrates and invertebrates (Nguyen et al., 2000). Concerning its function in C4da neuron development, this finding suggests that *mav* is secreted by the epithelium and its levels within the dendritic field are tightly regulated functioning as guidance cue for dendrite growth direction.

Based on in situ hybridization and RT-PCR analysis, *mav* is expressed throughout embryonic and larval stages and persists until adulthood. More detailed analysis of the spatial distribution of the transcript during development revealed that mav mRNA is ubiquitously distributed throughout the embryo at early syncytial blastoderm and post-cellular blastoderm stages (stages 1-5). During gastrulation and germ band elongation (stages 6±8 and stages 9±11, respectively), mav is located throughout the embryo at low levels and shows a dynamic expression pattern in germ layers forming the gut (stage 9-10). Besides gut expression, mav transcripts are also present in distinct segmental patches of cells likely belonging to the dorso-lateral epidermal region (Nguyen et al., 2000). This expression domain already indicates its function in axial determination and field organization.

Recently, the maternal maverick/GDF-15-like TGFβ ligand panda has been identified to function in the radial symmetry of the sea urchin embryo to direct the dorsal-ventral axis formation. It is known that dorsal-ventral axis formation is highly regulated through the expression of nodal. How maternal signals initiate axis formation is largely unknown. Haillot et al. provide evidence that panda mRNA is broadly distributed during early embryonic development but local expression of panda mRNA efficiently orients the dorsal-ventral axis,

which is achieved by restricting zygotic expression of nodal. Nodal encodes a cytokine belonging to the TGFβ superfamily but is not conserved in *Drosophila*. Phylogenetic analysis revealed that panda does not belong to classical BMP ligands, but can be classified as a member related to TGFβ that includes *mav* from *Drosophila* and GDF-15 from vertebrates (Haillot et al., 2015). Thus, the spatial activity of the maternal factor panda is both necessary and sufficient to regulate patterning along the dorsal-ventral axis. It is feasible that *mav* has an analog function by acting as a graded permissive signal in dendrite development of C4da sensory neurons.

Interestingly, the loss of *mav* function in C4da sensory neurons indicates its role in dendrite spreading, since first order dendrites are developed and these neurons mainly exhibited defects in the development of higher order branches. Moreover, epithelial *mav* overexpression results in an extreme increase of C4da dendrite terminals, which argues for *mav* function in dendrite branching. Unlike ectopic *Ret* overexpression, ectopic overexpression of *mav* does not affect dendrite dynamics, which may indicate that *mav* does not change the stability of C4da neuron dendrites, in line with a role as a permissive signal.
Interestingly, major branches of C4da neurons in mav^{ko} animals are well developed along the anterior-posterior and dorsal-ventral axis. Thus the loss of mav might have revealed a program for axial C4da dendrite guidance. It is likely that additional guidance cues like Fmi are responsible for proper dendritic field establishment of C4da neurons, as already described in the previous chapter in this study (chapter 11.1.3). Thus, mav might be provided by the epithelium to permit growth of C4da neuron dendrites in combination with other guidance cues to ensure full field coverage.

Concerning mav and its categorization within the TGFβ family, sequence analysis revealed that *mav* cannot be easily classified into one of a described TGFβ subfamilies, since its sequence exhibits features of both, BMP and TGFβ/Activin ligands. Based on sequence analysis, *mav* exhibits the highest conservation with BMP related ligands. However, mav contains nine characteristic cysteine residues within the potential ligand domain typical for TGFβ/dActivin ligands (Daopin et al., 1992; Nguyen et al., 2000). Therefore, it is difficult to classify mav into a specific subfamily TGFβ, since it also exhibits high similarity to both BMP3 and GDF-10/GDF-15 (with consideration of its pro-domain before cleavage). Consequently, it might be possible that mav encodes a member of a novel subfamily of TGFβ ligands.
The described mammalian homologs of *mav*, GDF-10 and GDF-15, have been characterized extensively and it has been shown that both are implicated in cancer. However, their function in dendrite development has not been investigated yet. The growth/differentiation factor 15/macrophage inhibiting cytokine-1 (GDF-15/MIC-1) was identified as a member of the TGFβ superfamily in adult rat tissues (Böttner et al., 1999). The comparison of the mature domain of the human protein with select members of the TGFβ superfamily revealed that

GDF-15/MIC-1 is a more distant member of the TGFβ superfamily. The comparison of the predicted rat, mouse and human GDF-15/MIC-1 proteins showed that all genes are composed of two exons that are separated by one single intron within the prepro-domain of the corresponding proteins. A TATA-like motif (TATAAA) is present in close proximity to the putative translation start codon indicating its conservation along the examined species. The tissue distribution of mouse GDF-15/MIC-1 mRNA by semi-quantitative RT-PCR revealed it is widely distributed in the brain and peripheral nervous system. With respect to its function, analysis revealed that GDF-15 is essential for neuronal survival since GDF-15 deficient mice showed progressive postnatal losses of motor and sensory neurons, and GDF-15 robustly promotes the survival of lesioned nigrostriatal dopaminergic neurons *in vivo* (Charalambous et al., 2013; Strelau et al., 2009). Due to the finding that homologs of *mav* are found in vertebrates and present within the peripheral nervous system, together with this study showing that *mav* is required for C4da dendrite development, it will be interesting to investigate if GDF-15/mav function is also linked to the development of sensory neurons in vertebrates.

BMP3, a further homolog of mav, has not been well investigated yet. In mammals, BMPs were first identified as factors to induce bone formation. Until now, it has been shown that these molecules are tightly regulated and involved in the development of almost all tissues, even during early developmental processes such as gastrulation and cellular polarization. Between vertebrates and invertebrates, different molecules of the BMP family share high identity (BMP2/3 and BMP5/6/7 are homologs of *dpp* and *gbb* in *Drosophila*, respectively). However, BMP3 also displays unique features and cannot be classified into the BMP or TGFβ/Activin subfamily. It has been shown that it acts as an antagonist for BMP and TGFβ/Activin pathways, since loss-of-function in mice induces higher bone mass and inhibits osteoblasts differentiation. These *in vivo* analyses indicate that BMP3 acts as an inhibitory factor, but how the expression of BMP3 is controlled is poorly understood (Bahamonde and Lyons, 2001; Lowery et al., 2013). Thus, whether BMP3 functions in dendrite development is completely unknown.

To gain more insight into *mav* expression and its function in dendrite development, some aspects have to be investigated in more detail. The analysis of the available mav-GFP-reporter revealed *mav* expression in the epithelial cells. This reporter comprised a GFP enhancer trap in the 5' genomic locus of *mav*. Since this insertion may cause defects or might not visualize the entire endogenous expression of *mav*, one next step will be the generation of a *mav* knock-in line using CRISPR/Cas9 to insert a tag in the endogenous locus of *mav*. This way, endogenous levels of *mav* can be analyzed at different developmental time points. This might clarify how *mav* is expressed and distributed in a spatial and temporal manner and might function during early dendrite development.

The use of a genomic *mav* duplication was only partially able to rescue the mav^{ko} phenotype. One explanation might be the presence of other genes in this duplicated genomic region, which encode for several cell-surface and additional proteins and potentially negatively affect C4da dendrite development. Their overexpression due to increased copy number might thus prevent a full rescue of the mav^{ko} phenotype. For instance, *Ephrin* and *Ephrin receptor tyrosine kinase* are located within this genomic fragment. Interestingly, in vertebrates Ret functions together with EphrinA (Bonanomi et al., 2012), which might be an additional putative interaction partner and impair Ret-mav signaling.

Since the expression of transgenic *UAS-mav* construct resulted in a strong phenotype, the use of large genomic constructs such as BACs and fosmids, which cover whole genes including all regulatory elements, might be an alternative approach to explore *mav* function under endogenous regulatory control and its ability to rescue the observed defects of mav^{ko} in C4da sensory neurons (Ejsmont et al., 2009).
Another aspect requiring further investigation is the influence of mav on C4da dendrite stability, as *mav* overexpression does not affect dendrite stability during short-time frames (5 min time points). Therefore, the influence of *mav* on C4da neuron dendrites will be investigated over longer time periods (24 hrs time points).
Finally, it is well known that adhesion between dendrites and the ECM plays an important role in dendrite development and mav^{ko} animals displayed a higher amount of dendrite crossing events. For that reason, the *mav* loss-of-function will be analyzed using an ECM-marker (viking-GFP) to investigate dendrite-ECM interaction of C4da neurons. Taken together, these experiments might help to understand novel function of mav in dendrite development.

11.3 Mav acts as guidance cue for C4da neuron dendrite growth

Examination of the mav GFP-reporter revealed that *mav* expression is located within the epithelium. Due to these results it can be postulated that TGFβ ligand *mav* is likely expressed and secreted by epithelial cells and affects the development of nearby located C4da neuron dendrites.
Interestingly, local overexpression of *mav* in the posterior domain of the C4da neuron receptive field redirected dendrite growth into the *mav* expression domain. In contrast, the knock-down of *mav* within the posterior field resulted in a reduction of C4da neuron dendrites and preferential anterior growth. This data showed that up- or downregulation of mav protein levels regulates dendrite growth preference of C4da neurons suggesting mav is acts as a local permissive guidance signal for C4da neuron dendrite growth.
Even more, it indicates that mav acts locally on C4da neuron dendrite growth since a mav's growth effect is restricted largely to the expression domain. The up- or downregulation of *mav* in the expression domain showed opposite effects on C4da neuron dendrite patterning. Ectopic overexpression of *mav* resulted in a growth preference into the expression domain, whereas RNAi-induced *mav*-knockdown resulted in less C4da neuron dendrites within the expression domain. Even more, the growth preference is shifted into the anterior compartment, most likely due to the remained endogenous *mav* expression. This effect nicely shows that the manipulation of local mav levels can affect the growth preference of C4da neurons. It can be postulated that dendrites directionally grow into a domain with higher amounts of mav. As soon as dendrites cover this area mav might be immediately internalized resulting in lower amounts of mav and less growth into this domain.

Interestingly, local manipulation of *mav* levels did not affect total dendrite length of C4da neuron dendrites, indicating that both the capacity of dendrite growth is limited and other factors are responsible for restricting dendrite growth. This might be either regulated by internal cues or by external signals to keep each dendritic field within its limit.
Like C4da sensory neurons in *Drosophila*, highly arborized mechanosensory PVD neurons in *C. elegans* display stereotypic dendritic arbors and serve as a model system for dendrite development. Here, Dong et al. and Salzberg et al. identified a tripartite ligand-receptor complex that is essential for the patterning of PVD dendrites. This complex consists of MNR-1/menorin and SAX-7/L1CAM proteins expressed in the hypodermis and the neuronal leucine-rich repeat transmembrane receptor DMA-1 expressed in sensory dendrites. Salzberg et al. provided evidence that MNR-1 acts as a contact-dependent or short-range cue together with the neural cell adhesion molecule SAX-7/L1CAM and functions at defined locations in the surrounding hypodermal tissue. The interaction is both necessary and sufficient to instruct spatially restricted growth and branching of PVD dendrites *in vitro* and *in vivo* (Dong et al., 2013; Liu and Shen, 2012; Salzberg et al., 2013; Ziegenfuss and Grueber, 2013).

These studies illustrate that the interplay and combined action of surface molecules expressed along dendrites and nearby tissue (e.g. epidermal cell, hypodermis) is highly controlled during neuronal development and required for receptive field formation in different species.

To get further insight if mav has a similar role in *Drosophila*, the generation of a tagged genomic *mav* transgene or knock-in (either with a fluorescent GFP marker or a HA-tag) will be highly useful, which would allow the visualization of endogenous mav localization. If the generated genomic reporter is fully functional, potential changes of mav distribution in control and Ret^{ko} backgrounds can be investigated *in vivo*. Since mav might be immediately internalized when dendrites cover a part of the receptive field, this would result in lower amounts of mav which might restrict further growth of nearby dendrites. Additionally, such a reagent will allow investigating if mav is internalized by C4da neurons in a Ret dependent manner.
These studies will help to identify the relationship between Ret and mav and the underlying mechanism for their common function in dendrite development.

11.4 Ret directly or indirectly acts as a novel TGFβ receptor for mav in dendrite development

The interaction of substrates and cells is one of the most important aspects in neuronal development. As discussed previously, many studies demonstrate the importance of cell surface protein distribution to determine cell compartments and cell polarization (Andre et al., 2015; Chen et al., 2008; Usui et al., 1999; Wu et al., 2013).
In this thesis, the TGFβ *mav* has been shown to be required for C4da sensory neuron development and its loss-of-function exhibits similar defects as Ret^{ko} larvae. This raises the question whether Ret and mav are acting as a novel receptor-ligand protein complex in this context. In the mammalian system, Ret receptor tyrosine kinase signaling is activated trough binding of soluble proteins belonging to the glial cell-derived neurotrophic factor (GDNF) family ligands (GFLs). This interaction further requires a ligand-binding subunit acting as a co-receptor, known as the GDNF family receptor α (GFRα) (Durbec et al., 1996, Trupp et al., 1996). Although *Drosophila* Ret shares homology with vertebrate RET and similar structural compartments in its extracellular domain, a homologous GDNF ligand has not been found in the *Drosophila* genome (Anders et al., 2001). Furthermore, *Drosophila* Ret does not bind GDNF. Rather, extracellular cadherin-like domains suggest a role for Ret in adhesion, although *Drosophila* Ret is unable of homophilic binding *in vitro* (Abrescia et al., 2005).

The hypothesis that mav is a potential ligand required for Ret signaling in C4da neurons was strengthened by a series of results. As previously described, C4da neurons in mav^{ko} animals phenocopied the *Ret* loss-of function effect. Localization of mav was observed in the nearby epidermis, which is a substrate for C4da neuron dendrites, and mav action depended on the presence of Ret. Mav^{ko}/Ret^{ko} transheterozygous animals exhibit morphological phenotypes in C4da neurons showing that *Ret* and *mav* are genetically linked, while double knock-out animals exhibited the same C4da phenotype as single *Ret* or *mav* knock-outs. Additionally, transgenic co-overexpression of *Ret* and *mav* was able to promote dendrite growth of C1da sensory neuron dendrites.
Moreover, the data collected in this thesis suggest that mav is upstream of Ret and might act as guidance cue for Ret-dependent C4da sensory neuron dendrite growth. First, transgenic *mav* expression in C4da neurons was able to rescue the heterozygous Ret mutant phenotype. The expression of a *mav* gene duplication rescued mav^{ko} phenotypes partially, but did not rescue Ret^{ko} or double knock-out defects suggesting that mav function requires Ret. These lines of evidence suggest that mav function is upstream of Ret. It also strengthens the hypothesis of both acting in same signaling pathway suggesting mav acts as a guidance cue for Ret-dependent C4da sensory neuron development.

11.4.1 Ret and mav signal in a multiprotein complex

The obtained data clearly demonstrate that *Ret* and *mav* are required for C4da dendrite growth. However, further effectors and interactions contribute to proper dendritic field organization, since major branches in both knock-out animals are already developed. Very recently, studies in C4da neurons by Meltzer et al. uncovered that the interaction of the transmembrane receptor Plexin and its ligand Semaphorin is involved in dendrite-ECM interaction. They showed that the loss-of-function of *sema-2b* exhibited severe crossing defects of C4da neuron dendrites due to dendrite adhesion defects to the ECM as shown for Ret in this study. In their study, they identified sema-2b as a secreted molecule derived from the epidermis, which functions as ligand for the neuronally expressed Plexin B receptor (Zlatic et al., 2009). This functional complex is required cell-autonomously in C4da neurons to mediate dendrite-ECM adhesion and was shown to interact with integrins, similarly to Ret (Meltzer et al., 2016; Soba et al., 2015).

As for C4da sensory neurons in *Drosophila*, Dong et al. identified a dendrite-substrate interaction essential for dendritic morphogenesis in *C. elegans* using the highly stereotyped PVD somatosensory neurons as model system. They identified mnr-1 and sax-7 acting as a receptor-ligand complex that functions between the developing PVD dendrites and the body wall hypodermal cells. *Mnr-1* (menorah-like dendrites of PVD neurons) encodes a member of the Fam151 family of proteins; *sax-7* encodes a Neuroglian/L1-CAM homolog of the immunoglobulin superfamily. Mutations of these genes reveal a striking loss and disorientation of higher-order dendrite branches demonstrating that both genes are required for PVD dendrite morphogenesis. The phenotype of *mnr-1* mutant was PVD specific, since the morphology of other neurons in the *C. elegans* nervous system appear to be unaffected. Lacking *sax-7* leads to very similar phenotypes as for *mnr-1*, and double mutant analysis demonstrated that both genes act in the same signaling pathway. As for mav in C4da neuron development, sax-7 protein forms a precise subcellular pattern in the hypodermis to interact with PVD dendrites, whereas mnr-1 localization is widespread. This suggests that sax-7 protein localization may provide an instructive cue for dendrite growth direction and together with mnr-1 represents a substrate for PVD dendrites (Dong et al., 2013; Salzberg et al., 2014).

Both studies demonstrate high similarity to Ret and mav and their function in C4da neurons. Analogous to Ret and mav, this specific receptor/ligand interaction is a perfect example of precisely controlled ligand secretion/presentation from a nearby tissue to regulate proper dendrite formation and patterning during development of different species. In addition, it supports the idea that Ret and mav form a functional multiprotein complex together with integrins or other cell surface proteins in order to organize complex branching C4da morphogenesis.

The obtained data showed that *mav* overexpression in C4da neurons was able to promote dendritic length, number of terminals, complexity in *Ret* heterozygous animals but not in the complete absence of *Ret*. This demonstrated that *mav* and *Ret* are functionally linked in the same genetic pathway with mav acting upstream of Ret.

However, the reciprocal effect on the number of terminal endings in heterozygous Ret^{ko} compared to complete Ret^{ko} larvae in *mav* overexpression experiment is until now hard to explain. Here, the overexpression of *mav* resulted in a significant increase of C4da neuron terminal dendrites in *Ret* heterozygous larvae, whereas in Ret^{ko} larvae the number of C4da neuron terminals was significantly decreased. It has to be investigated whether this effect was direct or indirect. It may indicate that mav can bind to other TGFβ receptors, e.g. punt (Fuentes-Medel et al., 2012). This aspect will be discussed in the following chapter (11.4.2).

Another explanation might be that mav interacts with a Ret-like protein in C4da sensory neurons and affects C4da dendrite development in a Ret-independent pathway. Maybe this potential interactor is expressed in a nearby tissue (e.g. epithelium) and can affect C4da neuron growth by an unknown mechanism. One candidate might be *Cad96Ca* (also known as *stitcher*) which is expressed in all ectodermal epithelia during mid- and late embryonic stages and shares high similarity with Ret containing cadherin domains (Fung et al. 2007). *Cad96Ca* supports re-epithelialization following wound healing by stimulating actin cable formation and cuticle repair in embryonic stages (Fung et al., 2008; Wang et al., 2009).

Alternatively, Ret and mav might need an unknown co-receptor to form a functional complex, similarly as GFRα co-receptors are required for Ret signaling in mammals. GFR-like proteins have been identified *in silico* in *Drosophila* and *C. elegans* but characterization revealed that this protein is not involved in Ret signaling in *Drosophila*, but is genetically linked with the *Drosophila* Ncam (neural cell adhesion molecule) homolog FasII to regulate fertility (Kallijärvi et al., 2012). Accordingly, the Ret signaling pathway in C4da sensory neurons is so far unclear.

For TGFβ signaling it has been reported that some receptors also require co-receptors for proper receptor-ligand interactions (Feng and Derynck, 2005). Candidates might be cell surface adhesion proteins as integrins. These glycoproteins function as heterodimeric transmembrane proteins and consist of an α and β subunit mediating contact with extracellular matrix components. Integrins feature a RGD-recognition and -binding domain to bind fibronectin in fibroblasts. Further, it has been shown that RGD-binding integrins (avb6 and avb8) are able to directly bind and activate TGFβ. This indicates that ECM and integrin actions are a critical central process to control the amount of TGFβ available for activation (Munger and Sheppard, 2011). Besides that, other protein without RGD-domains are able to bind integrins, e.g. adhesion molecules (ICAMs), collagens and laminin (Brown, 2000).

Recently, integrins have been identified to function together with the Ret receptor in a physical complex to control C4da neuron development and dendrite-ECM adhesion. Here, dendritic crossing defects in hypomorphic *Ret* mutants could be rescued by integrin

overexpression. However, integrins are not sufficient to rescue growth defects in *Ret* mutant C4da neurons (Soba et al., 2015).

Comparison of the *Ret* and *mav* phenotypes indicated that *Ret* is more heavily involved in crossing defects, whereas *mav* is prominently required for controlling dendritic growth and the number of terminals. This suggests that Ret-mav interaction might regulate dendritic growth, while Ret-integrin interaction might control the organization of dendrites within the dendritic field (chapter 11.1.2). Taken together, this might suggest that Ret, integrins and mav are functioning in a signaling complex. However, no RGD-domain (Arg-Gly-Asp) is found in the mav sequence suggesting that mav does not bind integrins directly.
Besides Ret-integrin interaction, it is published that Ret functions together with other cell surface proteins, such as transmembrane heparan sulfate proteoglycan (HSPG) syndecan-3 (Bespalov et al., 2011) or EphrinA (Bonanomi et al., 2012) implying that additional putative interaction partners might be implicated in Ret-mav signaling.

11.4.2 Ret-mav interaction in C4da neuron development does not depend on the non-canonical TGFβ signaling pathway

The identification of *mav* as being required for Ret-dependent C4da dendrite development in *Drosophila* raised the question whether classical TGFβ receptors may act in a functional signaling complex in this system. In *Drosophila*, the entire superfamily signaling network of TGFβ is subdivided into the BMP and Activin pathway and TGFβ receptors are classified into Type I and Type II receptors.
It has been shown that the expression of *mav* displays a similar pattern as the TGFβ type II receptor punt, which is described to activate dSmad2 in combination with the type I receptor babo (Gesualdi and Haerry, 2007). Further, studies by Fuentes-Medel et al. revealed that this ligand also interacts with punt and regulates presynaptic bouton growth at the *Drosophila* neuromuscular junction (NMJ) *in vivo*.
Very recently, the maternal Maverick/GDF15-like TGFβ ligand panda has been identified as regulator for dorso-ventral axis formation in the sea urchin embryo as previously discussed (chapter 11.2). Haillot et al. demonstrated that maternal panda mRNA is both necessary and sufficient to orient the dorsal-ventral axis during early embryonic development. For this function it requires the BMP type I receptors activin receptor-like kinases (Alk) Alk3/6 and Alk1/2 to transduce through intracellular BMP2/4 activation. The loss-of-function of both receptors results in a dramatic ventralization of the embryo. Further, this ventralization phenotype is mimicked by double inactivation of panda and Bmp2/4. Analysis revealed that this phenotype is caused by a massive ectopic expression of nodal - a TGFβ ligand - on the dorsal side, which is usually restricted by panda and BMP type I receptor interaction. Based

on phylogenetic analysis, panda is more related to TGFβ, which also includes mav in *Drosophila* and GDF15 in vertebrates (Haillot et al., 2015).
These two studies displayed mav/mav-like protein function in synaptic growth and axis formation by the interaction with their cognate TGFβ receptors. However in terms of novel function of mav in C4da sensory neuron development, nodal is not conserved in *Drosophila,* meaning that the results concerning panda and Alk might not be relevant for dendrite development.
The analysis of the known TGFβ receptors in *Drosophila* using mutant alleles or dominant-negative transgenes displayed no C4da neuron morphological defects. None of these mutants mimicked the *mav* loss-of-function phenotypes or displayed genetic interaction with Ret receptor. This strongly suggests that conventional TGFβ receptors are not involved in C4da sensory neuron development and Ret function. However, one possibility might be that maternal mRNA of one of these TGFβ receptors was masking the effect of the corresponding allele. Further, it might be possible that multiple redundant TGFβ receptors are involved in Ret-mav-dependent signaling. To exclude this option, the core downstream transducer required for canonical BMP and dActivin signaling, the co-Smad Medea (Smad4 homolog in mammals), has to be investigated more carefully.

It has to be mentioned that little is known about TGFβ function in the regulation of dendrite development. At least one study by Ting et al. could show that TGF signaling functions in regulating dendritic termination and thus dendrite development in *Drosophila*. In the *Drosophila* medulla, afferent-derived Activin restricts the dendritic field size of their postsynaptic partners to attain proper synaptic connectivity via babo. The loss-of-function of canonical Activin signaling in the downstream neurons resulted in enlarged dendritic field size and unspecific synaptic connections with neighboring photoreceptors (Ting et al., 2014).

Although TGFβ signaling is mainly transduced through downstream Smad activation, it has been shown that Smad-independent pathways can be activated in response to TGFβ in both vertebrates and invertebrates. For instance, it has been described that ERK-MAP kinase (MAPK) signaling can be activated through phosphorylation of the scaffold protein ShcA by TGFβ receptor ALK5. This activation leads to the recruitment of Grb and Sos, which induces Ras and thus MAPK signaling (Lee et al., 2007). Further, TGFβ can induce the activation of JNK and p38 MAPK signaling, but the detailed mechanism of how a MAP kinase cascade is activated by TGFβ receptors is not clear (Yamashita et al., 2008). Additional studies reported that the expression of chondroitin sulfate proteoglycans (CSPGs) is induced by TGFβ activity and mediated through Smad-independent activation of the PI3K/Akt/mTOR signaling pathway (Jahan and Hannila, 2015). This possible non-Smad activation might be also true for Ret activation through mav in C4da sensory neurons.

Together, this strengthens the idea that classical TGFβ signaling is not involved in C4da development and Ret might act either directly or indirectly as a novel TGFβ receptor for mav in dendrite development. Accordingly, non-canonical TGFβ signaling pathways might be involved in Ret-mav function in C4da neuron development

Future studies should be focused on the interplay between Ret and mav and their direct or indirect function in C4da dendrite development. Different biochemical assays (co-immunoprecipitation, immunohistochemical co-labeling, and proximity ligation assay) in *Drosophila* S2 cells will allow identifying whether Ret and mav are physically linked. For these analyses, the use of truncated *Ret* transgenes will help to understand the binding sites between both proteins. Besides that, Smad-independent signaling (Ras/MAP/ERK, JNK, PI3K/Akt/mTOR) will be followed up, since the canonical TGFβ signaling pathway is likely not involved in Ret-mav function in C4da dendrite development. As for Ret and mav interaction, biochemical assays and *in vivo* studies might help to uncover novel signaling partners. Apparently, the whole range of Ret ligand and signaling pathways is still largely unknown, although *Ret* exhibits a high sequence identity from mammals to *Drosophila* (Hahn and Bishop, 2001). These next studies will help to identify first, the relationship between Ret and mav and second, the underlying mechanism for their common function in dendrite development.

11.4.3 Ret and mav are sufficient to promote dendrite growth in heterologous neurons

This thesis work showed that mav can affect C4da neuron dendrite growth in a Ret-dependent manner. Astonishingly, *Ret* and *mav* are also sufficient to promote dendrite growth when ectopically expressed in C1da neurons, which endogenously do not express either *Ret* or *mav*.
C1da are described to develop during embryonic and early larval stages and typically extend few dendritic branches. At later larval stages their dendrites are stable and less dynamic due to low levels of actin compared to C3da neurons (Grueber et al., 2003; Jinushi-Nakao et al., 2007). It has been shown that C1da neurons express Abrupt, which acts to suppress arbor out-growth and branching compared to more complex da neuron subtypes as C3da or C4da neurons (Grueber et al., 2002). The overexpression of only *Ret* already resulted in mildly enhanced growth, which can be explained by the presence of endogenous *mav* in the extracellular space. This effect could be strongly enhanced by co-overexpression of *Ret* and *mav.* These results suggest again that Ret and mav act as a potential receptor-ligand pair.

Importantly, both the extracellular and intracellular domain of Ret are required for mav dependent C1da neuron dendrite growth. This highlights that both putative binding of mav as

a potential ligand for Ret and downstream signaling is involved in promoting growth in this system. The growth promoting effect of Ret/mav in C1da neurons further indicates that Ret and mav likely activate a general signaling pathway existing in many different tissues. Ret signaling has been shown to result in intracellular autophosphorylation of different tyrosine residues upon ligand binding, which consequently stimulate different downstream signaling pathways. These phosphorylated tyrosine residues provide docking sites for downstream effector proteins (including Ras/MAPK, Pi3K/Akt, PLCγ) as already mentioned previously (chapter 11.1.1). Most of the described pathways in Ret signaling are essential for fundamental genes implicated in developmental processes such as proliferation, growth and survival.

The growth promoting effect in C1da neurons might also activate signaling cascades regulating intracellular cytoskeleton structures or cytoskeletal-associated molecules. The activation of Ret by mav may modulate actin or/and microtubule polymerization and thus influence the restricted growth of C1da neurons, since Soba et al. have shown that Ret is linked to intracellular rac1 activity (Soba et al., 2015).

11.5 RanBPM function is linked to Ret

The analysis of Ret signaling in C4da dendrite development provided evidence that extracellular Ret receptor stimulation activates intracellular pathways. This was shown by analyzing transgenic Ret deletion construct and their capacity to rescue C4da morphology defects in Ret mutant animals (chapter 11.1).

Genome wide microarray analysis to find genes implicated in Ret signaling identified *Ran-binding protein M* (*RanBPM*) as a candidate based on strongly reduced transcript levels in Ret^{ko} C4da sensory neurons. Follow-up experiments revealed that *RanBPM* is expressed in C4da neurons and different allelic combinations of *RanBPM* mutants showed defects in C4da neuron dendrite development. Interestingly, *RanBPM* mutant defects were similar to the observed *Ret* loss-of-function phenotype. Furthermore, *RanBPM* and *Ret* showed genetic interaction resulting in a reduction of total dendritic length and terminal numbers of C4da neurons. This result shows that RanBPM is implicated in C4da dendrite development and that its function is linked to the Ret receptor.

In *Drosophila*, *RanBPM* was identified by a Gal4 enhancer trap screening and encodes two protein isoforms (short and long isoform) and displays high sequence similarity to two mammalian genes: *RanBPM* (or *RanBP9*) and *RanBP10*. Both share 68% amino acid identity, but differ in their N-terminal structure, since RanBP10 lacks the glutamine-rich region (Wang et al., 2004). In vertebrates, both RanBPM proteins are described to interact with different cell surface proteins and cell adhesion molecules by functioning as scaffolding protein to connect cell surface/cell adhesion proteins to transduce signaling. RanBPM molecules contain different conserved domains required for protein interaction and it was shown that RanBPM is able to bind the Met receptor and to interact with Tropomyosin-related kinase A (TrkA) through binding to a SPRY motif in the tyrosine kinase domain of the receptor (Wang et al., 2004; Yin et al., 2010; Yuan et al., 2006). It was further reported that RanBPM contributes to MAPK and Akt signaling by the interaction with the TrkB receptor, since overexpression of *RanBPM* can enhance BDNF-induced MAPK and Akt activation. The Trk receptor has a similar tyrosine kinase structure as Met and transduces BDNF (brain-derived neurotrophic factor) dependent signaling. BDNF belongs to the neurotrophin family and plays a critical role in neuronal survival, differentiation and morphogenesis. These studies support a function of RanBPM as a scaffold and signaling hub for cell surface proteins, which might include the Ret receptor.

RanBPM was also shown to be the plasma membrane and can interact with integrins. Denti et al. identified RanBPM as a novel downstream interaction partner of the cytoplasmic domain of the β1 integrin LFA-1. This protein-protein interaction was confirmed both *in vivo* and *in vitro* and by co-localization of both proteins at the plasma membrane. *In vitro* results indicated that LFA-1-mediated cell adhesion and RanBPM interaction contribute to the activation of a transcription factor AP-1-dependent promoter. Thus, RanBPM may regulate downstream signaling pathways of Ret through both signaling and transcriptional changes,

as it is involved in fundamental processes as cell proliferation, differentiation and survival (Denti et al., 2004).
In addition, RanBPM has recently been implicated in TGFβ signaling. Zhang et al. identified RanBPM as a novel binding partner for TGFβ receptor I (TβRI). TβRI has been shown to interact with TNF receptor associated factor (TRAF), an E3 ubiquitin protein ligase, which functions as a post-translational signal transducer of the NF-κB pathway (Zhang et al., 2014).

The genetic interaction between *RanBPM* and Ret^{ko} resulted in an enhancement of C4da neuron dendrite phenotype indicating a functional genetic link between both genes. Based on the knowledge about RanBPM protein-protein interaction and their genetic link in C4da neurons this might suggest that RanBPM interacts with the Ret receptor.
Performing rescue experiment in C4da neurons using *RanBPM* transgenes did not have the capacity to rescue C4da neuron defects in 3rd instar Ret^{ko} larvae. One possibility might be that RanBPM and the Ret receptor act in a multiprotein complex together with integrins, since Denti et al. demonstrated that RanBPM and integrin adhesion receptors can interact *in vivo* and *in vitro*, and Soba et al. provided evidence that Ret and integrins are interacting as functional complex required for C4da neuron dendrite development (Denti et al., 2004; Soba et al., 2015). However, the observed defects in *RanBPM* mutant larvae did not phenocopy the Ret loss-of-function completely; it is therefore possible that RanBPM is only one of several Ret interactors required for C4da neuron development.
Besides its suggested function as a scaffolding protein, RanBPM has been implicated in larval learning behavior. Scantlebury et al. reported that this protein is present in Kenyon cells (KC) of the larval mushroom body, which has been considered loosely equivalent to the hippocampus in the mammalian brain. The mushroom body has been well studied for its function in memory and learning in *Drosophila*. In their studies, Scantlebury et al. found that *RanBPM* mutants display defects in the modulation of locomotion by light indicated by reduced responses during an ON/OFF-light behavior assay. *RanBPM* mutant animals also exhibited deficits in feeding behavior and growth. However, the animals did not display any morphological disruptions within the nervous system. Interestingly, the targeted expression of *RanBPM* transgenes in Kenyon cells resulted in a rescue of all observed defects (Scantlebury et al., 2010).
These findings suggest an additional connection to Ret, since *Ret* loss-of-function larvae exhibited behavioral defects in locomotion and light avoidance as well. However, the behavioral assays differ between this and the previous study. As the C4da neuron specific transgenic Ret expression did not rescue the behavioral defects of Ret^{ko} animals, it might indicate a potential link to mushroom body function. It is therefore likely that Ret function is necessary in other tissues than C4da sensory neurons to completely rescue the behavioral deficits of Ret^{ko} animals, which has to be investigated further.

Taken together, these datasets indicate that RanBPM functions as a scaffolding protein in a variety of signal transduction pathways, is required for larval behavior in the nervous system and is connected to Ret function in C4da dendrite development.

Further detailed dissection of how RanBPM and Ret are linked should be focused on investigating whether both proteins are directly or indirectly connected and if the loss-of-function of one gene will influence the distribution of the other and vice versa. The application of Ret deletion transgenes, especially of the intracellular domain of Ret, will allow the identification of the putative interaction domain between RanBPM and Ret.

As Ret and TGFβ ligand mav are genetically linked and based the association of RanBPM with TGFβ signaling (Zhang et al., 2014)**,** it might be worthwhile to investigate a link with mav. The potential activation of downstream modulators within non-/canonical TGFβ pathways mediated by mav will further help decoding the underlying machinery of a putative functional complex of RanBPM, Ret and mav in dendrite development.

11.6 Ret expression in C4da neurons is required but not sufficient for nocifensive behavior of *Drosophila melanogaster* larvae

Besides morphological defects, Ret and mav loss-of-function analysis revealed similar functional C4da neuron sensory defects in light avoidance and nociceptive behaviour. This suggests that Ret and mav are required for C4da neuron dependent nociceptive responses since they function as larval light sensors (Xiang et al., 2010; Yamanaka et al., 2013) and nociceptors (Hwang et al., 2007; Zhong et al., 2010). Additionally, Ret^{ko} larvae displayed reduced crawling velocity and increased turning behaviour. Although C4da neuron specific Ret overexpression can rescue morphological defects in Ret mutant animals, it was insufficient for a robust functional rescue. If mav overexpression in mav^{ko} larvae is able to rescue behavioral defects remains to be shown.

The result that Ret overexpression did not rescue C4da function can be explained by several possibilities. Although defects on the morphological level are restored, the physiological functionality of C4da might still be disrupted. Further, the connectivity of postsynaptic partners might also be affected and the transmission of noxious stimuli to the CNS could be altered. Another possible explanation could be that overexpression of Ret above physiological levels impairs function even if it rescues C4da neuron morphology. Although obvious morphological axon defects were not detected in Ret^{ko} animals, single cell analysis might reveal defects explaining the lack of a behavioral recue. In addition, specific synaptic markers can be used to detect potential synaptic defects at pre- or postsynaptic sites. It is possible that the number of synapses or their localization is changed which would prevent restoring C4da functionality. Another reason might be that C4da neuron dependent behavior relies on additional neurons, which are directly or indirectly affected by *Ret*. Based on this possibility, a Gal4-insertion located in the genomic locus of Ret was used to investigate its expression pattern. It revealed that Ret was expressed in neurons located in the CNS, identified as prothoracicotropic hormone (ptth) producing neurons (studies by Alisa Gruschka, Master thesis, Šoba lab). Recently, ptth neurons were shown to function in light avoidance (Gong et al., 2010; Xiang et al., 2010; Yamanaka et al., 2013). Interestingly, ptth neurons in Ret^{ko} larvae exhibited axonal projection and misrouting defects. However, the overexpression of Ret in ptth neurons was not sufficient to restore morphology or behavioral phenotypes in a Ret^{ko} mutant background (studies by Alisa Gruschka, Master thesis, Šoba lab). Possibly, the co-expression of Ret in different neurons or tissues is necessary to restore the observed behavioral defects. As the Ret expression analysis in the CNS so far relied on a Gal4-insertion, which do not always reflect the correct or complete endogenous expression pattern, the generation of a fluorescently tagged Ret knock-in might reveal the Ret expression pattern and help to identify neuronal subsets required for its role in behavior.

Interestingly, it has been shown that Ret signaling is required for the peripheral and central targeting of mechanoreceptors. The skin is the largest sensory organ in mammals, as it is

innervated by many different types of sensory neurons, including pain-sensing nociceptors, temperature-sensing thermoreceptors and low-threshold mechanoreceptors (LTMRs), which transmit non-painful stimuli (touch, pressure, vibration) (Luo et al., 2009; Zimmerman et al., 2014). LTMRs are divided into different sensory neuron subtypes classified based on their adaptation response to a certain stimuli into rapidly (RA) or slowly adapting (SA) neurons. SA receptors are sensors firing continuously during a stimulus, while RA receptors are velocity detectors responding only to the onset and offset of stimulation. In the mammalian skin, Meissner and Pacinian corpuscles are innervated by RA LTMRs transmitting vibration and motion on the skin. The static mechanical stimulation is transmitted by activated SA LTMR Merkel cells. However, the development of RA and SA mechanoreceptors is largely unknown.

Virtually all sensory neuron somata reside in the dorsal root ganglion (DRG), from where they send stereotyped peripheral and central projections. It has been shown that subtypes of LTMRs can be identified shortly after DRG genesis. Recently, several studies could demonstrate that early Ret positive DRG neurons are developing into RA mechanoreceptors to form Meissner corpuscles, Pacinian corpuscles and longitudinal lanceolate endings. The specification of these LTMR sensory neuron subtypes is regulated by the selective expression of the transcription factor MafA in combination with the Ret receptor and its co-receptor GRFα2. Studies in mice have uncovered that loss of Ret signaling results in a severe disruption of specialized RA mechanoreceptor projections in the periphery and also in the CNS. Further, the differentiation and survival of cultured embryonic DRG neurons were selectively supported by Neurturin (NTN) and glial cell-derived neurotrophic factor (GDNF) known as ligands for Ret/GRFα2 (Bourane et al., 2009; Luo et al., 2009).

Taken together, it is an interesting parallel that the development of subsets of sensory neurons in *Drosophila* and mouse is Ret-dependent. In mice it remains to be seen if the loss of Ret function in sensory neurons might lead to nociceptive defects as well.

Interestingly, TGFβ signaling functions as a modulator for nociceptive processing as well, both in peripheral sensory neurons and in the CNS. Neuropathic pain models in rats suggest that TGFβ-1 acts as a mediator of nociception and exhibits protective functions against chronic neuropathic pain development (Echeverry et al., 2009). This is achieved by the inhibition of the neuroimmune responses of spinal microglia and astrocytes and further the activation of endogenous expression of pro-inflammatory cytokines (IL-1β and IL-6) within the spinal cord (Yan et al., 1992). In addition, BMP4 was shown to inhibit the development of thermal hyperalgesia (sensitized response to noxious stimuli) in rats, since pretreatment of glial precursor cells with BMP4 could indirectly protect against hyperalgesia (Davies et al., 2008). Within the PNS, Activins and BMPs are involved in the protection of damaged tissue from nociceptor hypersensitization (reviewed in Lantero et al., 2012).

These results might prompt future studies of a link between Ret and TGFβ ligands in vertebrates. It will be interesting to transfer the findings in this thesis to the vertebrate system, which might reveal conserved roles for Ret and mav within a common non-canonical signaling pathway.

12 CONCLUSION

The development and organization of a dendritic field is regulated by basic mechanisms including self-avoidance and tiling, and highly controlled by protein-protein and protein-substrate interactions (Grueber et al., 2002; M. E. Kim et al., 2012; Soba et al., 2007). Recent findings suggested the conserved receptor tyrosine kinase (RTK) Ret as a key regulator of dendrite development specifically in C4da sensory neurons (Soba et al., 2015).

In this thesis, novel functions of Ret in dendrite development and the underlying signaling pathway have been investigated in great detail.
This study revealed that loss of Ret in C4da neurons influences the patterning of dendrites and their ability to grow in a defined 2D space due to detachment defects between the extracellular matrix and C4da neuron dendrites. Interestingly, Ret is cell-autonomously required for dendrite and ECM interaction, since specific overexpression of full-length Ret in C4da neurons was able to rescue patterning and ECM detachment phenotypes. The dissection of Ret protein domain function showed that extracellular signals are transduced intracellularly and activate so far unknown signaling pathways, since Ret transgenes lacking the extra- or intracellular domains did not restore C4da neuron morphology. With respect to the different extracellular domains, Ret lacking either the Cadherin-like domain (CLD) or the Cysteine-rich domain (CRD) did not show rescue capacity. It can be postulated that lacking the CLD might prevent potential ligand or co-receptor binding to Ret. Based on the described function of the CRD, its absence might disrupt Ret dimerization and prevent intracellular signal transduction.

Ret intracellular domain analysis revealed that the tyrosine kinase domain is only partially involved in C4da neuron dendrite development. Surprisingly, kinase-dead Ret showed full rescue activity indicating that Ret tyrosine kinase activity is dispensable for Ret function. However, lack of the entire intracellular domain did not show to rescue any capacity. The alignment of human and *Drosophila* Ret indicates that several intracellular tyrosine residues are conserved and might be required for signal transduction. However, it remains to be shown which tyrosine residues are functionally relevant.

In the mammalian system, Ret is part of a functional complex consisting of a soluble ligand and a co-receptor. The identified Ret ligands belongs to the glial cell-derived neurotrophic factor (GDNF) family (GFLs) and Ret activation additionally requires a ligand-binding co-receptor, the GDNF family receptor α (GFRα) (P. Durbec et al., 1996; Trupp et al., 1996). However, GDNF is evolutionary not conserved in invertebrates. Yet members of the TGFβ ligand family display homology to GDNF which may suggest similar functions.
In this thesis, the TGFβ ligand mav was identified as a putative upstream ligand of Ret. Mav is likely secreted from the epithelium and epithelial mav overexpression induces C4da

neuron specific morphogenesis defects in a Ret-dependent manner (Figure 48). Based on the findings in this thesis, it can be hypothesized that mav acts as a local permissive growth cue for C4da neuron dendrites, which might grow preferentially towards regions with higher levels of mav. Once dendrites cover this area during development, mav might be immediately internalized by C4da neurons thus lowering local mav levels. This hypothesis has to be investigated in more detail.

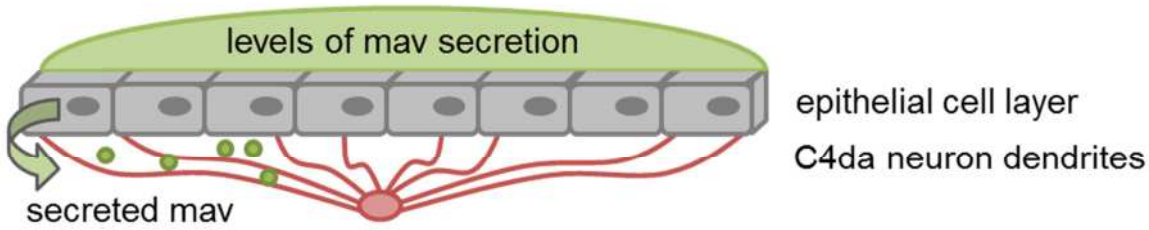

Figure 48. The TGFβ mav is expressed and likely secreted by epithelial cells. The presented data provides evidence that mav is secreted by the epithelium and acts as a guidance and growth cue for C4da neuron dendrites. The analysis of a mav reporter line further indicated a gradient of mav expression with its peak close to the soma of C4da neurons and decreasing levels distally.

Moreover, the generated mav knock-out (*mav*^{ko}) allele phenocopied the Ret loss-of-function phenotype confirming that mav is required for C4da neuron dendrite growth. The data presented here clearly show that Ret and mav are genetically linked and do not require classical TGFβ receptors and canonical TGFβ signaling for their function in C4da dendrite growth. Moreover, Ret and mav are sufficient to promote growth in heterologous neurons, which again depended on Ret extra- and intracellular domains. One can speculate that one or multiple general and ubiquitous signaling pathways are activated by Ret and mav. Together, this strengthens the hypothesis that Ret is a novel TGFβ-like receptor for mav required for C4da neuron dendrite development. Furthermore, it may indicate that Ret and TGFβ ligands have similar joint functions in vertebrates which will be interesting to investigate.

However, Ret dependent C4da neuron dendrite development requires additional interaction partners for correct receptive field innervation. Besides the observed growth defect, Ret mutant C4da neuron dendrites exhibit severe crossing defects due to impaired dendrite-ECM adhesion. Recently, it has been shown that Ret mediates dendrite-ECM adhesion through integrins. Integrins act as linkers between the ECM and the intracellular compartment anchoring the ECM to the cytoskeleton (Cabodi et al., 2010). This direct interplay between Ret and integrins activates downstream rac1 signaling and supports dendrite adhesion to the ECM. Soba et al. could show that in *Ret* mutant animals integrin overexpression was able to rescue crossing but not growth defects of C4da neuron dendrites (Soba et al., 2015).

Based on the results of this thesis, it can be postulated that the interaction of Ret and integrins might be responsible for adhesion and thus growth in a 2 dimensional space, while Ret and mav might primarily mediate dendritic growth to enable full coverage of the dendritic field (Figure 49).

These results nicely illustrate that the precisely controlled secretion of extracellular molecules like mav and multiprotein complex formation of ret regulate proper dendrite growth and patterning during development in a dose-dependent manner.

To get insight into Ret dependent intracellular signaling, a genome wide microarray analysis of *Ret*^{ko} C4da neurons was performed in collaboration with Jay Parrish and Charlie Kim. With the help of this analysis, the scaffolding protein RanBPM was identified as a candidate protein involved in Ret downstream signaling. RanBPM is indeed expressed in C4da neurons and loss-of-function analysis showed similar albeit weaker dendrite defects as observed in *Ret*^{ko} C4da neurons. Genetic interaction between RanBPM confirmed that RanBPM is indeed linked to Ret function in C4da neuron dendrite development. Based on these analyses, RanBPM might be a direct interaction partner of Ret required to transduce a subset of Ret dependent signals into the cell (Figure 49). However, whether this interaction is direct or indirect will be in focus of further studies.

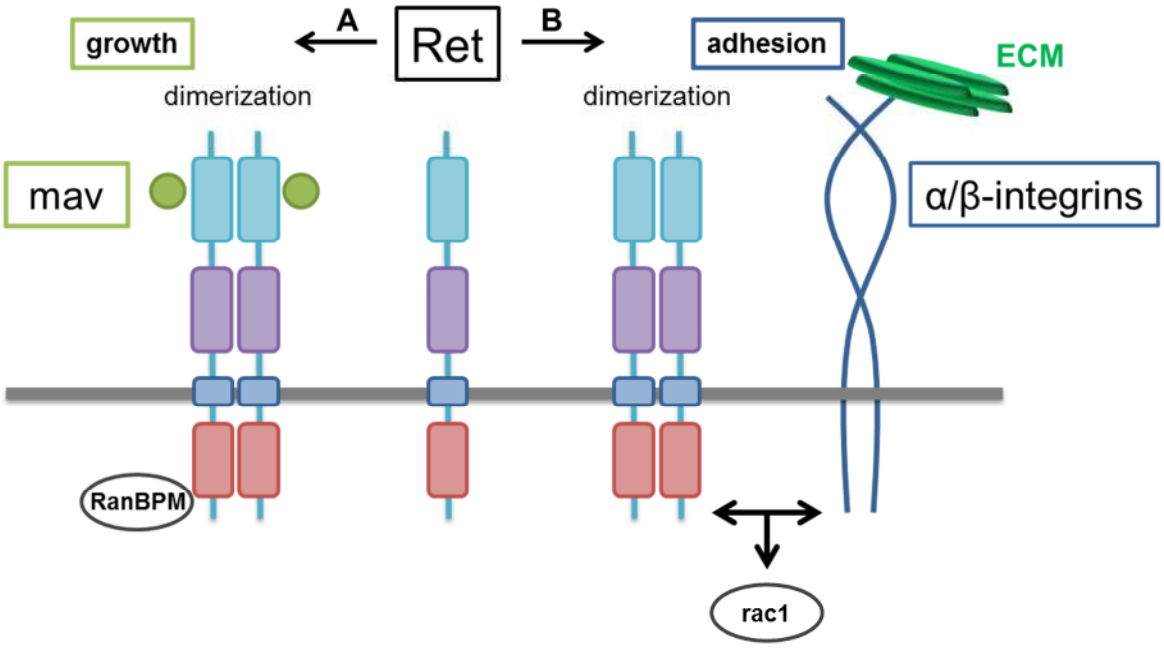

Figure 49. Ret function in C4da sensory neuron dendrite development in *Drosophila*. Schematic depiction of Ret interaction with its potential ligand mav (A) and integrins (B). The TGFβ ligand mav promotes C4da neuron dendrite growth in a Ret-dependent manner. Downstream signaling pathway analysis identified the scaffolding protein RanBPM as a potential Ret interaction and signaling partner. Moreover, proper Ret dependent C4da dendrite patterning requires additional interaction partners. Besides growth defects, C4da neuron dendrites also exhibit severe dendrite crossing defects. C4da neuron dendrites are attached to the ECM and it has been shown that Ret mediates dendrite-ECM adhesion through integrins. This potentially direct interaction activates downstream rac1 signaling and supports dendrite adhesion to the ECM.

In this thesis, the impact of Ret on C4da neuron dependent locomotion and nociceptive behavior of *Drosophila melanogaster* larvae was examined by investigating light avoidance and mechano-nociceptive behaviors. The data revealed that a loss of *Ret* leads to impaired nociceptive responses. Using a light/dark choice assay, Ret^{ko} larvae exhibited a clear light avoidance defect. In addition, larvae lacking Ret displayed reduced nocifensive rolling responses after noxious mechanical stimulation.

Although C4da neuron specific overexpression of Ret was sufficient to rescue dendritic development defects in Ret^{ko} larvae, the behavioral defects could not be mitigated.

These results point out that Ret is necessary for C4da neuronal development and their associated functions, but likely not sufficient to rescue C4da neuron or associated network functions.

Accordingly, Gong et al. showed that the modulation of specific hormone producing neurons within the larval brain, ptth neurons, can switch larval behavior from light aversion to attraction. These neurons might function as a control center for larval light avoidance by hormonal control of C4da neuron function (Gong et al., 2010). Detailed analysis revealed that Ret is likely expressed in ptth neurons and loss of Ret leads to an impaired axonal projection pattern of ptth neurons (master thesis performed by Alisa Gruschka, Soba lab). These results indicate that Ret has functions in neuronal development and larval behavior not only in C4da neurons but also in related circuit components. Consistently, the loss of the putative Ret receptor ligand, the TGFβ *mav*, also impaired both light avoidance behavior and mechano-nociception in *Drosophila* larvae. Thus, it will be interesting to investigate whether *mav* expression in specific tissues is sufficient to rescue these defects.

Taken together, these findings will help to understand the fundamental role of Ret in the development and function of neuronal circuits in *Drosophila*. Moreover, if the identified Ret dependent pathways turn out to be conserved, these studies will also pave the way for similar analyses in vertebrates.

13 APPENDIX

13.1 Plasmid maps

On the following pages, the generated UAS-transgenes containing the Ret cDNA (blue arrow) with different domain deletions for tissue specific rescue experiments are shown. Predicted domains are highlighted in green boxes: CLD (Cadherin-like domain), CRD (Cysteine-rich domain), TMD (transmembrane domain [without labeling]), TKD (tyrosine kinase domain). The localization of inactive Ret kinase mutation (K805M) is indicated by a red line. Additional features (white-cassette, 5xUAS, SV40 polyA, AttB) are shown in orange boxes and the selectable marker encoding a gene that refers to bacterial resistance to the antibiotic ampicillin (Amp) is shown as a blue arrow. The used restriction enzymes for each of these generated transgenes are indicated (see chapter 8.6). The name of the construct and its size are displayed in the center.

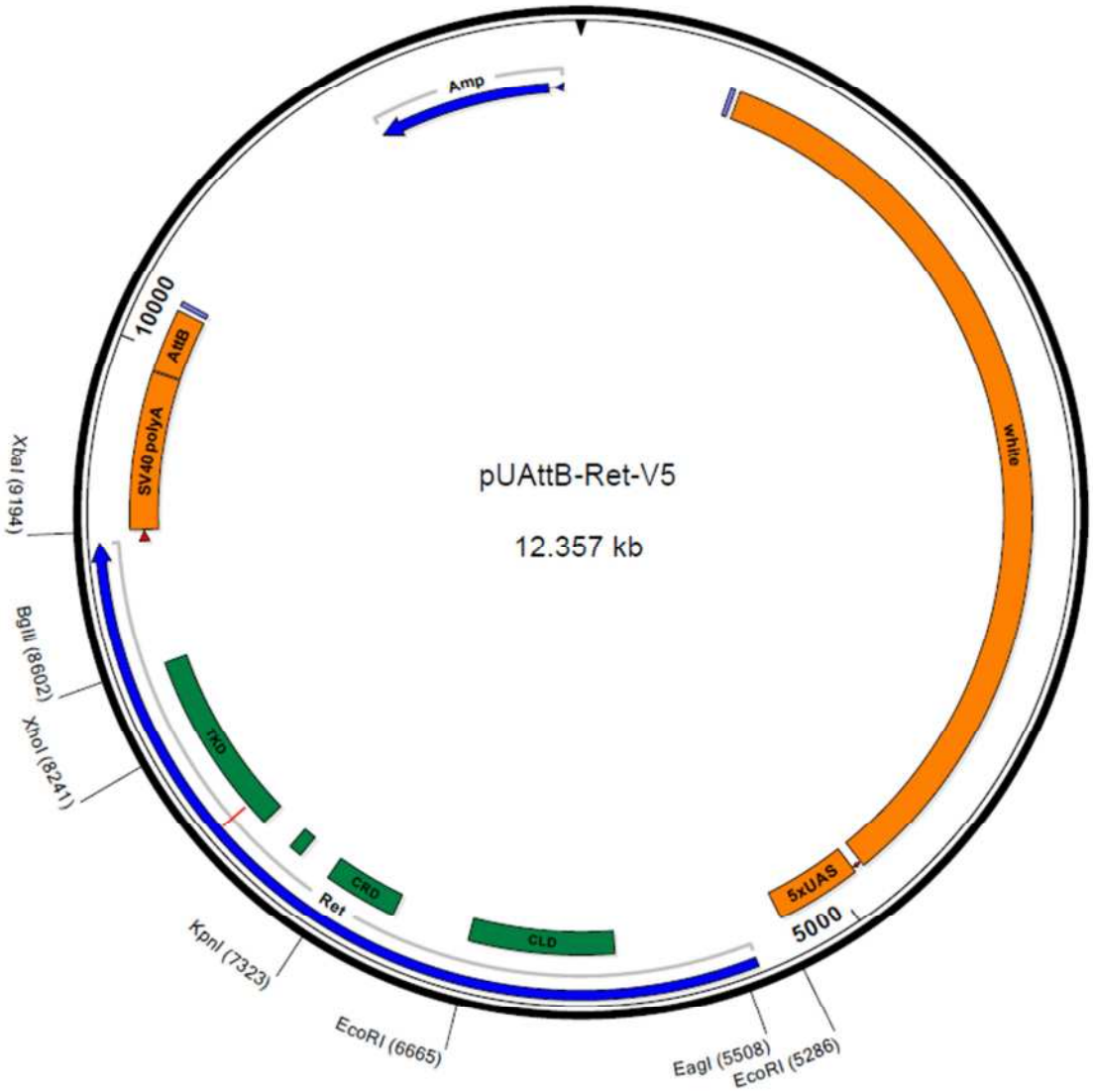

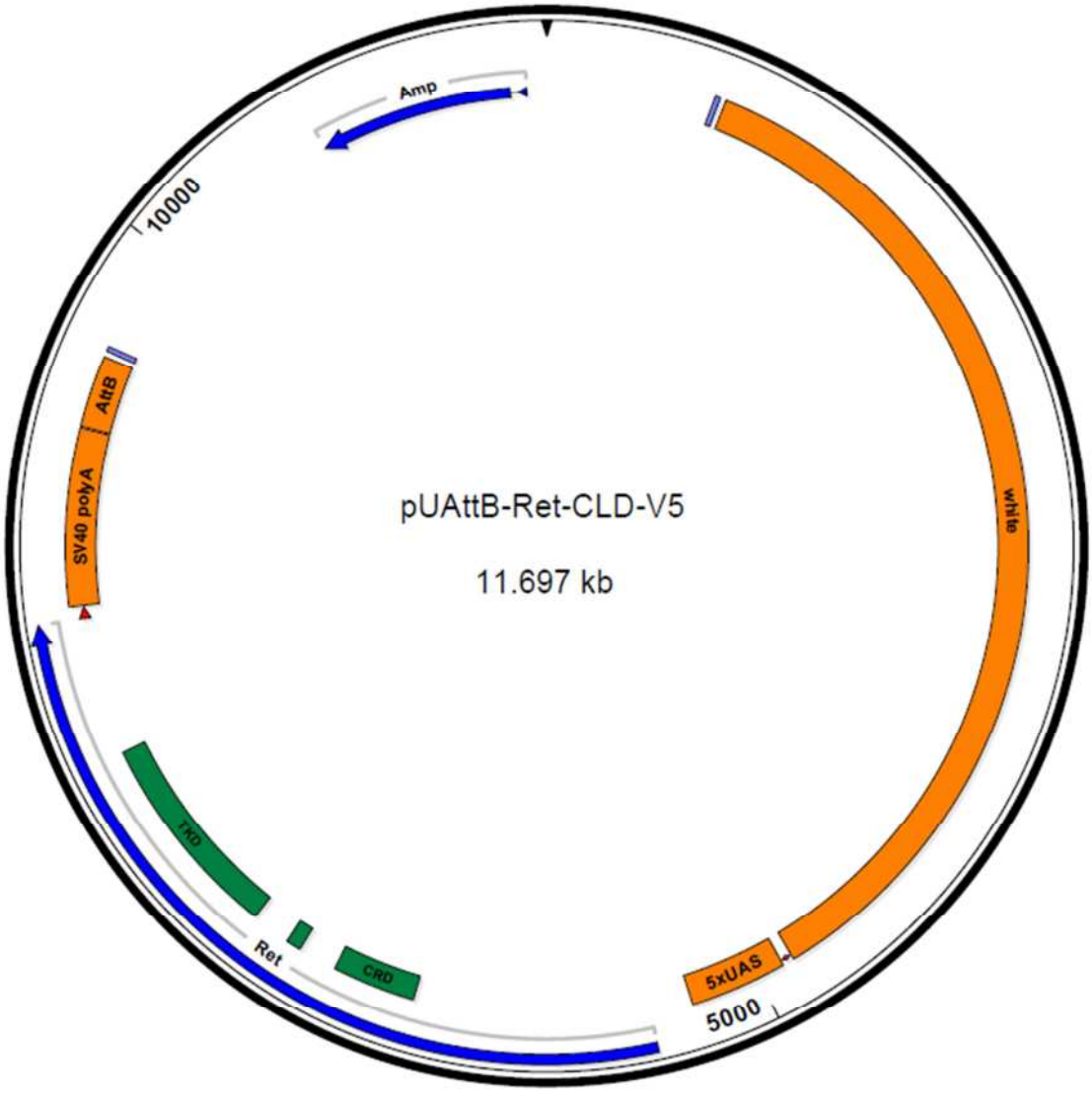
Amp
10000
AttB
SV40 polyA
pUAttB-Ret-CLD-V5
11.697 kb
white
TKD
Ret
CRD
5xUAS
5000

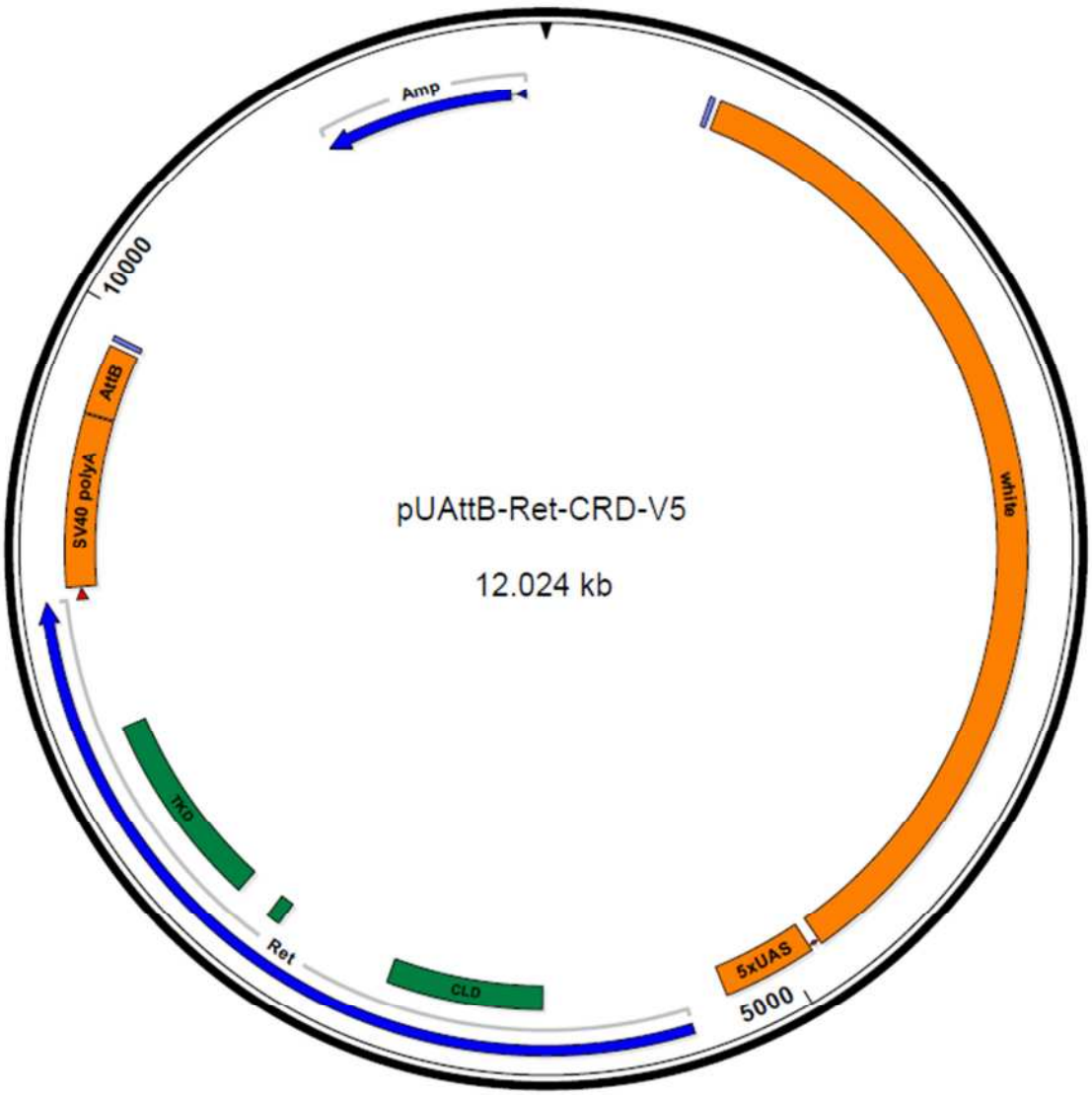
Amp
10000
AttB
SV40 polyA
pUAttB-Ret-CRD-V5
12.024 kb
white
TKD
Ret
CLD
5xUAS
5000

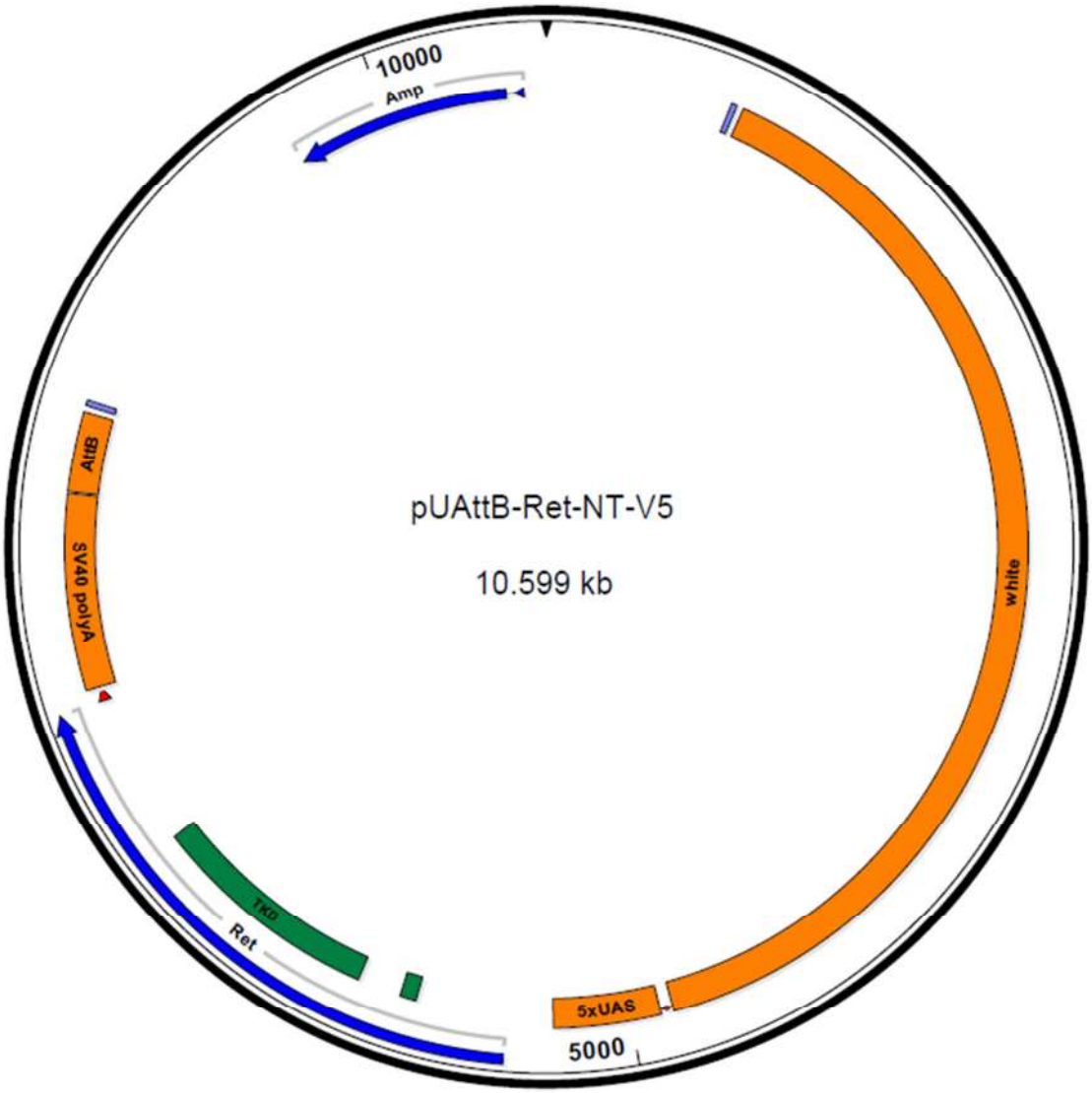
10000
Amp
pUAttB-Ret-NT-V5
10.599 kb
white
5xUAS
5000
Ret
1kb
SV40 polyA
attB

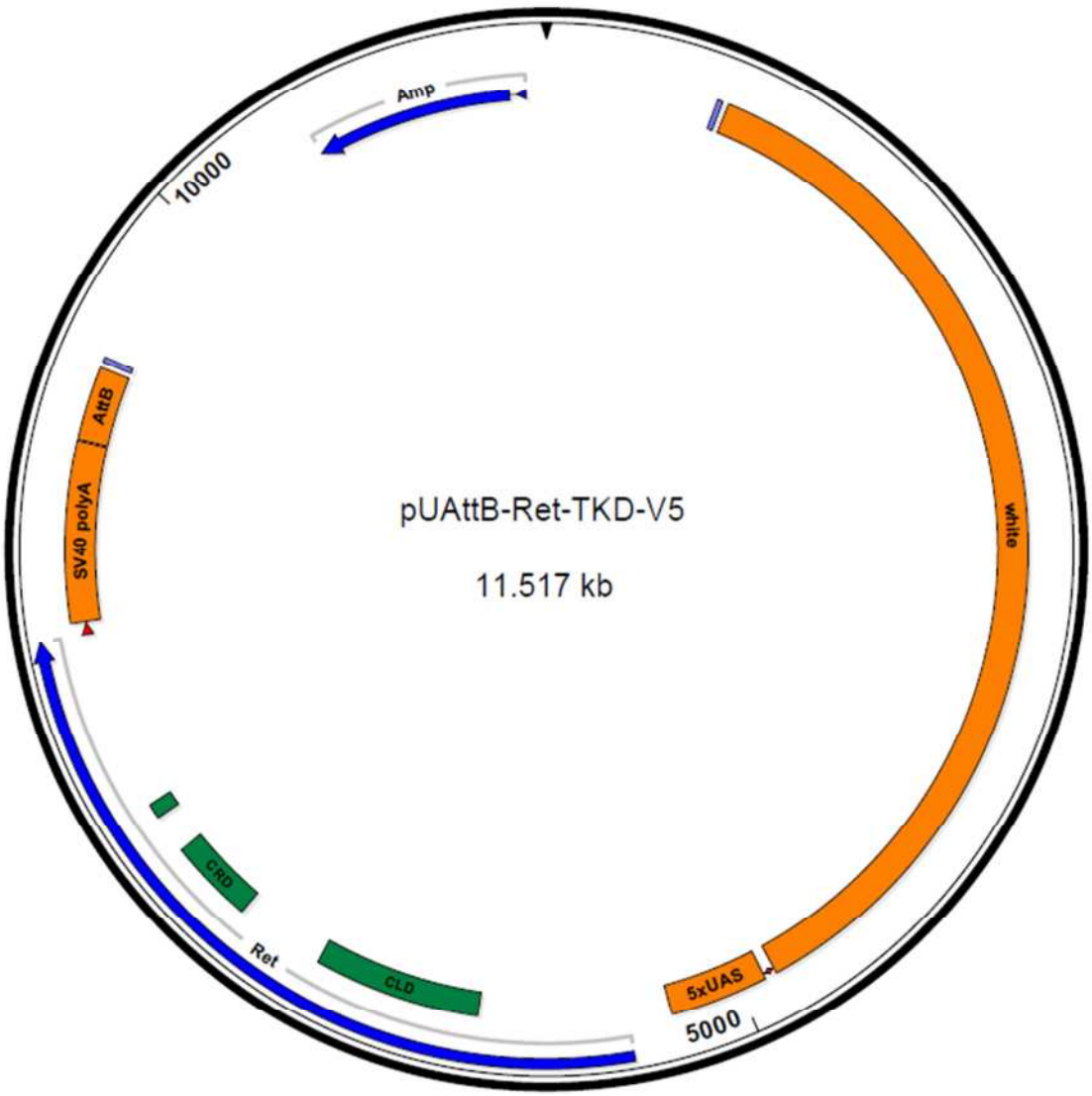
Amp
10000
AttB
SV40 polyA
pUAttB-Ret-TKD-V5
11.517 kb
white
CRD
Ret
CLD
5xUAS
5000

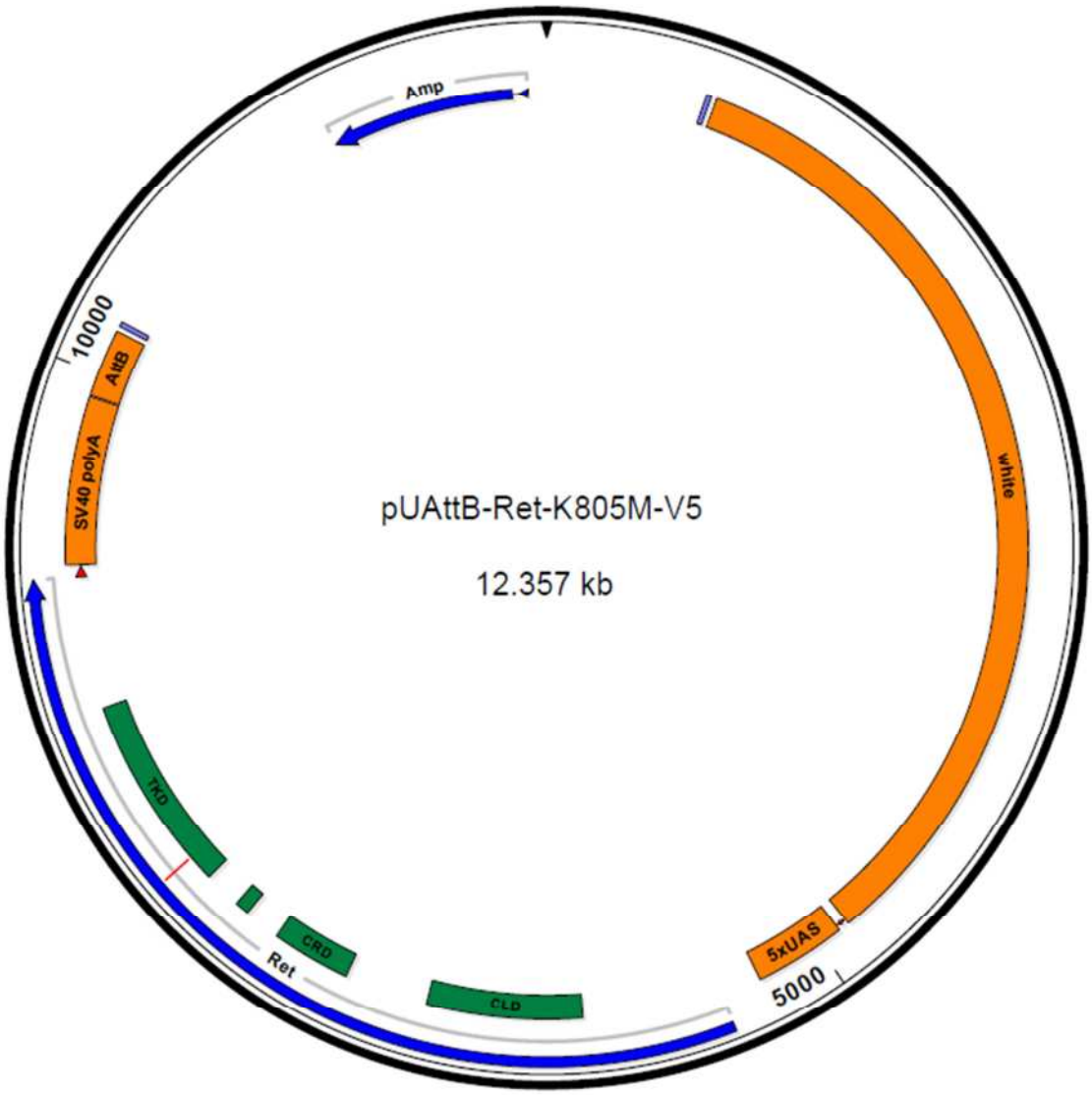
Amp
10000
AttB
SV40 polyA
pUAttB-Ret-K805M-V5
12.357 kb
white
5xUAS
5000
TKD
CRD
CLD
Ret

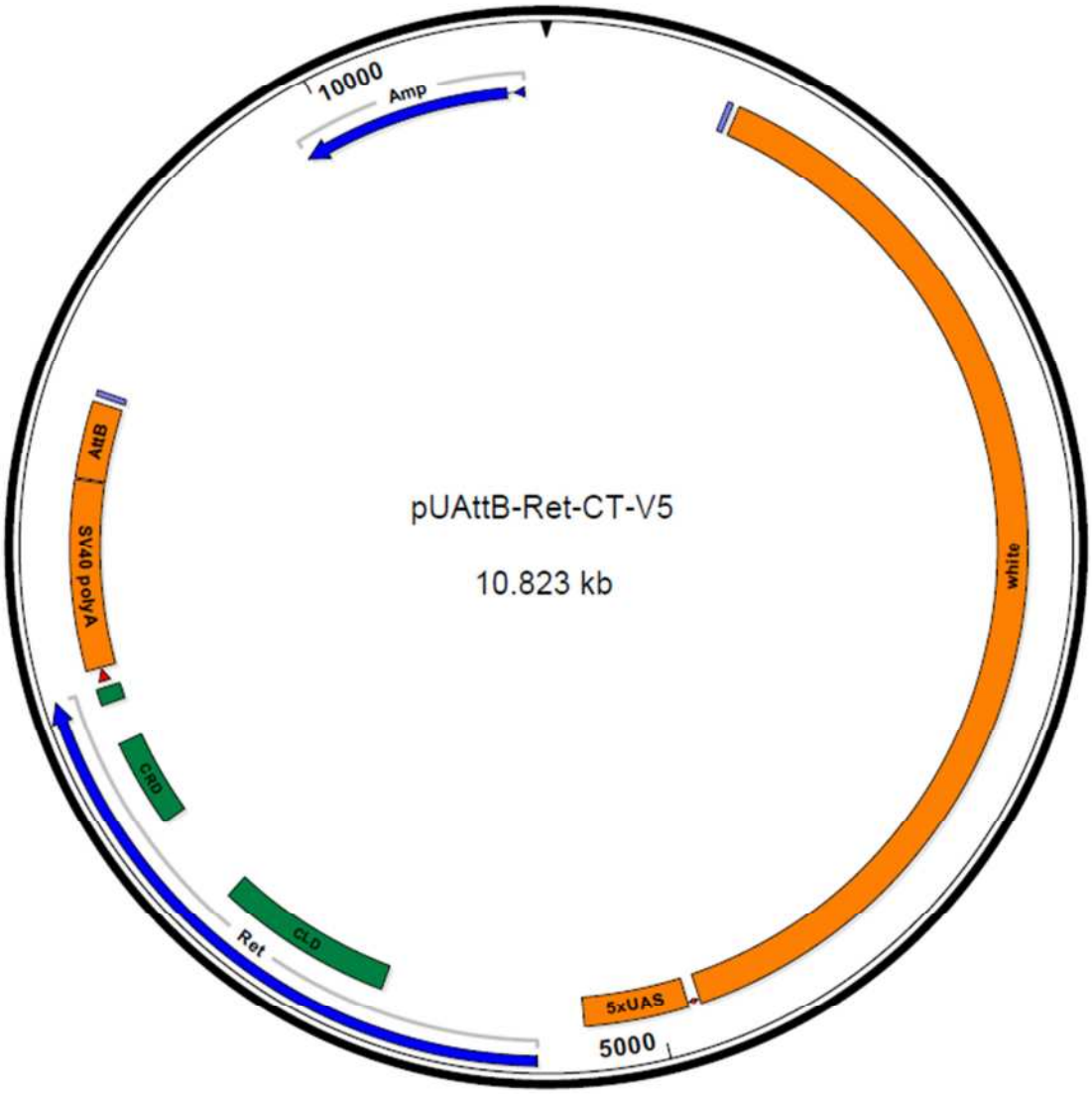
10000
Amp
pUAttB-Ret-CT-V5
10.823 kb
white
5xUAS
5000
Ret
CLD
CRD
SV40 polyA
attB

13.2 Sequence alignment of human RET and *Drosophila* Ret

Shown is the amino acid alignment of *Drosophila* Ret (dRet, NCBI Reference Sequence: NP_477044) and the vertebrate homolog of RET (Ret isoform a, GenBank: AEH95840.1) by Clustal W method using MegAlign DNASTAR Lasergene 12 software.

The different predicted domains are highlighted: CLD (Cadherin-like domain, blue), CRD (Cysteine-rich domain, purple), TMD (transmembrane domain, dark blue), TKD (tyrosine kinase domain, orange). The localization of inactive Ret kinase mutation is indicated in green (K805M). Each intracellularly located tyrosine residue is highlighted in red as potential phosphorylation motif.

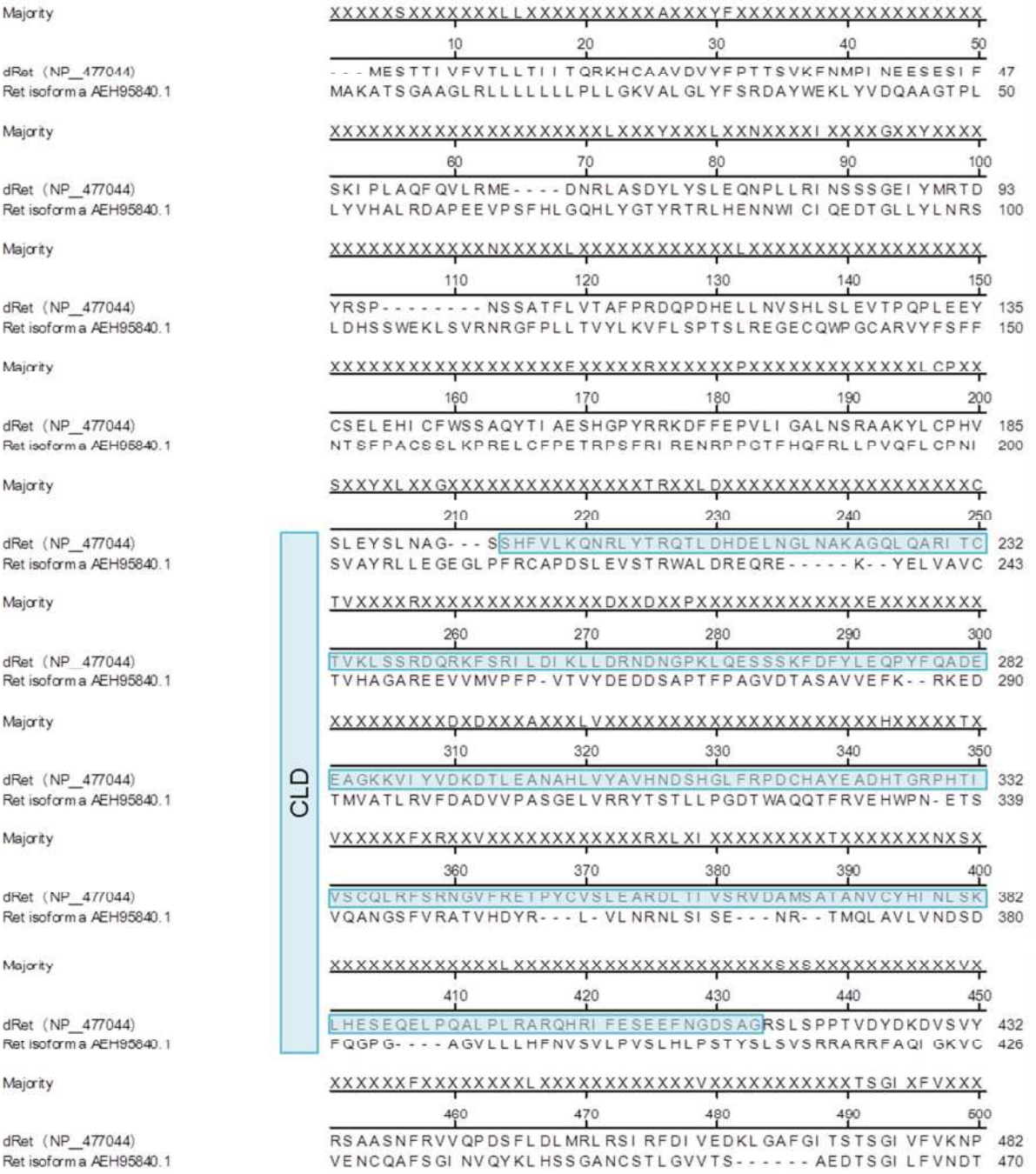

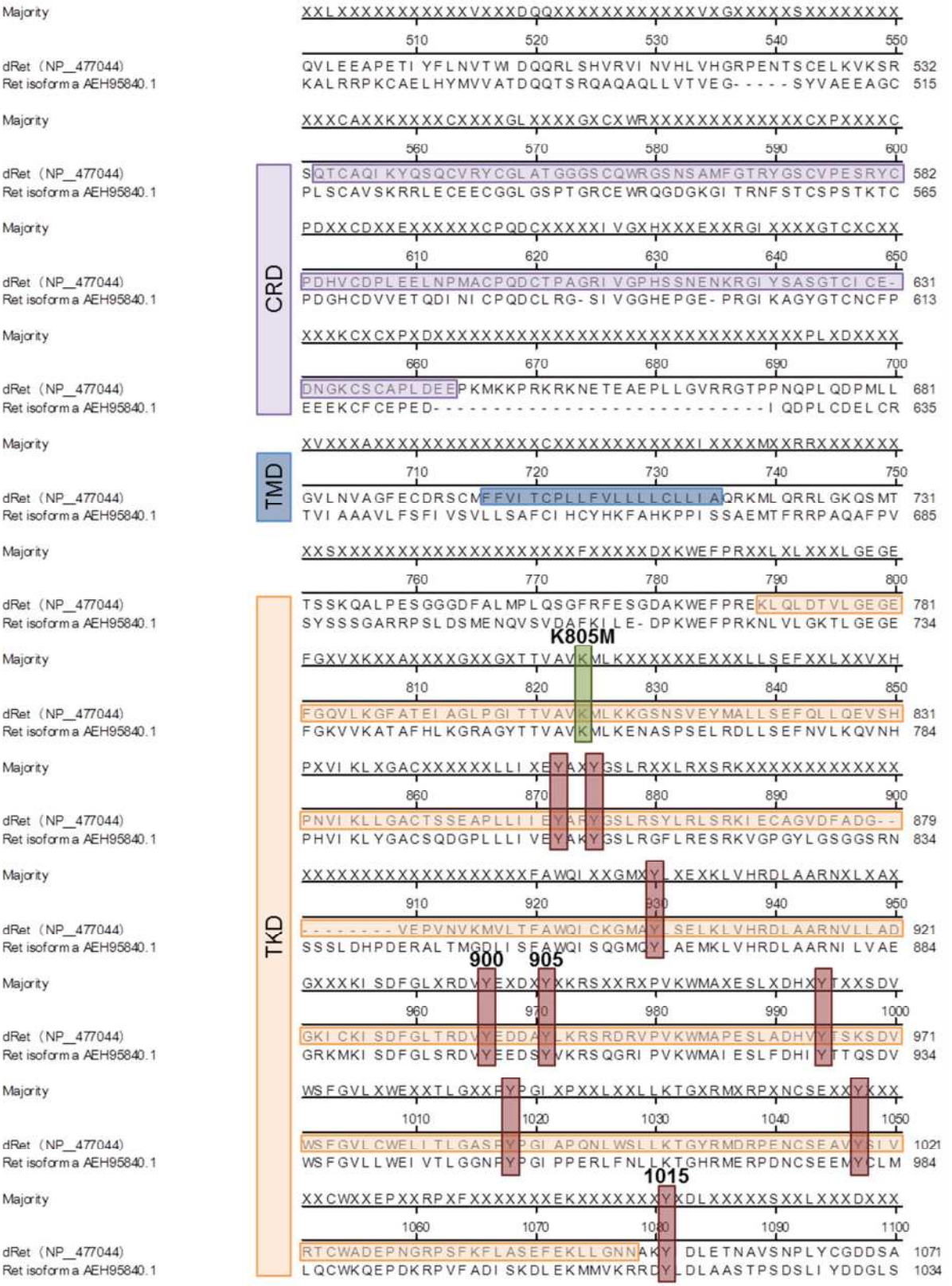
CRD
TMD
TKD
K805M
900
905
1015

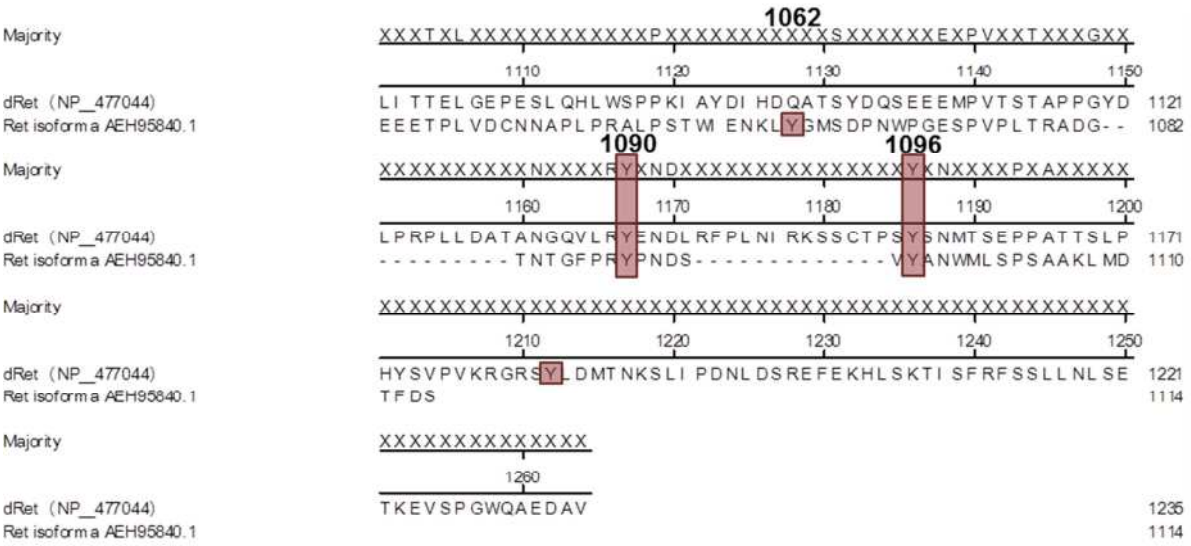
1062
Majority
1110
1120
1130
1140
1150
dRet (NP_477044) LI TTEL GEPESL QHL WSPPKI AYDI HDQATSYDQSEEEMPVTSTAPPGYD 1121
Ret isoforma AEH95840.1 EEETPL VDCNNAPL PRALPSTWI ENKLYGMSDPNWPGESPVPLTRADG- - 1082
1090
1096
Majority
1160
1170
1180
1190
1200
dRet (NP_477044) LPRPLL DATANGQVLRYENDL RFPL NI RKSSCTPSYSNMTSEPPATTSLP 1171
Ret isoforma AEH95840.1 - - - - - - - - - TNTGFPRYPNDS- - - - - - - - - - - - VYANWML SPSAAKL MD 1110
Majority
1210
1220
1230
1240
1250
dRet (NP_477044) HYSVPVKRGRSYL DMTNKSLI PDNL DSREFEKHLSKTI SFRFSSLLNL SE 1221
Ret isoforma AEH95840.1 TFDS 1114
Majority
1260
dRet (NP_477044) TKEVSPGWQAEDAV 1235
Ret isoforma AEH95840.1 1114

14 REFERENCES

Abrescia, C., Sjöstrand, D., Kjaer, S., Ibáñez, C.F., 2005. Drosophila RET contains an active tyrosine kinase and elicits neurotrophic activities in mammalian cells. FEBS Lett. 579, 3789–3796. doi:10.1016/j.febslet.2005.05.075

Ackley, B.D., 2014. Wnt-signaling and planar cell polarity genes regulate axon guidance along the anteroposterior axis in C. elegans. Dev. Neurobiol. 74, 781–96. doi:10.1002/dneu.22146

Adams, C.M., Anderson, M.G., Motto, D.G., Price, M.P., Johnson, W.A., Welsh, M.J., 1998. Ripped Pocket and Pickpocket, Novel. Cell 140, 143–152.

Airaksinen, M.S., Titievsky, A., Saarma, M., 1999. GDNF Family Neurotrophic Factor Signaling: Four Masters, One Servant? Mol. Cell. Neurosci. 13, 313–325. doi:10.1006/mcne.1999.0754

Amoresano, A., Incoronato, M., Monti, G., Pucci, P., de Franciscis, V., Cerchia, L., 2005. Direct interactions among Ret, GDNF and GFRalpha1 molecules reveal new insights into the assembly of a functional three-protein complex. Cell. Signal. 17, 717–27. doi:10.1016/j.cellsig.2004.10.012

Anders, J., Kjær, S., Ibáñez, C.F., 2001. Molecular Modeling of the Extracellular Domain of the RET Receptor Tyrosine Kinase Reveals Multiple Cadherin-like Domains and a Calcium-binding Site. J. Biol. Chem. 276, 35808–35817. doi:10.1074/jbc.M104968200

Andre, P., Song, H., Kim, W., Kispert, A., Yang, Y., 2015. Wnt5a and Wnt11 regulate mammalian anterior-posterior axis elongation. Development 142, dev.119065–. doi:10.1242/dev.119065

Arora, K., Levine, M.S., O'Connor, M.B., 1994. The screw gene encodes a ubiquitously expressed member of the TGF-beta family required for specification of dorsal cell fates in the Drosophila embryo. Genes Dev. 8, 2588–601. doi:10.1101/gad.8.21.2588

Ausubel, F., Brent, R., Kingston, R., Moore, D., Seidman, J., Smith, J., Struhl, K., 1992. Short Protocols in Molecular Biology. John Wiley Sons, New York p 917.

Bahamonde, M.E., Lyons, K.M., 2001. BMP3: to be or not to be a BMP. J. Bone Joint Surg. Am. 83-A Suppl, S56–S62.

Baloh, R.H., Tansey, M.G., Johnson, E.M., Milbrandt, J., 2000. Functional mapping of receptor specificity domains of glial cell line- derived neurotrophic factor (GDNF) family ligands and production of GFRα1 RET-specific agonists. J. Biol. Chem. 275, 3412–3420. doi:10.1074/jbc.275.5.3412

Bespalov, M.M., Sidorova, Y.A., Tumova, S., Ahonen-Bishopp, A., Magalhães, A.C., Kulesskiy, E., Paveliev, M., Rivera, C., Rauvala, H., Saarma, M., 2011. Heparan sulfate proteoglycan syndecan-3 is a novel receptor for GDNF, neurturin, and artemin. J. Cell Biol. 192, 153–169. doi:10.1083/jcb.201009136

Besset, V., Scott, R.P., Ibáñez, C.F., 2000. Signaling complexes and protein-protein interactions involved in the activation of the Ras and phosphatidylinositol 3-kinase pathways by the c-Ret receptor tyrosine kinase. J. Biol. Chem. 275, 39159–66. doi:10.1074/jbc.M006908200

Blochlinger, K., Bodmer, R., Jan, L.Y., Jan, Y.N., 1990. Patterns of expression of cut, a protein required for external sensory organ development in wild-type and cut mutant Drosophila embryos. Genes Dev. 4, 1322–31. doi:10.1101/gad.4.8.1322

Bloor, J.W., Brown, N.H., 1998. Genetic analysis of the Drosophila α(PS2) integrin subunit reveals discrete adhesive, morphogenetic and sarcomeric functions. Genetics 148, 1127–1142.

Bodmer, R., Jan, Y.N., 1987. Morphological differentiation of the embryonic peripheral neurons in Drosophila. Roux's Arch. Dev. Biol. 196, 69–77. doi:10.1007/BF00402027

Bonanomi, D., Chivatakarn, O., Bai, G., Abdesselem, H., Lettieri, K., Marquardt, T., Pierchala, B.A., Pfaff, S.L., 2012. Ret is a multifunctional coreceptor that integrates diffusible- and contact-axon guidance signals. Cell 148, 568–582. doi:10.1016/j.cell.2012.01.024

Bonkowsky, J.L., Thomas, J.B., 1999. Cell-type specific modular regulation of derailed in the Drosophila nervous system. Mech. Dev. 82, 181–184. doi:10.1016/S0925-4773(99)00007-6

Böttner, M., Laaff, M., Schechinger, B., Rappold, G., Unsicker, K., Suter-Crazzolara, C., 1999. Characterization of the rat, mouse, and human genes of growth/differentiation factor-15/macrophage inhibiting cytokine-1 (GDF-15/MIC-1). Gene 237, 105–111. doi:10.1016/S0378-1119(99)00309-1

Bourane, S., Garces, A., Venteo, S., Pattyn, A., Hubert, T., Fichard, A., Puech, S., Boukhaddaoui, H., Baudet, C., Takahashi, S., Valmier, J., Carroll, P., 2009. Low-Threshold Mechanoreceptor Subtypes Selectively Express MafA and Are Specified by Ret Signaling. Neuron 64, 857–870. doi:10.1016/j.neuron.2009.12.004

Brabant, M.C., Brower, D.L., 1993. PS2 integrin requirements in Drosophila embryo and wing morphogenesis. Dev Biol 157, 49–59. doi:10.1006/dbio.1993.1111

Brand, A.H., Perrimon, N., 1993. Targeted gene expression as a means of altering cell fates and generating dominant phenotypes. Development 118, 401–15. doi:10.1101/lm.1331809

Breuer, O., Lawhorn, C., Miller, T., Smith, D.M., Brown, L.L., 2005. Functional architecture of the mammalian striatum: Mouse vascular and striosome organization and their anatomic relationships. Neurosci. Lett. 385, 198–203. doi:10.1016/j.neulet.2005.05.029

Brower, D.L., Bunch, T. a, Mukai, L., Adamson, T.E., Wehrli, M., Lam, S., Friedlander, E., Roote, C.E., Zusman, S., 1995. Nonequivalent requirements for PS1 and PS2 integrin at cell attachments in Drosophila: genetic analysis of the alpha PS1 integrin subunit. Development 121, 1311–1320.

Brown, N.H., 2000. Cell-cell adhesion via the ECM: Integrin genetics in fly and worm. Matrix Biol. 19, 191–201. doi:10.1016/S0945-053X(00)00064-0

Brummel, T., Abdollah, S., Haerry, T.E., Shimell, M.J., Merriam, J., Raftery, L., Wrana, J.L., O'Connor, M.B., 1999. The Drosophila activin receptor Baboon signals through dSmad2 and controls cell proliferation but not patterning during larval development. Genes Dev. 13, 98–111. doi:10.1101/gad.13.1.98

Cabodi, S., del Pilar Camacho-Leal, M., Di Stefano, P., Defilippi, P., 2010. Integrin signalling adaptors: not only figurants in the cancer story. Nat. Rev. Cancer 10, 858–870. doi:10.1038/nrc2967

Campbell, I.D., Humphries, M.J., 2011. Integrin structure, activation, and interactions. Cold Spring Harb. Perspect. Biol. 3, 1–15. doi:10.1101/cshperspect.a004994

Charalambous, P., Wang, X., Thanos, S., Schober, A., Unsicker, K., 2013. Regulation and effects of GDF-15 in the retina following optic nerve crush. Cell Tissue Res. 353, 1–8. doi:10.1007/s00441-013-1634-6

Chen, W.S., Antic, D., Matis, M., Logan, C.Y., Povelones, M., Anderson, G.A., Nusse, R., Axelrod, J.D., 2008. Asymmetric Homotypic Interactions of the Atypical Cadherin Flamingo Mediate Intercellular Polarity Signaling. Cell 133, 1093–1105. doi:10.1016/j.cell.2008.04.048

Cheng, L.E., Song, W., Looger, L.L., Jan, L.Y., Jan, Y.N., 2010. The Role of the TRP Channel NompC in Drosophila Larval and Adult Locomotion. Neuron 67, 373–380. doi:10.1016/j.neuron.2010.07.004

Chi, X., Michos, O., Shakya, R., Riccio, P., Enomoto, H., Licht, J.D., Asai, N., Takahashi, M., Ohgami, N., Kato, M., Mendelsohn, C., Costantini, F., 2009. Ret-Dependent Cell Rearrangements in the Wolffian Duct Epithelium Initiate Ureteric Bud Morphogenesis. Dev. Cell 17, 199–209. doi:10.1016/j.devcel.2009.07.013

Chiariello, M., Visconti, R., Carlomagno, F., Melillo, R.M., Bucci, C., de Franciscis, V., Fox, G.M., Jing, S., Coso, O. a, Gutkind, J.S., Fusco, A., Santoro, M., 1998. Signalling of the Ret receptor tyrosine kinase through the c-Jun NH2-terminal protein kinases (JNKS): evidence for a divergence of the ERKs and JNKs pathways induced by Ret. Oncogene 16, 2435–45. doi:10.1038/sj.onc.1201778

Cong, L., Ran, F.A., Cox, D., Lin, S., Barretto, R., Habib, N., Hsu, P.D., Wu, X., Jiang, W., Marraffini, L.A., Zhang, F., 2013. Multiplex genome engineering using CRISPR/Cas systems. Science 339, 819–23. doi:10.1126/science.1231143

Constam, D.B., Robertson, E.J., 1999. Regulation of bone morphogenetic protein activity by pro domains and proprotein convertases. J. Cell Biol. 144, 139–49. doi:10.1083/jcb.144.1.139

Corey, D.P., García-Añoveros, J., Holt, J.R., Kwan, K.Y., Lin, S.-Y., Vollrath, M. a, Amalfitano, A., Cheung, E.L.-M., Derfler, B.H., Duggan, A., Géléoc, G.S.G., Gray, P. a, Hoffman, M.P., Rehm, H.L., Tamasauskas, D., Zhang, D.-S., 2004. TRPA1 is a candidate for the mechanosensitive transduction channel of vertebrate hair cells. Nature 432, 723–730. doi:10.1038/nature03066

Coste, B., Mathur, J., Schmidt, M., Earley, T.J., Ranade, S., Petrus, M.J., Dubin, A.E., Patapoutian, A., 2010. Piezo1 and Piezo2 are essential components of distinct mechanically activated cation channels. Science 330, 55–60. doi:10.1126/science.1193270

Crozatier, M., Vincent, A., 2008. Control of multidendritic neuron differentiation in Drosophila: The role of Collier. Dev. Biol. 315, 232–242. doi:10.1016/j.ydbio.2007.12.030

Dansereau, D.A., Lasko, P., 2008. RanBPM regulates cell shape, arrangement, and capacity of the female germline stem cell niche in Drosophila melanogaster. J. Cell Biol. 182, 963–977. doi:10.1083/jcb.200711046

Daopin, S., Piez, K. a, Ogawa, Y., Davies, D.R., 1992. Crystal structure of transforming growth factor-beta 2: an unusual fold for the superfamily. Science 257, 369–373. doi:10.1126/science.1631557

Davies, J.E., Pröschel, C., Zhang, N., Noble, M., Mayer-Pröschel, M., Davies, S.J.A., 2008. Transplanted astrocytes derived from BMP- or CNTF-treated glial-restricted precursors have opposite effects on recovery and allodynia after spinal cord injury. J. Biol. 7, 24. doi:10.1186/jbiol85

De Ferrari, G. V, Inestrosa, N.C., 2000. Wnt signaling function in Alzheimer's disease. Brain Res. Brain Res. Rev. 33, 1–12.

Denti, S., Sirri, A., Cheli, A., Rogge, L., Innamorati, G., Putignano, S., Fabbri, M., Pardi, R., Bianchi, E., 2004. RanBPM Is a Phosphoprotein That Associates with the Plasma Membrane and Interacts with the Integrin LFA-1. J. Biol. Chem. 279, 13027–13034.

doi:10.1074/jbc.M313515200
Devenport, D., Brown, N.H., 2004. Morphogenesis in the absence of integrins: mutation of both *Drosophila* β subunits prevents midgut migration. Development 131, 5405–5415. doi:10.1242/dev.01427
Dong, X., Liu, O.W., Howell, A.S., Shen, K., 2013. An extracellular adhesion molecule complex patterns dendritic branching and morphogenesis. Cell 155, 296–307. doi:10.1016/j.cell.2013.08.059
Donis-Keller, H., Dou, S., Chi, D., Carlson, K.M., Toshima, K., Lairmore, T.C., Howe, J.R., Moley, J.F., Goodfellow, P., Wells, S. a, 1993. Mutations in the RET proto-oncogene are associated with MEN 2A and FMTC. Hum. Mol. Genet. 2, 851–856. doi:10.1093/hmg/2.7.851
Drosten, M., Pützer, B.M., 2006. Mechanisms of Disease: cancer targeting and the impact of oncogenic RET for medullary thyroid carcinoma therapy. Nat. Clin. Pract. Oncol. 3, 564–74. doi:10.1038/ncponc0610
Duffy, J.B., 2002. GAL4 system in Drosophila: a fly geneticist's Swiss army knife. Genesis 34, 1–15. doi:10.1002/gene.10150
Durbec, P., Marcos-Gutierrez, C. V, Kilkenny, C., Grigoriou, M., Wartiowaara, K., Suvanto, P., Smith, D., Ponder, B., Costantini, F., Saarma, M., 1996. GDNF signalling through the Ret receptor tyrosine kinase. Nature 381, 789–93. doi:10.1038/381789a0
Durbec, P.L., Larsson-Blomberg, L.B., Schuchardt, A., Costantini, F., Pachnis, V., 1996. Common origin and developmental dependence on c-ret of subsets of enteric and sympathetic neuroblasts. Development 122, 349–58.
Durick, K., Gill, G.N., Taylor, S.S., 1998. Shc and Enigma are both required for mitogenic signaling by Ret/ptc2. Mol. Cell. Biol. 18, 2298–308.
Echeverry, S., Shi, X.Q., Haw, A., Liu, H., Zhang, Z., Zhang, J., 2009. Transforming growth factor-beta1 impairs neuropathic pain through pleiotropic effects. Mol. Pain 5, 16. doi:10.1186/1744-8069-5-16
Ejsmont, R.K., Sarov, M., Winkler, S., Lipinski, K. a, Tomancak, P., 2009. A toolkit for high-throughput, cross-species gene engineering in Drosophila. Nat. Methods 6, 435–7. doi:10.1038/nmeth.1334
Eketjäll, S., Fainzilber, M., Murray-Rust, J., Ibáñez, C.F., 1999. Distinct structural elements in GDNF mediate binding to GFRα1 and activation of the GFRα1-c-Ret receptor complex. EMBO J. 18, 5901–5910. doi:10.1093/emboj/18.21.5901
Emoto, K., He, Y., Ye, B., Grueber, W.B., Adler, P.N., Jan, L.Y., Jan, Y.N., 2004. Control of dendritic branching and tiling by the tricornered-kinase/furry signaling pathway in Drosophila sensory neurons. Cell 119, 245–256. doi:10.1016/j.cell.2004.09.036
Emoto, K., Parrish, J.Z., Jan, L.Y., Jan, Y.-N., 2006. The tumour suppressor Hippo acts with the NDR kinases in dendritic tiling and maintenance. Nature 443, 210–213. doi:10.1038/nature05090
Feng, X.-H., Derynck, R., 2005. Specificity and Versatility in Tgf-B Signaling Through Smads. Annu. Rev. Cell Dev. Biol. 21, 659–693. doi:10.1146/annurev.cellbio.21.022404.142018
Fuentes-Medel, Y., Ashley, J., Barria, R., Maloney, R., Freeman, M., Budnik, V., 2012. Integration of a retrograde signal during synapse formation by glia-secreted TGF-β ligand. Curr. Biol. 22, 1831–8. doi:10.1016/j.cub.2012.07.063
Fuerst, P.G., Bruce, F., Tian, M., Wei, W., Elstrott, J., Feller, M.B., Erskine, L., Singer, J.H., Burgess, R.W., 2009. DSCAM and DSCAML1 Function in Self-Avoidance in Multiple Cell Types in the Developing Mouse Retina. Neuron 64, 484–497. doi:10.1016/j.neuron.2009.09.027
Fuerst, P.G., Koizumi, A., Masland, R.H., Burgess, R.W., 2008. Neurite arborization and mosaic spacing in the mouse retina require DSCAM. Nature 451, 470–474. doi:10.1038/nature06514
Fung, S., Wang, F., Chase, M., Godt, D., Hartenstein, V., 2008. Expression profile of the cadherin family in the developing Drosophila brain. J. Comp. Neurol. 506, 469–488. doi:10.1002/cne.21539
Gao, F.B., Kohwi, M., Brenman, J.E., Jan, L.Y., Jan, Y.N., 2000. Control of dendritic field formation in Drosophila: the roles of flamingo and competition between homologous neurons. Neuron 28, 91–101. doi:10.1016/S0896-6273(00)00088-X
Gao, W.Q., Zheng, J.L., Karihaloo, M., 1995. Neurotrophin-4/5 (NT-4/5) and brain-derived neurotrophic factor (BDNF) act at later stages of cerebellar granule cell differentiation. J. Neurosci. 15, 2656–67.
Gesualdi, S.C., Haerry, T.E., 2007. Distinct signaling of Drosophila Activin/TGF-beta family members. Fly (Austin). 1, 212–221. doi:10.4161/fly.5116
Gire, V., 2004. Dysfunctional telomeres at senescence signal cell cycle arrest via Chk2. Cell Cycle 3, 1217–1220. doi:1167 [pii]
Gong, Z., Gong, Z., 2012. A molecular diffusion based utility model for Drosophila larval phototaxis. Theor. Biol. Med. Model. 9, 3. doi:10.1186/1742-4682-9-3
Gong, Z., Liu, J., Guo, C., Zhou, Y., Teng, Y., Liu, L., 2010. Two pairs of neurons in the central brain

control Drosophila innate light preference. Sci. (New York, NY) 330, 499–502. doi:10.1126/science.1195993

Gorczyca, D.A., Younger, S., Meltzer, S., Kim, S.E., Cheng, L., Song, W., Lee, H.Y., Jan, L.Y., Jan, Y.N., 2014. Identification of Ppk26, a DEG/ENaC Channel Functioning with Ppk1 in a Mutually Dependent Manner to Guide Locomotion Behavior in Drosophila. Cell Rep. 9, 1446–1458. doi:10.1016/j.celrep.2014.10.034

Green, P., Hartenstein, A.Y., Hartenstein, V., 1993. The embryonic development of the Drosophila visual system. Cell Tissue Res. 273, 583–98.

Greenspan, R.J., 2004. Fly Pushing: The Theory and Practice of Drosophila Genetics. Cold Spring Harb. Lab. Press. Cold Spring Harb. New York.

Grieco, M., Santoro, M., Berlingieri, M.T., Melillo, R.M., Donghi, R., Bongarzone, I., Pierotti, M. a., Della Porta, G., Fusco, A., Vecchio, G., 1990. PTC is a novel rearranged form of the ret proto-oncogene and is frequently detected in vivo in human thyroid papillary carcinomas. Cell 60, 557–63. doi:10.1016/0092-8674(90)90659-3

Grimm, J., Sachs, M., Britsch, S., Di Cesare, S., Schwarz-Romond, T., Alitalo, K., Birchmeier, W., 2001. Novel p62dok family members, dok-4 and dok-5, are substrates of the c-Ret receptor tyrosine kinase and mediate neuronal differentiation. J. Cell Biol. 154, 345–54. doi:10.1083/jcb.200102032

Grueber, W.B., Jan, L.Y., Jan, Y.N., 2003. Different levels of the homeodomain protein cut regulate distinct dendrite branching patterns of Drosophila multidendritic neurons. Cell 112, 805–818. doi:10.1016/S0092-8674(03)00160-0

Grueber, W.B., Jan, L.Y., Jan, Y.N., 2002. Tiling of the Drosophila epidermis by multidendritic sensory neurons. Development 129, 2867–2878.

Grueber, W.B., Ye, B., Yang, C.-H., Younger, S., Borden, K., Jan, L.Y., Jan, Y.-N., 2007. Projections of Drosophila multidendritic neurons in the central nervous system: links with peripheral dendrite morphology. Development 134, 55–64. doi:10.1242/dev.02666

Guo, Y., Wang, Y., Wang, Q., Wang, Z., 2014. The Role of PPK26 in Drosophila Larval Mechanical Nociception. Cell Rep. 9, 1183–1190. doi:10.1016/j.celrep.2014.10.020

Hahn, M., Bishop, J., 2001. Expression pattern of Drosophila ret suggests a common ancestral origin between the metamorphosis precursors in insect endoderm and the vertebrate enteric neurons. Proc. Natl. Acad. Sci. U. S. A. 98, 1053–1058. doi:10.1073/pnas.98.3.1053

Haillot, E., Molina, M.D., Lapraz, F., Lepage, T., 2015. The Maternal Maverick/GDF15-like TGF-β Ligand Panda Directs Dorsal-Ventral Axis Formation by Restricting Nodal Expression in the Sea Urchin Embryo. PLoS Biol. 13, e1002247. doi:10.1371/journal.pbio.1002247

Hakeda, S., Suzuki, T., 2013. Golden goal controls dendrite elongation and branching of multidendritic arborization neurons in drosophila. Genes to Cells 18, 960–973. doi:10.1111/gtc.12089

Halbleib, J.M., Nelson, W.J., 2006. Cadherins in development: cell adhesion, sorting, and tissue morphogenesis. Genes Dev. 20, 3199–214. doi:10.1101/gad.1486806

Han, C., Jan, L.Y., Jan, Y.-N., 2011. Enhancer-driven membrane markers for analysis of nonautonomous mechanisms reveal neuron-glia interactions in Drosophila. Proc. Natl. Acad. Sci. U. S. A. 108, 9673–8. doi:10.1073/pnas.1106386108

Han, C., Wang, D., Soba, P., Zhu, S., Lin, X., Jan, L.Y., Jan, Y.N., 2012. Integrins Regulate Repulsion-Mediated Dendritic Patterning of Drosophila Sensory Neurons by Restricting Dendrites in a 2D Space. Neuron 73, 64–78. doi:10.1016/j.neuron.2011.10.036

Hanks, S.K., Quinn, a M., Hunter, T., 1988. The protein kinase family: conserved features and deduced phylogeny of the catalytic domains. Science 241, 42–52. doi:10.1126/science.3291115

Hassan, J., Busto, M., Iyengar, B., Campos, A.R., 2000. Behavioral characterization and genetic analysis of the Drosophila melanogaster larval response to light as revealed by a novel individual assay. Behav. Genet. 30, 59–69.

Hattori, D., Millard, S.S., Wojtowicz, W.M., Zipursky, S.L., 2008. Dscam-Mediated Cell Recognition Regulates Neural Circuit Formation. Annu. Rev. Cell Dev. Biol. 24, 597–620. doi:10.1146/annurev.cellbio.24.110707.175250

Hernández, K., Myers, L.G., Bowser, M., Kidd, T., 2015. Genetic Tools for the Analysis of Drosophila Stomatogastric Nervous System Development. PLoS One 10, e0128290. doi:10.1371/journal.pone.0128290

Hofstra, R.M., Landsvater, R.M., Ceccherini, I., Stulp, R.P., Stelwagen, T., Luo, Y., Pasini, B., Höppener, J.W., van Amstel, H.K., Romeo, G., 1994. A mutation in the RET proto-oncogene associated with multiple endocrine neoplasia type 2B and sporadic medullary thyroid carcinoma. Nature 367, 375–6. doi:10.1038/367375a0

Huang, J., Zhou, W., Dong, W., Watson, A.M., Hong, Y., 2009. From the Cover: Directed, efficient, and versatile modifications of the Drosophila genome by genomic engineering. Proc. Natl. Acad. Sci. U. S. A. 106, 8284–8289. doi:10.1073/pnas.0900641106

Hughes, M.E., Bortnick, R., Tsubouchi, A., Bäumer, P., Kondo, M., Uemura, T., Schmucker, D., 2007. Homophilic Dscam interactions control complex dendrite morphogenesis. Neuron 54, 417–27. doi:10.1016/j.neuron.2007.04.013

Hwang, R.Y., Zhong, L., Xu, Y., Johnson, T., Zhang, F., Deisseroth, K., Tracey, W.D., 2007. Nociceptive Neurons Protect Drosophila Larvae from Parasitoid Wasps. Curr. Biol. 17, 2105–2116. doi:10.1016/j.cub.2007.11.029

Hynes, R.O., Zhao, Q., 2000. The evolution of cell adhesion. J. Cell Biol. 150, F89–96. doi:10.1083/jcb.150.2.F89

Jahan, N., Hannila, S.S., 2015. Transforming growth factor β-induced expression of chondroitin sulfate proteoglycans is mediated through non-Smad signaling pathways. Exp. Neurol. 263, 372–84. doi:10.1016/j.expneurol.2014.10.023

Jain, S., Encinas, M., Johnson, E.M., Milbrandt, J., 2006. Critical and distinct roles for key RET tyrosine docking sites in renal development. Genes Dev. 20, 321–333. doi:10.1101/gad.1387206

Jijiwa, M., Fukuda, T., Kawai, K., Nakamura, A., Kurokawa, K., Murakumo, Y., Ichihara, M., Takahashi, M., 2004. A targeting mutation of tyrosine 1062 in Ret causes a marked decrease of enteric neurons and renal hypoplasia. Mol Cell Biol 24, 8026–8036. doi:10.1128/MCB.24.18.8026-8036.2004

Jinek, M., Chylinski, K., Fonfara, I., Hauer, M., Doudna, J.A., Charpentier, E., 2012. A programmable dual-RNA-guided DNA endonuclease in adaptive bacterial immunity. Science 337, 816–21. doi:10.1126/science.1225829

Jinushi-Nakao, S., Arvind, R., Amikura, R., Kinameri, E., Liu, A.W., Moore, A.W., 2007. Knot/Collier and Cut Control Different Aspects of Dendrite Cytoskeleton and Synergize to Define Final Arbor Shape. Neuron 56, 963–978. doi:10.1016/j.neuron.2007.10.031

Kallijärvi, J., Stratoulias, V., Virtanen, K., Hietakangas, V., Heino, T.I., Saarma, M., 2012. Characterization of Drosophila GDNF Receptor-Like and Evidence for Its Evolutionarily Conserved Interaction with Neural Cell Adhesion Molecule (NCAM)/FasII. PLoS One 7, e51997. doi:10.1371/journal.pone.0051997

Kang, K., Pulver, S.R., Panzano, V.C., Chang, E.C., Griffith, L.C., Theobald, D.L., Garrity, P.A., 2010. Analysis of Drosophila TRPA1 reveals an ancient origin for human chemical nociception. Nature 464, 597–600. doi:10.1038/nature08848

Keene, A.C., Mazzoni, E.O., Zhen, J., Younger, M.A., Yamaguchi, S., Blau, J., Desplan, C., Sprecher, S.G., 2011. Distinct Visual Pathways Mediate Drosophila Larval Light Avoidance and Circadian Clock Entrainment. J. Neurosci. 31, 6527–6534. doi:10.1523/JNEUROSCI.6165-10.2011

Kim, M.E., Shrestha, B.R., Blazeski, R., Mason, C.A., Grueber, W.B., 2012. Integrins establish dendrite-substrate relationships that promote dendritic self-avoidance and patterning in drosophila sensory neurons. Neuron 73, 79–91. doi:10.1016/j.neuron.2011.10.033

Kim, S.E., Coste, B., Chadha, A., Cook, B., Patapoutian, A., 2012. The role of Drosophila Piezo in mechanical nociception. Nature 483, 209–212. doi:10.1038/nature10801

Kjær, S., Ibáñez, C.F., 2003. Identification of a Surface for Binding to the GDNF-GFRα1 Complex in the First Cadherin-like Domain of RET. J. Biol. Chem. 278, 47898–47904. doi:10.1074/jbc.M309772200

Knauf, J.A., Ouyang, B., Croyle, M., Kimura, E., Fagin, J.A., 2003. Acute expression of RET/PTC induces isozyme-specific activation and subsequent downregulation of PKC(epsilon) in PCCL3 thyroid cells. Oncogene 22, 6830–6838. doi:10.1038/sj.onc.1206829

Knowles, P.P., Murray-Rust, J., Kjaer, S., Scott, R.P., Hanrahan, S., Santoro, M., Ibáñez, C.F., McDonald, N.Q., 2006. Structure and chemical inhibition of the RET tyrosine kinase domain. J. Biol. Chem. 281, 33577–87. doi:10.1074/jbc.M605604200

Koike-Kumagai, M., Yasunaga, K., Morikawa, R., Kanamori, T., Emoto, K., 2009. The target of rapamycin complex 2 controls dendritic tiling of Drosophila sensory neurons through the Tricornered kinase signalling pathway. EMBO J. 28, 3879–92. doi:10.1038/emboj.2009.312

Komiyama, T., Sweeney, L.B., Schuldiner, O., Garcia, K.C., Luo, L., 2007. Graded expression of semaphorin-1a cell-autonomously directs dendritic targeting of olfactory projection neurons. Cell 128, 399–410. doi:10.1016/j.cell.2006.12.028

Kondo, S., Ueda, R., 2013. Highly improved gene targeting by germline-specific Cas9 expression in Drosophila. Genetics 195, 715–21. doi:10.1534/genetics.113.156737

Kowsky, S., Pöppelmeyer, C., Kramer, E.R., Falkenburger, B.H., Kruse, A., Klein, R., Schulz, J.B., 2007. RET signaling does not modulate MPTP toxicity but is required for regeneration of dopaminergic axon terminals. Proc. Natl. Acad. Sci. U. S. A. 104, 20049–20054. doi:10.1073/pnas.0706177104

Kramer, E.R., Aron, L., Ramakers, G.M.J., Seitz, S., Zhuang, X., Beyer, K., Smidt, M.P., Klein, R., 2007. Absence of Ret signaling in mice causes progressive and late degeneration of the nigrostriatal system. PLoS Biol. 5, 0616–0628. doi:10.1371/journal.pbio.0050039

Kramer, E.R., Knott, L., Su, F., Dessaud, E., Krull, C.E., Helmbacher, F., Klein, R., 2006. Cooperation between GDNF/Ret and ephrinA/EphA4 Signals for Motor-Axon Pathway Selection in the Limb. Neuron 50, 35–47. doi:10.1016/j.neuron.2006.02.020

Kurokawa, K., Kawai, K., Hashimoto, M., Ito, Y., Takahashi, M., 2003. Cell signalling and gene expression mediated by RET tyrosine kinase. J. Intern. Med. 253, 627–33. doi:1167 [pii]

Lahaye, L.L., Wouda, R.R., de Jong, A.W.M., Fradkin, L.G., Noordermeer, J.N., 2012. WNT5 interacts with the Ryk receptors doughnut and derailed to mediate muscle attachment site selection in Drosophila melanogaster. PLoS One 7, e32297. doi:10.1371/journal.pone.0032297

Lantero, A., Tramullas, M., Díaz, A., Hurlé, M.A., 2012. Transforming growth factor-β in normal nociceptive processing and pathological pain models. Mol. Neurobiol. 45, 76–86. doi:10.1007/s12035-011-8221-1

Lecuit, T., Sonnenberg, A., 2011. Cell-to-cell contact and extracellular matrix. Editorial overview. Curr. Opin. Cell Biol. 23, 505–7. doi:10.1016/j.ceb.2011.09.001

Lee, M.K., Pardoux, C., Hall, M.C., Lee, P.S., Warburton, D., Qing, J., Smith, S.M., Derynck, R., 2007. TGF-beta activates Erk MAP kinase signalling through direct phosphorylation of ShcA. EMBO J. 26, 3957–67. doi:10.1038/sj.emboj.7601818

Leppänen, V.-M., Bespalov, M.M., Runeberg-Roos, P., Puurand, U., Merits, A., Saarma, M., Goldman, A., 2004. The structure of GFRalpha1 domain 3 reveals new insights into GDNF binding and RET activation. EMBO J. 23, 1452–62. doi:10.1038/sj.emboj.7600174

Letsou, A., Arora, K., Wrana, J.L., Simin, K., Twombly, V., Jamal, J., Staehling-Hampton, K., Hoffmann, F.M., Gelbart, W.M., Massagué, J., 1995. Drosophila Dpp signaling is mediated by the punt gene product: a dual ligand-binding type II receptor of the TGF beta receptor family. Cell 80, 899–908. doi:10.1016/0092-8674(95)90293-7

Li, W., Wang, F., Menut, L., Gao, F.-B., 2004. BTB/POZ-zinc finger protein abrupt suppresses dendritic branching in a neuronal subtype-specific and dosage-dependent manner. Neuron 43, 823–34. doi:10.1016/j.neuron.2004.08.040

Liu, O.W., Shen, K., 2012. The transmembrane LRR protein DMA-1 promotes dendrite branching and growth in C. elegans. Nat. Neurosci. 15, 57–63. doi:10.1038/nn.2978

Lowery, J.W., LaVigne, A.W., Kokabu, S., Rosen, V., 2013. Comparative Genomics Identifies the Mouse Bmp3 Promoter and an Upstream Evolutionary Conserved Region (ECR) in Mammals. PLoS One 8, e57840. doi:10.1371/journal.pone.0057840

Luo, W., Enomoto, H., Rice, F.L., Milbrandt, J., Ginty, D.D., 2009. Molecular Identification of Rapidly Adapting Mechanoreceptors and Their Developmental Dependence on Ret Signaling. Neuron 64, 841–856. doi:10.1016/j.neuron.2009.11.003

Mali, P., Esvelt, K.M., Church, G.M., 2013. Cas9 as a versatile tool for engineering biology. Nat. Methods 10, 957–63. doi:10.1038/nmeth.2649

Manié, S., Santoro, M., Fusco, A., Billaud, M., 2001. The RET receptor: Function in development and dysfunction in congenital malformation. Trends Genet. 17, 580–589. doi:10.1016/S0168-9525(01)02420-9

Marqués, G., Bao, H., Haerry, T.E., Shimell, M.J., Duchek, P., Zhang, B., O'Connor, M.B., 2002. The Drosophila BMP type II receptor Wishful Thinking regulates neuromuscular synapse morphology and function. Neuron 33, 529–43. doi:10.1016/S0896-6273(02)00595-0

Massagué, J., 2000. How cells read TGF-beta signals. Nat. Rev. Mol. Cell Biol. 1, 169–178. doi:10.1038/35043051

Massagué, J., 1998. Tgf-B Signal Transduction. Annu. Rev. Biochem. 67, 753–791. doi:10.1146/annurev.biochem.67.1.753

Matsubara, D., Horiuchi, S.Y., Shimono, K., Usui, T., Uemura, T., 2011. The seven-pass transmembrane cadherin Flamingo controls dendritic self-avoidance via its binding to a LIM domain protein, Espinas, in Drosophila sensory neurons. Genes Dev. 25, 1982–1996. doi:10.1101/gad.16531611

Matthews, B.J., Kim, M.E., Flanagan, J.J., Hattori, D., Clemens, J.C., Zipursky, S.L., Grueber, W.B., 2007. Dendrite self-avoidance is controlled by Dscam. Cell 129, 593–604. doi:10.1016/j.cell.2007.04.013

Mauthner, S.E., Hwang, R.Y., Lewis, A.H., Xiao, Q., Tsubouchi, A., Wang, Y., Honjo, K., Skene, J.H.P., Grandl, J., Tracey, W.D., 2014. Balboa binds to pickpocket in vivo and is required for mechanical nociception in drosophila larvae. Curr. Biol. 24, 2920–2925. doi:10.1016/j.cub.2014.10.038

Meltzer, S., Yadav, S., Lee, J., Soba, P., Younger, S.H., Jin, P., Zhang, W., Parrish, J., Jan, L.Y., Jan, Y.-N., 2016. Epidermis-Derived Semaphorin Promotes Dendrite Self-Avoidance by Regulating Dendrite-Substrate Adhesion in Drosophila Sensory Neurons. Neuron. doi:10.1016/j.neuron.2016.01.020

Mishra, B., Ghannad-Rezaie, M., Li, J., Wang, X., Hao, Y., Ye, B., Chronis, N., Collins, C. a, 2014.

Using microfluidics chips for live imaging and study of injury responses in Drosophila larvae. J. Vis. Exp. e50998. doi:10.3791/50998
Mulligan, L.M., 2014. RET revisited: expanding the oncogenic portfolio. Nat. Rev. Cancer 14, 173–86. doi:10.1038/nrc3680
Munger, J.S., Sheppard, D., 2011. Cross talk among TGF-β signaling pathways, integrins, and the extracellular matrix. Cold Spring Harb. Perspect. Biol. 3, a005017. doi:10.1101/cshperspect.a005017
Murakami, H., Yamamura, Y., Shimono, Y., Kawai, K., Kurokawa, K., Takahashi, M., 2002. Role of Dok1 in cell signaling mediated by RET tyrosine kinase. J. Biol. Chem. 277, 32781–90. doi:10.1074/jbc.M202336200
Murooka, T.T., Mempel, T.R., 2012. Integrin and Cell Adhesion Molecules. Methods in Molecular Biology 757, 247–257. doi:10.1007/978-1-61779-166-6
Myers, S.M., Eng, C., Ponder, B.A., Mulligan, L.M., 1995. Characterization of RET proto-oncogene 3' splicing variants and polyadenylation sites: a novel C-terminus for RET. Oncogene 11, 2039–45. doi:10.1016/j.devcel.2010.10.021.Steroid
Nagata, K., Duggan, A., Kumar, G., García-Añoveros, J., 2005. Nociceptor and Hair Cell Transducer Properties of TRPA1, a Channel for Pain and Hearing. J. Neurosci. 25, 4052–4061. doi:10.1523/JNEUROSCI.0013-05.2005
Neely, G.G., Keene, A.C., Duchek, P., Chang, E.C., Wang, Q.P., Aksoy, Y.A., Rosenzweig, M., Costigan, M., Woolf, C.J., Garrity, P.A., Penninger, J.M., 2011. TrpA1 regulates thermal nociception in Drosophila. PLoS One 6, e24343. doi:10.1371/journal.pone.0024343
Neumann, C., Cohen, S., 1997. Morphogens and pattern formation. Bioessays 19, 721–9. doi:10.1002/bies.950190813
Nguyen, M., Parker, L., Arora, K., 2000. Identification of maverick, a novel member of the TGF-beta superfamily in Drosophila. Mech. Dev. 95, 201–6. doi:10.1016/S0925-4773(00)00338-5
Ohiwa, M., Murakami, H., Iwashita, T., Asai, N., Iwata, Y., Imai, T., Funahashi, H., Takagi, H., Takahashi, M., 1997. Characterization of Ret-Shc-Grb2 complex induced by GDNF, MEN 2A, and MEN 2B mutations. Biochem. Biophys. Res. Commun. 237, 747–51. doi:10.1006/bbrc.1997.7225
Polleux, F., Giger, R.J., Ginty, D.D., Kolodkin, A.L., Ghosh, A., 1998. Patterning of cortical efferent projections by semaphorin-neuropilin interactions. Science 282, 1904–6. doi:10.1126/science.282.5395.1904
Polleux, F., Morrow, T., Ghosh, A., 2000. Semaphorin 3A is a chemoattractant for cortical apical dendrites. Nature 404, 567–73. doi:10.1038/35007001
Port, F., Chen, H.-M., Lee, T., Bullock, S.L., 2014. Optimized CRISPR/Cas tools for efficient germline and somatic genome engineering in Drosophila. Proc. Natl. Acad. Sci. U. S. A. 111, E2967–76. doi:10.1073/pnas.1405500111
Puram, S. V, Bonni, A., 2013. Cell-intrinsic drivers of dendrite morphogenesis. Development 140, 4657–71. doi:10.1242/dev.087676
Purro, S.A., Galli, S., Salinas, P.C., 2014. Dysfunction of Wnt signaling and synaptic disassembly in neurodegenerative diseases. J. Mol. Cell Biol. 6, 75–80. doi:10.1093/jmcb/mjt049
Purves, D., Augustine, G.J., Fitzpatrick, D., Hall, W.C., Lamantia, A.-S., McNamara, J.O., Williams, S.M., 2011. Neuroscience, 5th ed.
Raftery, L.A., Sutherland, D.J., 1999. TGF-beta family signal transduction in Drosophila development: from Mad to Smads. Dev. Biol. 210, 251–68. doi:10.1006/dbio.1999.9282
Ramon y Cajal S, 1911. Histologie du systeme nerveux de l'homme et des vertebres.
Read, R.D., Goodfellow, P.J., Mardis, E.R., Novak, N., Armstrong, J.R., Cagan, R.L., 2005. A drosophila model of multiple endocrine neoplasia type 2. Genetics 171, 1057–1081. doi:10.1534/genetics.104.038018
Richardson, D.S., Rodrigues, D.M., Hyndman, B.D., Crupi, M.J.F., Nicolescu, A.C., Mulligan, L.M., 2012. Alternative splicing results in RET isoforms with distinct trafficking properties. Mol. Biol. Cell 23, 3838–50. doi:10.1091/mbc.E12-02-0114
Riesgo-Escovar, J.R., Hafen, E., 1997. Drosophila jun kinase regulates expression of decapentaplegic via the ets-domain protein Aop and the ap-1 transcription factor Djun during dorsal closure. Genes Dev. 11, 1717–1727. doi:10.1101/gad.11.13.1717
Robertson, J.L., Tsubouchi, A., Tracey, W.D., 2013. Larval Defense against Attack from Parasitoid Wasps Requires Nociceptive Neurons. PLoS One 8, 1–9. doi:10.1371/journal.pone.0078704
Romeo, G., Ronchetto, P., Luo, Y., Barone, V., Seri, M., Ceccherini, I., Pasini, B., Bocciardi, R., Lerone, M., Kääriäinen, H., 1994. Point mutations affecting the tyrosine kinase domain of the RET proto-oncogene in Hirschsprung's disease. Nature 367, 377–378. doi:10.1038/367377a0
Rong, Y.S., 2002. Gene targeting by homologous recombination: A powerful addition to the genetic arsenal for Drosophila geneticists. Biochem. Biophys. Res. Commun. 297, 1–5.

doi:10.1016/S0006-291X(02)02066-1
Rosso, S.B., Sussman, D., Wynshaw-Boris, A., Salinas, P.C., 2005. Wnt signaling through Dishevelled, Rac and JNK regulates dendritic development. Nat. Neurosci. 8, 34–42. doi:10.1038/nn1374
Rozario, T., DeSimone, D.W., 2010. The extracellular matrix in development and morphogenesis: a dynamic view. Dev. Biol. 341, 126–40. doi:10.1016/j.ydbio.2009.10.026
Ruco, L.P., Stoppacciaro, A., Ballarini, F., Prat, M., Scarpino, S., 2001. Met protein and hepatocyte growth factor (HGF) in papillary carcinoma of the thyroid: Evidence for a pathogenetic role in tumourigenesis. J. Pathol. 194, 4–8. doi:10.1002/path.847
Runeberg-Roos, P., Virtanen, H., Saarma, M., 2007. RET(MEN 2B) is active in the endoplasmic reticulum before reaching the cell surface. Oncogene 26, 7909–15. doi:10.1038/sj.onc.1210591
Rusmini, M., Griseri, P., Matera, I., Pontarini, E., Ravazzolo, R., Mavilio, D., Ceccherini, I., 2014. Expression variability and function of the RET gene in adult peripheral blood mononuclear cells. J. Cell. Physiol. 229, 2027–2037. doi:10.1002/jcp.24660
Ryder, E., Russell, S., 2003. Transposable elements as tools for genomics and genetics in Drosophila. Brief. Funct. Genomic. Proteomic. 2, 57–71. doi:10.1093/bfgp/2.1.57
Saarma, M., 2000. GDNF - a stranger in the TGF-β superfamily? Eur. J. Biochem. 267, 6968–6971. doi:10.1046/j.1432-1327.2000.01826.x
Salzberg, Y., Díaz-Balzac, C.A., Ramirez-Suarez, N.J., Attreed, M., Tecle, E., Desbois, M., Kaprielian, Z., Bülow, H.E., 2013. Skin-derived cues control arborization of sensory dendrites in Caenorhabditis elegans. Cell 155, 308–20. doi:10.1016/j.cell.2013.08.058
Salzberg, Y., Ramirez-Suarez, N.J., Bülow, H.E., 2014. The proprotein convertase KPC-1/furin controls branching and self-avoidance of sensory dendrites in Caenorhabditis elegans. PLoS Genet. 10, e1004657. doi:10.1371/journal.pgen.1004657
Sambrook, J., Fritsch, E., Maniatis, T., 1989. Molecular Cloning: A Laboratory Manual. Cold Spring Harb. Lab. Press. Cold Spring Harb. NY. doi:http://dx.doi.org/10.1016/0092-8674(90)90210-6
Sawin-McCormack, E.P., Sokolowski, M.B., Campos, A.R., 1995. Characterization and genetic analysis of Drosophila melanogaster photobehavior during larval development. J. Neurogenet. 10, 119–35.
Scantlebury, N., Zhao, X.L., Moncalvo, V.G.R., Camiletti, A., Zahanova, S., Dineen, A., Xin, J.H., Campos, A.R., 2010. The Drosophila gene RanBPM functions in the mushroom body to regulate larval behavior. PLoS One 5, e10652. doi:10.1371/journal.pone.0010652
Schalm, S.S., Ballif, B.A., Buchanan, S.M., Phillips, G.R., Maniatis, T., 2010. Phosphorylation of protocadherin proteins by the receptor tyrosine kinase Ret. Proc. Natl. Acad. Sci. U. S. A. 107, 13894–13899. doi:10.1073/pnas.1007182107
Schmierer, B., Hill, C.S., 2007. TGFbeta-SMAD signal transduction: molecular specificity and functional flexibility. Nat. Rev. Mol. Cell Biol. 8, 970–82. doi:10.1038/nrm2297
Schmucker, D., Clemens, J.C., Shu, H., Worby, C. a, Xiao, J., Muda, M., Dixon, J.E., Zipursky, S.L., 2000. Drosophila Dscam is an axon guidance receptor exhibiting extraordinary molecular diversity. Cell 101, 671–84. doi:10.1016/S0092-8674(00)80878-8
Schuchardt, A., D'Agati, V., Larsson-Blomberg, L., Costantini, F., Pachnis, V., 1994. Defects in the kidney and enteric nervous system of mice lacking the tyrosine kinase receptor Ret. Nature 367, 380–383. doi:10.1038/367380a0
Segouffin-Cariou, C., Billaud, M., 2000. Transforming ability of MEN2A-RET requires activation of the phosphatidylinositol 3-kinase/AKT signaling pathway. J. Biol. Chem. 275, 3568–3576. doi:10.1074/jbc.275.5.3568
Shi, Y., Massagué, J., 2003. Mechanisms of TGF-beta signaling from cell membrane to the nucleus. Cell 113, 685–700.
Soba, P., Han, C., Zheng, Y., Perea, D., Miguel-Aliaga, I., Jan, L.Y., Jan, Y.N., 2015. The ret receptor regulates sensory neuron dendrite growth and integrin mediated adhesion. Elife 2015. doi:10.7554/eLife.05491
Soba, P., Zhu, S., Emoto, K., Younger, S., Yang, S.J., Yu, H.H., Lee, T., Jan, L.Y., Jan, Y.N., 2007. Drosophila Sensory Neurons Require Dscam for Dendritic Self-Avoidance and Proper Dendritic Field Organization. Neuron 54, 403–416. doi:10.1016/j.neuron.2007.03.029
Song, W., Onishi, M., Jan, L.Y., Jan, Y.N., 2007. Peripheral multidendritic sensory neurons are necessary for rhythmic locomotion behavior in Drosophila larvae. Proc. Natl. Acad. Sci. U. S. A. 104, 5199–5204. doi:10.1073/pnas.0700895104
Sprecher, S.G., Cardona, A., Hartenstein, V., 2011. The Drosophila larval visual system: High-resolution analysis of a simple visual neuropil. Dev. Biol. 358, 33–43. doi:10.1016/j.ydbio.2011.07.006
St Johnston, D., 2002. The art and design of genetic screens: Drosophila melanogaster. Nat. Rev. Genet. 3, 176–88. doi:10.1038/nrg751

Stewart, A., Tsubouchi, A., Rolls, M.M., Tracey, W.D., Sherwood, N.T., 2012. Katanin p60-like1 Promotes Microtubule Growth and Terminal Dendrite Stability in the Larval Class IV Sensory Neurons of Drosophila. J. Neurosci. 32, 11631–11642. doi:10.1523/JNEUROSCI.0729-12.2012

Strelau, J., Strzelczyk, A., Rusu, P., Bendner, G., Wiese, S., Diella, F., Altick, A.L., von Bartheld, C.S., Klein, R., Sendtner, M., Unsicker, K., 2009. Progressive postnatal motoneuron loss in mice lacking GDF-15. J. Neurosci. 29, 13640–8. doi:10.1523/JNEUROSCI.1133-09.2009

Surís, A., Smith, J., Powell, C., North, C.S., 2013. Interfering with the reconsolidation of traumatic memory: sirolimus as a novel agent for treating veterans with posttraumatic stress disorder. Ann. Clin. Psychiatry 25, 33–40. doi:10.1016/j.drudis.2011.09.009

Sweeney, L.B., Chou, Y.-H., Wu, Z., Joo, W., Komiyama, T., Potter, C.J., Kolodkin, A.L., Garcia, K.C., Luo, L., 2011. Secreted semaphorins from degenerating larval ORN axons direct adult projection neuron dendrite targeting. Neuron 72, 734–47. doi:10.1016/j.neuron.2011.09.026

Takahashi, M., 2001. The GDNF/RET signaling pathway and human diseases. Cytokine Growth Factor Rev. 12, 361–373. doi:10.1016/S1359-6101(01)00012-0

Takahashi, M., Ritz, J., Cooper, G.M., 1985. Activation of a novel human transforming gene, ret, by DNA rearrangement. Cell 42, 581–588. doi:10.1016/0092-8674(85)90115-1

Ting, C.Y., McQueen, P.G., Pandya, N., Lin, T.Y., Yang, M., Venkateswara Reddy, O., O'Connor, M.B., McAuliffe, M., Lee, C.H., 2014. Photoreceptor-derived activin promotes dendritic termination and restricts the receptive fields of first-order interneurons in Drosophila. Neuron 81, 830–846. doi:10.1016/j.neuron.2013.12.012

Tracey, W.D., Wilson, R.I., Laurent, G., Benzer, S., 2003. painless, a Drosophila gene essential for nociception. Cell 113, 261–273. doi:10.1016/S0092-8674(03)00272-1

Trupp, M., Arenas, E., Fainzilber, M., Nilsson, A.S., Sieber, B.A., Grigoriou, M., Kilkenny, C., Salazar-Grueso, E., Pachnis, V., Arumäe, U., 1996. Functional receptor for GDNF encoded by the c-ret proto-oncogene. Nature 381, 785–9. doi:10.1038/381785a0

Tsubouchi, A., Caldwell, J.C., Tracey, W.D., 2012. Dendritic filopodia, ripped pocket, NOMPC, and NMDARs contribute to the sense of touch in Drosophila larvae. Curr. Biol. 22, 2124–2134. doi:10.1016/j.cub.2012.09.019

Twombly, V., Blackman, R.K., Jin, H., Graff, J.M., Padgett, R.W., Gelbart, W.M., 1996. The TGF-beta signaling pathway is essential for Drosophila oogenesis. Development 122, 1555–1565.

Usui, T., Shima, Y., Shimada, Y., Hirano, S., Burgess, R.W., Schwarz, T.L., Takeichi, M., Uemura, T., 1999. Flamingo, a seven-pass transmembrane cadherin, regulates planar cell polarity under the control of Frizzled. Cell 98, 585–595. doi:10.1016/S0092-8674(00)80046-X

Valnegri, P., Puram, S. V, Bonni, A., 2015. Regulation of dendrite morphogenesis by extrinsic cues. Trends Neurosci. 38, 439–47. doi:10.1016/j.tins.2015.05.003

Venken, K.J.T., Simpson, J.H., Bellen, H.J., 2011. Genetic manipulation of genes and cells in the nervous system of the fruit fly. Neuron 72, 202–230. doi:10.1016/j.neuron.2011.09.021

Vieira, P., Thomas-Crusells, J., Vieira, A., 2003. Internalization of glial cell-derived neurotrophic factor receptor GFRα1 in the absence of the ret tyrosine kinase coreceptor. Cell. Mol. Neurobiol. 23, 43–55. doi:10.1023/A:1022593001155

Wang, D., Li, Z., Schoen, S.R., Messing, E.M., Wu, G., 2004. A novel MET-interacting protein shares high sequence similarity with RanBPM, but fails to stimulate MET-induced Ras/Erk signaling. Biochem. Biophys. Res. Commun. 313, 320–326. doi:10.1016/j.bbrc.2003.11.124

Wang, S., Tsarouhas, V., Xylourgidis, N., Sabri, N., Tiklová, K., Nautiyal, N., Gallio, M., Samakovlis, C., 2009. The tyrosine kinase Stitcher activates Grainy head and epidermal wound healing in Drosophila. Nat. Cell Biol. 11, 890–895. doi:10.1038/ncb1898

Wang, X., 2013. Structural studies of GDNF family ligands with their receptors - Insights into ligand recognition and activation of receptor tyrosine kinase RET. Biochim. Biophys. Acta - Proteins Proteomics 1834, 2205–2212. doi:10.1016/j.bbapap.2012.10.008

Wassle, H., Peichl, L., Boycott, B.B., 1981. Dendritic territories of cat retinal ganglion cells. Nature 292, 344–345.

Weigmann, K., Klapper, R., Strasser, T., Rickert, C., Technau, G., Jäckle, H., Janning, W., Klämbt, C., 2003. FlyMove--a new way to look at development of Drosophila. Trends Genet. 19, 310–1. doi:10.1016/S0168-9525(03)00050-7

Wojtowicz, W.M., Flanagan, J.J., Millard, S.S., Zipursky, S.L., Clemens, J.C., 2004. Alternative splicing of Drosophila Dscam generates axon guidance receptors that exhibit isoform-specific homophilic binding. Cell 118, 619–633. doi:10.1016/j.cell.2004.08.021

Wojtowicz, W.M., Wu, W., Andre, I., Qian, B., Baker, D., Zipursky, S.L., 2007. A Vast Repertoire of Dscam Binding Specificities Arises from Modular Interactions of Variable Ig Domains. Cell 130, 1134–1145. doi:10.1016/j.cell.2007.08.026

Worby, C. a, Vega, Q.C., Zhao, Y., Chao, H.H., Seasholtz, A.F., Dixon, J.E., 1996. Glial cell line-derived neurotrophic factor signals through the RET receptor and activates mitogen-activated

protein kinase. J. Biol. Chem. 271, 23619–22.
Wu, J., Roman, A.-C., Carvajal-Gonzalez, J.M., Mlodzik, M., 2013. Wg and Wnt4 provide long-range directional input to planar cell polarity orientation in Drosophila. Nat. Cell Biol. 15, 1045–55. doi:10.1038/ncb2806
Xiang, Y., Yuan, Q., Vogt, N., Looger, L.L., Jan, L.Y., Jan, Y.N., 2010. Light-avoidance-mediating photoreceptors tile the Drosophila larval body wall. Nature 468, 921–6. doi:10.1038/nature09576
Yamanaka, N., Romero, N.M., Martin, F. a, Rewitz, K.F., Sun, M., O'Connor, M.B., Léopold, P., 2013. Neuroendocrine control of Drosophila larval light preference. Science 341, 1113–6. doi:10.1126/science.1241210
Yamashita, M., Fatyol, K., Jin, C., Wang, X., Liu, Z., Zhang, Y.E., 2008. TRAF6 mediates Smad-independent activation of JNK and p38 by TGF-beta. Mol. Cell 31, 918–24. doi:10.1016/j.molcel.2008.09.002
Yan, H.Q., Banos, M.A., Herregodts, P., Hooghe, R., Hooghe-Peters, E.L., 1992. Expression of interleukin (IL)-1β, IL-6 and their respective receptors in the normal rat brain and after injury. Eur. J. Immunol. 22, 2963–2971. doi:10.1002/eji.1830221131
Yan, Z., Zhang, W., He, Y., Gorczyca, D., Xiang, Y., Cheng, L.E., Meltzer, S., Jan, L.Y., Jan, Y.N., 2013. Drosophila NOMPC is a mechanotransduction channel subunit for gentle-touch sensation. Nature 493, 221–5. doi:10.1038/nature11685
Yee, G., Hynes, R., 1993. A novel, tissue-specific integrin subunit, beta nu, expressed in the midgut of Drosophila melanogaster. Development 118, 845–858. doi:8076521
Yin, Y.X., Sun, Z.P., Huang, S.H., Zhao, L., Geng, Z., Chen, Z.Y., 2010. RanBPM contributes to TrkB signaling and regulates brain-derived neurotrophic factor-induced neuronal morphogenesis and survival. J. Neurochem. 114, 110–121. doi:10.1111/j.1471-4159.2010.06745.x
Yoshikawa, S., Bonkowsky, J.L., Kokel, M., Shyn, S., Thomas, J.B., 2001. The derailed guidance receptor does not require kinase activity in vivo. J. Neurosci. 21, RC119.
Yoshikawa, S., McKinnon, R.D., Kokel, M., Thomas, J.B., 2003. Wnt-mediated axon guidance via the Drosophila Derailed receptor. Nature 422, 583–588. doi:10.1038/nature01522
Yuan, Q., Xiang, Y., Yan, Z., Han, C., Jan, L.Y., Jan, Y.N., 2011. Light-induced structural and functional plasticity in Drosophila larval visual system. Science 333, 1458–62. doi:10.1126/science.1207121
Yuan, Y., Fu, C., Chen, H., Wang, X., Deng, W., Huang, B.R., 2006. The Ran binding protein RanBPM interacts with TrkA receptor. Neurosci. Lett. 407, 26–31. doi:10.1016/j.neulet.2006.06.059
Zaidel-Bar, R., Itzkovitz, S., Ma'ayan, A., Iyengar, R., Geiger, B., 2007. Functional atlas of the integrin adhesome. Nat. Cell Biol. 9, 858–67. doi:10.1038/ncb0807-858
Zhang, J., Ma, W., Tian, S., Fan, Z., Ma, X., Yang, X., Zhao, Q., Tan, K., Chen, H., Chen, D., Huang, B.-R., 2014. RanBPM interacts with TβRI, TRAF6 and curbs TGF induced nuclear accumulation of TβRI. Cell. Signal. 26, 162–72. doi:10.1016/j.cellsig.2013.09.019
Zhang, L., Huang, Y., Chen, J.Y., Ding, Y.Q., Song, N.N., 2015. DSCAM and DSCAML1 regulate the radial migration and callosal projection in developing cerebral cortex. Brain Res. 1594, 61–70. doi:10.1016/j.brainres.2014.10.060
Zheng, Y., Wildonger, J., Ye, B., Zhang, Y., Kita, A., Younger, S.H., Zimmerman, S., Jan, L.Y., Jan, Y.N., 2008. Dynein is required for polarized dendritic transport and uniform microtubule orientation in axons. Nat. Cell Biol. 10, 1172–1180. doi:10.1038/ncb1777
Zhong, L., Hwang, R.Y., Tracey, W.D., 2010. Pickpocket Is a DEG/ENaC Protein Required for Mechanical Nociception in Drosophila Larvae. Curr. Biol. 20, 429–434. doi:10.1016/j.cub.2009.12.057
Ziegenfuss, J.S., Grueber, W.B., 2013. SAX-7 and menorin light the path for dendrite morphogenesis. Cell 155, 269–71. doi:10.1016/j.cell.2013.09.029
Zihlmann, K.B., Ducray, A.D., Schaller, B., Huber, A.W., Krebs, S.H., Andres, R.H., Seiler, R.W., Meyer, M., Widmer, H.R., 2005. The GDNF family members neurturin, artemin and persephin promote the morphological differentiation of cultured ventral mesencephalic dopaminergic neurons. Brain Res. Bull. 68, 42–53. doi:10.1016/j.brainresbull.2004.10.012
Zimmerman, A., Bai, L., Ginty, D.D., 2014. The gentle touch receptors of mammalian skin. Science 346, 950–4. doi:10.1126/science.1254229
Zlatic, M., Li, F., Strigini, M., Grueber, W., Bate, M., 2009. Positional cues in the Drosophila nerve cord: Semaphorins pattern the dorso-ventral axis. PLoS Biol. 7, e1000135. doi:10.1371/journal.pbio.1000135